ORGANO- AND INORGANO-ORGANO-MODIFIED CLAY MATERIALS IN THE REMEDIATION OF ENDOCRINE DISRUPTING CHEMICALS (EDCs) AND ARSENIC CONTAMINATED WATER

A Thesis submitted
in partial fulfilment of the requirements for the Degree of

Doctor of Philosophy

in

Chemistry

By
THANHMINGLIANA
Regd. No. : MZU/PhD/481 of 15.05.2012

DEPARTMENT OF CHEMISTRY
SCHOOL OF PHYSICAL SCIENCES
MIZORAM UNIVERSITY,
TANHRIL, AIZAWL- 796004

August, 2015

MIZORAM UNIVERSITY
(A central University under the Act of Parliament)
Department of Chemistry
School of Physical Sciences

Dr. Diwakar Tiwari
Professor

CERTIFICATE

This is to certify that the thesis entitled '*Organo- and inorgano-organo-modified clay materials in the remediation of endocrine disrupting chemicals (EDCs) and arsenic contaminated water*' submitted by ***Mr. Thanhmingliana,*** for the degree of ***Doctor of Philosophy*** in the Mizoram University, Aizawl, Mizoram, embodies the record of original investigations carried out by him under my supervision. He has been duly registered and the thesis presented is worthy of being considered for the award of the Ph.D. degree. This work has not been submitted for any degree in any other university.

Dated: 11th August, 2015

(DIWAKAR TIWARI)
Supervisor

Tanhril Campus, Aizawl, Mizoram 796004, India: Ph. 0389-2330832 (0): Cell: 09862323015 Fax: 0389-2330834: Email: diw-tiwari@yahoo.com

Declaration of the Candidate

Mizoram University

August, 2015

I, Thanhmingliana, hereby declare that the subject matter of this thesis is the record of work done by me, that the contents of this thesis did not form basis of the award of any previous degree to me or to the best of my knowledge to anybody else, and that the thesis has not been submitted by me for any research degree in any other University/Institute.

This is being submitted to the Mizoram University for the degree of Doctor of Philosophy in Chemistry.

(THANHMINGLIANA)
Candidate

(Dr. MUTHUKUMARAN R.)
Head

(Prof. DIWAKAR TIWARI)
Supervisor

ACKNOWLEDGEMENTS

I sincerely express my heartfelt gratitude to my research supervisor, *Prof. Diwakar Tiwari*, Department of Chemistry, Mizoram University, for his active guidance and constant support throughout my research work. His devotion to his work, passion for scientific research and valuable suggestions highly encourages me in the field of scientific research; improve my knowledge as well as my research skill.

I express my sense of gratitude to the present and former Deans, *Prof. R.C. Tiwari* and *Prof. R.K. Thapa*, School of Physical Sciences, MZU for their support and encouragements in accomplishing the research work.

I also convey my sincere thanks to *Dr. Muthukumaran, R.*, Head of the Department of Chemistry, MZU, for allowing me to carry out my Ph.D. activities in the Department; and to all other faculty members of the Department, *viz., Dr. Zodinpuia Pachuau, Dr. N. Mohandas Singh, Dr. Rajkumar Mishra, Dr. Ved Prakash Singh*, for their encouragement and support. I also thank to all the non-teaching staff of the Department of Chemistry, MZU, for their valuable help and cooperation.

I express my sincere thanks to the Principal *Dr. Tawnenga* and Vice Principal *Dr. C. Prof. J.V. Hluna*, Pachhunga University College, for their support and for allowing me to pursue my research program at MZU.

I offer my special thanks to *Prof. Seung Mok Lee* and his team, Department of Environmental Engineering, Catholic Kwandong University, Gangneung, Korea, for part of my work was undertaken in their institution with their kind support, and for carrying out the analysis of my sample.

I am immensely thankful to *Dr. H. Lalhlenmawia,* Head, Department of Pharmacy, RIPANS, Aizawl and his staff *Ms. Lalchawimawii* for supporting my work with the HPLC facilities and for their kind assistance with the handling of the instrument.

I really appreciate the hospitality and care extended to me by *Mrs. Alka Tiwari* and *Aditi* at all times. I offer my sincere gratitude to them.

I truly offer my earnest thanks to my colleague and fellow research scholar, *Mr. C. Lalhriatpuia*, who always stands with me and lend me a helping hand in every part of my work. My special gratitude is extended to *Dr. Lalhmunsiama*, for all his valuable helps in the collection of data and analysis of samples.

Valuable support and encouragement that I had received from all my colleagues during my research career is worth to be mentioned. I would like to mention, in particular, the supports of *Dr. Grace Skariah,* Head, Department of Chemistry, Pachhunga University College; my colleagues *Dr. Raghvendu Pathak*, *Mr. Jay Prakash Rajan*, *Dr. K. Vanlaldinpuia* and *Dr. Chanambam Victory Devi*; and the non-teaching staff, *viz*., *Mr. C. Thansanga*, *Mr. Lalsawikima* and *Mr. Ramdinthara*, of the Department of Chemistry, Pachhunga University College. I extend my deep gratitude to them.

I am very happy to acknowledge the cooperation and help I received from all my fellow research scholars in the Department of Chemistry. I thank *Dr. C. Laldawngliana*, *Dr. Lalramnghaki Pachuau*, *Dr. Samuel Lallianrawna*, *Mr. Lalhmingliana Hnamte*, *Mr. Lalrosanga*, *Miss Rebecca Lalmuanpuii*, *Mr. Joseph Lalhruaitluanga*, *Mr. John Vanlalhruaia*, *Mr. Lalsaimawia Sailo*, *Miss Jacqueline Lalthlengliani*, *Miss Lalchhingpuii*, *Mr. Zirlianngura* and others for their support and helping hand, which had been rendered while carrying out my research work. It is my pleasure to mention the help of *Dr. A. Jamsheera*, Research Assistant and *Mr. Brojen Singh*, Sr. Laboratory Technician, Chemistry Department. I put forth my deep sense of gratitude to them.

My deepest gratitude to my beloved mother *Mrs. C. Lalnuntluangi*, my wife *Mrs. Malsawmtluangi* and all my family members for their endless love, constant support and prayers which make it possible to accomplish my research work.

Above all, I thank the Almighty God for his blessings, protection and guidance which enable me to fulfill this research success.

(THANHMINGLIANA)

CONTENTS

CHAPTER – 1

CHAPTER – 2

CHAPTER – 3

CHAPTER–4

Appendix: ***Published Journals Papers***

ORGANO- AND INORGANO-ORGANO-MODIFIED CLAY MATERIALS IN THE REMEDIATION OF ENDOCRINE DISRUPTING CHEMICALS (EDCs) AND ARSENIC CONTAMINATED WATER

CHAPTER 1

INTRODUCTION

1. INTRODUCTION

1.1. BACKGROUND

Reliable access of clean and affordable water is considered one of most basic humanitarian goals, and remains a major global challenge for the 21st century (Qu et al., 2013). Having it available in adequate quantity and quality contributes to the maintenance of health. The total amount of water available on this planet has been estimated at 1.4 billion cubic kilometers. About 97.5% of the earth's water is present in the oceans and seas, and is seemingly unfit for human consumptions because of its high salt content. However, the remaining 2.5%, which is fresh water, a larger fraction (68.7%) is in the form of ice caps, glaciers and permanent snow. The remaining unfrozen fresh water is available as ground water (30.1%) and surface water (1.2%). Only 20.56% of the available surface water (i.e., 0.25% of total global fresh water reserves or only 0.007% of total earth's water) found in lakes and rivers, is readily accessible for direct human consumption (Gleick, 1993; Greenlee et al., 2009). The balance of water supply and demand is affected regionally by a broad range of factors, including population growth, increasing urbanization, intergovernmental relations, political and policy choices, social factors, technological growth, and uncertainties of climate (Plappally and Lienhard, 2012).

According to the World Health Organization (WHO), the scarcity of water resources has created challenges for over 40% of the world population, i.e., more than 2 billion people have no access of enough and clean water (Fu et al., 2014) and almost 1 billion people yet to access of cleaned/improved drinking water sources (Qu et al., 2013). Inadequate access of clean water and sanitation has become one of the pervasive problems affecting human health in developing countries which further may worsen in coming decades. In India, only 20% of communities had access to wastewater treatment plants in the past and the problems posed by waterborne pathogens caused about 80% of illnesses (Fosshage, 2014). Water shortages have plagued many communities, and humans have long searched for a solution to Earth's meager fresh water supplies. Today, the production of potable water has become a worldwide concern; for many communities, projected population growth and demand exceed conventional available water resources. For most, solutions such as water conservation and water transfer or dam construction are not sufficient methods to cope with increasing demand and, in many cases, decreasing supply. Traditional fresh water resources such as lakes, rivers and groundwater are overused or misused; as a result, these resources are either diminishing or becoming saline. Countries continue to develop and expansion of cities, only few new water resources are available to support daily fresh water needs (Greenlee et al., 2009).

The rapid pace of industrialization, population expansion and unplanned urbanization had largely contributed to the severe water pollution. The main sources of freshwater pollution are attributed to a discharge of untreated sanitary and toxic industrial wastes, dumping of industrial effluents and runoff from agricultural fields. The amount of waste disposed in water reservoirs around the world increased manifolds over the last few decades. Statistical data on ocean pollution reveals that every year 14 billion pounds of wastes are disposed in the oceans all over the world. Pollutants discharged into waterbodies can be toxic to aquatic life and causes natural water resources unfit as potable water sources (Bhatnagar and Sillanpää, 2010). The world faces severe and growing challenges maintaining water quality. Therefore, receives overgrowing demand of wastewater treatment plants. In the recent years, diverse technologies have been introduced for the treatment of municipal, domestic, industrial and nuclear wastewater. The fundamental procedures being used in these innovative wastewater treatment technologies are of physical, chemical and biological in nature (Sehar et al., 2013).

It is noted that a large number of pollutants are found at levels exceeding the permissible concentrations which pose a serious threat to the efficiency of wastewater treatment technologies being employed currently. Many research studies are dedicated investigating various aspects of the wastewater treatment technologies and it is found that waste pollutants can be removed as well as treated by different methods. The wastewater treatment processes however; must comply with standards that ensure environmental protection, whilst be efficient to minimize the socio-economic burden (Ainger et al., 2009). The main priorities for wastewater treatment (WWT) are effluent quality, cost, energy efficiency and nutrient removal/recovery. Regulatory agencies aim to improve local environmental health using advanced forms of WWT. The development of wastewater treatment technology is critical to improve the long-term sustainability of the necessary treatment capacity (Hassard et al., 2014). A number of technologies are available at varying degree of success to control water pollution. Some of them are coagulation, foam flotation, filtration, ion exchange, aerobic and anaerobic treatment, advanced oxidation processes, solvent extraction, adsorption, electrolysis, microbial reduction and activated sludge. However, most of them require substantial financial input and their use is restricted due to cost factors overriding the importance of pollution control (Bhatnagar and Sillanpää, 2010).

The conventional methods of water treatment are effective to some extent, but they have some drawbacks such as production of large volumes of sludge, requirement of high energy, problems associated with fouling and generation of huge byproducts (Mook et al., 2014). Among various available water treatment technologies, adsorption process is considered better because of convenience, ease of operation and simplicity of design (Faust and Aly, 1987; Bhatnagar and Sillanpää, 2010). Further, this process can remove/minimize variety of pollutants; thus possesses wider applicability in water pollution control. It is thus highly attractive for water treatment, especially in the developing countries, which are most heavily affected by water contamination (Unuabonah and Taubert, 2014). Besides the fact that adsorption is able to provide advantages, adsorbents also circumvent the production of large amounts of sludge usually associated with some other alternative wastewater treatment techniques like precipitation, which obviously increases the overall cost of water treatment (Ho and McKay, 1999a); this is another advantage of adsorption over other water treatment techniques.

A number of materials are extensively investigated as adsorbents in water pollution control. The choice of adsorbent for the treatment of a specific wastewater with specific chemical pollution characteristics is based on the concentration and type of the micropollutants present in the wastewater, the efficiency/cost ratio and the adsorption capacity of the adsorbent for the pollutant(s) of interest. Since the volume of the water to be treated is generally large, the adsorbent to be used in the process should possess high selectivity for the pollutant(s) of interest. Moreover, it should be non-toxic, easily recoverable from filters, re-generable, cost effective and abundance in nature (Bhattacharyya and Gupta, 2008). Some of the significant examples of high-performance adsorbents that have been developed include clays and modified clays, silica gel/beads, activated alumina, zeolites, polymeric resins, activated carbon, low cost adsorbents from industrial and municipal wastes\by-products like fly ash, slag, sludge, red mud etc., and agricultural wastes and biomasses (Bhatnagar and Sillanpää, 2010; Unuabonah and Taubert, 2014). Among these, clay and their modified forms have received widespread attention for their use as adsorbents of organic micropollutants and inorganic ions from aqueous medium because of their easy availability and comparatively less cost.

1.2. FATE OF POLLUTANTS AND THEIR TOXICITY

1.2.1. Arsenic

Arsenic (As, atomic number 33) is widely distributed on the earth, ranking 20th in abundance in the earth's crust, 14th in seawater, and 12th in the human body (Mandal and Suzuki, 2002). Since its isolation in 1250 A.D., it has been used in various fields such as medicine, electronics, metallurgy, pesticides and wood preservatives (Sharma and Sohn, 2009). Arsenic exists in four different oxidation states: arsenate (+5), arsenite (+3), elemental arsenic (0) and arsine (−3). More than 245 minerals contain arsenic and the ultimate source of arsenic pollution is natural processes and anthropogenic activities such as weathering, mining, burning of fossil fuels and pesticide applications. The levels of arsenic in unpolluted surface water and groundwater vary typically from 1–10 μg/L. In freshwater, the variation is in the range of 0.15–0.45 μg/L (Bissen and Frimmel, 2003). In seawater, the concentration of arsenic is usually less than 2 μg/L (Ng, 2005). Natural geological sources of arsenic in drinking water are one of the most significant causes of arsenic contamination around the world (Sharma and Sohn, 2009).

The World Health Organization (WHO) set a guideline of 10 μg/L as the drinking water standard for total arsenic. At present, millions of people worldwide are suffering from chronic arsenic poisoning (Hughes et al., 2011) mainly due to consumption of As-contaminated water and food. Arsenic contamination in the environment is becoming a serious public health problem in several regions. It is interesting to note that, As was used to cure acute promyelocytic leukemia in humans; on the other hand, As caused adverse health effects in human (Sun et al., 2014). Arsenic is toxic to both plants and animals and inorganic arsenicals are proven carcinogens in humans (Ng, 2005); and the toxicity of arsenic to human health ranges from skin lesions to cancer of the brain, liver, kidney, and stomach (Smith et al., 1992). Inorganic arsenic is classified as 1A class human carcinogen (Devesa et al., 2004). A wide range of arsenic toxicity is studied which depends on arsenic speciation. Generally inorganic arsenic species are more toxic than organic forms to living organisms, including humans and other animals. The oral LD50 for inorganic arsenic ranges from 15–293 mg(As)/kg and 11–150 mg(As)/kg body weight in rats and other laboratory animals respectively (Ng, 2005; Petrick et al., 2000; Sharma and Sohn, 2009). Exposure to arsenic trioxide by ingestion of 70–80 mg was reported to be fatal for humans (Vallee et al., 1960). However, different organic arsenic species possess varied toxicity. For example, as final arsenic metabolites, monomethylarsonic acid (MMA^{V}) and dimethylarsinic acid (DMA^{V}) are less toxic than inorganic arsenic, whereas the toxicity of intermediate metabolites such as monomethylarsonous acid (MMA^{III}) and dimethylarsinous acid (DMA^{III}) are much more toxic than inorganic arsenic. The toxicity of various arsenic species increases in the order of $As^{V}<MMA^{V}<DMA^{V}<As^{III}<MMA^{III}\approx DMA^{III}$ (Petrick et al., 2000; Sun et al., 2014).

Arsenite (As^{III}) is usually more toxic than arsenate (As^{V}). The toxicity of trivalent arsenic is related to its high affinity for the sulfhydryl groups of biomolecules such as glutathione (GSH) and lipoic acid and the cysteinyl residues of several enzymes (Aposhian and Aposhian, 2006). The formation of As^{III}–sulfur bonds results in various harmful effects inhibiting the activities of enzymes such as glutathione reductase, glutathione peroxidases, thioredoxin reductase, and thioredoxin peroxidase. An example of As^{III}–S bond formation is the 1:3 complex of As with Cys-containing tripeptide GSH, which shows unusually high stability constant. As^{III}–GSH conjugates are detected in the bile of rats (Sharma and Sohn, 2009). It is generally accepted that pentavalent arsenicals do not directly bind to sulfhydryl groups to cause toxic effects; however, a recent study reported that sulfide-activated pentavalent arsenic could bind with sulfhydryl group of GSH (Raab et al., 2007). In terrestrial environment, arsenic is mainly present as inorganic arsenic, which exists as pentavalent (As^{V})

under aerobic condition and trivalent (As^{III}) under anaerobic environment. However, As^{III} and As^{V} exert toxicity at different levels. As^{III} is typically present as a neutral species ($As(OH)_3^0$, $pK_a = 9.2$) in aqueous solution at physiological pH. As^{V} is present as an oxyanions in solution, i.e., $H_2AsO_4^-$ and $HAsO_4^{2-}$ at pH 5–7. After entering the cells in animals and humans, As^{V} is rapidly reduced to As^{III} (Sun et al., 2014).

Both trivalent and pentavalent inorganic and organic arsenicals are detected in the urine of individuals after chronic exposure of arsenic and in cell medium following *in vitro* exposure of arsenic (Devesa et al., 2004). Arsenic induces epidemiological toxicity, damaging organisms by producing excess ROS (reactive oxygen species). Arsenic is also cytotoxic and genotoxic. In addition, it is well known that chronic exposure to arsenic can lead to arsenicosis, including skin lesions, black-foot disease, peripheral vascular disease and cancers (Sun et al., 2014). Besides being a carcinogen, arsenic also causes a number of non-cancerous multi–systemic diseases including dermal disease, cardiovascular disease, hypertension and diabetes mellitus (Centeno et al., 2002). Researchers pointed out that trivalent arsenicals (As^{III}, MMA^{III} and DMA^{III}) can induce diabetes via disrupting glucose metabolism based on intact pancreatic islets from mice (Douillet et al., 2013). In addition, As^{III} induces inhibition of pyruvate and α-ketoglutarate dehydrogenase and causes for diabetes (Navas-Acien et al., 2006). Cardiovascular disease is closely associated with hypertension. There are several pathways for arsenic-induced hypertension, including promoting inflammation activity and endothelial dysfunction, altering vascular tone in blood vessels, and affecting kidney function (Abhyankar et al., 2012).

1.2.2. Endocrine Disrupting Chemicals (EDCs)

Endocrine disrupting compounds (EDCs) are chemicals with the potential to elicit negative effects on the endocrine systems of humans and wildlife (Campbell et al., 2006). The US Environmental Protection Agency (USEPA) defines an EDC as: "*An exogenous agent that interferes with the synthesis, secretion, transport, binding, action, or elimination of natural hormones in the body that are responsible for the maintenance of homeostasis, reproduction, development, and/or behavior*" (USEPA, 1997). These are broadly classified into several categories, such as hormones (natural and synthetic estrogen or steroids), pharmaceuticals and personal care products (PPCPs), industrial chemicals, pesticides, combustion byproducts, and surfactants (Campbell et al., 2006). The USEPA tried to establish the Endocrine Disruptor Screening Program (EDSP) to develop official screening methods and toxicity testing strategies for approximately 87,000 compounds. The European Organization for Economic Co-operation and Development (OECD) also put an effort to develop a reliable method to confirm the significance of EDCs (Hecker et al., 2007). However, the proposed methods have not yet been fully accepted within scientific communities (Snyder et al., 2003).

Despite of great efforts to prepare official guidelines of EDCs, their definition and terms are still quite ambiguous. Although many natural and synthetic chemicals are widely considered as EDCs, numerous chemicals present in the environment still remain unidentified and are considered suspicious as potential EDCs (Chang et al., 2009). EDCs are attributed to disturb the reproductive system in humans and wildlife (Oaks et al., 2004; Campbell et al., 2006). Human exposure to these chemicals in the environment is a critical concern with unknown long-term impacts. Natural and synthetic EDCs are released into the environment by humans, animals and industry; mainly through sewage treatment systems before reaching the receiving bodies (soil, surface water, sediment and ground water) (Liu et al., 2009). Given that many of the EDCs identified as potential to cause an estrogenic response even at very low concentrations (parts per billion to parts per trillion), it is of greater concern that a measurable concentrations of many of these chemicals are found in wastewater, surface waters, sediments, groundwater, and even in drinking water. Wastewater treatment plants are found as a source of EDCs (Snyder et al., 2003; Campbell et al., 2006).

1.2.2.1. Bisphenol A (BPA)

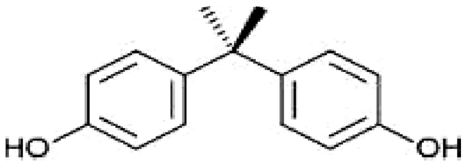

Figure 1.1. Structure of BPA.

Bisphenol A has become ubiquitous in the environment for last 80 years because of its presence in a multitude of products including food and beverage packaging, flame retardants, adhesives, building materials, electronic components, and paper coatings (Flint et al., 2012). Release of this occurs with chemical manufacture, transport and processing. Post-consumer releases are primarily via effluent discharge from municipal wastewater treatment plants, leaching from landfills, combustion of domestic waste and the natural breakdown of plastics in the environment (Crain et al., 2007; USEPA, 2010). Release of BPA to the environment exceeds over a million pounds per year (USEPA, 2010). The tolerable daily intake of BPA was established at 25 μg/kg bodyweight/day by the Health Canada and 50 μg/kg bodyweight/day by the United States and the European Food Safety Authority (EFSA) (Krishnan et al., 2010), but EFSA recommended the current tolerable daily intake (TDI) be lowered from its current level of 50 μg/kg bw/ day (or 0.05 mg/kg/bw/day) to 5 μg/kg bw/day (0.005 mg/kg/bw/day) (EFSA, 2014).

BPA occurs, relatively, at high concentrations (up to 21µg/L) in rivers and lakes worldwide (Crain et al., 2007). In China, BPA is detected up to 0.19µg/L in the surface seawaters, 3.92 µg/L in rivers/lakes/ ponds, and 370 µg/L in wastewaters (Huang et al., 2012). In order to gain basic understanding of the effects of BPA, many research groups were tested its effects on wildlife. Several studies have reported that BPA at higher concentrations caused several adverse effects especially on reproduction. For example, in the freshwater Ramshorn snail (*Marisa cornuarietis*), exposure levels >1.0 mg/L were found to result in superfeminization (additional female organs, enlarged sex glands, oviduct deformities and increased fecundity), oviduct rupture and mortality (Oehlmann et al., 2000). In the mollusk (*Mytilus edulis*), spawning induction, as well as oocyte and ovarian follicle damage, was observed following BPA exposure for 3 weeks at 50 mg/L (Aarab et al., 2006). Alo et al. (2005) found that 80 mg/L BPA alters the activity of neural estrogen receptors that regulate growth hormone in the Mediterranean rainbow wrasse (*Coris julis*), potentially impairing reproduction and development in this sequentially hermaphroditic species. Fathead minnows exhibited altered sex cell type ratios (increased percentage of spermatocytes) following 1 mg/L BPA exposure, which reduces the numbers of mature spermatozoa at 16 mg/L (Sohoni et al., 2001). Altered sex steroid levels were also found in the marine turbot (*Psetta maxima*) at the exposure of BPA 59 mg/L (Labadie and Budzinski, 2006). Furuya et al. (2002) shows the delayed growth of comb, wattle, and testes in male chickens as received with oral doses of BPA as low as 2 mg/1000 g body weight every two days for up to 23 weeks of exposure. In field voles (*Microtus agrestis*) exposure to 250 mg/kg/day results in increase testosterone levels (Nieminen et al., 2002). Studies of the effects of BPA exposure on mammal currently rely on data from laboratory studies on model organisms, which indicate many adverse effects on rodents at high BPA levels. Such effects include advanced puberty, increased obesity, pregnancy complications, defects in male and female reproductive organs, prostate effects, and increases in malignancies (Flint et al., 2012).

1.2.2.2. 17α-Ethynylestradiol (EE2)

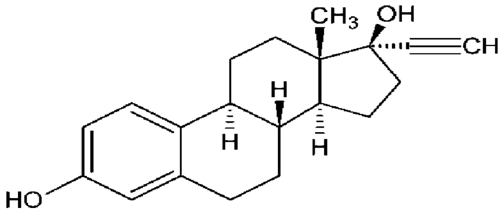

Figure 1.2. Structure of EE2.

17α-ethynylestradiol, also known as EE2 is a synthetic estrogen compound and is a derivative of the natural hormone, estradiol (E2). EE2 is used in almost all modern formulations of combined oral contraceptive pills and hormone replacement therapy for the treatment of osteoporosis, menstrual disorders, prostate and breast cancer, and other ailments, to improve productivity by promoting growth, prevent and treat reproductive disorders in livestock and to develop single-sex populations of fish to optimize the growth in aquaculture (Han et al., 2013; Aris et al., 2014). A survey on best-selling drugs published by Pharmacy Times® in 2010 found that EE2 was used as an active pharmaceutical ingredient in five of the top 200 prescribed drugs in the U.S. under different brand names (Bartholow, 2011). Mazellier et al. (2008) stated that EE2 is used for the treatment of estrogen deficiencies and oral contraceptives with doses ranging from 15 to 50µg. In France, EE2 is widely used by women (30–40µg per pill) and about 60%, ranging from 20–44 years old women (Muller et al., 2010).

Humans and livestock excrete a considerable quantity of hormones. Human urine is considered as one of the main sources of EE2 (Pauwels et al., 2008). The combined farm animal population, for example, sheep and poultry, generates around four times more estrogen than the human population in the UK (Johnson et al., 2000), and the annual level of estrogen excretion by farm animals is reached approximately 33 tons in the European Union and 49 tons in the United States (Tang et al., 2013). These hormones penetrate the surface and ground water systems through sewage treatment plants (STPs), septic systems, from the industrial sources that run the synthetic hormone production facilities, from aquaculture runoff, and through agricultural runoff when sewage and manure are used as fertilizer (Aris et al., 2014). In fact, treated sewage effluents constitute the major source of environmental EE2 due to the inadequate removal of EE2 in STPs. Orally ingested EE2 undertakes extensive metabolism in the liver, principally via oxidation at C17 ethinyl triple bond and aromatic hydroxylation at C2/C4 on steroid nucleus, prior to excretion via urine and feces. Human metabolism transforms EE2 into biologically inactive sulfate and glucuronide forms (Han et al., 2013); however, partial degradation in STPs and natural environment de-conjugates EE2 metabolites and renders them estrogenically active again (Atkinson et al., 2012). Larcher and Yargeau (2013) explained the treatment process in wastewater treatment plants (WWTPs) is incomplete and insufficient to remove EE2, resulting the measured concentrations of EE2 even up to 62 ng/L from WWTP effluents. Cargouët et al. (2004) also reported that high level of free EE2 is detected in domestic wastewater at 7 ng/L and in the effluent of WWTP of up to 42 ng/L. Li et al. (2013) estimated that the concentration of EE2 in reclaimed water would still be 8.7 ng/L, which is much higher than the predictive non-effect concentration (PNEC) of EE2 (0.002 ng/L) even though the effluent of WWTP in China with a treatment capacity of 2,00,000 m^3/d was treated by ozonation and microfiltration to produce reclaimed water. Hence, EE2 was detected in treated drinking water and was found significantly in the German drinking water at 0.5 ng/L (Atkinson et al., 2012). The presence of this compound in drinking water poses a serious public health concern.

It has become a widespread problem in aquatic environments because of its high resistance to the process of degradation, its ultra-high estrogenicity and its tendency to absorb organic matter, accumulate in sediment and concentrate in biota (Aris et al., 2014). The Endocrine Disruptor Knowledge Base (EDKB), which is jointly published by the U.S. Food and Drug Administration (USFDA) and National Center for Toxicological Research (NCTR), identifies EE2 as the most potent estrogenic chemical in all endocrine-disrupting chemicals discovered to date (USFDA, 2012). In January 2012, the European Commission announced a proposal to limit EE2 in European water bodies to an annual average below 0.035 ng/L under its Water Framework Directive, which has sparked wide ranged debate due to the potentially high treatment costs (Han et al., 2013). In Australia, the risk of human exposure to EE2 through affected drinking water is a real concern in water-stressed regions where the drinking water supply is augmented by recycled water produced from municipal wastewater effluents (Ying et al., 2004). The Australian Guidelines for Water Recycling recommended a maximum level of 1.5 ng/L EE2 in drinking water augmented with recycled water, which represents the lowest threshold in a suite of ten targeted estrogens due to the high estrogenicity of EE2 (Middleton et al., 2008). EE2 shows the highest estrogenic potency in the *in vitro* tests compared to the other estrogens E2 and E1. However, toxicity of EE2 varies and is dependent on the studied species and *in vitro* or *in vivo* assays which are used for studies (Aris et al., 2014).

The toxic potential of estrogen compounds to various organisms has been extensively studied. Numerous experiments prove that EE2 is very toxic to a large number of exposed organisms. Endocrine-disrupting effects of EE2, both *in vivo* and *in vitro*, are observed in freshwater fish species in both laboratory and field studies at ng/L levels. Several studies have shown that exposure to concentrations of EE2 in the range of those detected in the environment, elicit the synthesis of the egg-yolk precursor vitellogenin, increases incidences of histological aberrations, and causes the feminization of male fish (Dussault et al., 2009). Both field and laboratory studies have provided abundant evidence concerning the effects of exposure to these chemicals, such as the increase of plasma vitellogenin in male and female fish, accelerates proportions of intersex fish, decreases egg and sperm production, reduces gamete quality, complete feminization of male fish, reduces fertility and fecundity and also behavioral changes (Larcher and Yargeau, 2013; Aris et al., 2014). It can directly or indirectly reduce the fate of survival, the growth of early-life stage of organisms, and reproductive success (e.g., fertility and hatching success), and also impact on the population level (Yan et al., 2012).

Other than aquatic organisms, the vertebrates, including mammals have shown to be sensitive to EE2, particularly during their postnatal development (PND). For example, Vosges et al. (2008) reported that male rats that are exposed to EE2 in their drinking water for 3 weeks at a concentration of 0.1 and 1 ppm (PND 22–PND 43) are found to affect significantly the ponderal growth of the animals. Males exposed to 10 ng/mL of EE2 in drinking water from PND 5 onwards conceived a significantly higher proportion (25%) of small litters (one to five pups) than the control males (0–3%). Delclos et al. (2009) reported that 50 ppb of EE2 can affect the exposed Sprague Dawley rats, by decreasing body weight, accelerating the vaginal opening, and altering the estrous cycles in young animals. At higher doses, anogenital distance was subtly affected and significantly increased the incidence of uterine lesions (a typical focal hyperplasia and squamous metaplasia). Exposure during development (from gestational day 7 to postnatal day 8) to oral micromolar doses of EE2 permanently disrupted the reproductive tract of male rats (Larcher et al., 2012).

1.2.2.3. Diclofenac sodium (DFS)

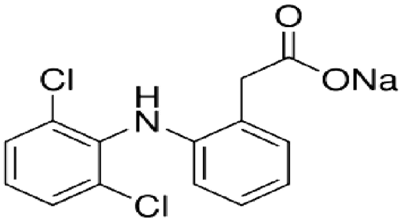

Figure 1.3. Structure of DFS.

Diclofenac, a phenylacetic acid derivative is a non-steroidal anti-inflammatory drug (NSAID) with analgesic, anti-inflammatory, and antipyretic properties. The sodium salt of diclofenac (DFS) is often used to treat osteoarthritis, rheumatoid arthritis, ankylosing spondylitis, and mild to moderate pain. It is also recommended to reduce menstrual pain, dysmenorrhea etc. (Vogna et al., 2004; Zhang et al., 2008). Diclofenac is a most commonly used analgesic in the world and is commercially available in various formulations including ones for oral administration. The global consumption of diclofenac is estimated to be approximately 940 tons per year; with a defined daily dose of 100 mg. Approximately 65% of the dose is excreted through urine, mainly as hydroxylated metabolites conjugated to glucuronides after enterohepatic circulation (Zhang et al., 2008; Fent et al., 2006). However, the actual amount of metabolites in the feces is still not clear. DFS is generally removed only about 30% in conventional sewage treatment plants (STPs). Because of its low biodegradability and its limited sorption properties onto activated sludge, DFS is detected in STP−effluent and surface water even up to 4.7 μg/L and 1.2 μg/L, respectively, and even in groundwater and tap water at concentrations up to 380 ng/L and below 10 ng/L, respectively (Aguinaco et al., 2012; Fent et al., 2006). Diclofenac has also been detected in rivers, groundwater, hospital effluents and drinking water at the order of ng/L (Santos et al., 2010). DFS is considered to be one of the most important compounds in terms of ecotoxicity and persistence in the environment (Wang et al., 2014).

Recent studies have shown that diclofenac inhibits the activity of cyclooxygenases and DNA synthesis through multiple mechanisms (Chae et al., 2015). Diclofenac is assigned to pregnancy category C prior to 30 weeks gestation and to category D starting at 30 weeks of gestation by the United States Food and Drug Administration (USFDA, 2011). Even though the toxicity and teratogenicity of diclofenac are measured, conflicting data is published for different animal model systems. Fetal neuronal cell apoptosis is significantly induced in diclofenac-treated pregnant rats (Gokcimen et al., 2007). Additionally, diclofenac-treated rodents deliver fetuses with severe morphological abnormalities such as defects of the palate, limbs, and ductus arteriosus (Chae et al., 2015). Diclofenac-treated Medaka fish embryos also show decreased survival rates, shrunken yolks, and hemorrhage (Nassef et al., 2010). These studies clearly suggest diclofenac toxicity during embryogenesis, although it seems to be safe for embryos at considerably lower doses. Diclofenac is thought to affect damage in renal and gastrointestinal tissues in several vertebrate taxa and its accidental exposure in the veterinary use as resulted in the near extinction of critically endangered Asian vulture populations. This causal relationship is subsequently confirmed under controlled experimental conditions in both captive Asian and African white-backed vultures (*G. africanus*) (Oaks et al., 2004). For this reason diclofenac was highlighted as a particular environmental concern. Saravanan et al. (2011) reported that diclofenac interferes with the biochemical functions of fish and leads to tissue damage even at environmentally relevant concentrations.

Ng et al. (2008) demonstrated that DFS could induce cellular apoptosis. In addition diclofenac have shown to induce uricemia in the chicken (Naidoo et al., 2007). Zebra mussels exposed to the environmentally relevant (nominal) concentration of 1 µg/L of diclofenac shows signs of oxidative stress with elevated lipid peroxidation levels. At higher concentration of 1000 µg/L the defense mechanism of Glutathione-S-transferase (GST) and Metallothionein (MT) are induced by diclofenac (Schmidt et al., 2011). Among the NSAID, diclofenac shows the most acutely toxic nature with the effects being observed at concentrations below 100 mg/L (Cleuvers, 2003). Chronic toxicity trials performed on rainbow trout (*Oncorhynchus mykiss*) evidenced cytological changes in the liver, kidneys and gills for the exposure of 28 days at just 1 µg/L of diclofenac. At the concentration of 5 µg/L, renal lesions are evident as well as drug bioaccumulation in the liver, kidneys, gills and muscle (Santos et al., 2010). Brown trout (*Salmo trutta f. fario*) showed similar cytological damage and a reduction of haematocrit values after 21 days of exposure using 0.5 µg/L of this active substance (Hoeger et al., 2005). Schmitt-Jansen et al. (2007) evaluated both diclofenac phytotoxicity and its photochemical products on the unicellular chlorophyte *Scenedesmus vacuolatus*. Inhibition of algal reproduction by the parent compound only occurred at a concentration of 23 mg/L, hence indicating no specific toxicity. However, the threat significantly increased when metabolites were produced from 53 h of exposure to daylight. Diclofenac also inhibited the growth of marine phytoplankton *Dunaliella tertiolecta* at concentrations of 25 mg/L and above, and for this organism, 96 h EC_{50} of 185.69 mg/L is found (DeLorenzo and Fleming, 2008).

1.2.2.4. Tetracycline (TC)

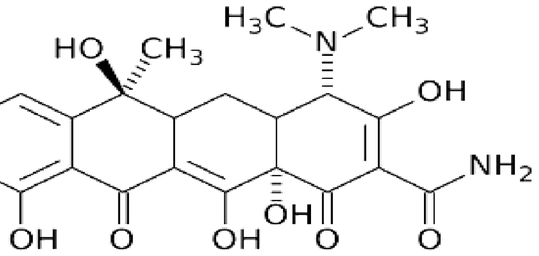

Figure 1.4. Structure of TC.

Tetracycline is a broad-spectrum antibiotic employed in the treatment of bacterial infections such as Rocky Mountain spotted fever, syphilis, pneumonia, respiratory tract infection, amoebic infections and gonorrhea (Heaton et al., 2007). TC is most commonly used to treat acne vulgaris and other skin disorders like rosacea and perioral dermatitis (Farombi et al., 2008). It is also employed in aquaculture and the livestock industry as one typical antibiotic (Niu et al., 2013). The consumption of tetracycline for veterinary purposes is significantly high comparing to other classes of antibiotics (Kim et al., 2014). The emergence of bacterial resistance limited its practical uses. In spite of this, however, according to the National Ambulatory Medical Care Survey, of visit to office-based physicians in the United States (2007) tetracycline among other counterpart drugs was prescribed either as a new medication or as a continued medication. Moreover, the drug has gained wide acceptance in the third world countries because of its easy accessibility, availability and cost effectiveness. As such, the drug can be abused due to self-prescribing, which is rife in this part of the world (Farombi et al., 2008).

It enters into the environmental matrices by direct runoff and excretion as unmetabolized drugs or active metabolites and degradation products (Niu et al., 2013). The widespread occurrence of pharmaceuticals is demonstrated by a number of monitoring studies (Kim et al., 2014). Previous researches showed that nearly 90% of antibiotics could be excreted with the urine and up to 75% in animal feces, which leads to 70%–80% of antibiotics loads, enters into the city sewage system as their parent form. However, the normal sewage treatment system cannot eliminate antibiotics completely, which results in residual antibiotics in the effluent. It was reported that the removal rate of tetracycline was only 30% in WWTP. This could become a risk both to the environment and human health. Recently, it is reported that TC is detected in surface water, wastewater and soils, as well as drinking water, while the detected concentration is in the range of ng/L – µg/L (Yang et al., 2013). The occurrence of cumulated TC in the environment can induce genetic exchange, increases the resistance of bacteria against drugs, and subsequently threatens human health.

Thus, it is of great importance to develop effective technology for eliminating TC from water (Niu et al., 2013).

Tetracycline is a well-known antibiotic that induces Nonalcoholic steatohepatitis, NASH (a combination of lipid accumulation in the liver and associated liver lesions, such as lipid peroxidation and cell necrosis/apoptosis) in human and rodents since the first description in 1951 (Lepper et al., 1951). Tetracycline-induced NASH has been extensively reported in studies *in vivo* (Shen et al., 2009). Inhibition on mitochondrial β-oxidation of fatty acids largely determined tetracycline-induced steatohepatitis in mice (Freneaux et al., 1988). Besides, tetracycline was suggested to block the tricarboxylic acid cycle and respiratory chain in mitochondria in rats (Fromenty and Pessayre, 1995). Triglyceride accumulation and lipid peroxidation is also detected, followed by the increase of serum alanine and aspartate aminotransferases in rodents and human. Tetracycline toxicity is partly evidenced basing on a few *in vitro* studies using hepatocyte monolayer. The reduced metabolism of fatty acid and lipid accumulation are observed in tetracycline-treated hepatocytes from either rats or dogs while oxidative stress is demonstrated in rat hepatocytes as well as in human hepatocytes. In addition, the decrease of mitochondrial membrane potential is detected in human hepatocytes by treatment of tetracycline. Thus, these results by monolayer culture concerned lipid accumulation, oxidative stress or mitochondrial lesion which only reflected a part of cellular alternations without systematic description (Xu et al., 2008; Shen et al., 2009).

Tetracycline is known to cause a number of biochemical dysfunctions and suspected to induce testicular damage to animals and humans. Administration of tetracycline caused a reduction in the epididymal sperm motility, percentage of live spermatozoa, sperm count, increased in abnormal sperm morphology as well as induction of adverse histopathologic changes in the testes. Tetracycline-induced hepatotoxicity characteristically caused fatty infiltration of the liver and liver parenchymal cell damage. Studies have also reported that the drug causes hyperglycemia as well as injury to the pancreas (Asha et al., 2007; Farombi et al., 2008). Mechanisms by which tetracycline elicits these effects are not well understood, however, reactive oxygen species (ROS) are implicated. Tetracycline causes significant oxidative stress in the liver and pancreas of rats by reducing the levels of antioxidant enzymes and glutathione (GSH), and elevating the levels of lipid peroxide formed (Asha et al., 2007). Immunohistochemical expression of oxidative stress-related markers such as 8-hydroxy deoxyguanosine, heme oxygenase-1 and superoxide dismutase (SOD) is detected in the livers of rats treated with tetracycline (Kikkawa et al., 2006).

1.3. ARSENIC REMOVAL TECHNIQUES

Arsenic removal from aquatic environment is not an easy task because of the variable oxidation states of arsenic and the environmental matrix associated thereof. From a technical point of view, the physicochemical and microbiological characteristics of the waters and the available materials in the region will determine the convenient way of technology to adopt for speciation and removal of arsenic. The selection of the method depends greatly on arsenic speciation and chemical composition of the water. All technologies rely on a few basic chemical processes that can be applied alone, simultaneously or in sequence. Mostly, the arsenic removal technologies are efficient when the element is in the pentavalent state, because it is present in the form of oxyanions, mainly $H_2AsO_4^-$ and $HAsO_4^{2-}$ at a wide pH range 2–12, while the trivalent form is uncharged at pH below 9.2 (H_3AsO_3). This is the reason why many arsenic remediation methods used; are deployed a prior oxidation step. However, oxidation without the other physical or chemical transformations could not help to remove the arsenic from aqueous solutions (Litter et al., 2010).

The purpose of oxidation is to convert soluble As(III) to more easily removable As(V) species, followed by precipitation of As(V). This is essential for anoxic groundwater, since As(III) is the predominant form near neutral pH. As(V) adsorbs more easily onto solid surfaces than As(III) and thus, oxidation followed by adsorption is thought to be effective for the removal of As (Mondal et al., 2013). Simple direct aeration is slow, but a number of chemicals, including chlorine, hypochlorite, ozone, permanganate, hydrogen peroxide, manganese oxides, ferrate and Fenton's reagent (H_2O_2/Fe^{2+}) can be employed to accelerate oxidation (Ahmed, 2002; USEPA, 2000a). Photochemical oxidations is found to be a convenient way of As(III) oxidation. Chlorine is an efficient/effective oxidant, but it may react with organic matter, producing toxic and carcinogenic trihalomethanes as by-products. Potassium permanganate effectively oxidizes arsenite, and it may be a widely available inexpensive reagent suitable for many developing nations. Hydrogen peroxide is an effective oxidant if the raw water contains dissolved iron, which often occurs in conjunction with arsenic contamination, allowing the occurrence of Fenton reactions (Litter et al., 2010). Thus, an adequate selection of oxidants in relation with aquatic chemistry and water composition is a pertinent step to achieve a high removal efficiency of aqueous As oxidation. Moreover, due to several drawbacks, oxidation alone is not considered as an effective method for the removal of As (Mondal et al., 2013).

The most common technologies include processes that can be used alone or mostly in combinations, such as oxidation, precipitation/coprecipitation, adsorption onto coagulated flocs, lime treatment, adsorption onto suitable surfaces, the use of ion exchange resins, membrane technologies etc. (Newcombe and Möller, 2008; Sharma and Sohn, 2009).

1.3.1. Precipitation/Co-precipitation

Among the conventional technologies, precipitation/co-precipitation is frequently used technology to treat arsenic-contaminated waters. Precipitation/co-precipitation uses chemicals to transform dissolved contaminants into insoluble solids, or form another insoluble solid onto which dissolved contaminants are adsorbed. The solids are then removed from the liquid phase by filtration (Jain and Singh, 2012). By adding calcium, magnesium, manganese (II) or iron (III) salts to As(V) solutions, As-containing solids are obtained that can be removed through sedimentation or filtration. However, the method is generally not suitable because of the instability of most of the solids, also inadequate for direct disposal, although it can be used to palliate the problem in mining sites where those salts are present naturally (Ladeira et al., 2002). The effectiveness of this technology is less likely to be reduced by characteristics and contaminants other than arsenic, compared to conventional water treatment technologies. Systems using this technology generally require skilled operators; therefore, precipitation/co-precipitation is more cost effective on a large scale where labor costs can spread over a larger amount of treated water produced (Jain and Singh, 2012).

1.3.2. Coagulation/flocculation and filtration

This is common technique for the removal of arsenic from ground water. The addition of coagulant followed by the formation of floc is a potential way that has been used to remove As from groundwater. Positively charged cationic coagulants reduce the negative charge of the colloids and, as a result, larger particles are formed due to the aggregation of particles (Choong et al., 2007). Arsenic is removed in the pentavalent form, which adsorbs onto coagulated flocs and can then be removed by filtration. The commonly used coagulants are aluminium sulfate $Al_2(SO_4)_3$, ferric chloride ($FeCl_3$) and ferrous sulfate ($FeSO_4$). Iron salts are being generally found better removal agents. Filtration is a necessary step. Coagulation–filtration technology is simple, only common chemicals are used, installation costs are small and it can be easily applied for large water volumes (Litter et al., 2010). However, a problem with this technique is the safe separation of the ferric hydroxide precipitate, for example by filtration or sedimentation. Further, relatively large volumes of As-containing sludge is formed which needs a careful handling (Jain and Singh, 2012). The management of contaminated sludge is important for safeguarding the environment from secondary pollution and thus reduces the feasibility of applying this method in field conditions (Mondal et al., 2013).

1.3.3. Lime softening

In presence of water and carbonic acid, lime forms calcium carbonate, that readily adsorbs arsenic and the process ends with a coagulation step. The method is efficient to treat water with high hardness, especially at $pH > 10.5$. The addition of chlorine to oxidize As(III) is needed. The disadvantages are: (i) a very high pH in the resulting water (10–12), which implies a further acidification step; (ii) a very high dose of coagulant is needed; (iii) relatively low removal efficiencies (generally not less than 1 mg/L), secondary treatments is required (Kartinen and Martin, 1995; Newcombe and Möller, 2008; USEPA, 2000a).

1.3.4. Membrane processes

Membrane processes are considered a promising technology for removing As from groundwater in view of the drinking water production. Generally four different types of membrane processes, i.e., microfiltration (MF), ultrafiltration (UF), nanofiltration (NF) and reverse osmosis (RO) are used for the treatment of As contaminated water. The separation by these processes depends on the pore size of the membrane; for MF and UF membranes, separation is achieved via mechanical sieving while for NF and RO membranes, capillary flow or solution diffusion are responsible for the separation (Choong et al., 2007). From the possible membrane processes, MF or UF, which uses low-pressure membranes (large nominal pore sizes, 10–30 psi) are not completely adequate since the arsenical species are very small and can traverse the membranes (Litter et al., 2010). For improving the removal efficiency, some particle size increasing techniques was applied, such as coagulation and flocculation (Ghurye, 2004).

NF and RO are high pressure techniques and are able to remove dissolved As from water to an appreciable level provided that the feed water contains a very low amount of suspended solids. NF membranes are generally negatively charged at neutral and alkaline solution. Separation of As is caused due to electrostatic repulsion between the anionic As species and the charge of the membrane (Donnan exclusion) as well as the small size of the pores of the membrane. Therefore, although NF gives satisfactory results in the removal of As(V) from the solution, but the persistent problem of this technique is the removal of the uncharged As(III) species in the near-neutral pH range. Thus, NF without oxidative pretreatment is not sufficient to remove total As from an aqueous solution and is not able to provide water quality below the maximum contaminant level (MCL) (Mondal et al., 2013). In RO, an external pressure is applied to reverse natural osmotic flow, and water flows from a more concentrated saline solution through the semipermeable membrane, which has a thin microporous surface that rejects impurities but allows water to pass through. Since only a small amount of raw water (10–15%) passes through the membrane in NF and RO, these processes are suitable for household or applications where only a small amount of treated water is required. Operation and maintenance requirements for membranes are minimal: no chemicals are needed, and maintenance consists of only ensuring a reasonably constant pressure, and periodic cleaning of the membranes. The main disadvantages, especially for

RO, are low water recovery rates (typically 10–20%), high electrical consumption, relatively high capital and operating costs (expensive membranes), and the risk of membrane fouling. High concentrations of suspended solids, organic matter, humic acids, hardness, sulfides, ammonium, nitrite, methane, etc. interfere in removal of arsenic and only low levels of arsenic can be treated. Discharge of rejected water (20–25% of the influent) or brine is also a concern; therefore, the technology is not much useful in areas where water is scarce. The method provides good As(V) but poor As(III) removal, and oxidation is difficult because residual oxidants can damage the membranes (Litter et al., 2010).

1.3.5. Ion exchange resins

Synthetic ion exchange resins, generally of polymeric matrix (polystyrene cross-linked with divinylbenzene), linked to charged functional groups, could be applied for As removal; quaternary amine groups, $-N^{+}(CH_3)_3$, are the preferred groups (Litter et al., 2010). Anion exchange resins are commonly used for the treatment of As where the oxy-anionic species of arsenate ($H_2AsO_4^{1-}$, $HAsO_4^{2-}$ and AsO_4^{3-}) are effectively exchanged with the anionic charged functional groups of the resin, thus producing effluents with low concentrations of As(V) (Choong et al., 2007). Since arsenite usually exists as a neutral molecule and is not exchanged, oxidation of As(III) to As(V) is an important pretreatment step for ion exchange processes. Before passing As contaminated water, the resin bed is usually flushed with HCl so as to implant labile Cl^{-} on the surface of the resin, which is later easily exchanged with As. Thus, the effluent contains a considerable amount of Cl^{-} and additional secondary treatment is needed to improve the quality (Mondal et al., 2013). Competing anions, especially sulfate, TDS, selenium, fluoride, and nitrate, interfere strongly and play a significant role in the removal of As via ion exchange. Reports suggest that sulfate is preferentially exchanged than As for commercial resins and thus, less water could be treated for high sulfate water than for low sulfate water (Höll, 2010). Additionally, clogging of the resin takes place due to iron precipitation and suspended solids in aqueous solution (Kartinen and Martin, 1995; USEPA, 2000a; Mondal et al., 2013). Therefore, the life cycle of the resin becomes very low and increases the cost of operation. Moreover, during regeneration of resins, As rich brine solutions are produced which may again lead to the environmental release of As (Cundy et al., 2008). Ion exchange or membrane processes are quite expensive in nature and they are not relevant in the context of costs (Jain and Singh, 2012).

1.4. EDCs REMOVAL TECHNIQUES

Various separation or degradation techniques are considered as potential treatment option for the efficient and effective removal of EDCs from water bodies. Unfortunately, many chosen treatment option could not consistently conform to the desired removal efficiency level. One possible reason might be due to sub-micro level concentration and varying physical and chemical nature of EDCs. Removal efficiencies of individual EDCs vary depending on unit operations and processes commonly used in WWTP (Barceló, 2003). Therefore, proper removal process for an individual target compound needs to be carefully selected in accordance with the characteristic property of each EDC (Chang et al., 2009). Certainly the existing water and wastewater treatment plants have been designed for the best in the treatment and removal of contaminants and eutrophicating pollution loads, especially those which are specified in the existing regulations. However, the occurrence of the new 'unregulated' micro-contaminants such as EDCs requires advanced treatment. Furthermore, EDCs possessed a wide range of chemical properties and thus success in removal varies greatly depending upon their particular chemical nature (Bolong et al., 2009).

Physicochemical treatment such as coagulation-flocculation process was, in general, unable to remove EDCs. However, advanced treatment like UV and ion-exchange do improve the removal of EDCs, yet they are insufficient to be considered as feasible removal options (Bolong et al., 2009). A study conducted by Westerhoff et al. (2005) using a bench-scale simulation water treatment plant model and natural waters spiked with 30 pharmaceuticals to 80 different EDCs yielded no significant removal except using activated carbon (powder) and oxidation via chlorination and ozonation. Chemical treatment such as coagulation, flocculation or lime softening shows ineffective removal of EDCs and PPCPs. These findings are also made by Adams et al. (2002) where several EDCs (*viz*., carbadox, sulfadimehoxine and trimethoprim) was not removed by metal salt coagulants (aluminium sulfate and ferric sulfate).

Among the different options available for the removal of EDCs biological processes, membrane filtration and advanced oxidation processes (AOPs) are applied and assessed by several authors. However, each removal option possesses advantages and limitations (Silva et al., 2012).

1.4.1. Membrane process

Membrane process is gaining wide use for organic contaminant removal in wastewater treatment. Membrane filtration technology such as reverse osmosis (RO) and nanofiltration (NF) membranes is reported to be efficient in removing organic micro-contaminants such as EDCs including steroid hormones, pesticides, and pharmaceuticals and personal care chemicals (PPCPs) (Chang et al., 2009; Liu et al., 2009; Silva et al., 2012). Removal by membranes occurs by a combination of processes such as adsorption, size exclusion and charge repulsion. These three main mechanisms were so much interrelated and have significant influence on EDCs rejection that in turn causes the removal performances which can be very different and varied from compound to compound (Bolong et al., 2009). Their rejection efficiency is strongly dependent on membrane operating conditions (like flux and water feed quality), membrane properties (e.g., permeability, pore size, surface charge and hydrophobicity/hydrophilicity), membrane fouling and parameters like pH, temperature and salinity (Silva et al., 2012). Studies show that the rejection efficiency of EDCs by membranes also strongly depends on EDCs' physicochemical properties, such as molecular weight, octanol-water partition coefficient (K_{ow}), water solubility and electrostatic property and so on. In comparing membrane types over most cases, EDCs rejection rate by reverse osmosis is highest, followed by nano-membrane types, then ultra-membranes, with the rejection of micro-membranes as the lowest (Liu et al., 2009).

1.4.2. Biological treatment

Among the conventional biological wastewater treatment systems, the activated sludge process is most widely used around the globe, and as the proportion of removal by primary settling, chemical precipitation, aerating volatilization and sludge absorption is small. The majority of EDCs in wastewater is regarded to be removed by biodegradation (Andersen et al., 2003; Braga et al., 2005). However, most of the EDCs removal was not always complete by existing WWTPs and they remained fluctuating with concentrations in effluent, and discharge of such effluents is the main reason for the wide distribution and occurrence of EDCs in surface waters, ground waters, and even in drinking waters. Incomplete removal of EDCs by existing WWTPs not only results from the fluctuation of EDC levels in the influent, but the type of processes applied in the WWTPs as well as operational conditions (Liu et al., 2009). Moreover, it should be noted that, for estrogens, as for any chemical, the biodegradation products can be more harmful than the parent substance (Silva et al., 2012).

1.4.3. Advanced oxidation processes

Advanced oxidation processes (AOPs) are considered as highly competitive water treatment technology for the removal of several classes of EDCs which are difficult to remove by conventional techniques (Oller et al., 2011), but at present most of the results are from laboratory research based on artificial sewage. The essential mechanisms of AOPs are mineralization of pollutants in wastewater to CO_2 or transference of pollutants to some other metabolite products by some strong oxidizers through oxidation-reduction reactions (Liu et al., 2009). The removal efficiency is generally proportional to the oxidation power, and is a function of the contaminant structure and oxidant dose. Particularly, the chemical structure of target compounds affects the oxidation rate of EDCs (Chang et al., 2009). To increase the removal effect, some combinations such as UV/O_3, UV/H_2O_2, UV/Fenton etc. are widely applied in the removal of EDCs. These methods are characterized by the generation of the hydroxyl radical (•OH), for which the higher redox potential provides enhanced oxidation of contaminants (Liu et al., 2009). However, it must be pointed out that under certain circumstances, AOPs can be a cause of concern. These processes may render harmful by-products or transformation products due to their reactivity with water matrix components or micropollutants, which can have similar or increased estrogenicity relative to the parent compounds. On this basis, the disappearance of the original compound does not necessarily imply that the treatment is efficient (Silva et al., 2012). However, careful selection is needed as reaction of these chemicals is found to be reactive and produce byproducts, of which the effects are unknown (Bolong et al., 2009).

1.5. ADSORPTION

According to IUPAC, adsorption is an increase in the concentration of a dissolved substance at the interface of a condensed and a liquid phase (or a gaseous phase) due to the operation of surface forces (IUPAC, 1997). It is considered to be a process of selective partitioning of the adsorbent species to the interface in preference to the bulk and is the result of interactions of such species with the surface species on the solid. It is sometimes difficult or impossible to discriminate experimentally between adsorption and absorption, in such cases it is convenient to use the non-committal term ‘sorption’ (together with its derived terms sorbent, sorbate, sorptive). This term is also used as a general term to cover both adsorption and absorption when both are known to occur simultaneously (IUPAC, 1971).

Adsorption of molecules on solids from solution is important in controlling a variety of interfacial processes such as mineral flotation and other solid–liquid separation processes, flocculation\dispersion, blood clotting, and micellar flooding of oil wells. Adsorption results from energetically favorable interactions between the solid adsorbate and the solute species. Adsorption of surfactants on minerals from aqueous or organic solutions is often a complex process since it can be influenced by all components of the system: solid, solvent, and solute. Several interactions such as electrostatic attraction, covalent bonding, hydrogen bonding or nonpolar interactions between the adsorbate and the adsorbent species, and lateral interaction between the adsorbed species as well as their desolvation can contribute to the adsorption process (Birdi, 2009).

1.5.1. Physisorption and Chemisorption

The interactions responsible for adsorption can be either physical or chemical in nature. Therefore, adsorption is broadly classified into two categories, physical adsorption or physisorption and chemical adsorption or chemisorption, depending on the nature of the forces involved (Adamson, 1982). Physisorption is defined as adsorption in which the forces involved are intermolecular forces (van der Waals forces) of the same kind as those responsible for the imperfection of real gases and the condensation vapors, and this could not involve a significant change in the electronic orbital patterns of the species involved (IUPAC, 1997). Physical adsorption is usually a weak and reversible and associated with small energy changes. The van der Waals forces and electrostatic forces are primarily responsible for physical adsorption which is also characterized by the high rate of adsorption and formation of multilayers (Parfitt and Rochester, 1983).

Chemisorption on the other hand is the adsorption which results from chemical bond formation (strong interaction) between the adsorbent and the adsorbate in a monolayer coverage onto the solid surface (IUPAC, 1997). Chemical adsorption occurs through covalent bonding between the adsorbate and the surface species on the solid. Chemical adsorption normally involves an activation stage and is characterized by relatively higher energy changes and a low rate of adsorption. The adsorption is usually strong, irreversible and specific, and is limited to a monolayer. A distinction between physical and chemical adsorption can usually be made from the temperature dependence of the adsorption process. In case of physical adsorption, the adsorption generally decreases with increasing temperature while in the case of chemisorption, it increases. However, it must be noted that the distinction between physical and chemical adsorption is an arbitrary one and in many cases an intermediate or combined character of adsorption is encountered. Under favorable conditions, both processes can occur simultaneously or alternately (Dabrowski, 2001). In some cases, like adsorption of gases on metal surfaces, physisorption may take place initially, followed by adsorbent-adsorbate reactions, resulting in chemisorption (Zangwill, 1988; Birdi, 2009).

1.5.2. Factors affecting Adsorption

There are several factors controlling adsorption which also influences the mechanism governing the adsorption process (Birdi, 2009; Parfitt and Rochester, 1983); and these are briefly discussed here:

1. *Nature of the surface*: The physical characteristics of the solid (surface area, porosity, etc.) determine the area available for adsorption while the chemical nature of the surface determines the reactivity of the surface toward a given solute. The heterogeneity and the presence of adsorbed impurities also affect the adsorption process.
2. *Chemical structure of the solute and its interactions with the solvent*: The structure (hydrocarbon chain length, branching, nature and location of polar functional groups) of the solute and its interactions with the solvent (solubility, complexation and micellization) show a marked effect on its adsorption.
3. *Nature of the solvent*: The solvent influences the adsorption by interacting with the surface and/or the solute thereby weakening the interaction between the solute and the surface. The chemical nature of the solvent and its polarity are important properties in question.
4. *Nature of interactions between the surface and the adsorbed solute*: The structure and orientation of the adsorbed layer depends upon the relative strength of the interaction between the surfactant and the surface and the surfactant association behavior in the bulk

solution. An example of such an interaction in aqueous system is the electrostatic interaction between the charged surface sites and the charged surfactant molecules.

5. *Temperature*: Temperature affects adsorption altering the properties of the solute, surface, solvent as well as their mutual interactions. Usually physical adsorption, which is weak, decreases with increase in temperature probably due to the increased solubility of the solute. The effect of temperature on chemisorption depends on the nature of the chemical reaction taking place at the surface. Chemisorption usually increases within a temperature range, and decreases above the range.

1.6. SOME COMMON ADSORBENTS

A number of materials have been extensively investigated as low-cost adsorbents in water pollutions control. Some of the important ones are detailed below:

1.6.1. Activated carbon

Activated carbon (AC) is the most popular and widely used adsorbent for the removal of pollutants from wastewater. AC is produced by a process consisting of raw material dehydration and carbonization followed by activation and it generally has a very porous structure with a large surface area ranging from 600 to 2000 m^2/g (Bhatnagar and Sillanpää, 2010). In particular, the effectiveness of adsorption on AC for the removal of a wide variety of pollutants from wastewaters has made it an ideal alternative to other expensive treatment options. The large capacity to adsorb pollutants is mainly due to their structural characteristics and their porous texture which gives them a large surface area, and their chemical nature which is easily modified by chemical treatment in order to increase their properties (Ahmaruzzaman, 2008). It is found to be a versatile adsorbent, which can remove diverse types of pollutants such as metal ions, anions, phenols, detergents, pesticides, humic substances, chlorinated hydrocarbons and many other chemicals (Bhatnagar and Sillanpää, 2010). Joseph et al. (2013) utilize powder activated carbon (PAC) which removes more than 90% of both BPA and EE2 and this outperforms the single-walled carbon nanotubes (SWCNTs) and multiwalled carbon nanotubes (MWCNTs). Commercial AC is extensively used for As(III) and As(V) adsorption from water (Mohan and Pittman Jr., 2007). AC adsorption was investigated in arsenic and antimony removal from copper electrorefining solutions (Navarro and Alguacil, 2002). A huge arsenic sorption capacity (2860 mg/g) is obtained on this coal-derived commercial carbon.

1.6.2. Zeolites

Zeolites are basically hydrated alumino-silicates having micro-porous structure that can accommodate a wide variety of cations without any change in structure. Their structures consist of a three dimensional frameworks, having a negatively charged lattice. The negative charge is balanced by cations which are exchangeable with certain cations in solutions. It has been received increasing attention for pollution control in wastewater treatment. At present, there are 191 unique zeolite frameworks identified, and over 40 naturally occurring zeolite frameworks are known (Chiban et al., 2012), but only seven (mordenite, clinoptilolite, chabazite, erionite, ferrierite, phillipsite, and analcime) occur with abundance and having adequate purity to be exploited (Navarro and Alguacil, 2002). The most abundant and frequently studied zeolite is clinoptilolite, a mineral of the heulandite group. However, most zeolites are made synthetically; some of them are made for commercial use while others synthesized to study their chemistry. The characteristics and applications of zeolites have been reviewed by Ghobarkar et al. (1999). High ion-exchange capacity and relatively high specific surface area, and more importantly their relatively cheap prices, makes zeolites attractive adsorbents. Another advantage of zeolites over resins is their ion selectivity generated by their rigid porous structures. Zeolites are becoming widely used as alternative materials in areas where adsorptive applications are required (Ahmaruzzaman, 2008). Both ion exchange and adsorption properties of zeolites are used for the selective separation of cations from aqueous solution. Zeolites received increasing attention for pollution control as standard components in wastewater treatment. The adsorption characteristic of phenol and 4-chlorophenol by surfactant-modified zeolite was investigated by Kuleyin (2007). Wang and Peng (2010) reviewed natural zeolites utilization in water and wastewater treatment. Xu et al. (2002) studied adsorption and removal of As(V) from drinking water by aluminium-loaded shirasu-zeolite and found its effectiveness over a wide range of pH (3 to 10). Common competing anions such as chloride, nitrate, sulfate etc. show insignificant effect on As(V) adsorption but phosphate greatly interfered the sorptive removal.

1.6.3. Activated alumina

The activated alumina (AA) comprises a series of non-equilibrium forms of partially hydroxylated alumina oxide, Al_2O_3. In general, as a hydrous alumina precursor is heated, hydroxyl groups are driven off leaving a porous solid structure of activated alumina. It is a porous, granular material having good sorption properties. AA grains are having a typical diameter of 0.3–0.6 mm and high surface area ranging from 200 to 300 m^2/g (Bhatnagar and Sillanpää, 2010). AA receives attention as an adsorbent and was first employed as adsorptive medium for the removal of arsenic from water supplies (USEPA, 2000b). The reported adsorption capacity of AA ranges from 0.003 to 0.112 g of arsenic per gram of AA. It is available in different mesh sizes and its particle size affects contaminant removal efficiency. Up to 23,400 bed volumes of wastewater can be treated before AA requires regeneration or disposal and replacement with new media. The adsorption of salicylic acid and polyacrylic acid on two aluminas with different porous volume and on a non-porous alumina was investigated by Thomas et al. (1995). In the study of Adsorption parameters (enthalpy of adsorption, free energy of adsorption) of several alkanes, cyclic hydrocarbons, aromatic hydrocarbons and chlorinated compounds on different adsorbents (alumina, zeolites and activated carbon), it was found that mesoporous alumina presents lower enthalpy of adsorption than the microporous materials (Díaz et al., 2004). The selectivity of AA towards As(III) is poor, owing to the overall neutral molecular charge at pH levels below 9.2. Therefore, pre-oxidation of As(III) to As(V) is critical. Previous studies show that an optimum pH range 5.5 – 6.0 showed more that 98% of arsenic removal (USEPA, 2003; Jain and Singh, 2012). Singh and Pant (2004) conducted the equilibrium studies which reveals that As(III) ions possess high affinity towards activated alumina at pH 7.6. Both Freundlich and Langmuir adsorption isotherms are well fitted to the experimental data. Thermodynamic parameters depict the exothermic nature of adsorption and the process is spontaneous and favorable. The results suggest that activated alumina is an effective alternative at least in the removal of As(III) from aqueous solutions.

1.6.4. Biosorbents and Biomasses

Biological materials, such as chitin, chitosan, yeasts, fungi or bacterial biomass are used as chelating and complexing adsorbents in order to concentrate and to remove the pollutants from water. Chitin, a long-chain polysaccharide, is the most widely occurring natural carbohydrate polymer next to cellulose. Chitosan, one of the common bioadsorbents, is produced from chitin, which is the structural element in the exoskeleton of crustaceans (shrimp, crab, shellfish etc.) (Chiban et al., 2012). The annual worldwide crustacean shells production is to be estimated 1.2×10^6 tonnes and the recovery of chitin and protein from this waste is an additional source of revenue (Teng et al., 2001). These bioadsorbents and their derivatives contain a variety of functional groups which can sequester the pollutants. The chitosan exhibited a high affinity to phenolic compounds. Various researches on chitosan in recent past indicated that chitosan is a good adsorbent for heavy metals as well. The evaluation of applicability of chitin and chitosan as adsorbent material to solid phase extraction of phenol and chlorophenols was studied by Rhee et al. (1998). Dambies et al. (2000) assessed the adsorption of As(V) onto molybdate-impregnated chitosan gel bead and reported that the sorption capacity was increased with the impregnation at an optimum pH 3. Powdered chitosan, obtained from shrimp shell, was converted into bead form (Chen and Chung, 2006) and used to remove arsenic from water in both batch and dynamic process.

The use of biomass for wastewater treatment is increasing because of its availability in large quantities and at low prices. Algae, fungi and bacteria are examples of biomass-derived sorbents for several metals. Recent literature on the methods of removal of phenol and their compounds from wastewater focuses on adsorption and microbial biodegradation process (Ahmaruzzaman, 2008). The potential use of the fungus *Phanerochaete chrysosporium* to remove phenols (phenol, *o*-chlorophenol, *p*-chlorophenol and 2,4,6-trichlorophenol) from aqueous solutions is evaluated by Denizli et al. (2004). Biosorption is capable of removing traces of heavy metals and other elements from dilute aqueous solutions. Brierley (1990) reviewed how bacteria, fungi and algae take up toxic metal ions. Rmalli et al. (2005) demonstrated that dried powdered roots of the water hyacinth rapidly reduces the arsenic concentrations (200 μg of arsenic/L) in water as within 60 min of contact the arsenic level reaches less than 10 ppb which is maximum permissible limit for drinking water recommended by the World Health Organization.

1.6.5. Agricultural and forest wastes

The use of agricultural waste materials is found economical and eco-friendly due to their unique chemical composition, availability in abundance, renewable nature and low cost. This implies a viable option of water and wastewater remediation. Agricultural materials, particularly those containing cellulose show potential sorption capacity for various pollutants. The basic components of agricultural waste materials include hemicellulose, lignin, lipids, proteins, simple sugars, water, hydrocarbons, and starch, containing variety of functional groups (Bhatnagar and Sillanpää, 2010). Sawdust is an abundant by-product of the wood industry that is either used as cooking fuel or as packing material. Sawdust is easily available in the countryside at zero or negligible price (Garg et al., 2004). It contains various organic compounds (lignin, cellulose and hemicellulose) with polyphenolic groups that are useful for binding phenolic compounds through different mechanisms. Another waste product from the timber industry is bark, a polyphenol-rich material, which is found to be effective in removing phenols from water solutions. Because of its low cost and high availability, bark is very attractive adsorbent (Ahmaruzzaman, 2008).

During last few decades, various agricultural wastes are explored as low-cost adsorbent. Some of them include the shells and/or stones of fruits like nuts, peanuts, olive wastes, almonds, apricots stones and cherries; and wastes resulting from the production of cereals such as rice, maize and corn as well as sugar cane bagasse and coir pith. The agricultural and forest waste materials are used in their natural form or with some physical or chemical modification (Bhatnagar and Sillanpää, 2010). Bras et al. (1999) tested the ability of pine bark to remove organochlorine pesticides from aqueous solutions. The results showed that approximately 97% of heptachlor, aldrin, endrin, dieldrin, DDT, DDD and DDE were removed from 1.0 to 10.0 μg/L solutions. Li et al. (2010a) studied the removal efficiency of polycyclic aromatic hydrocarbons (PAHs), namely, phenanthrene and pyrene on raw and modified pine bark. They proposed that pine bark is good adsorbent for the removal of PAHs and its efficiency is significantly enhanced by acid hydrolysis. Hardwood (Beech) sawdust with 13% moisture content was used as an adsorbent by Asfour et al. (1985) for the removal of basic dye Astrazone Blue FRR 69 from aqueous solutions. The results indicated that the capacity of hardwood for adsorption of basic dye was increased with increase in solution temperature, i.e., from 82.2 mg dye/g of wood at 25 °C to 105.7 mg dye/g of wood at 80 °C. Manganese immobilized activated carbon samples prepared from rice hulls and areca nut waste were used for arsenic removal from water (Lalhmunsiama et al., 2012). The simultaneous presence of background electrolytes concentration ($NaNO_3$) could not significantly affect the uptake of these two ions which inferred that the sorption of As(III) and As(V) by these solids predominantly occurred through strong chemical forces and may ultimately form 'inner-sphere' complexes. The kinetic data was best fitted to the pseudo-first order kinetic model. Untreated rice husk was utilized for aqueous arsenic remediation (Amin et al., 2006). Complete removal (using rice husk in columns) for both As(III) and As(V) was achieved under the following conditions: initial As concentration, 100 μg/L; rice husk amount, 6 g; average particle size, 780 and 510 μm; flow rate, 6.7 and 1.7 mL/min; and pH, 6.5 and 6.0, respectively.

1.6.6. Industrial and municipal wastes as low-cost adsorbents

A number of industrial wastes are investigated with or without treatment as adsorbents in the removal of pollutants from wastewaters. Because of their low cost and local availability, industrial solid wastes/by-products such as fly ash and red mud are used as adsorbents for the removal of pollutants. Fly ash is a waste material originating in great amounts in combustion processes. The high percentage of silica and alumina in fly ash makes it a good candidate for utilization as an inexpensive adsorbent for bulk use (Ahmaruzzaman, 2008). Fly ash possess a surface area of 15.6m^2/g. Its properties are extremely variable and depend strongly on its origin (Wang et al., 2005). Singh and Nayak (2004) investigated the potential of fly ash, for removing nitro-substituted phenols, i.e., *o*-nitrophenol, *m*-nitrophenol and *p*-nitrophenol. A special iron-abundant fly ash was used to develop a novel adsorbent for As(V) removal from wastewater through simple chemical processes (Li et al., 2009). The adsorption capacity for arsenic removal was found to be 19.46 mg/g. Another abundant industrial by-product/waste which was converted into low-cost potential adsorbent material is red mud. Red mud is a ferric hydroxide material, the by-product of smelting and refining of ores, mainly bauxite processing residue discarded in alumina production (Ahmaruzzaman, 2008). Red mud was used for the removal of phenol, 2-chlorophenol, 4-chlorophenol, and 2,4-dichlorophenol from wastewater (Gupta et al., 2004). Arsenic adsorption on red mud was pH dependent and an acidic solution having pH range 1.1 to 3.2 favored As(V) removal while alkaline aqueous medium (pH $\approx$ 9.5) was effective for As(III) removal (Altundogan et al., 2000). Heat and acid treated red mud was also reported having good adsorption capacity for arsenic (Altundogan et al., 2002).

1.7. REVIEW OF LITERATURE

The term clay refers to a naturally occurring material composed primarily of fine-grained aluminosilicate materials, which generally attain plasticity at appropriate water contents and turns harden when dried or fired. Clay contains phyllosilicates and it contains other materials that impart plasticity of materials (Gugenheim and Martin, 1995). The crystal structure of clay minerals, with a few exceptions, consists of sheets, firmly arranged in structural layers. The individual layers are composed of two, three or four sheets. These sheets are formed either by tetrahedra $[SiO_4]^{4-}$, abbreviated as tetrahedral 'T', or by octahedra $[AlO_3(OH)_3]^{6-}$, termed as octahedral 'O'. The interiors of tetrahedrons and octahedrons contain smaller metal cations, their apices being occupied by oxygen from which some are connected with protons (as OH). All these fundamental structural elements are arranged to form a hexagonal network with each sheet. According to the number and ratio of sheets in the fundamental structural units results the charge of the layers (Lee and Tiwari, 2012).

Broadly, the crystalline clay minerals are classified into seven groups: (i) The kaolinite and serpentine group, typical two-sheet phyllosilicates, where the T:O ratio is 1:1 and the charge of the two-sheet layer (unit cell) is 0 e/uc (electron charges per unit cell). (ii) The group of micas, three-sheet phyllosilicates, where the T:O ratio is 2:1 and the charge of the three-sheet layer (unit cell) is ≤ 2 e/uc. (iii) The vermiculite group, the expanding three-sheet phyllosilicates, where the T:O ratio is 2:1 and the charge of the three-sheet layer (unit cell) is 1.2 to 1.8 e/uc. (iv) The group of smectites, strongly expanding three-sheet phyllosilicates, where the T:O ratio is 2:l and the charge of the three-sheet layer (unit cell) is 0.5 to 1.2 e/uc. (v) The pyrophyllite and the talc group, non-swelling three-sheet phyllosilicates, where the T:O ratio is 2:1 and the charge of the three-sheet layer is 0 e/uc. (vi) The group of chlorites, four-sheet silicates, where the T:O:O ratio is 2:1:1 and the charge of the four-sheet layer is 1.1 to 3.3 e/uc. (vii) The palygorskite and sepiolite group having the layer-fibrous structure (Konta, 1995; Lee and Tiwari, 2012).

Bentonite is natural clay containing mainly the smectite and kaolinite groups. Smectite is fairly an expanding three-sheet phyllosilicates, where the T:O ratio is 2:l and the charge of the three-sheet layer (unit cell) is 0.5 to 1.2 e/uc (negative charge). Smectite groups refer to non-metallic clay composed of hydrated sodium aluminium silica with a formula of $(Ca,Na,H)(Al,Mg,Fe,Zn)_2(Si,Al)_4O_{10}(OH)_2 \cdot nH_2O$. In addition, the isomorphous substitution causes a net negative charge on the clay surface by the replacement of Mg^{2+} or Zn^{2+} for Al^{3+} in the octahedral layer, and Al^{3+} for Si^{4+} in the tetrahedral sheets (Zhu et al., 2000). Therefore, bentonite shows fairly high cation exchange capacity (CEC). The high specific surface area enables it to a useful material for adsorption/absorption of several ionic or polar compounds. On the other hand, kaolinite and serpentine group is having two-sheet phyllosilicates, where T:O ratio is 1:1 and the charge of the two-sheet layer (unit cell) is 0 e/uc. Kaolinite group clays are having the general formula of $Al_2Si_2O_5(OH)_4$. The octahedral site is occupied by Al^{3+} in the dioctahedral, whereas these sites are filled with Mg^{2+} and Fe^{2+} in trioctahedral minerals (Park et al., 2011b). Illite clays are interlayer-deficient dioctahedral minerals of the mica group. They are three-sheet phyllosilicates, where the T:O ratio is 2:1 and the charge of the three-sheet layer (unit cell) is ≤ 2 e/uc. Illite clays possess a structure very similar to that of muscovite, but are typically deficient in alkalis, with less Al substitution for Si. The general formula for illites is $K_yAl_4(Si_{8-y},Al_y)O_{20}(OH)_4$, usually with $1<y<1.5$, but in the case of possible charge imbalances, Ca and Mg are substituted for K. The K, Ca, and Mg interlayer cations prevent the inclusion of water into the clay structure (Alvarez-Puebla et al., 2005).

The ionic substitutions in the structure are controlled by the chemistry of the environment and the kinetics of reactions occurring during the formation and development of clay minerals. Isomorphous substitution within silicate layers is responsible for the presence of exchangeable cations within the interlamellar region (Konta, 1995). The negative charge of structural layers is naturally compensated by cations adsorbed within the interlayer space. The most common exchangeable cations occurring within the interlayer spaces are K^+, Na^+, Ca^{2+}, Mg^{2+} and H^+. Therefore, the electrical charge possessed by the clay minerals along with the porosity at micro level, surface functional groups as well the exchangeable cations present in the crystal structure makes it viable natural adsorbent for attenuation of several contaminants from aqueous solutions (Lee and Tiwari, 2012). The adsorption capabilities of clay result from their large surface area and exchange capacities. The negative charge on the structure of clay minerals enables clay to attract and hold cations such as heavy metals (Bailey et al., 1999).

Therefore, a number of studies are conducted using clays to show their effectiveness in removing several metal ions. The removal performance of montmorillonite and kaolinite for lead and cadmium was investigated by Srivastava et al. (1989). It was found that the adsorption capacity of Pb^{2+} and Cd^{2+} was significantly higher for montmorillonite than the kaolinite, and the sorption capacity increases with increasing pH. Further, the adsorption on montmorillonite follows the Langmuir adsorption model. The adsorption of lead on Thai kaolin and clay consisting mainly of kaolinite and illite was studied (Chantawong et al., 2001). It was reported that the maximum adsorption capacity of both materials was found to be 1.41 and 4.29 mg of Pb^{2+}/g, respectively. The adsorption was followed both Langmuir and Freundlich models of isotherm. It was also observed that the presence of co-ions such as Cd(II), Cr(VI), Cu(II), Ni(II), and Zn(II) was greatly reduced the lead uptake from aqueous solution. Jiang et al. (2010) showed that kaolinite clay was used to remove metal ions such as

Pb(II), Cd(II), Ni(II) and Cu(II) from aqueous solutions in both single and multi-metal ions. They observed that the interactions of metal ions with the solid surface were predominantly chemical in nature, the adsorption sites were non-uniform and nonspecific in nature. The adsorption of Cd^{2+} and Zn^{2+} from aqueous solution was investigated using natural bentonite (Pradas et al., 1994). It was reported that Cd^{2+} was adsorbed two times higher than Zn^{2+} due to the fact that Cd^{2+} possessed less polarizing effects on the surface charge of bentonite than zinc ions. Khan et al., (1995) reported that the sorption process of strontium on bentonite was endothermic in nature. Besides, bentonite clay was also applied for the removal of cesium (Oscarson et al., 1994) and in radioactive waste management studies (Pusch, 1992).

Although clay minerals are natural porous materials and showed effectiveness for removing several metal ions, however, the pristine clay minerals showed insignificant sorption capacity and selectivity towards several organic pollutants having non- or low-polarity and the anionic impurities such as As(V), As(III), Cr(VI) etc. (Tiwari and Lee, 2012). Clay minerals possess insignificant affinity for organics because hydration of the clay mineral surface tends to reduce accessibility of the interlayer spaces to aromatic molecules. Many studies reported that naturally occurring clays are ineffective for the adsorption of anionic contaminants, and hydrophobic or non-polar organic pollutants due to the hydrophilic nature of their surfaces and charges (Park et al, 2011b). Furthermore, the difficulty experienced in recovering clay particles from solutions after adsorption process makes them even less attractive as adsorbents for industrial water treatment. This ultimately makes regeneration of these colloidal particles quite difficult. Again these clay minerals do lose a substantial amount of their adsorption capacities when they are regenerated for reuse (Unuabonah and Taubert, 2014). Most of the clay materials showed less settling capacity hence, limiting its wider practical implication in several waste water treatment operations.

To increase the ability of clays to remove low- or non-polar organic and anionic water pollutants, it is necessary to modify the pristine clay minerals structures. The permanent negative charge in the crystal structures of clay minerals and the presence of exchangeable cations within the interlayer space makes them suitable for modification by a short chain and long chain organic cations. The modifications of clay minerals with suitable organic molecule by cation exchange enhances the properties of clay minerals from highly hydrophilic to increasingly hydrophobic and then makes it suitable for the attenuation of several non-polar or slightly polar organic or even anionic water pollutants (Alkaram et al., 2009). Similarly, the hybrid materials obtained by simultaneously pillaring with poly(hydroxo metal) cations and intercalation of suitable organic cations showed an enhanced applicability in waste water treatment since this could not only be effective in the removal of inorganic pollutants but also showed fair affinity towards the organic impurities as well. Furthermore, these hybrid materials show achievable settling capacity makes easy for solid/aqueous separation (Lee and Tiwari, 2012).

A number of studies were conducted relating the effect of organic cation and the properties of clay minerals on the specific properties of the resultant organo-modified clay. Generally, for swelling clay minerals the basal spacing of organoclay increases with the alkyl chain length and the concentration of the organic cation. It was reported that longer the surfactant chain length and having higher the charge density of the clay, ultimately caused further apart interlayer space of clay structure (Baron et al., 1999). The modification of the swelling clay with a cationic surfactant not only results in an increase interlayer spacings but also exposure of the new sorption sites of clay (Park et al., 2012). Wang et al. (2001) prepared organo-clays with different alkylammonium chain lengths. Three-dimensional framework of clay retains the high molecular weight surfactants primarily on the outer surface, whereby at sufficient loading of surfactant/or organic molecules forms a bilayer. This bilayer formation results in a reversal of the charge on the external surface of the clay, providing sites where anions can possibly be retained and cations repelled, while neutral species can partition into the hydrophobic core introduced. These modified minerals provide primarily a hydrophobic environment towards the retention of organic molecules having less or no polarity (Li and Bowman, 1997; Alkaram et al., 2009).

However, the interlayer distance also depends upon the way the onium ion chains organizes themselves in the organoclay. In order to describe the structure of the interlayer in organo-clays, one has to know the negative charge originates in the silicate layer, the cationic head group of the alkylammonium molecule preferentially residues at the layer surface, leaving the organic tail radiating away from the surface (Alexandre and Dubois, 2000). The alkyl chain length and the charge density of the clay layer are responsible for the arrangement of intercalated organic cations in the organoclays. In the classical model, organic cations only form monolayers in the adsorptive clays intercalated with short-chain alkyl ammonium ions. When the grafting density is low, the long chain surfactant molecules usually lie flat with the molecular axis of their methylene chain parallel to the sheet of the clay. In contrast, bilayers, pseudo-trimolecular arrangement or paraffin complexes could be found in the organophilic clays intercalated with increasing grafting density or with long chain surfactant cations. As highly charged clay minerals intercalated with alkylammonium ions, more paraffin-type structures was found (Lagaly, 1986; Alexandre and Dubois, 2000). In some cases, the alkyl chains form paraffin-type structures rather than pseudo-trimolecular layers since the paraffin-type aggregation allows better fit of the ammonium groups to the surface oxygen atoms than it is the case for close-packed chains in pseudo-trimolecular layers (Lagaly, 1986; de Paiva et al., 2008).

Quaternary ammonium organo-clays are divided into two groups depending on the structure of the organic cation and the mechanism of sorption. The first group called adsorptive clays are synthesised with quaternary ammonium cations (QACs) containing short-chain alkyl groups and/or a benzyl group, such as benzyltriethylammonium (BTEA) or tetramethylammonium (TMA)/trimethylphenylammonium (TMPA). Sorption on this type of organoclay is characterized by Langmuir-type isotherms, which are commonly associated with specific sorption sites. On the other hand, if the QACs contain a long-chain alkyl group, such as hexadecyltrimethylammonium (HDTMA) and didodecyldimethylammonium (DDDMA) clays, the group of organo-clays is called organophilic clay. The sorption of this group is characterized by linear isotherms over a wide range of solute concentrations. The different sorptive behavior of the two organo-clays (adsorptive clays and organophilic clays) is further described for its possible environmental applications. The modified clay derived from long-chain alkylammonium ions creates an organic partition medium through the conglomeration of the flexible alkyl chains, whereas the clay from small quaternary ammonium ions could not form partition phases. Instead surface adsorption sites for non-ionic solute uptake exists as discrete entities on the clay layers because of the small alkyl-chain ions (Groisman et al., 2004; Park et al., 2011b).

The alteration of clay properties by adsorbed organic materials was, in fact, known from the earliest use of clay by man about 7000 BC. The Greek profited by the interaction of clays with vegetable tannins probably to obtain distinct clay fractions for red-black decors. The likely used of urea for preparation of very thin walled-porcelain during the Sung period in China is a further striking example of the practical application of clay-organic interactions (Lagaly, 1984). Although, the practical application in the environmental studies was first discussed by McBride et al. (1975), however, several reports indicated that the organo-clay was obtained date back in 1920's with intercalation of the organic molecules into interlayer space of clay minerals, soon after the introduction of X-ray diffraction in 1913 (de Paiva et al., 2008). One of the earliest paper appeared, by Smith (1934) reported to the saturation of bentonite clay with nicotine. Gieseking (1939) found methylene blue to be very effective in replacing interlayer cations. These results suggested the possibility of using ammonium ions of the NH_3R^+, $NH_2R_2^+$, NHR_3^+, and NR_4^+ types to throw more light on the mechanism of cation exchange with clay minerals. The montmorillonite, beidellite and nontronite types of clay minerals were treated with solutions of the hydrochlorides or hydro iodides of various amines. Clay minerals can adsorb the organic ions, giving rise to a basal spacing greater than those of the same clay minerals saturated with smaller cations such as calcium or hydrogen. Similarly, MacEwan (1944) was seeking means to identify montmorillonite with ease and discovered that treatment with glycerol resulted in its intercalation into the interlayer region of montmorillonite. Jordan (1949) investigated some of the factors involved with the swelling of organoclays and the extent of the conversion of the clay from hydrophilic to hydrophobic nature. Organophilic bentonites were prepared by the interaction of bentonite with various aliphatic ammonium salts. The swelling of the organoclays was studied in several organic liquids and liquid mixtures. Jordan concluded that the degree of solvation depends on at least three factors: 1) the extent of the surface coating of the clay particles by organic matter; 2) the degree of saturation of the exchange capacity of the clay mineral by organic cations; and 3) the nature of the organic liquid.

The hydrophobic organoclays with high uptake capacity of organics was actually employed to remove aromatic wastes from water and the effectiveness of organo-clays for the remediation of organic contaminants was found seven times more powerful than the activated carbon (Alther, 2002). Sheng et al. (1996) showed that aqueous phase of NOCs such as benzene, nitrobenzene, chlorobenzene, trichloroethylene, and carbon tetrachloride were significantly removed using layer silicate clays modified with HDTMA. In the comparison of long and short-chain organoclays, the long-alkyl chain organoclay was more effective adsorbent for NOCs than the short alkyl chain organoclay (Groisman et al., 2004). It was also reported previously that the adsorption of NOCs to organophilic clays derived from long-alkyl chains such as HDTMA or benzyldimethyltetradecylammonium chloride (BDTDA) was studied. Moreover, the materials were studied for relatively low solute uptake, isotherm linearity, partition behavior, correspondence between organic carbon normalized sorption coefficients (K_{oc}) and the octanol water partition coefficients (K_{ow}), and inverse dependence on water solubility. In contrast, sorption of NOCs to adsorptive clays modified from short alkyl chains such as TMA or TMPA was characterized by relatively strong solute uptake, isotherm nonlinearity, shape selectivity, surface adsorption behavior, and progressively lower uptake of larger aromatic molecules (Dentel et al., 1998; Park et al., 2011b).

Modifications of clay are conducted in view of its possible applications in the diverse area of research. The modifications of clay are carried out with the exchange reactions using numerous QACs of the general form $[(CH_3)_3NR]^+$ or $[(CH_3)_2NRR']^+$, where R is a large alkyl hydrocarbon which exchanges the inorganic cations, *viz*., Na^+ or Ca^{2+} present within the interlayer of clay, resulting the organo-clay having significantly high organophilic character (Boyd et al., 1988). Several studies were conducted for the removal of phenol or phenolic impurities from aqueous solutions using organo-clay materials. The locally available clay basaltic clay and bentonite were modified with HDTMA and TMPA for the phenol removal (Richards and Bouazza, 2007). The structural studies suggested that bentonite possessed same surface area as of incoming organic cation, i.e., HDTMA hence; they assumed the cations were arranged in single or double layers. However, the basaltic clay possessed with significantly less surface area than HDTMA hence, the arrangement was likely to be semi tri-layer type (i.e., the head of the cation chain lay flat and the tails of adjacent sheets interlocked) or paraffin style (i.e., cation chains arranged diagonally within layers) (Jordan, 1949). It was further demonstrated that a paraffin arrangement of long chain cations produced more effective partitioning phase than other arrangements (Jaynes and Boyd, 1990).

The sorption of phenol, p-nitrophenol and aniline to the synthesized dual-cation and anion-cation organo-bentonite was studied and demonstrated that at lower sorptive concentrations the sorption was a dominant mechanism whereas at higher sorptive concentrations partitioning of contaminant was dominated (Zhu et al., 2000). Mortland et al. (1986) studied the sorption of phenol, 3-chlorophenol, 3,5-dichlorophenol, 3,4,5-trichlorophenol and 2,4,6-trichlorophenol using the HDTMA and TMPA modified montmorillonite. The sorption capacity of phenols and its chlorinated congeners was improved when the modified montmorillonite with HDTMA or TMPA were applied. It was noted that the adsorption of phenols and chlorinated phenols was independent of the water solubility of the solute. Surfactant-modified bentonite was synthesized by replacing the adsorbed Na^+ with long-chain alkyl quaternary ammonium cation HDTMA (Rawajfih and Nsour, 2006). The sorption capacity of phenols was increased with chlorine addition (phenol < p-chlorophenol < 2,4-dichlorophenol). The adsorptive behavior was affected by the properties of phenols.

The attapulgite, a commercial product was modified with sonication as well by stirring method using organic compound, i.e., octadecyltrimethylammonium chloride (ODTMA) (Huang et al., 2007). Further, the organo-modified clay was utilized in the removal of phenol and it was showed that the uptake of phenol followed second order rate law and Freundlich adsorption isotherm suited well for the equilibrium concentration dependence studies. The affinity of organo-clays modified with quaternary ammonium salts much depend on the modifier polarity of incoming organo cations. p-nitrophenol, phenol and aniline were removed using the commercial organo-clays, *viz.,* Cloisite-10A, Cloisite-15A, Cloisite-30B and Cloisite-93A which were organically modified (Ko et al., 2007). The sorption of these pollutants caused for further penetration of d(001)-spacing as indicated by the XRD results. Moreover, it was suggested that the suspension pH could hardly affect the removal. In a line, HDTMA and phenyltrimethylammonium bromide (PTMA) modified bentonite and kaolinite (both commercial product) were assessed for the removal of phenol from aqueous solutions (Alkaram et al., 2009). Significantly higher uptake of phenol occurred for these two organo-clays and endothermic type of sorption process followed the pseudo-second-order rate law.

Sericite was modified with HDTMA and alkyldimethylbenzylammonium chloride (AMBA), which was then employed in the removal of phenol, from aqueous solutions (Tiwari et al., 2015). Batch reactor data showed that an increase in sorbate concentration favored the uptake whereas an increase in pH caused for a significant decrease in percent uptake of phenol. Equilibrium state concentration dependence data were well modelled with the Freundlich adsorption isotherm. Cetyltrimethylammonium bromide (CTAB) exchanged montmorillonite was employed in the removal of benzoic acid from aqueous solutions (Yan et al., 2007b). Sorption results were optimized and showed that the uptake was followed pseudo-second-order rate equation and proceeded with the partitioning mechanism. In a line, other report demonstrated the organically modified bentonites for the removal of benzoic acid and hydroquinone from aqueous solutions (Yildiz et al., 2005). Toluene retention using TMA-montmorillonite from aqueous solution was discussed and suggested that an interlayer sorption takes place, which was also correlated with the IR data (Vidal and Volzone, 2009). The uptake of toluene was increased for organo-modified montmorillonite to *ca.* 110 times comparing to the pristine montmorillonite sample.

The work was reported on the sorption and co-sorption of 1,2,4-trichlorobenzene and tannic acid using several organo-clays (Dentel et al., 1998). The presence of hydrophilic tannic acid was almost unaffected with the 1,2,4-trichlorobenzne sorption onto the organo-clays, which showed that no site competition existed between these two pollutants. Moreover, the competitive sorption of polycyclic aromatic hydrocarbons (PAH) was investigated on to the organo-zeolites obtained with exchange process using stearyl dimethylbenzylammonium chloride (SDBAC) (Lemic et al., 2007). However, the studies conducted by Groisman et al. (2004) showed that compounds with low to intermediate hydrophobicity (log K_{OW} 2.5 to 3.8) were more strongly sorbed on to the short-chain organo-clays, whereas the more hydrophobic compounds (log K_{OW} 5.2 to 6.1) were better sorbed by the long-chain organo-clays. Previously, Nzengung et al. (1996) showed the organic co-solvent effects on to the sorption equilibrium of hydrophobic organic chemicals using HDTMA, TMPA and BDTDA modified montmorillonite.

Further, simultaneous sorption of phosphate and phenanthrene was assessed using the inorgano-organo-bentonite (i.e., Fe-pillared-CTMAB-modified-bentonite) from aqueous solutions (Ma and Zhu, 2006). More than 95% phosphate and 99% phenanthrene were removed simultaneously and the uptake of these pollutants followed Langmuir adsorption isotherm with pseudo-second order rate kinetics. These results suggested that distinct sorption sites were available for the two different pollutants. Similarly, the competitive sorption of lead and phenol was studied in an attempt to utilize these organo-clays at the studied field conditions (Yan et al., 2007a). The presence of Pb(II) suppressed phenol sorption onto the Na^+ or Ca^{2+}-montmorillonite whereas; phenol showed little effect on the Pb(II) sorption. However, the HDTMA-montmorillonite could hardly show the competitive sorption among these two. They assumed that these two pollutants were likely to be sorbed with different domains of the solids. Lead was sorbed with the coordination bonds of montmorillonite whereas phenol was supposed to be attached with the van der Waals forces operating in between the sorbent and sorbate ions.

It was observed that the organo or inorgano-organo-clays with hydrophobic in nature and possessed with organophilic character have a greater tendency to sorb the non-ionic organic compounds, however, several studies showed that they equally possessed significant sorption capacity towards the ionizable organic impurities as well. 3,6-dichloro-2-methoxy benzoic acid (dicamba; weakly-acidic pesticides) was removed by the HDTMA and DODMA exchanged smectites (Zhao et al., 1996). The different sorption capacities obtained for dicamba using these organo-modified clays was correlated with the basal spacing expansion and the arrangement of alkylammonium ions within interspace of clays as well the organic carbon content. Hsu et al. (2000) reported the removal of weakly acidic pesticide 2,4-dichlorophenoxy propionic acid from the aqueous solutions using HDTMA modified clay. The principal mechanism proposed was the partitioning which was in accordance to the previous report suggested for the removal of organic pollutants with organo-clay materials (Boyd et al., 1988). Similar partitioning mechanism was suggested for the removal of 1,2,4-trichlorobenzene (1,2,4-TCB) by organo-clays (Dentel et al., 1998). Lee et al. (1989) indicated adsorptive mechanism for the similar uptake, although obtained a linear isotherm for the sorption of 1,2,3-TCB onto TMA-modified smectite.

In the studies of Hermosin et al. (2001) and Carrizosa et al. (2003), organo-clays as possible carriers in controlled-release formulations of bentazone and dicamba as an example of mobile and persistent acidic herbicides reduces the total leaching losses from 55% to 90%, and reduced fenuron up to 78%. Their finding suggests the potential use of organoclays as barriers for immobilising pesticides and herbicides derived from point sources. Groisman et al. (2004) investigated the efficiency of organo-clays with different sizes of alkyl chains in removing organic pollutants from the pesticide mixtures. The sorption by a long-chain ODTMA-organoclay was less affected by competition with accompanying compounds and background materials, while a short-chain TMA-organoclay was very sensitive for competitive sorption. Additionally, the different clay materials, viz., montmorillonite, illite, muscovite, sepiolite and palygorskite modified with ODTMA were used for the removal of penconazole, linuron, alachlor, atrazine and metalaxyl (Sanchez-Martin et al., 2006). It was concluded that the uptake of these pesticides depended largely on the ODTMA saturation. However, the ODTMA sorption capacity on to the clay depends mainly on the charge density of the clay minerals. In a line, the same research group studied the long-chain organic cation structure in the sorption of penconazole and metalaxyl fungicides using the dihexadecyldimethyl ammonium (DHDDMA) bromide modified clays (Rodríguez-Cruz et al., 2008). They obtained that DHDDMA modified clays increased the sorption of fungicides by clay depended to the type of clay (higher for layered clays than for non-layered clays), and on the fungicide hydrophobicity (higher for penconazole with K_{OW} = 3.72 than for metalaxyl with K_{OW} = 1.75).

The efficiency of ODTMA-organoclays was measured in the immobilization of organic pesticides in a sandy soil (Rodríguez-Cruz et al., 2007). The result indicated that almost complete immobilization of linuron, the most hydrophobic pesticide, was obtained Adsorption behaviour of the herbicide prometrone by diverse organoclays was observed by Socías–Viciana et al. (1998). Two different natural smectites (high charge SAz and low charge SWy) and those treated with two akylammonium cations (octadecylammonium and HDTMA) were assessed. The organo-clay characteristics favouring the prometrone sorption were the high charge density, quaternary alkylammonium in the interlayer and organic cation saturation slightly below CEC. However, for low charge smectite, primary alkylammonium and organic cation saturation above CEC promoted herbicide adsorption. Similar adsorption behavior was reported by Carrizosa et al., (2001) who investigated the influence of adsorption-desorption of DICAMBA, selected as a model of very mobile and leachable herbicides, on two smectites modified with different amounts of alkylammonium cations such as octadecyl-(C18), hexadecyltrimethyl (HDT)-, and dioctadecyldimethyl (DOD)-ammonium of 50% or 100% of the clays' CEC. They further reported that the desorption isotherms were reversible except in organoclays with C18 and DOD cations as a result of the stronger polar contribution in the primary alkylammonium and the difficulty for diffusion in the bulky organo-clays.

Vesicle-clay complexes in which positively charged vesicles composed of DDDMA were adsorbed on to montmorillonite removed efficiently anionic (sulfentrazone, imazaquin) and neutral (alachlor, atrazine) pollutants from water bodies (Undabeytia et al., 2008). A synergistic effect on the adsorption of atrazine was observed when all pollutants were present simultaneously and the column results indicated higher removal capacity achieved comparing to the activated carbon. Efficiency of benzyldimethylhexadecylammonium (BDMHDA) modified montmorillonite for the removal of two antibiotics groups: tetracyclines (tetracycline, oxytetracycline and chlortetracycline) and sulfonamides (sulfamethoxazole, sulfisoxazole and sulfamethizole) from water were demonstrated by Polubesova et al. (2006). It was concluded that the system was very efficient for the removal of both tetracyline and sulphonamide antibiotics from water and even in the presence of dissolved organic matter. The efficiency of antibiotic removal from water was reported to be significantly higher than the usual activated carbon. Three organo-montmorillonites were prepared using three surfactants, viz., cetyltrimethylammonium bromide (CTMAB), 3-(N,N-dimethylhexadecylammonio)-propane sulfonate (HDAPS) and 1,3-bis(hexadecyldimethylammonio)-propane dibromide (BHDAP) and their adsorption behaviors toward sulfamethoxazole (SMX) were investigated (Lu et al., 2014). The adsorption mechanism was reported to be dominated by electrostatic interaction, while hydrophobic interaction played a secondary role. Rahardjo et al. (2011) obtained CTAB-bentonite by microwave heating and the adsorption of ampicillin was investigated. Based on the evaluation of the physical meaning of fitted isotherm parameters of different models, it was reported that Toth equation represented the equilibrium data better than other temperature dependent form of Langmuir, Freundlich and Sips models.

Liu et al. (2012) compared tetracycline (TC) adsorption capacity of Na-montmorillonite (Na-mont) with six organo-montmorillonites (organo-monts) obtained with three quaternary ammonium cations (QACs) having different alkyl-chain lengths. It was reported that the processes of TC adsorption on to the tested samples could be well fitted by the pseudo-second-order equation. Both the Langmuir and Freundlich models fitted the adsorption isotherms. The TC adsorption to the organo-montmorillonite was increased significantly with decreasing the pH below 5.5 because of the electrostatic interaction, and a high QACs loading showed better than a low loading at around pH 3. An aluminium-pillared bentonite clay (Al-NaBt) and inorganic–organic clays (IOCs) obtained by surfactant modification of Al-NaBt with 1-hexadecylpyridinium bromide was used in the removal of salicylic acid, clofibric acid, carbamazepine, and caffeine (Cabrera-Lafaurie et al., 2012). The IOCs are modified with Co^{2+}, Cu^{2+}, or Ni^{2+} to induce complexation-like adsorbate–adsorbent interactions at ambient conditions. The studies show that, in general, the Ni^{2+}IOCs exhibited the greatest interaction with salicylic and clofibric acids, while the Co^{2+}adsorbents are found fairly high sorption capacities for caffeine at lower sorptive concentrations. All the metal-modified IOCs showed comparable adsorption capacities in the case of carbamazepine, probably due to the lack of availability of particular functional groups with this adsorbate.

The same group used fixed-beds of transition metal (Co^{2+}, Ni^{2+} or Cu^{2+})-IOCs to study single- and multi-component non-equilibrium adsorption of a set of PPCPs (Pharmaceuticals and personal care products) from water (Cabrera-Lafaurie et al., 2015). Adsorption capacities for single components revealed that copper(II)-IOC possess better affinity toward salicylic and clofibric acid. However, multi-component adsorption tests showed a considerable decrease in adsorption capacity for acids and an unusual selectivity toward carbamazepine depending on the transition metal. It was attributed to a combination of competition between PPCPs for adsorption sites, adsorbate–adsorbate interactions, and plausible pore blocking caused by carbamazepine. The cobalt(II)-IOC bed that was partially calcined to fractionate the surfactant moiety showcased the best selectivity toward caffeine, even during multi-component adsorption which was due to a combination of a mildly hydrophobic surface and interaction between the PPCP and cobalt(II). In the study of Chen et al. (2014), an organo-bentonite modified with CTMAB was utilized as sorbent for the removal of nitrosodiphenylamine (NDPhA) and its precursor diphenylamine (DPhA) from aqueous solution. The sorption kinetics of both NDPhA and DPhA was best described by the pseudo-second-order model. The sorption isotherm for NDPhA was nearly linear, indicating that partition process was dominant in the sorption of NDPhA. However, the nonlinear sorption isotherm of DPhA was best represented by the Slips model because both partition and electrostatic interaction were involved in the sorption of DPhA. Two organoclays were synthesized by modifying Na-exchanged montmorillonite (Mt) with benzyldecyltrimethylammonium (BDTA) cationic surfactant and the tri-ethyleneglycol mono-n-decylether($C_{10}E_3$), a non-conventional nonionic surfactant and used for the sorption efficient of three micro-pollutants namely, benzene, dimethyl-phthalate and paraquat (Guégan et al., 2015).

In another study, Polyethersulfone (PES)–organophilic montmorillonite (OMMT) hybrid particles, with various proportions of OMMT, were successfully used for the removal of bisphenol A (BPA) from aqueous solution (Cao et al., 2009). Pseudo-second order kinetic model and Langmuir isotherm provided the best fit for the adsorption of BPA onto the PES–OMMT. Furthermore, adsorbed BPA could be effectively leached by ethanol, which indicated that the hybrid materials could be reused. Ca-montmorillonite modified with two surfactants, dodecyltrimethylammonium bromide (DDTMA) and HDTMA was demonstrated in the effective removal of BPA from aqueous solutions (Zheng et al., 2013). The hydrophobic phase and positively charged surface created by the loaded surfactant molecules was responsible for the attenuation of BPA. The adsorption of BPA onto organo-clays was well described by pseudo-second order kinetic model and the Langmuir isotherm. In addition, the adsorption process was spontaneous and exothermic based on the adsorption thermodynamic study. The organo-clays intercalated with longer chain surfactant molecules possessed greater adsorption capacity for BPA even under alkaline conditions. Similar observation was reported by Park et al. (2014) on the remediation of bisphenol A (BPA) from aqueous solutions using organoclays synthesized from montmorillonite (MMT) with different types of organic surfactant molecules, *viz*., DDTMA, HDTMA and DDDMA. Cai et al. (2013) reported the successful removal of natural hormones- testosterone (Te) and 17*β*-estradiol (E2) from the constructed wetland system (CWS) treated dairy farm wastewater with organoclay sorbent.

The pillaring of clay materials with the inorganic metals, *viz.,* Al, Fe, Cr, Ti etc. showed good settling capacity however, showed very little affinity towards the organics in the aqueous solutions. However, the partial/or complete modification of these intercalated clays with organic cationic surfactants possessed fairly a good sorption capacity for the organic pollutants as well (Bouras et al., 2001). Srinivasan and Fogler, (1990) applied the inorgano-organo clays in the removal of benzo(α)pyrene and chlorophenols from industrial wastewaters. Montmorillonite was pillared with the help of inorganic ion aluminium (Al_2O_3) and hence, the surface of the motmorillonite (Mt) as well the pillared montmorillonite (PMt) was modified using hexadecyl pyridine (HDPY-Br). Results indicated that both these modified solids enhanced greatly the uptake of phenols. Pillaring of montmorillonite was carried out with Al(III), Fe(III) and Ti(IV), and followed by co-adsorption of CTAB (Bouras et al., 2007). These materials were then used for the removal of diuron (3-(3,4-dichlorophenyl)-1,1-dimethylurea and its degradation products viz., 3-(3,4-dichlorophenyl)-1-methylurea; 1-(3,4-dicholorophenyl)urea; and 2,4-dichloroaniline. The removal efficiency of these solids was in the order of CTA-Ti_xH_y-montm > CTA-$Fe_x(OH)_y$-montm > CTA-$Al_x(OH)_y$-montm towards these pesticides. The mechanism of these pesticides sorption onto the organo–inorgano-clays was suggested as van der Waals attraction between the pesticides and the alkyl chains of the CTA cations.

Important features of these inorgano-organo-clays were reported to be that they possessed two different sorption sites capable of removing different types of pollutants, i.e., organic and inorganic pollutants from the aqueous solutions simultaneously apparently, with an enhanced sorption capacity (Ma and Zhu, 2006; Yan et al., 2007a). Ma and Zhu (2006) investigated the feasibility of utilizing inorgano-organo-bentonite (IOB). Bentonite mineral was modified with both Fe polycations and CTMAB. The IOB was explored successfully in simultaneously removal of phosphate and phenanthrene from aqueous solutions. They also indicated that the solid separation of IOB from aquatic phase was greatly improved compared to organobentonite and pristine bentonite. Similarly, a series of IOBs was synthesized by intercalating bentonite with both CTMAB and hydroxy-aluminium at varied ratios (Zhu and Zhu, 2007). Sorption experiments with phenol, *p*-chlorophenol, 2,4-dichlorophenol, 2-naphthol, nitrobenzene, *p*-nitrotoluene or naphthalene together with phosphate was demonstrated that IOBs could simultaneously remove organic compounds and phosphate from waters. Partitioning and ligand exchange mechanism was suggested for the organic and phosphate pollutants, respectively. CTMAB and hydroxy-aluminium (Al_{13}) were used to intercalate with bentonite simultaneously or sequentially to prepare series of inorganic–organic bentonites (IOBs) and their sorptive characteristics towards naphthalene and phosphate were investigated (Zhu et al., 2009b). The resulting IOBs were as effective as the CTMAB modified bentonites in the attenuation of naphthalene from aqueous solutions, and they were shown to be more effective in the sorption of phosphate from waters than the Al_{13} pillared bentonite.

The greater advantages of the organo-clays are towards the removal of several anionic contaminants particularly the inorganic oxyanions. The intercalation of cationic surfactants not only changes the surface properties from hydrophilic to hydrophobic but also greatly increases the anions adsorption capacity especially when surfactant loading exceeds the CEC of clay. The formation of surfactant bilayer resulted to charge reversal of the clay surface and the positive charge will eventually attract the anions (Li and Bowman, 1997; 2001). Based on these unique properties, studies intended towards its possible applications in the remediation of waters contaminated with several inorganic pollutants including the inorganic oxyanions. The immobilization of hydrophilic anionic contaminant like nitrate was studied using the HDTMA modified clays (bentonite, kaolinite and halloysite) (Xi et al*.,* 2009). The HDTMA modified bentonite showed very high removal capacity for nitrate of 12.83 mg/g. Montmorillonite-modified with cetylpyridinium bromide showed significant efficiency towards the Cr(VI) removal which was slightly decreased with the increase in pH from 3.0 to 6.0 (Brum et al., 2010). The equilibrium concentration dependence modeling suggested the applicability of Langmuir adsorption isotherm. The work of Li and Bowman (2001) intended to assess the applicability of natural kaolinite modified with HDTMA for the sorption of several inorganic oxyanions, *viz*., nitrate, arsenate and chromate. Sorption of each oxyanion was well-described by the Langmuir isotherm. Sorption of oxyanions on organo-kaolinite was at least two orders of magnitude greater than their sorption on unmodified kaolinite. They also mentioned that properly prepared organoclays could remove oxyanions, as well as nonpolar organics, from contaminated waters.

The influence of removal capacity of chromate on rectorite modified by stearyl trimethylammonium chloride (STAC) and ODTMA was investigated previously (Hong et al., 2008). The adsorption of Cr(VI) was tested as a function of pH, temperature, and initial chromate to rectorite ratio at batch scale operations. It was concluded that the Cr(VI) adsorption by STAC-modified rectorite was strongly dependent to pH as STAC-rectorite adsorbs chromate effectively in acidic solutions. The adsorption of Cr(VI) was maximum at pH 4 and the change in enthalpy of the adsorption was −9.4 kJ/mol, indicated retention of Cr(VI) on STAC-rectorite was proceeded with weak physical forces. They assumed that the uptake of negatively charged Cr(VI) ions within the interlayer regions of STAC-modified rectorite was due to electrostatic forces derived from the polarized water molecules and positively charged groups of the STAC cations. Similar result was found by Krishna et al. (2000) and they revealed that pH was highly responsible for the adsorption capacity of organo-clays modified with HDTMA. It was found that the amount of adsorbed chromate decreased with increasing pH and become negligible at and above pH 8. The specific rate constant of Cr(VI) species on modified montmorillonite was rapid and equilibrium was attained within 30 min and the process followed with first order rate kinetics.

In a line, chromate and molybdate was removed from aqueous solutions with the help of cetylpyridinium-bentonite under the batch and column studies and it was suggested that the uptake of these ions proceeded via ‘ion exchange’ mechanism (Atia, 2008). Previously, novel aluminium-pillared surfactant-modified-sericite using organic cations HDTMA and AMBA were found useful in the removal of As(III) and As(V) (Tiwari and Lee, 2012). It was further observed that increase in sorptive concentration enhanced the uptake of these pollutants and the 1000 times increase in ionic strength, i.e., background electrolyte concentration ($NaNO_3$) caused an insignificant decrease in As(V) removal, which inferred that As(V) was adsorbed specifically onto the solid surface. However, it was affected greatly with As(III) pointed that As(III) was sorbed mainly through electrostatic or even with weak van der Waals attractive forces. pH dependence data showed that arsenic removal was greatly affected by the change in solution pH. The simultaneous presence of phenol in the removal of As(III) or As(V) showed insignificant change in arsenic removal by these materials which pointed that different sorption sites were available for these two different contaminants. Octadecylbenzyldimethylammonium surfactant modified-bentonites prepared by varied dose of cationic surfactants were employed in the significant removal of As(V) and As(III) from aqueous solutions (Su et al., 2011). The adsorption kinetics was fitted well to the pseudo-second-order rate model. They also reported that adsorption of As(V) and As(III) was strongly dependent to solution pH and addition of anions could not affect As(III) adsorption, while they clearly suppressed the adsorption of As(V).

1.8. SCOPE OF THE PRESENT INVESTIGATION

Environmental pollution with arsenic and Endocrine Disrupting Chemicals (EDCs) has become a global concern. Therefore, removal of these pollutants from contaminated waters is one of the greatest concerns in order to protect the aquatic environment and terrestrial life. Certainly, the existing water and wastewater treatment plants are designed for the best in treatment and removal of contaminants, especially those which are specified in the existing regulations. However, the occurrence of new emerging micro-contaminants such as EDCs which possess a wide range of chemical properties, success in their removal varies greatly upon their particular properties and thus requires effective treatment process. In light of more popular appreciation of environmental issues, pressures have arisen to address and minimize production of contaminants and to remove contaminants present in natural systems. A number of technologies are available with varying degree of success to control these pollutions. However, most of them require substantial financial input and their use is restricted because of cost factors overriding the importance of pollution control. Among various available water treatment technologies, adsorption process is considered better because of convenience, ease of operation and simplicity of design.

A number of materials are extensively investigated as adsorbents in water pollution control. Among these, clays and their modified forms is received widespread attention for their use as adsorbents of organic pollutants like EDCs and arsenic oxyanions in environmental clean-up in particular the remediation of aquatic environment. The electrical charge possessed by the clay minerals along with the porosity at micro level, surface functional groups as well the exchangeable cations present within the crystal structure makes it a viable natural adsorbent for several pollutants in the treatment of contaminated waters. However, materials are shown insignificant sorption capacity and selectivity towards several organic pollutants along with the anionic impurities. But modifications of clay minerals with appropriate organic molecule or even with inorgano-organo molecules enable it suitable for the attenuation of several organic/inorganic impurities.

Therefore, in order to enhance the applicability and selectivity of clay minerals are to be modified or functionalized using a suitable organic or inorganic-organic molecule/cation. The permanent negative charge within the crystal structures of clay materials and presence of exchangeable cations makes them suitable for surface modification using the organic cationic surfactants. Three-dimensional framework of clay retains the high molecular weight surfactants primarily on the outer surface, whereby at sufficient loading of surfactant/or organic molecules forms a bilayer. This bilayer formation results in a reversal of the charge on the external surface of the clay, providing sites where anions can possibly be retained and cations repelled, while neutral species can partition into the hydrophobic core introduced. On the other hand, surfactant retention occurs within the interlayer space of clay and other layers of silicates present. These modified forms provide primarily a hydrophobic environment towards the retention of several organic molecules having less or no polarity.

Therefore, keeping in view, the present investigation deals with the modification of naturally abundant bentonite clay and locally available clay with hexadecyltrimethylammonium bromide (HDTMA) to obtain the organo-modified clays and aluminium pillared-HDTMA modified clay (inorgano-organo-modified clay), the application of which could provide more viable, eco-friendly, cost effective and efficient treatment technology. The modified solids were then employed in the efficient removal of As(III), As(V), and some EDCs, viz., Bisphenol A (BPA), 17α-ethynylestradiol (EE2), Diclofenac sodium salt (DFS) and Tetracycline hydrochloride (TC) from the aqueous solutions under different physico-chemical parametric studies which could helped in scaling up the laboratory data to pilot or large scale treatment of contaminated water.

CHAPTER 2

METHODOLOGY

2. METHODOLOGY

2.1. MATERIALS

Bentonite clay (BC) was procured from a commercial supplier and it was mined near Bhuj, Gujarat, India. Local clay (LC) was collected from Phullen Village, Aizawl District, Mizoram, India.

2.2. CHEMICALS AND APPARATUSES

The water used for entire solution preparations and other analytical studies was purified with the Millipore water purification system (Milli–Q$^+$). Electronic balance (Sartorius, Model: BS224S–CW, Sensitivity: 0.1mg) was used for taking weights of chemicals and clay materials. A pH–meter (Thermo Scientific, Model: Orion 2 Star, pH Benchtop) was utilized for the entire pH measurements. Before using, the pH meter was calibrated with the supplied buffer solutions. Syringe filter (PVDF filter membrane, 25 mm diameter and porosity of 0.45 μm) was obtained from Whatman, USA, which was used for filtration of samples in batch and column experiments. Glass bead (0.5 mm to 1 mm) used for packing of glass column was obtained from HiMedia, India.

The chemicals employed in the experiments were procured from different sources. Hexadecyltrimethylammonium bromide, bisphenol A, 17α–ethynylestradiol, diclofenac sodium salt, tetracycline hydrochloride and iminodiacetic acid were obtained from Sigma–Aldrich, USA. Aluminium(III) chloride, sodiumhexametaphosphate, sodium dithionite, hydrochloric acid, sodium nitrate, sodium hydrogen carbonate, di-sodium hydrogen phosphate, acetic acid (glacial), acetonitrile (HPLC grade), methanol (HPLC grade), HPLC water, citric acid monohydrate and tri–sodium citrate dihydrate were procured from Merck, India. Sodium hydroxide was obtained both from Merck, India and Duksan Pure Chemicals Co. Ltd., Korea. Sodium chloride, hydrogen peroxide, sodium carbonate and sodium chloride were purchased from HiMedia, India. Sodium meta-arsenite and disodium hydrogen arsenate heptahydrate were obtained from Wako Pure Chemical Industries Ltd., Japan. Copper(II) sulfate, ammonium sulfate, sodium phosphate and nitric acid were obtained from Duksan Pure Chemicals Co. Ltd., Korea. Glycine was procured both from Duksan Pure Chemicals Co. Ltd., Korea and HiMedia, India. Manganese(II) chloride tetrahydrate was procured from Duksan Pure Chemicals Co. Ltd., Korea and S.D. Fine Chemical Ltd., India. Ethylenediaminetetraacetic acid (EDTA) was purchased both from Duksan Pure Chemicals Co. Ltd., Korea and Loba Chemie Pvt. Ltd., India. Cadmium(II) sulfate was obtained from Kanto Chemical Co. Inc., Japan. Cadmium(II) chloride and Copper(II) chloride were obtained from DBH Laboratory reagents, India. Oxalic acid was procured both from Merck, India and Shinyo Pure Chemical Co. Ltd., Japan.

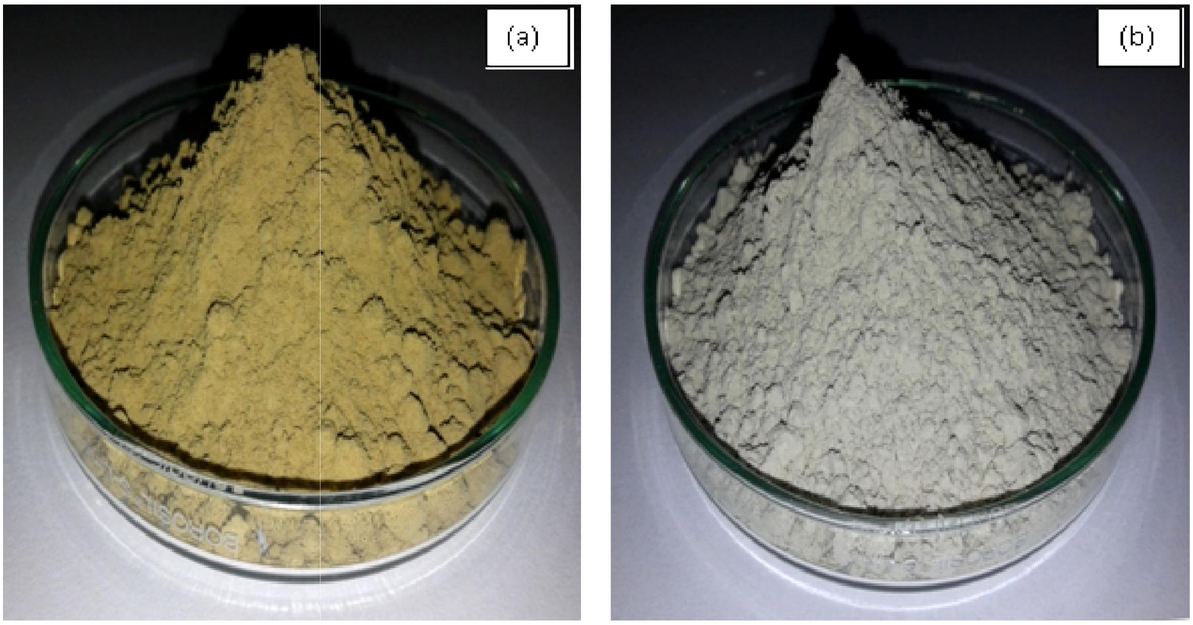

Fig 2.1. (a) Bentonite Clay, and (b) Local Clay.

2.2.1. Ultraviolet–Visible (UV–Vis) spectroscopy

Spectrophotometry is the analytical technique based on measuring the amount of light absorbed by a sample solution at a given wavelength. The UV–Vis Spectroscopy uses electromagnetic radiations between 190 nm to 800 nm and is divided into the ultraviolet (UV, 190–400 nm) and visible (VIS, 400–800 nm) regions. This technique is complementary to fluorescence spectroscopy, in that fluorescence deals with transitions from the excited state to the ground state, while absorption measures transitions from the ground state to the excited state (Skoog et al., 2007). Since the absorption of ultraviolet or visible radiation by a molecule leads transitions among electronic energy levels of the molecule, it is also often called as electronic spectroscopy. The term implies that these relatively high energy photons disturb the electron distribution within the molecule. Since atoms or molecules absorb UV–visible radiation at different wavelength, spectroscopy/spectrometry is often used in physical and analytical chemistry for the identification of substances through the spectrum emitted from or absorbed by them. The greater the number of molecules that absorb light of a given wavelength, the greater the extent of light absorption and higher the peak intensity in the absorption spectrum. If there are only a few molecules that absorb radiation, the total absorption of energy is less and consequently lower intensity peak is observed (Kumar, 2008). This makes the basis of Beer–Lambert law which states that the fraction of incident radiation absorbed is proportional to the number of absorbing molecules in its path.

When radiation passes through a solution, the amount of light absorbed or transmitted is an exponential function of the molecular concentration of the solute and also a function of path length of radiation passes through the sample. It can be represented as (Equation 2.1):

$$\log \frac{I_o}{I} = \varepsilon\, c\, l = A \qquad \text{...(2.1)}$$

Where I_o = Intensity of the incident light (or the light intensity passing through a reference cell)

I = Intensity of light transmitted through the sample solution

c = concentration of the solute in mol/L

l = path length of the sample in cm

ε = molar absorptivity or the molar extinction coefficient of the substance whose light absorption is under investigation. It is a constant and is a characteristic of a given absorbing species (molecule or ion) in a particular solvent at a particular wavelength. ε is numerically equal to the absorbance of a solution of unit molar concentration (c = 1) in a cell of unit length (l = 1) and its units are liters/moles/cm. However, it is customary practice to omit the units. Thus, if the path length and the molar absorptivity are known and the absorbance is measured, the concentration of the substance (or the number density of absorbers) can be deduced. The most common use of absorbance measurements is to determine the concentration of a solute.

The internal structure of a molecule may respond to radiant energy by more than just electronic transitions. In some molecules, bonding electrons also have natural resonant frequencies that give rise to molecular vibration while others exhibit a phenomenon known as rotation. Because the differences in energy levels associated with vibration and rotation are much smaller than those involved in electronic transitions, excitation will occur at correspondingly longer wavelengths. For most absorbing species, especially in the solution, absorption peaks do not appear as sharp lines at highly differentiated wavelengths, but rather as bands of absorption over a range of wavelengths. A principal reason is that an electronic transition is frequently accompanied by vibrational transitions between electronic levels (vibrational fine structure) (Hollas, 2005). In the same way each vibrational level is associated with rotational levels so that an absorption spectrum due to an electronic transition may well be a complex structure, with contributing components from vibrational and rotational absorption.

Spectrophotometer is a device to measure light intensity as a function of the wavelength of light. The basic parts of a spectrophotometer are having a light source, a sample holder, a diffraction grating or monochromator to separate the different wavelengths of light, and a detector. The radiation source is often a tungsten filament (300–2500 nm), a deuterium arc lamp which is continuous over the ultraviolet region (190–400 nm), and more recently light emitting diodes (LED) and Xenon Arc Lamps for the visible wavelengths. The detector is typically a photodiode or a charge–coupled device (CCD). Photodiodes are used with monochromators, which permit them only light of a single wavelength reaches the detector. Diffraction gratings are used with CCDs, which collects light of different wavelengths on different pixels. In the present investigation, UV–Visible Spectrophotometer (Thermo Electron Corporation, England; Model: UV1) was used to measure the absorbance of solutions containing EDCs so as to obtain the concentrations.

2.2.2. Atomic Absorption Spectroscopy (AAS)

Atomic absorption spectroscopy (AAS) is an analytical technique used for the qualitative and quantitative determination of the elements present in different samples. AAS was developed by Alan Walsh in mid of 1950. In this spectroscopy, the atoms in the ground state absorb the energy and converted into the gaseous state. When a solution containing metallic species is aspirated into a flame, the vapour of metallic species will be obtained.

Some of the metal atoms raised the energy level sufficiently high to emit the characteristic radiation of the metal. These ground state atoms of a particular element are receptive of light radiation of their own specific resonance wavelength. Thus, when a light of this wavelength is allowed to pass through a flame, part of that light will be absorbed and the absorption will be proportional to the density of the atoms in the flame. Thus in the AAS, one determines the amount of light absorbed. Once the value of this absorption is determined, the amount of the metallic atoms can be obtained since the absorption is proportional to the density of the atoms in the flame.

In 1955, Walsh suggested the use of cathode lamps to provide an emission of the appropriate wavelength (Walsh, 1955); and the use of a flame to produce neutral atoms that would absorb the emission as they crossed through its path. Metal ions in a solution are converted to the atomic state by means of a flame. Light of the appropriate wavelength is supplied and the amount of light absorbed is measured against a standard curve. The technique of flame atomic absorption spectroscopy (FAAS) requires a liquid sample to be aspirated, aerosolized, and mixed with combustible gases, such as acetylene and air or acetylene and nitrous oxide. The mixture is ignited in a flame whose temperature ranges from 2100 to 2800^{o}C. During combustion, atoms of the element of interest in the sample are reduced to free, unexcited ground state atoms, which absorb light at characteristic wavelengths which are element specific and accurate to 0.01–0.1 nm. To provide element specific wavelengths, a light beam from a lamp whose cathode is made of the element being determined is passed through the flame. A device such as photon multiplier can detect the amount of reduction of the light intensity due to absorption by the analyte, and this can be directly related to the amount of the element in the sample.

FAAS is a very common technique for detecting metals and metalloids in environmental samples. It is a very convenient, reliable, simple and widespread technique and has an acceptable level of accuracy for most analytes. The technique is based on the fact that ground state metals absorb light at specific wavelengths, as such making use of absorption spectrometry to assess the concentration of an analyte in a sample. It requires standards with known analyte content to establish the relation between the measured absorbance and the analyte concentration and relies therefore on Beer–Lambert law. In short, the electrons of the atoms in the atomizer can be promoted to higher orbitals (excited state) for a short period of time (nanoseconds) by absorbing a defined quantity of energy (radiation of a given wavelength). This amount of energy, i.e., wavelength, is specific to a particular electronic transition in a particular element. In general, each wavelength corresponds to only one element, and the width of an absorption line is only of the order of a few picometers (pm), which gives the technique of its elemental selectivity. There is no vibrational or rotational energy level that would widen the lines to bands in the spectrum like it happens in the case of UV–Vis spectroscopy. The radiation flux without a sample and with a sample in the atomizer is measured using a detector, and the ratio between the two values (the absorbance) is converted to analyte concentration or mass using Beer–Lambert's law stating that the absorbance of an absorbing analyte is proportional to its concentration.

Fast Sequential Atomic Absorption Spectrometer (Model AA240FS, Varian, Australia) was employed in the present investigation for the quantitative estimation of arsenic concentrations. FS–FAAS is a sequential multi–element technique that keeps the advantages of conventional FAAS. FS–FAAS is a sequential multi–element technique that keeps the advantages of conventional Flame Atomic Absorption Spectrometer (FAAS), for example ease of use. The sequential mode of this instrument allows the measurement of a sequence of analytes in decreasing order of wavelengths in one monochromator scan. By measuring all elements in one solution before proceeding to subsequent ones, the total analysis time is reduced and the results are obtained as soon as the sample analysis is finished. It is also possible to use the reference–element technique in a way that the application of the correction factors is performed automatically by the instrument software (Miranda and Pereira–Filho, 2009).

2.3. METHODS

2.3.1. Separation/purification of local clay

Bentonite clay was used after simple washing with distilled water and dried at 90°C in a drying oven without further purification. However, the local clay collected from the field of Mizoram was having several impurities hence, was thoroughly separated using the standard ‘Procedures for Soil Analysis’, International Soil Reference and Information Centre (ISRIC, 2002). In brief, the field sample was air dried, carefully crushed using a pestle and mortar and sieved with 30 BSS (British Standard Sieve) (500 microns) followed with 60 BSS (250 microns) to remove coarser particles like plant debris, gravel, rock fragments, etc. It was homogenized in water and allowed to pass through 100 BSS (0.15mm or 150 microns) to remove the larger sand and silt fraction. H_2O_2 (30%) was added in small increments until decomposition of organic matter is completed. After removal of any remaining H_2O_2, the supernatant was removed by decantation or by using a siphon and then treated with 10% acetic acid solution (v/v) to remove carbonates present. Deferration was thoroughly done with sodium dithionite in a buffer solution (0.3 M sodium citrate and 0.1 M sodium bicarbonate). After dispersion with a dispersing agent (40.0 g $(NaPO_3)_6$ and 10.0 g Na_2CO_3 in 1 L water), the clay fraction was separated by the pipette method. The pipette method was based on the slower sedimentation of clay compared to the silt and sand fraction. The suspension (mixture of clay, silt and sand) in water after the dispersion was allowed to settle in the settling cylinder/container. Temperature of the suspension was recorded and the clay fraction (upper part) was separated as indicated, and the process was repeated several times with the addition of more water after each separation. The depth at which the clay fraction was collected as a function of temperature and after the indicated settling time (5½ hours) is given below in Table 2.1:

Table 2.1: Fractions of clay collected as a function of temperature after indicated settling time.

Temp. (°C)	20	21	22	23	24	25	26	27	28	29	30
Depth (in cm) to be taken after 5½ hrs.	7.1	7.2	7.4	7.6	7.8	8.0	8.2	8.4	8.6	8.8	9.0

The dried bentonite or local clay sample was crushed in a mortar and sieved to obtain 100 BSS mesh size particles (0.150 mm) and stored in an airtight container for experimentation.

2.3.2. Determination of cation exchange capacity (CEC) of clay

The cation exchange capacity (CEC) is a measure of the quantity of negatively charged sites on clay material surfaces which is compensated by the exchangeable positively charged ions (cations) attached with weak electrostatic forces. It is usually expressed as milliequivalents per 100 grams (meq/100 g) of clay (Ross and Ketterings, 2011).

The bentonite and local clay powders were subjected to its cation exchange capacity (CEC) determination using the standard USEPA Method 9080 (http://www.epa.gov/osw/hazard/testmethods/sw846/pdfs/9080.pdf). Briefly, the clay sample was mixed with an excess of sodium acetate solution resulting in an exchange of the added sodium cations for the matrix cations. The sample was then washed with isopropyl alcohol. An ammonium acetate solution was added, which replaced the adsorbed sodium with ammonium. The concentration of displaced sodium was then determined.

2.3.3. Preparation of organo–modified clay

The bentonite or local clay was organically modified using the organic cation (i.e., HDTMA). The wet cation exchange process was followed as: 20 g of each clay (BC or LC) powder was taken separately into 1 L of HDTMA solution containing 1.0 CEC of respective clay (Boyd et al., 1988; Bowman et al., 2002). The slurry was refluxed for 48 h at 60°C under constant stirring. The slurry was filtered and the clay solid was washed several times with purified water. The organo–modified bentonite or local clay was then dried at 60–70°C in a drying oven. The solids were grounded and sieved to 100 BSS mesh sizes and then stored in an airtight polyethylene bottle. The HDTMA–modified bentonite and local clay were then labeled as BCH and LCH samples, respectively.

2.3.4. Preparation of inorgano–organo–modified clay

The bentonite or local clay was simultaneously pillared with aluminium and modified with organic cation, viz., HDTMA as to obtain the bentonite clay–Al–HDTMA (BCAH) or local clay–Al–HDTMA (LCAH) hybrid materials. A simple wet synthesis was followed as described elsewhere (Tiwari and Lee, 2012; Khalaf et al., 1997). In brief, aluminium pillaring solution was prepared mixing 100 mL of 0.4 mol/L NaOH and 100 mL of 0.2 mol/L aluminium chloride solutions under vigorous and constant stirring. The solution mixture was kept 7 days for ageing at room temperature. Further, in this aluminium solution a known amount of HDTMA (equivalent to 1:1 CEC of clay) was mixed under stirred conditions. BC or LC clay powder (4 g) in 300 mL of water was then taken in a round bottom flask. To this clay suspension, HDTMA mixed with aluminum pillaring solution was introduced and stirred for *Ca*. 5 h at room temperature. The slurry was then kept at room temperature for another 2 days. The modified bentonite or local clay was separated carefully and the solids were washed with plenty of distilled water as to obtain materials free from the chlorides hence, free from surfactants. It was then dried at 60–70°C in a drying oven and grounded gently in a mortar. It was sieved to 100 BSS mesh sizes and the powder (BCAH or LCAH) was kept in an airtight polyethylene bottles for further investigations.

2.3.5. Characterization of hybrid materials

The metal oxides present in the bentonite and local clay samples were obtained with the XRF analytical method using an X–Ray Fluorescence Spectrometer (Model: ZSX 100e, Rigaku, Japan). The surface morphology of the hybrid materials along with the pristine clay was obtained by taking the SEM images using a Field Emission Scanning Electron Microscope (S–4700, Hitachi, Japan). X–ray diffraction (XRD) data was recorded using the X–ray diffraction machine (PANalytical, Netherland; Model X'Pert PRO MPD). Cu K_α radiation having wavelength 1.5418 Å was used for X–ray diffraction. FT–IR (Fourier transform– infrared) data was collected for these materials using a FT–IR machine (Bruker, Tensor 27, USA) by the KBR disk method. The specific surface area, pore volume and pore size of the solids were obtained by nitrogen adsorption and desorption using the BET Analyzer (Macsorb HM machine, Model–1201, Japan).

2.3.6. Determination of pH_{PZC} of the solids

The point of zero charge (pH_{PZC}) is the pH at which the net surface charge on the solid is zero. It is assumed that at $pH < pH_{PZC}$, the surface carries net positive charge, while at $pH > pH_{PZC}$ the surface possesses net negative charge (Al–Degs et al., 2000). The pH_{PZC} of the solid was determined by the pH drift method (Franz et al., 2000; Faria et al., 2004). In brief, a series of 0.1 M $NaNO_3$ solution (100 mL each) was prepared using the CO_2 free water in different narrow mouth bottles. The pH of the solution in each bottle was adjusted to pH values of 2 to 11 by adding 0.1 M HCl or 0.1 M NaOH solutions. 0.1 g of the solid sample was then added to each bottle and the flasks were capped tightly and agitated for 24 hours at 25°C. The final pH of the solutions was recorded and a graph was plotted between $pH_{Initial}$ and pH_{Final}. The point of intersection of this curve with the $pH_{Initial} = pH_{Final}$ linear plot yielded the point of zero charge.

2.3.7. Batch reactor experiment

Batch experiment was performed to obtain adsorption data with the effect of sorptive pH, initial sorptive concentration, and background electrolyte concentration and contact time in order to find out the mechanisms involved at solid/solution interface (Tiwari et al., 2007). The stock solutions of appropriate concentrations of each sorptive samples were prepared dissolving the appropriate amounts of As(III), As(V), BPA, EE2, DFS or TC in distilled water and the desired concentrations for the batch reactor experiments were obtained by the successive dilution of stock solutions. The adsorption of As(III), As(V), BPA, EE2, DFS or TC was investigated taking 0.1 g of the solid sample in 50 mL of sorptive solution. The solution mixture was equilibrated using an automatic shaker (KUKJE, Shaking Incubator, Korea model 36–SIN–125 or Incubator Shaker, TM Weiber, ACMAS Technologies Pvt. Ltd., India) for 24 hours at 25±1°C. 0.45 μm syringe filter was used for filtering the equilibrated solution. The bulk sorptive concentration was measured using Fast Sequential Atomic Absorption Spectrometer (Model AA240FS, Varian) for As(III) and As(V); and UV–Visible spectrophotometer (Model: UV1, Thermo Electron Corporation, USA) for EDCs. The absorbance was measured at 276 nm, 280 nm, 276 nm and 360 nm for BPA, EE2, DFS and TC respectively. HPLC system (Pump model: 515, Waters, USA) equipped with UV-Vis detector (Model: 2489, Waters, USA) with Symmetry ® C18 (5 µm, 4.6 x 250 mm) column was used for concentration measurement in the studies of the effect of co-existing ions for EDCs. The mobile phase was used acetonitrile:water (55:45, v/v) for BPA, acetonitrile:water:acetic acid (70:29:1, v/v) for EE2 and DFS, and 0.01 M oxalic acid–acetonitrile–methanol (45:35:20, V/V) for TC, with a flow rate of 1.0 mL/min. The detector was set at 276 nm, 280 nm, 276 nm and 360 nm for BPA, EE2, DFS and TC respectively. The Calibration curve was obtained with the standard sorptive solutions having different concentrations. The data were then utilized to calculate the percent removal using Equation 2.2:

$$\%\ \text{Removal} = \frac{C_0 - C_e}{C_0} \times 100 \qquad \text{...(2.2)}$$

where C_o and C_e are the initial and final sorptive concentrations, respectively.

2.3.7.1. Effect of pH

Solution pH is an important parameter during the adsorption process. The solution pH can affect the surface charge of the adsorbent, the degree of ionization of the different pollutants, the dissociation of functional groups in the active sites of the adsorbent as well as the structure of the adsorbate molecule. The solution pH would affect both aqueous chemistry and surface binding sites of the adsorbent (Ai et al., 2011; Bazrafshan et al., 2013). Therefore, there is a specific pH range, which favors the uptake of adsorption processes. The effect of pH was conducted maintaining the sorptive solution pH between pH 2.0 to 10.0 for

As(III) and As(V); sorptive equilibrium solution pH between pH 4.0 to 10.0 for EDCs; with the sorptive concentrations of ~10.0 mg/L for As(III), As(V), BPA, DFS or TC, and ~5.0 mg/L for EE2 and suspensions were equilibrated for 24 hours at a constant temperature 25±1°C. Further, the sorption experiments were conducted as detailed before in Chapter 2.3.7. The results obtained were reported as percent removal as a function of pH of the sorptive solution.

2.3.7.2. Effect of sorptive concentration

The initial sorptive concentration is an important factor to be determined in adsorption studies because the rate and uptake of sorptive solution by a sorbent are dependent upon its initial concentration in solution. It also makes the application of equilibrium adsorption isotherm models (Dawodu and Akpomie, 2014). In batch adsorption processes, the initial sorptive concentration in the solution plays a key role as a driving force to overcome the mass transfer resistance between the solution and solid phase (Mustaqeem et al., 2013). The effect of initial sorptive concentration was studied between 1.0 mg/L to 20.0 mg/L for As(III), As(V), BPA, DFS or TC, and 1.0 mg/L to 10.0 mg/L for EE2; at the sorptive pH 4.5 for As(III) and As(V), and pH ~7.0 for EDCs; with 24 hour equilibrium time and at 25±1°C. The sorption experiments were conducted as detailed in Chapter 2.3.7. The results were reported as percent removal as a function of the initial sorptive concentration.

2.3.7.3. Effect of background electrolyte concentration

The ionic strength dependence sorption data are generally used to distinguish between nonspecific and specific adsorption. Specific adsorption is characterized by more selective and less reversible reactions, including chemisorbed inner–sphere complexes; and nonspecific adsorption (or ion exchange), which involves rather weak and less selective outer–sphere complexes (Bradl, 2004). Outer sphere complexes involve only electrostatic interactions and are strongly affected by the ionic strength of aqueous phase, while inner sphere complexes involve much stronger covalent or ionic binding and are only weakly affected by the ionic strength (Scheidegger et al., 1996). Ionic strength is the other key factor that controls the electrostatic interactions. Thus, these interactions, either attractive or repulsive, could be reduced increasing the ionic strength of sorptive solution. This is due to a screening effect of the surface charge produced by the added salt. Therefore, when the electrostatic interaction between the surface and the adsorptive species is repulsive, or the surface concentration is sufficiently high, an increase in ionic strength will increase the adsorption. Conversely, when the electrostatic interactions are attractive, or the surface concentration is sufficiently low, an increase of the ionic strength will diminish the adsorption (Moreno–Castilla, 2004). Hence, keeping in view the background electrolyte ($NaNO_3$) concentration was increased from 0.001 mol/L to 0.1 mol/L in the solution keeping the initial As(III) and As(V) concentrations of 10.0 mg/L; sorptive solution pH of 4.5; with 24 hour equilibrium time and at $25\pm1^{o}C$. For EDCs, the background electrolyte (NaCl) concentrations was increased from 0.0001 mol/L to 0.1 mol/L keeping the initial sorptive concentrations of 10.0 mg/L for BPA, DFS or TC, and 5.0 mg/L for EE2; solution pH ~7.0; with 24 hour equilibrium time and at 25±1°C. The results were reported as percent removal as a function of background electrolyte concentration.

2.3.7.4. Effect of contact time

The study of sorption kinetics in wastewater treatment is significant as it provides valuable insights into the reaction pathways and enables to deduce the mechanism of sorption reactions. In addition, the kinetic studies describe the solute uptake rate, which in turn controls the residence time of sorbate uptake at the solid–solution interface. Therefore, it is important to predict the rate at which the pollutant is removed from aqueous solutions in order to design appropriate wastewater treatment plants (Ho and McKay, 1999b). The effect of contact time was studied at different intervals of time keeping the initial sorptive concentrations of ~10.0 mg/L for As(III), As(V), BPA, DFS or TC, and ~5.0 mg/L for EE2; sorptive pH of 4.5 for As(III) and As(V), and at pH ~7.0 for EDCs, and at constant temperature of 25±1°C. The results were reported as percent removal as a function of time.

2.3.7.5. Effect of coexisting ions

The sorption of As(III), As(V) and EDCs was conducted in presence of cations and anions separately, keeping the arsenic concentration of 10.0 mg/L at pH~4.5 and temperature 25±1°C. As usual the sorptive solutions were equilibrated for 24 hour with a solid dose of 2 g/L. Concentrations of the coexisting ion was taken as 50.0 mg/L. The cations chosen were Cd(II), Cu(II) and Mn(II); whereas the anions taken were sulfate, oxalate, phosphate, glycinate, iminodiacetate (IDA), and ethylenediaminetetraacetate (EDTA) ions for arsenic; and nitrate, phosphate, glycinate, IDA and EDTA for EDCs. The results were then presented as percent removal as a function of coexisting ion concentration.

2.3.7.6. Effect of phenol on arsenic removal

The hybrid materials were utilized to assess the effect of phenol on the As(III) and As(V) removal, at varying concentrations of phenol from 2.0 mg/L to 15.0 mg/L, with the arsenic concentration of 10.0 mg/L, at pH 4.5 and temperature 25±1°C, and the solution was equilibrated for 24 hour with a constant solid dose of 2 g/L. Batch experiments were carried out as detailed before in Chapter 2.3.7. Results were evaluated as percent removal of arsenic as a function of initial phenol concentration, and also the amount of phenol removed as a function of initial phenol concentrations.

2.3.8. Adsorption isotherm modeling

Equilibrium isotherm models are introduced over the years based on different basic assumptions. Some of the models have gained more importance than others due to their simplicity and, in some cases, due to their ubiquitous applicability. Accuracy of an isotherm model is generally a function of number of independent parameters introduced with the model, while its popularity in relation to the process application is generally a function of its mathematical simplicity (Malek and Farooq, 1996). Adsorption equilibrium is established when the sorptive solution is in contact with the adsorbent for sufficient time, with its adsorbate concentration in the bulk solution is apparently in a dynamic balance with the interface concentration. Usually, the mathematical correlation which constitutes an important role towards the modeling analysis, operational design and applicable practice of the adsorption system, is usually depicted by graphical expression of the solid phase concentration against its residual concentration. Its physicochemical parameters together with the underlying thermodynamic assumptions provide information of the adsorption mechanism, surface properties as well as the degree of affinity of the adsorbents (Foo and Hameed, 2010). Among several available adsorption isotherm models, two models are common to formulate adsorption equilibrium data:

2.3.8.1. Langmuir adsorption isotherm

Langmuir isotherm model assumes monolayer adsorption, i.e., the adsorbed layer is in molecular thickness and adsorption occur at a fixed number of definite localized sites, that are identical and equivalent, with no lateral interaction and steric hindrance between the adsorbed molecules, even on adjacent sites. In its derivation, Langmuir isotherm refers to homogeneous adsorption; all sites possess equal affinity for the adsorbate with each molecule possesses constant enthalpies and sorption activation energy (Kundu and Gupta, 2006). The linearized Langmuir adsorption model (Tiwari et al., 2007) in its usual form is adopted for the estimation of maximum uptake (q_o) at various initial concentrations (Equation 2.3):

$$\frac{C_e}{q} = \frac{1}{q_o b} + \frac{C_e}{q_o} \qquad \text{...(2.3)}$$

where q is the amount of solute adsorbed per unit weight of adsorbent (mg/g) at equilibrium; C_e the equilibrium bulk sorptive concentration (mg/L); q_o the Langmuir monolayer adsorption capacity, i.e., the amount of solute required to occupy all the available sites in unit mass of solid sample (mg/g) and b is the Langmuir constant (L/g).

2.3.8.2. Freundlich adsorption isotherm

Freundlich isotherm is the earliest known relationship describing the non–ideal and reversible adsorption, not restricted to the formation of monolayer. This empirical model is applied to multilayer adsorption, with non–uniform distribution of adsorption heat and affinities over the heterogeneous surface. Nowadays, Freundlich isotherm is widely applied in heterogeneous systems especially for organic compounds or highly interactive species on activated carbon and molecular sieves (Foo and Hameed, 2010). The linearized form of

Freundlich equation (Tiwari et al., 2007) is given in Equation 2.4:

$$\log a_e = \frac{1}{n} \log C_e + \log K_f \qquad ...(2.4)$$

where a_e and C_e are the amount adsorbed (mg/g) and bulk sorptive concentration (mg/L) at equilibrium, respectively, and K_f and $\frac{1}{n}$ are the Freundlich constants referring to adsorption capacity and adsorption intensity or surface heterogeneity, respectively.

2.3.9. Adsorption kinetic modeling

A number of adsorption processes for pollutants are studied in an attempt to find a suitable explanation for the mechanisms and kinetics involved in the uptake of pollutants by the employed solids. In order to investigate the mechanisms of adsorption, various kinetic models are suggested, and in recent years, adsorption mechanisms involving kinetic–based models are reported. Numerous kinetic models described the reaction order of adsorption systems based on solution concentration; and also the reaction orders based on the capacity of the adsorbents are also presented previously (Ho, 2006).

Time dependence data are utilized to conduct the kinetic modeling for three different kinetic models, *viz*., pseudo–first order (PFO) (Azizian, 2004), pseudo–second order (PSO) (Ho and McKay, 1998) and fractal–like pseudo–second order (FL–PSO) (Haerifar and Azizian, 2012) to its non–linear forms as given in Equations 2.5, 2.6 and 2.7 respectively, in order to establish the best fitted model for the studied systems:

$$q_t = q_e(1 - \exp(-k_1 t)) \qquad \ldots(2.5)$$

$$q_t = \frac{k_2 q_e^2 t}{1 + k_2 q_e t} \qquad \ldots(2.6)$$

$$q_t = \frac{k q_e^2 t^{\alpha}}{1 + k q_e t^{\alpha}} \qquad \ldots(2.7)$$

where q_t and q_e are the amount of sorbate removed at time t and removal capacity at equilibrium, respectively. k_1 and k_2 are the pseudo–first and pseudo–second order rate constants, respectively. Similarly, the constants k and α are referred to the rate constant and fractal constant, respectively. The pseudo–first–order kinetic model which is theoretically derived by the Lagergren could show the properties of the Langmuir rate at initial times of adsorption or close to equilibrium. Similarly, theoretical studies indicate that the rate coefficient of pseudo–second–order model, i.e., k_2 is virtually a complex function of the initial concentration of the sorbing species (Azizian, 2004). However, the FL–PSO model approach basically imply to the fact that there are different paths of adsorption that take place in adsorption and the adsorption rate coefficient is a function of time (Haerifar and Azizian, 2012). A non–linear least square fitting is conducted for the estimation of unknown parameters.

2.3.10. Column experiments

Column experiments were performed as detailed previously Tiwari et al. (2007). It was conducted using a glass column (1 cm inner diameter) packed with 0.25 or 0.5 g of modified clay solid (kept middle in the column); below and above to this, *Ca*. 2.0 g of virgin sand particles (14–16 BSS) was placed and then the column was packed with glass beads. Sorptive solution of *Ca*. 5.0 or 10.0 mg/L, at pH ~7.0 for BPA, EE2, DFS or TC was pumped upward from the bottom of the column using a peristaltic pump (KrosFlo Research I Peristaltic Pump, Spectrum Laboratories Inc., California, USA) at a constant flow rate of 1.0 mL/min, and at a constant temperature of 25±1°C. Effluent solutions were collected using a fraction collector (Spectra/Chrom CF–2 Fraction Collector, Spectrum Laboratories Inc., California, USA). The collected effluents were filtered using 0.45 µm syringe filter and their concentrations were measured using UV–Vis spectrophotometer.

The breakthrough data were further utilized to optimize the loading capacity of specific EDCs by the hybrid material under dynamic conditions employing the Thomas equation (Equation 2.8) (Thomas, 1944):

$$\frac{C_e}{C_o} = \frac{1}{1 + e^{(K_T(q_o m - C_o V))/Q}} \qquad \ldots(2.8)$$

where C_e and C_o are the concentrations of effluents and an influent solution of EDC (mg/L), respectively; K_T refer to the Thomas rate constant (L/min/mg); q_o is the maximum amount of EDC loaded (mg/g) under the specified column conditions; m is the mass of hybrid materials taken in column (g); V is the throughput volume (L); and Q is the flow rate of pumped EDC solution (L/min). The column data were then fitted to a non–linear Thomas equation using the least square fitting method to estimate two unknown variables, i.e., K_T and q_o.

Figure 2.2. Experimental setup of column reactor.

CHAPTER 3

RESULTS AND DISCUSSION

3. RESULTS AND DISCUSSION

3.1. CHARACTERISATION OF MATERIALS

3.1.1. SEM analysis of the surface morphology of materials

The surface morphology of the pristine clays along with the hybrid materials was obtained taking the FE–SEM images of these solids. The images obtained are returned in Figure 3.1.1 (a–f) for these solids. The images clearly show that the bentonite clay (BC) and local clay (LC) possesses relatively compact and ordered surface structures, while the modified solids show more heterogeneous and disordered surface structures. It is assumed that the water molecules or the exchangeable cations present within the interspace of clay are exchanged with the HDTMA cations, and it firmly occupied the space within the interspace of clay. Also the surface structure of the modified solids seems more porous in nature. Further, for BCAH and LCAH solids, distinct and very fine particles are observed onto the surface, and perhaps aluminium is aggregated/ immobilized as aluminium oxide/hydroxide onto the solid surface. It may also likely to pillar the clay sheet structure once entered within the interspace.

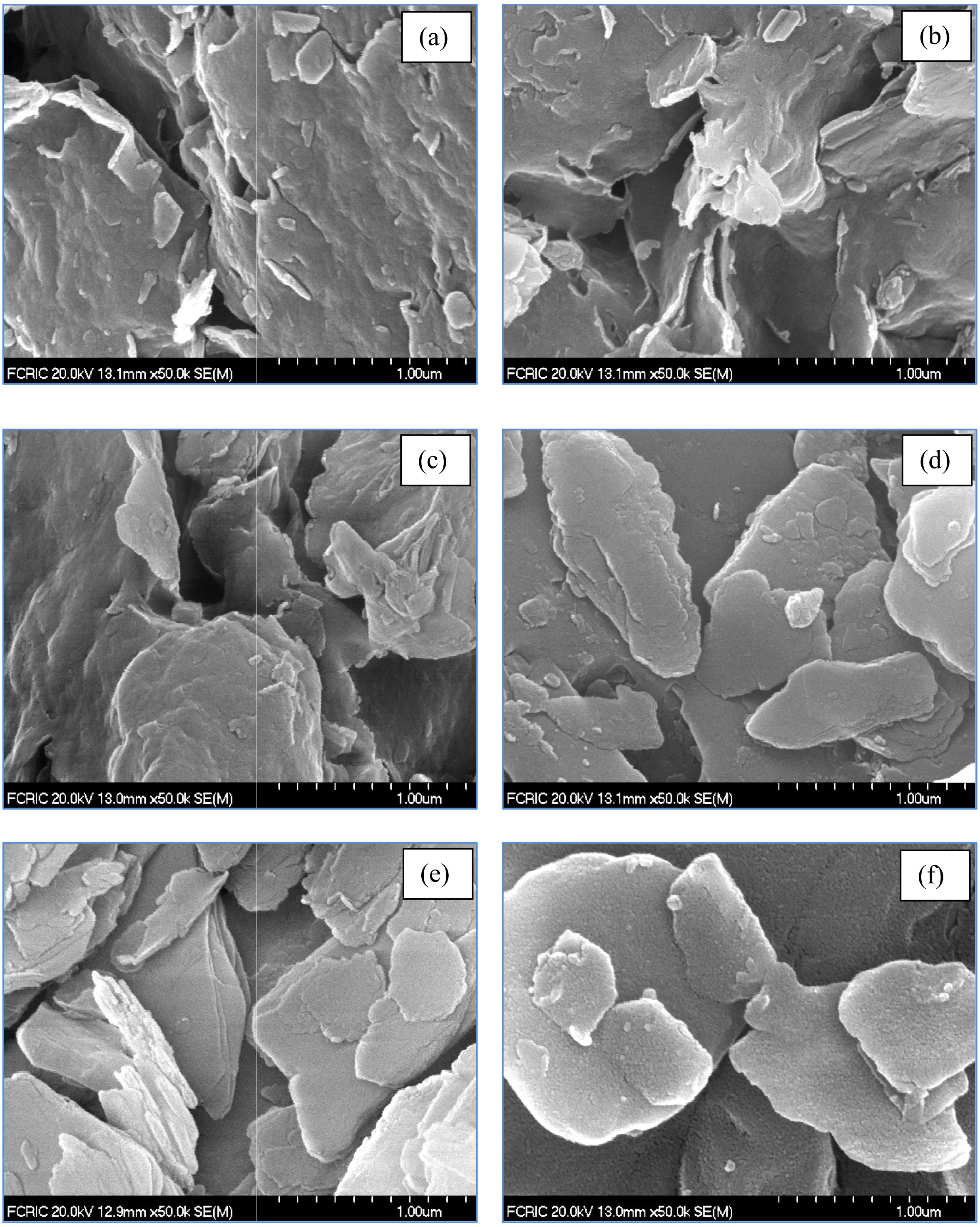

Figure 3.1.1. SEM images of (a) BC; (b) BCH; (c) BCAH; (d) LC; (e) LCH and (f) LCAH.

3.1.2. X-ray fluorescence (XRF) analysis

The bentonite and local clay was subjected for elemental composition using the XRF analytical method which was further optimized to the mineral oxides present with natural clays, BC and LC. The results are then tabulated in Table 3.1.1. It is clearly observed from the table that both the clay samples possess mainly the oxides of silicon, aluminium and iron. Also a notable amount of Na, Mg and K is present; which are likely to be exchangeable cations lying within the interspace of clay. Moreover, it is noteworthy that the composition of metal oxides for both the clay is found almost identical.

Table 3.1.1. Various components present in bentonite and local clay sample as estimated by the XRF analysis.

Components	**Mass Percentage**	
	Bentonite	**Local Clay**
Na_2O	2.11	2.17
MgO	2.77	2.72
Al_2O_3	21.87	21.89
SiO_2	54.51	54.57
P_2O_5	0.13	0.13
K_2O	1.39	1.38
CaO	0.98	0.95
TiO_2	2.51	2.47
Cr_2O_3	0.04	0.04
MnO	0.17	0.19
Fe_2O_3	12.46	12.45

3.1.3. X–ray diffraction (XRD) analysis

X-ray diffraction analysis was conducted for the solids, *viz*., BC, BCH, BCAH, LC, LCH and LCAH. The results are presented graphically in Figure 3.1.2 (a) and (b) respectively for the bentonite and local clay based solids. The sharp diffraction peaks observed for these solids with a definite d-spacing makes possible to assign the peaks of different mineral phases of the clay materials. XRD data of bentonite and local clay are matched with the standard ICDD (International Centre for Diffraction Data) reference pattern. It is noted that both the clay samples contained with quartz, smectite, illite and kaolinite minerals; with varying percent composition as characteristic peaks are assigned in the XRD diffraction pattern. Further, quantitatively, it is evaluated that bentonite is having 43.71%, 23.17%, 1.73% and 31.39% of quartz, smectite, kaolinite and illite, respectively. Similarly, local clay contained with 79.35%, 6.20%, 0.45% and 14.01%, respectively of quartz, smectite, kaolinite and illite. The other visible diffraction peaks are, perhaps, due to the presence of some impurity. The XRD pattern of modified clay samples is almost identical to its pristine clay, with a slight change in d-values and intensities of peaks.

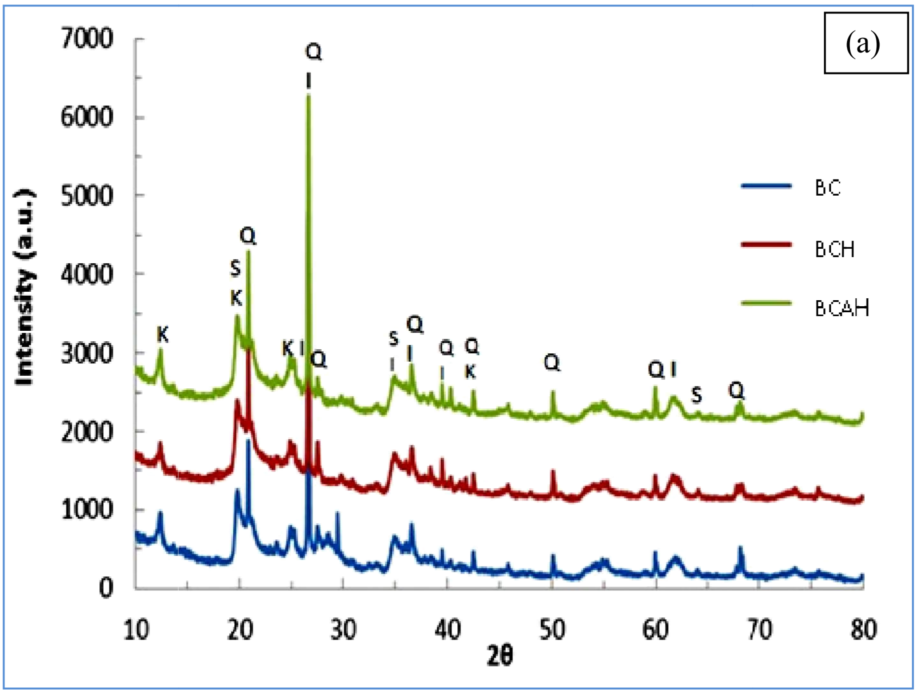

Figure 3.1.2 (a). X–ray diffraction pattern of BC, BCH and BCAH.

[S: Smectite; K: Kaolinite; Q: Quartz; and I: Illite].

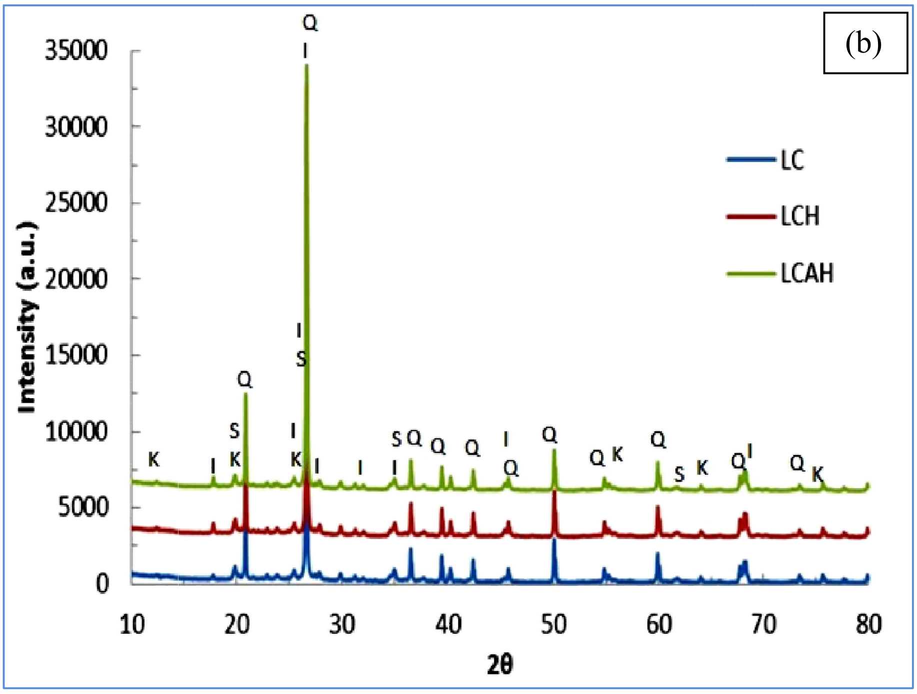

Figure 3.1.2 (b). X–ray diffraction pattern of LC, LCH and LCAH.

[S: Smectite; K: Kaolinite; Q: Quartz; and I: Illite].

3.1.4. Fourier–transform infra–red spectroscopic (FT–IR) analysis

FT–IR spectra of the bentonite and local clay based samples are presented in Figure 3.1.3 (a) and (b), respectively. The intense bands at 1110 and 1030 cm^{-1} are those of the Si–O stretching vibrations. Similarly, couple of IR bands centred around 695 cm^{-1} and 795 cm^{-1} is assigned to the quartz Si–O vibrations. The peak at 3620 cm^{-1} originates from the structural Al_2OH stretching (Tabak et al.; 2011; Jović–Jovičić et al., 2010; Aroke and El–Nafaty, 2014). The peak at 910 cm^{-1} originates from the Al–Al–OH hydroxyl bending vibrations. The vibrational frequency band at 880 cm^{-1} is assigned to OH deformation linked to Fe^{2+} and Fe^{3+}. The peak at 753 cm^{-1} corresponds to Si–O deformation (Aroke and El–Nafaty, 2014; Eisazadeh et al., 2012). A broad peak at 3420 cm^{-1} belongs to OH stretching of H–bonded water. Similarly, a peak at 1640 cm^{-1} belongs to the OH deformational mode of water (Tabak et al., 2011; Slimani et al., 2014). This clearly indicates the presence of hydroxyl groups within the clay sheets and the water molecules present within the interlayer space of clay. It is interesting to note that the modified samples, i.e., BCH, BCAH, LCH or LCAH, possess two distinct bands at 2925 and 2850 cm^{-1}. The bands are associated with asymmetric and symmetric C–H stretching vibrations of $–CH_2$, respectively. A band at 1480 cm^{-1} is assigned to the bending mode of CH_2 (Slimani et al., 2014; Jović–Jovičić et al., 2010; Aroke and El–Nafaty, 2014). This confirms the introduction of HDTMA within the clay network for all these modified solids.

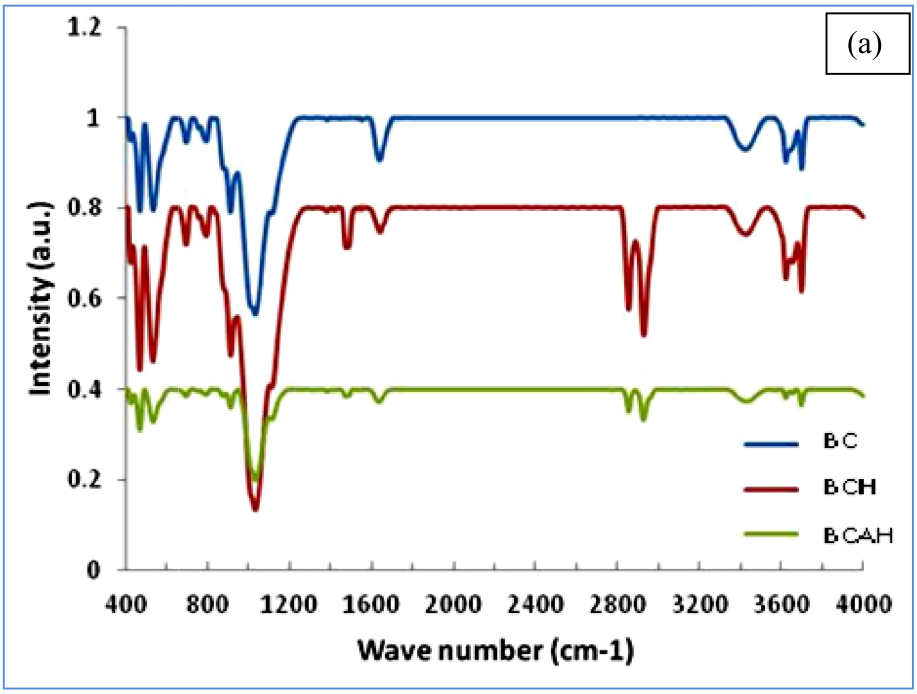

Figure 3.1.3 (a). FT-IR spectra of bentonite and modified bentonite samples.

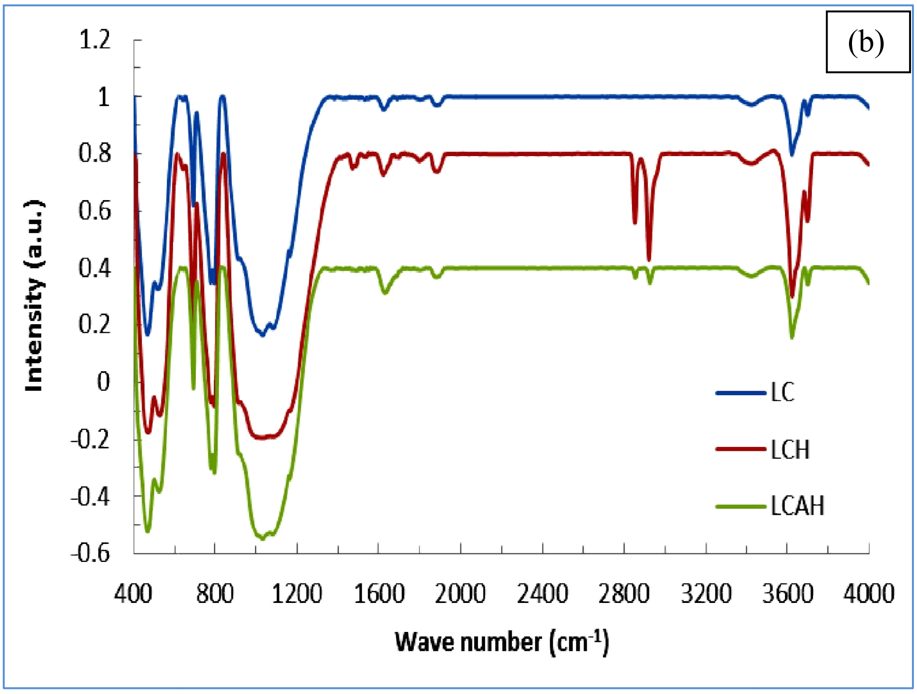

Figure 3.1.3 (b). FT-IR spectra of local clay and modified local clay samples.

3.1.5. Point of zero charge (pH_{PZC}) of the samples

The point of zero charge (pH_{PZC}) is defined as the pH value at which the net charge of the solid surface is zero, i.e., the surface of the material carries neither positive nor negative charges (Khormaei et al., 2007). Point of zero charge determination of these solids is also important in elucidating the adsorption mechanism involved at solid solution interface. At a pH lower than the pH_{PZC}, the solid carries a net positive surface charge, and at a pH higher than the pH_{PZC}, the surface carries a net negative charge because of the acidic dissociation of surface functional groups. The pH_{PZC} obtained for the solid samples are summarized in Table 3.1.2 and the plot is shown in Figure 3.1.4. As seen in the table, it is observed that the modified samples show lower pH_{PZC} values compare to their corresponding pristine clay samples. The pH_{PZC} of the local clay based samples show somewhat lower values compare to the corresponding bentonite based samples.

Table 3.1.2. The pH_{PZC} obtained for BC, BCH, BCAH, LC, LCH and LCAH samples.

Sl. No.	**Samples**	**pH_{PZC}**
1	BC	9.8
2	BCH	8.2
3	BCAH	6.1
4	LC	5.8
5	LCH	5.5
6	LCAH	5.5

Figure 3.1.4. Plot of initial pH vs final pH.

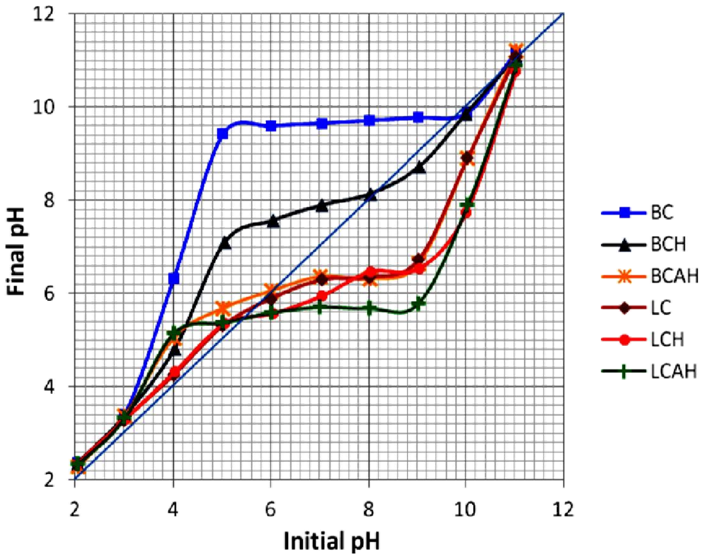

3.1.6. BET analysis of the samples

The BET specific surface area, pore volume and pore size of these solids, viz., BC, BCH, BCAH, LC, LCH and LCAH were obtained by the nitrogen adsorption and desorption and the values evaluated are returned in Table 3.1.3. It is seen from the table that very high value of the BET specific surface is obtained for the unmodified bentonite sample (BC) having low pore volume and pore size. The high specific surface area of BC is due to the presence of a higher percentage of smectite, kaolinite and illite compare to quartz/silica content (*cf.* Chapter 3.1.3). However, the HDTMA– or Al–HDTMA–modified bentonite materials show a remarkable decrease of specific surface area and an increase in pore size (diameter) and pore volume of the materials. It is due to the fact that the HDTMA or aluminium occupied the interspace and caused to decrease in specific surface area, whereas the propping up of the interlayer caused to enhance the pore size and pore volume of the solids. Similar results were reported previously in the HDTMA modified montmorillonite using a regulated loading of HDTMA (Juang et al., 2007). On the other hand, the unmodified local clay (LC) shows very low specific surface area, i.e., 2.94 m^2/g; due to the compact surface structure of LC which contained dominantly of silica/quartz. However, the presence of HDTMA or Al–HDTMA caused the relative increase in the specific surface area as well as a decrease in pore diameter of the modified solids. It was reported previously that the specific surface area of sand was increased with the manganese oxide coating of the sand solid (Lee et al., 2010).

Table 3.1.3. BET pore size, specific pore volume and specific surface area values of the clay and hybrid materials.

Materials	Pore Size (nm)	Specific pore volume (cm^3/g)	BET Specific surface area (cm^2/g)
BC	4.98	0.010	80.86
BCH	36.60	0.050	4.68
BCAH	27.45	0.075	9.55
LC	30.67	0.025	2.94
LCH	13.12	0.045	11.87
LCAH	8.04	0.010	4.55

3.2. BATCH REACTOR STUDIES

3.2.1. Effect of pH

3.2.1.1. As(III) and As(V)

The uptake of As(III) and As(V) was obtained as a function of solution pH (2.0 to 10.0), as detailed previously in Chapter 2.3.7.1. The results are tabulated in Table 3.2.1(a–f) and 3.2.2 (a–f); and then presented graphically in Figure 3.2.1 and 3.2.2, respectively, for As(III) and As(V). In general, relatively higher uptake of As(III) or As(V) is occurred at moderate pH values, i.e., pH 4–7. However, relatively, a lower uptake of arsenic is occurred at extremely low and high pH values, i.e., *Ca*. 2.0 and 10.0. In order to demonstrate the mechanism involved at solid/solution interface, it is important to discuss the speciation of As(III) and As(V) in aqueous solution as well the pH_{PZC} of these solids employed. The point of zero charge of the solids is found to be 9.8, 8.2, 6.1, 5.8, 5.1 and 5.1 for the samples BC, BCH, BCAH, LC, LCH and LCAH respectively. The materials are positively charged below this pH and carry a net negative charge above this pH. A simple acidic dissociation of surface functional groups could be deduced with Equation 3.1:

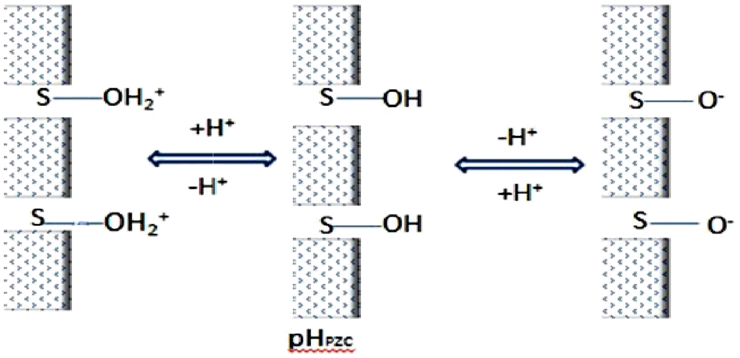

…(3.1)

where ′S′ represents the surface having the aluminium or silicon sites. The pH_{PZC} of the local clay based samples show somewhat lower values, whereas the bentonite and modified bentonite possess slightly higher pH_{PZC} values. The aluminium pillared samples, i.e., BCAH possess much lower pH_{PZC} (i.e., 6.1) compare to its corresponding pristine bentonite sample having pH_{PZC} of 9.8. This decrease is due to the sufficient loading of aluminium along with the HDTMA.

The speciation of As(III) and As(V) was carried out previously which demonstrated that up to pH 8.0 the dominant species of As(III) was the neutral H_3AsO_3; and beyond this pH, the negatively charged species $H_2AsO_3^-$ was gradually dominating in aqueous solutions (Lalhmunsiama et al., 2012). Relatively low uptake of As(III) that occurred at lower pH values, i.e., pH ~2.0 is due to the fact that at this pH there could be a strong competition between the H^+ ions and even the neutral arsenic species toward the surface and this hindered the attraction of arsenic species toward the solid surface (Tiwari et al., 2014). However, with the increase in pH, the surface become uncharged or the charge density decreases, which make possible for the van der Waals attractive forces to dominate which results in an enhanced uptake of As(III) by these solids, i.e., BCH, BCAH, LCH and LCAH. It seems that the aluminium pillaring insignificantly affect the uptake of As(III) since almost similar percent removal is achieved by the solids BCH and BCAH; and also by LCH and LCAH. Similar mechanism was proposed for the uptake of As(III) by the titanium oxide nanoparticles (Nabi et al., 2009). The van der Waals attractive sorption was reported previously for As(III) by the iron modified sand samples (Vaishya and Gupta, 2004). However, the other report showed that thiol–functionalized silica coated activated alumina sorbed As(III) by strong chemical bonds with the sulfhydryl group (Hao et al., 2009). Further, at very high pH values (pH~10.0), since the surface and arsenic species, both possess negative charges, a strong repulsive force causes for a considerable decrease in percent uptake of As(III) by these solids.

Table 3.2.1(a). Effect of pH on the removal of As(III) by BC.

pH	Initial conc. (mg/L)	Final conc. (mg/L)	% Removal
2	8.37	7.56	9.68
3	8.37	6.12	26.88
4	8.37	5.87	29.87
5	8.37	6.18	26.16
6	8.37	6.24	25.45
7	8.37	6.63	20.79
8	8.37	6.80	18.76
9	8.37	6.65	20.55
10	8.37	6.75	19.35

Table 3.2.1 (b). Effect of pH on the removal of As(III) by LC.

pH	Initial conc. (mg/L)	Final conc. (mg/L)	% Removal
2	8.37	7.77	7.17
3	8.37	7.03	16.01
4	8.37	6.94	17.08
5	8.37	6.92	17.32
6	8.37	6.59	21.27
7	8.37	7.20	13.98
8	8.37	7.39	11.71
9	8.37	7.47	10.75
10	8.37	7.77	8.00

Table 3.2.1(c). Effect of pH on the removal of As(III) by BCH.

pH	**Initial conc. (mg/L)**	**Final conc. (mg/L)**	**% Removal**
2	9.49	3.9	58.90
3	9.49	3.55	62.59
4	9.49	3.53	62.80
5	9.49	3.39	64.28
6	9.49	2.91	69.34
7	9.49	2.93	69.13
8	9.49	3.11	67.23
9	9.49	4.22	55.53
10	9.49	4.79	49.53

Table 3.2.1 (d). Effect of pH on the removal of As(III) by LCH.

pH	**Initial conc. (mg/L)**	**Final conc. (mg/L)**	**% Removal**
2	9.49	4.76	49.84
3	9.49	4.73	50.16
4	9.49	4.17	56.06
5	9.49	4.70	50.47
6	9.49	5.32	43.94
7	9.49	5.90	37.83
8	9.49	6.44	32.14
9	9.49	6.83	28.03
10	9.49	6.99	26.34

Table 3.2.1(e). Effect of pH on the removal of As(III) by BCAH.

pH	**Initial conc. (mg/L)**	**Final conc. (mg/L)**	**% Removal**
2	8.37	3.34	60.10
3	8.37	3.07	63.32
4	8.37	2.63	68.58
5	8.37	2.46	70.61
6	8.37	2.08	75.15
7	8.37	2.57	69.30
8	8.37	3.12	62.72
9	8.37	3.03	63.80

Table 3.2.1 (f). Effect of pH on the removal of As(III) by LCAH.

pH	**Initial conc. (mg/L)**	**Final conc. (mg/L)**	**% Removal**
2	8.37	3.89	53.52
3	8.37	3.85	54.00
4	8.37	3.83	54.24
5	8.37	3.54	57.71
6	8.37	3.72	55.56
7	8.37	4.41	47.31
8	8.37	4.70	43.85
9	8.37	4.98	40.50

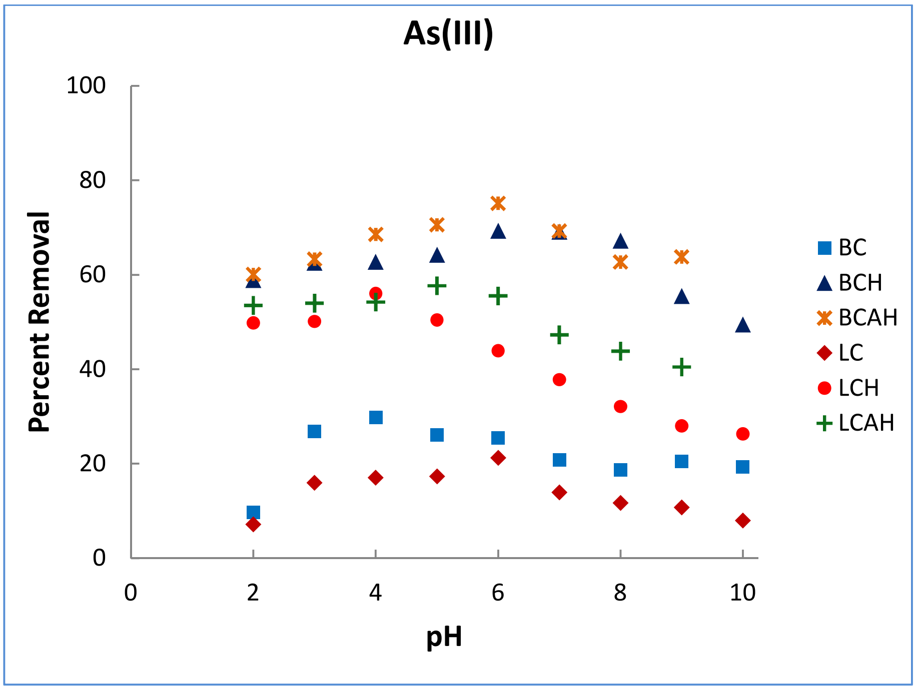

Figure 3.2.1. Removal of As(III) by the materials as a function of pH.

On the other hand, As(V) speciation studies showed that the oxyanionic species $H_2AsO_4^-$ was dominant within the pH region of 3.5 to 5.5. Further, within the pH region of 6.0 to 10.0, $HAsO_4^{2-}$ species was dominant in aqueous solutions. Moreover, below pH 3.5 the un–dissociated species of arsenic (H_3AsO_4) occurred mainly in solution (Lalhmunsiama et al., 2012). These species are important in deducing the mechanism involved at solid and surface interface. Figure 3.2.2 and Table 3.2.2 (e and f) clearly show that with the increase in pH from 2.0 to 4.0, there is an apparent increase in percent uptake of As(V) by BCAH and LCAH solids which further attains almost a constant percent uptake up until the pH ~7.0; and beyond pH 7.0 there is a significantly decrease percent uptake of As(V). Since the acidic dissociation of H_3AsO_4 is taking place at low pH and slowly the percent of $H_2AsO_4^-$ species increases in solutions, and also the surface carries positive charges; this gradually facilitates in sorption of As(V). The driving force, perhaps, is electrostatic attraction followed by the strong chemical bond formation. But within the pH region *Ca*. 4.5 to 6.2, the uptake of As(V) attains to its maximum value. It is due to the strong electrostatic attraction and, possibly, followed by a strong inner sphere complexation at the surface. The inner sphere complexation is suggested based on the other study as well, i.e., background electrolyte studies. The possible mechanism of As(V) sorption at the solid surface is suggested as given below in Equation 3.2:

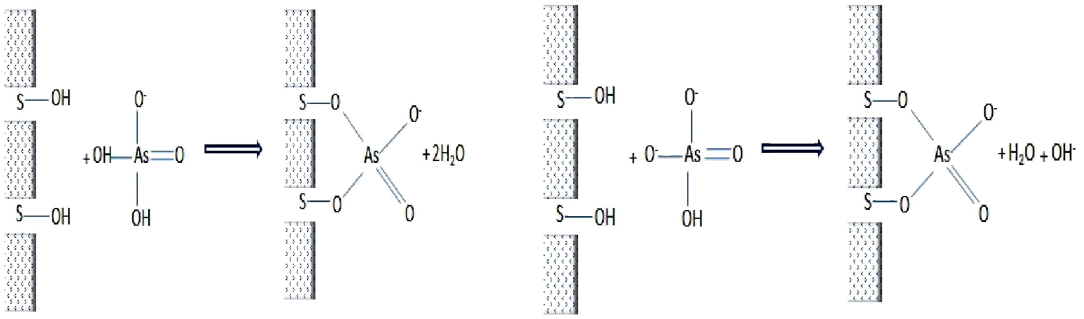

…(3.2)

pH 3.2 to 4.0 pH 4.5 to 6.0

The strong inner sphere complexation was suggested for As(V) sorption at pH 5.0 using hybrid inorgano–organo polymeric materials (Iesana et al., 2008). It was suggested that at pH 5.0 the positively charged adsorption site, i.e., $FeOH_2^+$ attracted the oxyanions of arsenic ($H_2AsO_4^-$) by the coulombic interactions, and the oxyanion could form inner sphere complexes with the surface active sites. The Poly(vinylidene fluoride) PVDF–zirconia blend flat sheet membrane also showed a high uptake of As(V) at pH *Ca*. 5.0 and was suggested for the inner sphere complexation between the arsenic oxyanions and surface functional groups (Zheng et al., 2011). Constant and high percent uptake within the pH region 4 to 10 was suggested as a strong chemisorptive uptake of As(V) by the aluminium–loaded Shirasu–zeolite (Xu et al., 2002). On further increase in pH, i.e., above pH 7.0 there is a strong decrease in percent uptake of As(V). It is due to strong electrostatic repulsions operating between the negatively charged surface and the oxyanions of As(V). This greatly hinders the sorption to proceed.

On the other hand, the HDTMA modified samples, i.e., BCH and LCH show insignificantly higher removal of As(V) compare to the virgin bentonite clay and local clay solids. It is assumed that a feeble electrostatic attraction restricts these oxyanions to enter within the interspace, and hence to form therein a strong chemical bond with the residual active sites given by the aluminol or silanol groups of clay sheets. The positive end of the HDTMA may take part in the electrostatic attraction of As(V) from aqueous solution, provided the cation is loaded in a little excess of CEC value. Similar electrostatic attraction was suggested previously for the sorption of several anions by the HDTMA modified kaolinite (Li and Bowman, 2001). Moreover, it was reported previously that the incorporation of cationic surfactants within the clay interspace enhances the anions sorption capacity, especially when the surfactant loading exceeds to the CEC of clay (Lee and Tiwari, 2012; He et al., 2010). Since, the loading of the HDTMA is regulated to 1:1 CEC of clay in this study, the surface lacks with excess charge density. Therefore, it restricts the uptake of As(V) by the solids BCH and LCH. The nature of binding could reaffirm with the background electrolyte studies as conducted in later sections.

Figure 3.2.2 and Table 3.2.2 (a–f) also demonstrated that the aluminium pillared clay samples possess remarkably a higher removal capacity for As(V) compare to the HDTMA modified samples of clay. This clearly indicates that the loaded aluminium take part predominantly in the sorption of As(V) species than the HDTMA. Therefore, the pillaring of aluminium could be a synergistic effect as it could provide good mechanical strength of the material with enhanced settling capacity along with the remarkably high removal capacity for arsenic. The pristine clay samples, i.e., bentonite and local clay, on the other hand, possess an extremely low sorption capacity for both pollutants i.e., As(III) and As(V) species. This enables that the modified clay materials, in particular, the aluminium pillared clays are having good applicability in the remediation of ground water contaminated with arsenic. Overall, BCAH and LCAH possess significantly higher removal capacity for the As(V) compare to the As(III) which is in a line to the other report where zero–valent iron was sorbing higher amount of As(V) than As(III) (Tyrovola et al., 2006).

Table 3.2.2 (a). Effect of pH on the removal of As(V) by BC.

pH	Initial conc. (mg/L)	Final conc. (mg/L)	% Removal
2	10.42	7.02	32.63
3	10.42	7.46	28.41
4	10.42	7.68	26.30
5	10.42	7.49	28.12
6	10.42	7.75	25.62
7	10.42	6.96	33.21
8	10.42	7.31	29.85
9	10.42	7.77	25.43
10	10.42	8.01	23.13

Table 3.2.2 (b). Effect of pH on the removal of As(V) by LC.

pH	Initial conc. (mg/L)	Final conc. (mg/L)	% Removal
2	10.42	8.05	22.74
3	10.42	7.75	25.62
4	10.42	7.58	27.26
5	10.42	8.16	21.69
6	10.42	7.95	23.70
7	10.42	7.82	24.95
8	10.42	8.03	22.94
9	10.42	8.52	18.23
10	10.42	8.61	17.37

Table 3.2.2 (c). Effect of pH on the removal of As(V) by BCH.

pH	Initial conc. (mg/L)	Final conc. (mg/L)	% Removal
2	10.58	7.72	27.03
3	10.58	7.28	31.19
4	10.58	6.55	38.09
5	10.58	7.12	32.70
6	10.58	7.22	31.76
7	10.58	7.33	30.72
8	10.58	7.65	27.69
9	10.58	7.61	28.07
10	10.58	8.28	21.74

Table 3.2.2 (d). Effect of pH on the removal of As(V) by LCH.

pH	Initial conc. (mg/L)	Final conc. (mg/L)	% Removal
2	10.53	7.72	29.49
3	10.53	7.28	34.10
4	10.53	6.55	41.76
5	10.53	7.55	31.27
6	10.53	7.67	30.01
7	10.53	7.92	27.39
8	10.53	8.22	24.24
9	10.53	8.64	19.83
10	10.53	8.42	22.14

Table 3.2.2 (e). Effect of pH on the removal of As(V) by BCAH.

pH	Initial conc. (mg/L)	Final conc. (mg/L)	% Removal
2	8.74	2.05	76.54
3	8.74	1.2	86.27
4	8.74	0.24	97.25
5	8.74	0.13	98.51
6	8.74	0.11	98.74
7	8.74	0.73	91.65
8	8.74	1.5	82.84
9	8.74	1.28	85.35
10	8.74	2.37	72.88

Table 3.2.2 (f). Effect of pH on the removal of As(V) by LCAH.

pH	Initial conc. (mg/L)	Final conc. (mg/L)	% Removal
2	9.70	4.43	54.33
3	9.70	3.34	65.57
4	9.70	2.47	74.54
5	9.70	2.66	72.58
6	9.70	2.88	70.31
7	9.70	2.22	77.11
8	9.70	2.64	72.78
9	9.70	3.44	64.54
10	9.70	4.12	57.53

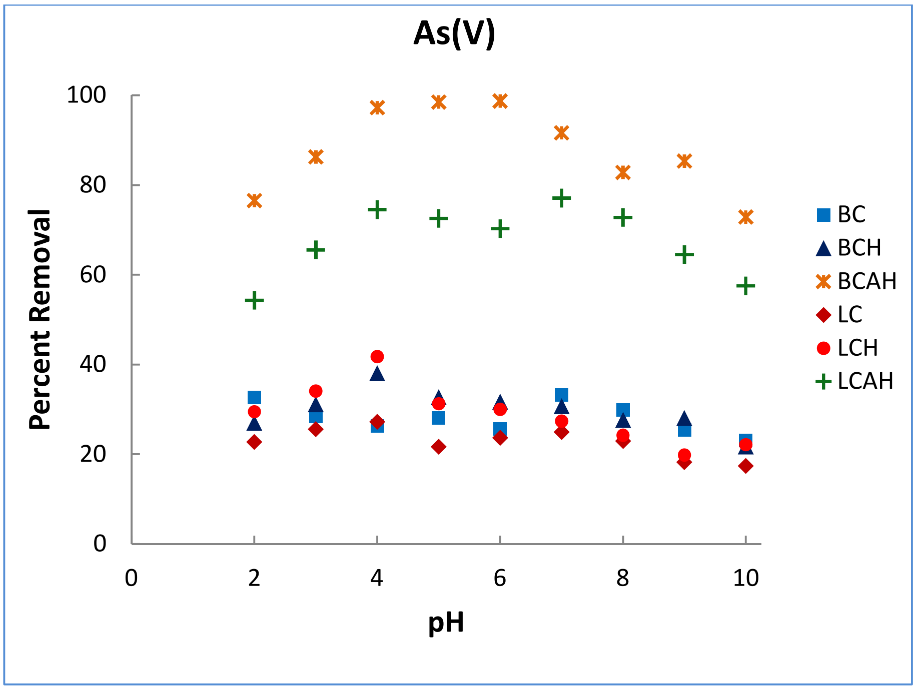

Figure 3.2.2. Removal of As(V) by the materials as a function of pH.

3.2.1.2. BPA

The pH dependence removal of BPA by the solids was studied for a wide range of solution pH (~4.0 to 10.0), taking ~10.0 mg/L BPA solution, and with a solid dose of 2 g/L. The experiments were conducted as detailed previously in Chapter 2.3.7.1. The data obtained are shown in Table 3.2.3 (a–f) and also presented graphically in Figure 3.2.3. BPA is having acid dissociation constant (pK_a) value of 9.6 to 10.2 (Yoon et al., 2003); and therefore would appreciably ionize and carry a negative charge only at higher pH levels. The pH dependence studies show that increase in pH from 4.0 to 9.0 is not significantly affecting the removal of BPA. But a slightly decrease sorption of BPA is observed on further increase in pH from the 9.0 to 10.0. Further, hybrid materials show very high percent uptake of BPA (at pH~7 *Ca*. 98% for BCH and BCAH, *Ca*. 95% for LCH and *Ca*. 90% for LCAH) under the studied pH range compare to the unmodified clay which achieves only less than 33% removal. Previously, it was reported that the organoclays with higher surfactant loadings and those prepared with longer chain surfactant molecules were less influenced by the solution pH and consistently possessed relatively high sorption capacity even under the alkaline conditions (Zheng et al., 2013). The introduction of cationic surfactant molecules within the clay structures notably enhanced the hydrophobic core with increased organophilic nature (Park et al., 2011a). The alkylammonium molecule preferentially resides at the layer surface, which leaves the organic tail radiating away from the surface and providing a hydrophobic environment (Alexandre and Dubois, 2000). This possibly causes BPA to partition at the hydrophobic core introduced.

Relatively, the Al-pillared HDTMA modified local clay shows a slightly lower uptake of BPA, possibly due to less loading of the HDTMA cation which reduces the hydrophobic core within the clay structure. LCAH also possesses lower specific pore volume and pore size which is responsible for the lower percent removal comparing to the other hybrid materials. On the other hand, BPA is present as neutral molecule if the solution pH goes below its pK_a values. For pH > pK_a, BPA molecules are mostly ionized to mono– or divalent anions with deprotonation. Hence, the repulsive electrostatic interactions between the negatively charged organo-clays and the bisphenolate anions are the main reasons for the reduction of the adsorption capacity at very high alkaline pH conditions, i.e., at pH ≈ 10.0 (Joseph et al., 2011). These results therefore enable that the hybrid materials provide a strong hydrophobic core for effective partitioning of BPA and hence a high attenuation of BPA is achieved by the modified solids from aqueous solutions.

Table 3.2.3 (a). Effect of pH on the removal of BPA by BC.

pH	Initial conc. (mg/L)	Final conc. (mg/L)	% Removal
4.09	9.93	6.81	31.47
5.71	10.00	6.74	32.64
7.04	10.00	6.74	32.64
8.17	10.07	7.01	30.34
9.10	10.42	7.57	27.34
9.69	10.07	7.49	27.58

Table 3.2.3 (b). Effect of pH on the removal of BPA by LC.

pH	Initial conc. (mg/L)	Final conc. (mg/L)	% Removal
4.13	10.35	7.92	23.49
6.21	10.35	7.99	22.82
7.69	10.42	8.19	21.34
7.81	10.42	8.33	20.01
9.81	10.42	8.82	15.34

Table 3.2.3 (c). Effect of pH on the removal of BPA by BCH.

pH	Initial conc. (mg/L)	Final conc. (mg/L)	% Removal
3.98	10.35	0.21	97.99
6.21	10.35	0.14	98.66
8.16	10.42	0.07	99.34
8.67	10.42	0.28	97.33
9.79	10.42	0.28	97.33

Table 3.2.3 (d). Effect of pH on the removal of BPA by LCH.

pH	Initial conc. (mg/L)	Final conc. (mg/L)	% Removal
3.98	10.35	0.49	95.30
6.06	10.35	0.42	95.97
7.28	10.42	0.56	94.66
9.00	10.42	0.83	92.00
10.04	10.42	1.32	87.34

Table 3.2.3 (e). Effect of pH on the removal of BPA by BCAH.

pH	Initial conc.	Final	%

Table 3.2.3 (f). Effect of pH on the removal of BPA by LCAH.

pH	Initial	Final	% Removal

	(mg/L)	conc.	Removal
		(mg/L)	
4.13	10.35	0.21	97.99
6.03	10.35	0.14	98.66
6.72	10.42	0.07	99.34
7.53	10.42	0.14	98.67
8.35	10.42	0.07	99.34
9.84	10.42	0.56	94.66

	conc.	conc.	
	(mg/L)	(mg/L)	
3.98	10.35	1.04	89.93
5.01	10.35	0.90	91.27
5.86	10.42	0.97	90.67
6.93	10.42	1.04	90.00
7.85	10.42	1.18	88.66
9.96	10.42	1.67	84.00

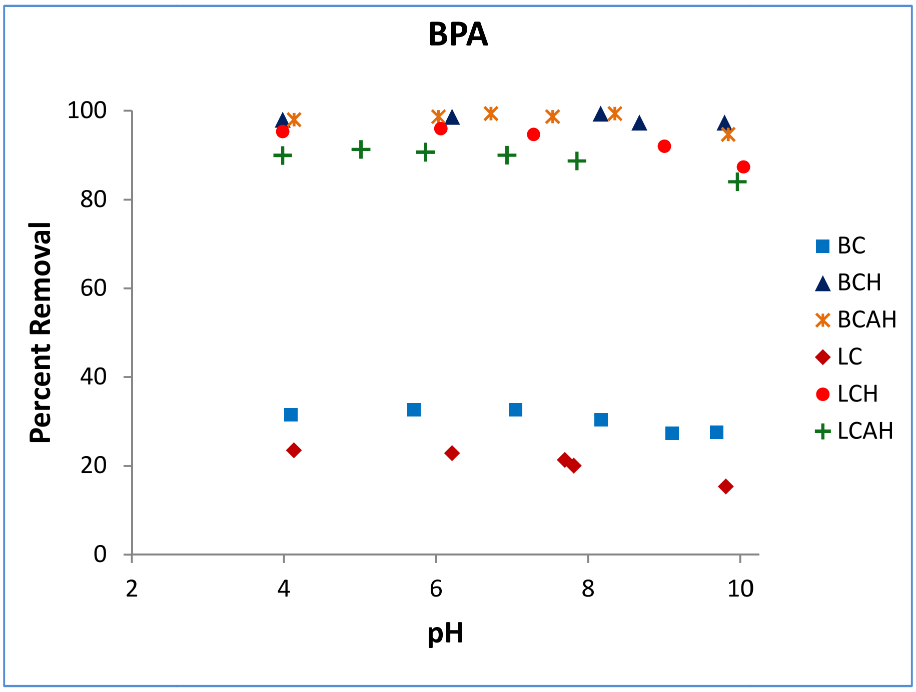

Figure 3.2.3. Removal of BPA by the materials as a function of pH.

3.2.1.3. EE2

The pH dependence removal of EE2 by these hybrid materials along with the pristine clay was studied for a pH range from ~4.0 to 10.0 and the results are returned in Table 3.2.4 (a–f) and presented graphically in Figure 3.2.4. EE2 is having acid dissociation constant (pK_a) value of 10.5 (Joseph et al., 2011; Al–Khateeb et al., 2014); and thus would carry a negative charge only at higher pH values. The pH dependence studies show that increase in pH from 4.0 to 9.0 insignificantly affects the removal of EE2. Hybrid materials show a very high percent uptake of EE2 (at pH~7 *Ca*. 94% for BCH, BCAH, LCH and *Ca*. 84% for LCAH) under the studied pH range comparing to the unmodified clay (< 43% removal). The introduction of HDTMA within the clay structures provides the hydrophobic core with enhanced organophilic nature which possibly causes EE2 to partition at the hydrophobic core introduced. However, LCAH sample shows relatively lower uptake of EE2 which is due to the less loading of the HDTMA cation which reduces the hydrophobic core within the clay structure; finds again in a line with the lower specific pore volume and pore size compared to the other hybrid materials. A decrease in percent removal is observed as the solution pH is increased to ~10.0; could be attributed to the repulsion between the ionized or negatively charged EE2 with the negatively charged solid surface. Joseph et al, (2011) and Al-Khateeb et al, (2014) also reported that adsorption of EE2 on carbon nanotubes was not notably affected by change in pH up to 9. However, a slight decreased in adsorption was observed on increasing the pH to 11.0. They also suggested that the hydrophobic interaction was more prominent driving force in the adsorption process. A similar observation was reported by Feng et al. (2010) on the adsorption of EE2 onto the inactivated sewage sludge.

Table 3.2.4 (a). Effect of pH on the removal of EE2 by BC.

pH	Initial	Final	%

Table 3.2.4 (b). Effect of pH on the removal of EE2 by LC.

pH	Initial	Final	%

	conc. (mg/L)	**conc. (mg/L)**	**Removal**
4.17	5.69	3.62	36.36
6.15	5.69	3.28	42.43
8.30	5.69	3.28	42.43
9.24	5.52	3.28	40.62
9.84	5.52	3.62	34.37

	conc. (mg/L)	**conc. (mg/L)**	**Removal**
4.01	5.69	3.97	30.30
6.44	5.69	3.62	36.36
7.61	5.69	3.62	36.36
9.12	5.52	3.79	31.25
9.81	5.52	4.14	25.00

Table 3.2.4 (c). Effect of pH on the removal of EE2 by BCH.

pH	**Initial conc. (mg/L)**	**Final conc. (mg/L)**	**% Removal**
4.07	5.69	0.52	90.91
6.61	5.69	0.34	93.94
7.96	5.69	0.34	93.94
8.14	5.69	0.34	93.94
9.24	5.52	0.86	84.38
9.77	5.52	1.03	81.25

Table 3.2.4 (d). Effect of pH on the removal of EE2 by LCH.

pH	**Initial conc. (mg/L)**	**Final conc. (mg/L)**	**% Removal**
4.06	5.69	0.69	87.87
6.21	5.69	0.35	93.94
7.43	5.69	0.52	90.91
8.17	5.52	0.52	90.63
10.05	5.52	1.38	75.00

Table 3.2.4 (e). Effect of pH on the removal of EE2 by BCAH.

pH	**Initial conc. (mg/L)**	**Final conc. (mg/L)**	**% Removal**
4.07	5.69	0.52	90.91
6.00	5.69	0.35	93.94
6.71	5.69	0.35	93.94
7.81	5.52	0.35	93.75
8.57	5.52	0.52	90.63
10.14	5.52	1.03	81.25

Table 3.2.4 (f). Effect of pH on the removal of EE2 by LCAH.

pH	**Initial conc. (mg/L)**	**Final conc. (mg/L)**	**% Removal**
4.24	5.69	0.86	84.85
5.27	5.69	0.86	84.85
5.53	5.69	0.86	84.85
6.67	5.52	0.86	84.38
7.97	5.69	1.03	81.82
9.77	5.52	1.55	71.88

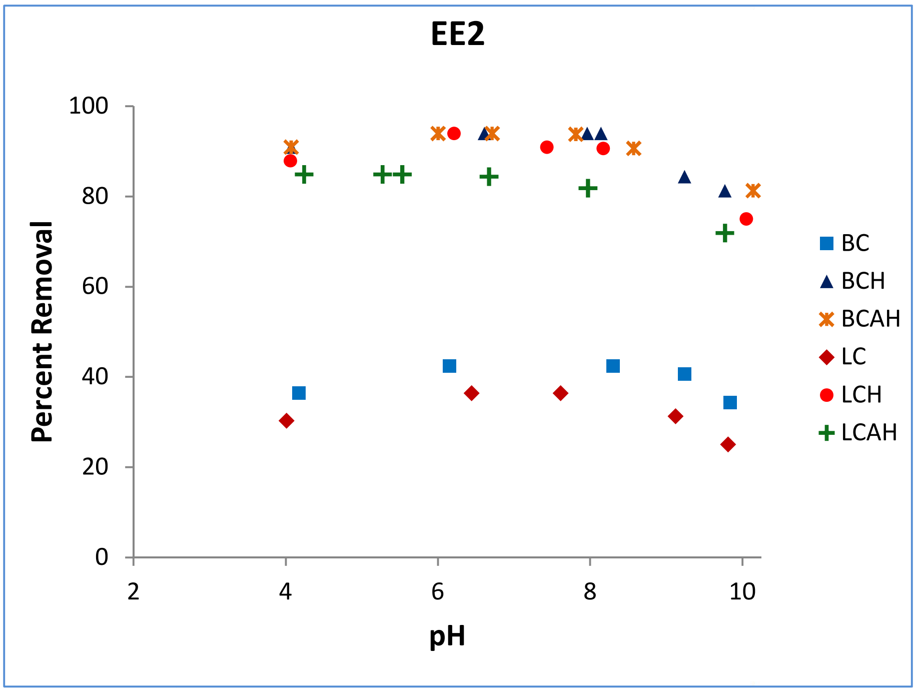

Figure 3.2.4. Removal of EE2 by the materials as a function of pH.

3.2.1.4. DFS

The pH dependence sorption data obtained for DFS are tabulated in Table 3.2.5 (a–f) and also presented in Figure 3.2.5. Diclofenac is having low dipole moment, and low acid dissociation constant (pK_a) value of 4.21 (Meloun et al., 2007). This implies that diclofenac carries net negative charge beyond pH 4.2. The sorption of DFS by these hybrid materials show that very high percent uptake (at pH~7, *Ca*. 98% for BCH, BCAH, LCH and *Ca*. 84% for LCAH) is obtained under the studied pH range. Very high percent removal of DFS achieved is not remarkably affected by the solution pH although a slightly decrease percent uptake is observed at very high pH values by these hybrid materials. The uptake is therefore almost independent of the charge carried by the solid or solute species. Therefore, the possible mechanism of diclofenac sodium uptake by these modified solids is primarily demonstrated by the fact that the introduction of organic cation (HDTMA) with the clay network enhances the organophilic behaviour of the surface having a strong hydrophobic end.

This possibly causes DFS to partition at the hydrophobic core introduced. However, somewhat decreased percent removal is observed, at least in the LCAH sample, on further increase in pH, i.e., above pH ~9.0. Relatively, LCAH shows lower uptake of DFS possibly due to less loading of the HDTMA cation which reduces the hydrophobic core within the clay structure. On the other hand, the pristine bentonite and local clay show much lower uptake (< 30% at pH~7) of DFS which is further decreased with increasing the solution pH and reached about 18% at pH 10.1. These results therefore enabled that the hybrid materials provide a strong hydrophobic core for the effective partitioning of DFS and hence a high attenuation of diclofenac is achieved by the modified solids.

Table 3.2.5 (a). Effect of pH on the removal of DFS by BC.

pH	Initial conc. (mg/L)	Final conc. (mg/L)	% Removal
3.97	1.88	1.32	29.82
6.15	8.38	5.81	30.70
8.36	9.51	7.26	23.61
8.14	9.67	7.33	24.23
9.30	9.57	7.66	20.00
10.12	9.67	7.66	20.82

Table 3.2.5 (b). Effect of pH on the removal of DFS by LC.

pH	Initial conc. (mg/L)	Final conc. (mg/L)	% Removal
3.87	2.11	1.49	29.69
6.21	8.48	6.01	29.19
7.19	10.40	7.43	28.57
7.84	10.10	7.56	25.16
10.11	10.46	8.61	17.66

Table 3.2.5 (c). Effect of pH on the removal of DFS by BCH.

pH	Initial conc. (mg/L)	Final conc. (mg/L)	% Removal
3.87	2.01	0.07	96.72
6.12	9.31	0.10	98.94
7.93	9.27	0.13	98.58
8.22	10.03	0.07	99.34
8.74	10.13	0.20	98.05
9.74	10.13	0.30	97.07

Table 3.2.5 (d). Effect of pH on the removal of DFS by LCH.

pH	Initial conc. (mg/L)	Final conc. (mg/L)	% Removal
3.83	2.11	0.10	95.31
5.84	8.48	0.17	98.05
7.44	10.40	0.46	95.56
8.12	10.10	0.59	94.12
10.11	10.46	1.42	86.44

Table 3.2.5 (e). Effect of pH on the removal of DFS by BCAH.

pH	Initial conc. (mg/L)	Final conc. (mg/L)	% Removal
4.12	2.01	0.10	95.08
4.99	9.27	0.13	98.58
6.31	10.03	0.17	98.36
8.06	10.03	0.30	97.04
10.12	10.13	0.63	93.81

Table 3.2.5 (f). Effect of pH on the removal of DFS by LCAH.

pH	Initial conc. (mg/L)	Final conc. (mg/L)	% Removal
3.85	2.11	0.26	87.50
5.84	8.48	1.06	87.55
7.27	10.40	1.68	83.81
8.82	10.10	2.01	80.07
10.07	10.46	3.53	66.25

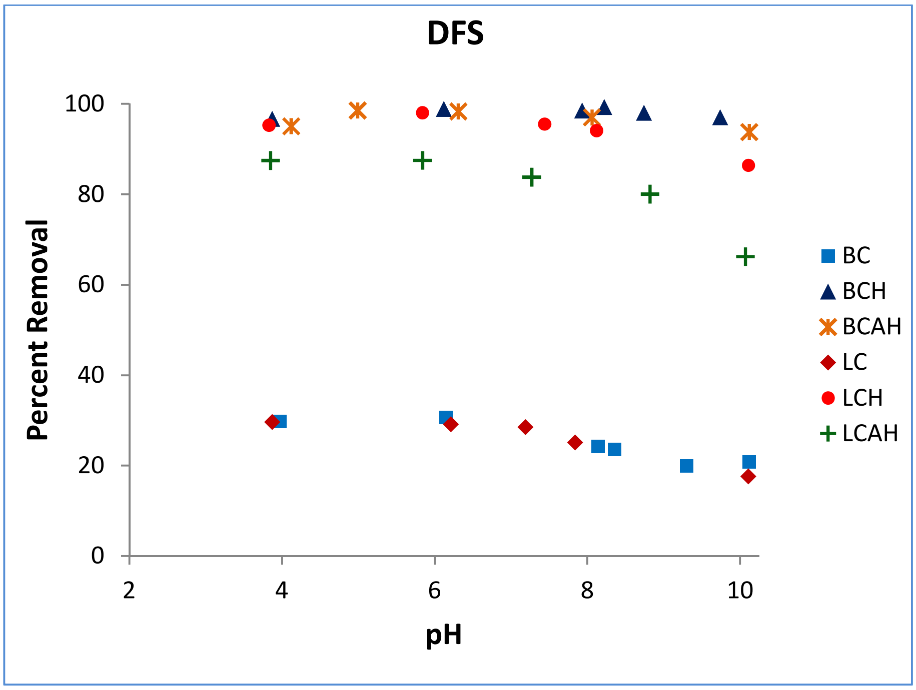

Figure 3.2.5. Removal of DFS by the materials as a function of pH.

3.2.1.5. TC

The pH dependence sorption data of TC are shown in Table 3.2.6 (a–f) and presented graphically in Figure 3.2.6. TC is having several polar/ionizable groups; including amino, carboxyl, phenol, alcohol and ketone. It is having three acid dissociation constants (pK_a) values of 3.3, 7.7, and 9.7; and exist as a cationic, zwitterionic and anionic species under acidic, moderately acidic to neutral, and alkaline conditions, respectively (Gao et al., 2012). The pH dependence studies indicate that TC adsorption by the modified and unmodified samples show different trends. The hybrid materials show a very high percent uptake of TC (at pH~7 *Ca*. 99% for BCH, BCAH and LCH; and *Ca*. 92% for LCAH) under the studied pH range. It is noted that increase in pH from 4.0 to 10.0, insignificantly affect the removal of TC employing the modified materials, even though a slight decrease in percent removal at lower and higher pH values is observed. The decrease in percent removed could be ascribed due to the electrostatic repulsion between the ionized TC and oppositely charged solid samples. Therefore, the possible mechanism of TC uptake by these modified solids is the partitioning mechanism. Unmodified clay samples, however, show markedly decrease percent removal on increasing the pH from 4.0 to 10.0. The removal is higher at pH 4 (*Ca*. 98%), decrease to some extent at *Ca*. pH 6 (*Ca*. 70% removal) and remains nearly constant up to pH 8.5, and then there is a sharp decrease at *Ca*. pH 10 (< 30% removal). At lower pH, the dominant TC species is the cationic species TCH_3^+ and electrostatic interaction is favored for the high TCH_3^+ adsorption onto the positively charged surface; while at moderate pH range, the zwitterionic species $TCH_3^{\pm}$ which carries no net charge is the dominant TC species. The lower removal at higher pH is attributed to the repulsion of TCH^- (or even TCH^{2-}) anions and the negatively charged surfaces (Parolo et al., 2008; Gao et al., 2012).

Table 3.2.6 (a). Effect of pH on the removal of TC by BC.

pH	Initial conc. (mg/L)	Final conc. (mg/L)	% Removal
4.44	9.50	0.18	98.10
6.27	9.91	2.67	73.05
7.40	10.05	3.26	67.57
8.16	10.05	3.30	67.12
8.50	10.00	3.58	64.25
8.64	9.55	3.67	61.61
9.83	9.14	6.52	28.71

Table 3.2.6 (b). Effect of pH on the removal of TC by LC.

pH	Initial conc. (mg/L)	Final conc. (mg/L)	% Removal
4.01	9.50	0.23	97.62
6.07	10.05	2.94	70.72
6.22	9.00	2.76	69.35
7.50	10.05	3.30	67.12
7.94	10.00	3.39	66.06
8.58	9.10	4.03	55.72
9.85	9.14	6.88	24.75

Table 3.2.6 (c). Effect of pH on the removal of TC by BCH.

pH	Initial conc. (mg/L)	Final conc. (mg/L)	% Removal
4.01	9.46	2.44	74.17
5.62	10.05	0.50	95.04
6.54	10.05	0.14	98.65
7.70	10.00	0.14	98.64
9.19	9.10	0.63	93.04
10.04	9.10	1.67	81.59

Table 3.2.6 (d). Effect of pH on the removal of TC by LCH.

pH	Initial conc. (mg/L)	Final conc. (mg/L)	% Removal
3.96	9.50	2.31	75.71
5.89	10.05	0.41	95.95
6.96	10.05	0.09	99.10
7.36	10.00	0.05	99.55
9.37	9.10	0.41	95.53
10.03	9.10	1.45	84.08

Table 3.2.6 (e). Effect of pH on the removal of TC by BCAH.

pH	Initial conc. (mg/L)	Final conc. (mg/L)	% Removal
4.00	9.00	2.44	72.87
4.65	9.14	1.40	84.65
5.37	10.05	0.95	90.54
6.91	10.05	0.09	99.10
7.66	10.00	0.09	99.10
8.80	9.10	0.00	100.00
9.97	9.10	1.04	88.55

Table 3.2.6 (f). Effect of pH on the removal of TC by LCAH.

pH	Initial conc. (mg/L)	Final conc. (mg/L)	% Removal
4.24	9.14	2.81	69.31
4.38	9.50	2.54	73.32
5.26	10.05	1.27	87.39
5.92	10.05	0.95	90.54
6.87	10.00	0.77	92.31
8.94	9.10	1.09	88.06
10.06	9.10	2.94	67.66

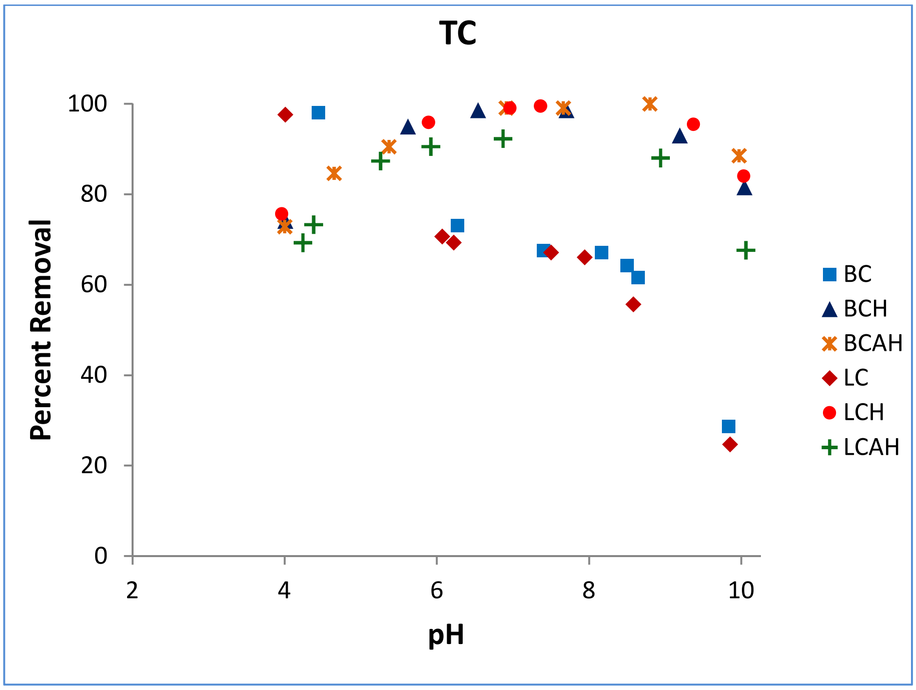

Figure 3.2.6. Removal of TC by the materials as a function of pH.

3.2.2. Effect of sorptive concentration

3.2.2.1. As(III) and As(V)

The concentration dependence removal of As(III) and As(V) was studied for a wide range of initial arsenic concentration, i.e., from ~2.0 mg/L to 15.0 mg/L for As(III) and from ~2.0 mg/L to 18.0 mg/L for As(V) at a constant pH 4.5. The experiments were conducted as discussed in Chapter 2.3.7.2. Results are presented in Table 3.2.7 (a–d) and 3.2.8 (a–d) and also shown graphically in Figures 3.2.7 and 3.2.8, respectively, for As(III) and As(V). It is revealed that increasing the concentration of arsenic, apparently causes to decrease the percent uptake of arsenic from aqueous solutions. More quantitatively, on increasing the As(III) concentration from 2.46 to 15.60, the corresponding decrease in As(III) is from 77.64% to 32.18% for BCH solid, from 70.73% to 28.21% for BCAH solid, from 56.50% to 20.83% for LCH solid and from 52.44% to 22.82% for LCAH solids. Similarly, on increasing the initial As(V) concentrations, i.e., from 3.66 mg/L to 17.92 mg/L for BCH and LCH; and from 1.82 mg/L to 18.66 mg/L for BCAH and LCAH, the corresponding decrease in percent removal of As(V) is from 97.81% to 35.88% for BCH, from 100.00% to 82.26% for BCAH, from 74.86 to 17.35% for LCH, and from 100.00% to 45.55% for LCAH solids. The results indicate the strong affinity of these hybrid materials towards the arsenic species in aqueous solutions.

Table 3.2.7 (a). Effect of As(III) initial concentration on the removal by BCH.

Initial conc. (mg/L)	Final conc. (mg/L)	% Removal
2.46	0.55	77.64
4.99	1.75	64.93
7.74	3.76	51.42
10.10	5.45	46.04
15.60	10.58	32.18

Table 3.2.7 (b). Effect of As(III) initial concentration on the removal by LCH.

Initial conc. (mg/L)	Final conc. (mg/L)	% Removal
2.46	1.07	56.50
4.99	2.34	53.11
7.74	4.62	40.31
10.10	6.58	34.85
15.60	12.35	20.83

Table 3.2.7 (c). Effect of As(III) initial concentration on the removal by BCAH.

Initial conc. (mg/L)	Final conc. (mg/L)	% Removal
2.46	0.72	70.73
4.99	1.95	60.92
7.74	4.16	46.25
10.10	5.79	42.67
15.60	11.20	28.21

Table 3.2.7 (d). Effect of As(III) initial concentration on the removal by LCAH.

Initial conc. (mg/L)	Final conc. (mg/L)	% Removal
2.46	1.17	52.44
4.99	2.68	46.29
7.74	4.87	37.08
10.10	6.75	33.17
15.60	12.04	22.82

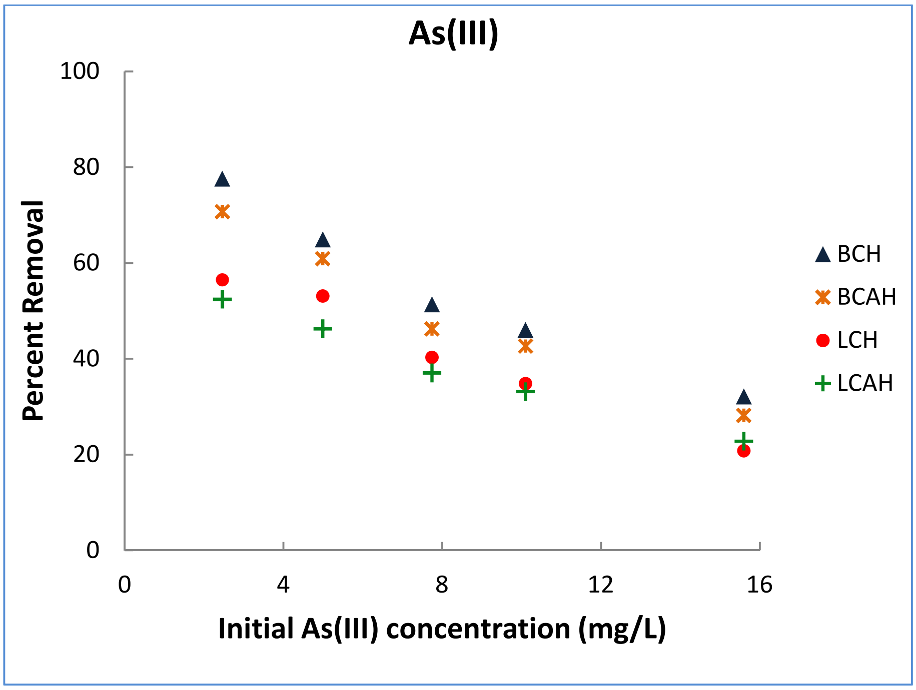

Figure 3.2.7. Removal of As(III) by the hybrid materials as a function of initial As(III) concentration.

Table 3.2.8 (a). Effect of As(V) initial concentration on the removal by BCH.

Initial conc. (mg/L)	Final conc. (mg/L)	% Removal
3.66	0.08	97.81
6.48	2.66	58.95
10.25	4.95	51.71
13.00	7.03	45.92
17.92	11.49	35.88

Table 3.2.8 (b). Effect of As(V) initial concentration on the removal by LCH.

Initial conc. (mg/L)	Final conc. (mg/L)	% Removal
3.66	0.92	74.86
6.48	3.60	44.44
10.25	6.41	37.46
13.00	8.30	36.15
17.92	13.46	24.89

Table 3.2.8 (c). Effect of As(V) initial concentration on the removal by BCAH.

Initial conc. (mg/L)	Final conc. (mg/L)	% Removal
1.82	0	100.00
4.07	0	100.00
6.71	0.24	96.42
8.73	0.65	92.55
13.14	1.40	89.35
18.66	3.31	82.26

Table 3.2.8 (d). Effect of As(V) initial concentration on the removal by LCAH.

Initial conc. (mg/L)	Final conc. (mg/L)	% Removal
1.82	0	100.00
4.07	0	100.00
6.71	0.49	92.70
8.73	2.00	77.09
13.14	5.91	55.02
18.66	10.16	45.55

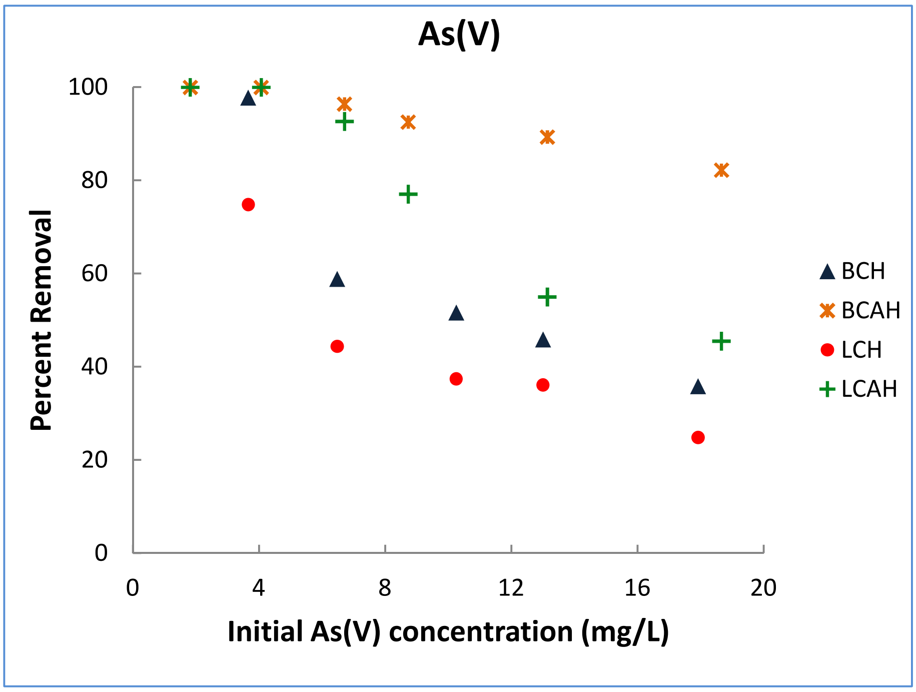

Figure 3.2.8. Removal of As(V) by the hybrid materials as a function of initial As(V) concentration.

3.2.2.2. BPA

The concentration dependence removal of BPA was studied for a wide range of initial BPA concentrations from *Ca.* 1.0 mg/L to 20.0 mg/L, at pH ~7.0, and with a solid dose of 2 g/L. The detailed experimental procedures are given in Chapter 2.3.7.2, and the results obtained are presented in Tables 3.2.9 (a–d) and Figure 3.2.9. Figure reveals that the very high percent uptake of BPA is not much affected by increasing the initial BPA concentration in the concentration range studied. The high percent removal of BPA at varying initial BPA concentrations indicates the strong affinity of hybrid materials towards the attenuation of BPA from aqueous solution. However, a slightly less removal of BPA is observed using the LCAH solid. This is due to the less loading of HDTMA with the clay solids and the lower specific pore volume and pore size. The results are consistent with the pH dependence study. Further, a bit of lower percent removal of BPA is observed at lower concentration. Quantitatively, on increasing the BPA concentration from 1.18 mg/L to 20.00 mg/L, the corresponding increase in percent removal is from 94.16% to 99.66%, 94.16% to 98.96%, 88.23% to 97.57% and 81.25% to 94.77%; for BCH, BCAH, LCH and LCAH solids, respectively.

Table 3.2.9 (a). Effect of BPA initial concentration on the removal by BCH.

Initial conc. (mg/L)	Final conc. (mg/L)	% Removal
1.18	0.07	94.16
2.01	0.07	96.57
5.07	0.14	97.26
7.64	0.21	97.28
10.28	0.07	99.33
15.21	0.07	99.55
20.00	0.07	99.66

Table 3.2.9 (b). Effect of BPA initial concentration on the removal by LCH.

Initial conc. (mg/L)	Final conc. (mg/L)	% Removal
1.18	0.14	88.23
2.01	0.14	93.10
5.07	0.21	95.90
7.64	0.35	95.46
10.28	0.42	95.94
15.21	0.49	96.80
20.00	0.49	97.57

Table 3.2.9 (c). Effect of BPA initial concentration on the removal by BCAH.

Initial conc. (mg/L)	Final conc. (mg/L)	% Removal
1.18	0.07	94.16
2.01	0.07	96.57
5.07	0.07	98.64
7.64	0.14	98.18
10.28	0.14	98.65
15.21	0.21	98.63
20.00	0.21	98.96

Table 3.2.9 (d). Effect of BPA initial concentration on the removal by LCAH.

Initial conc. (mg/L)	Final conc. (mg/L)	% Removal
1.11	0.21	81.25
2.08	0.28	86.66
5.21	0.56	89.33
7.08	0.76	89.22
9.72	0.90	90.71
15.07	1.04	93.09
19.93	1.04	94.77

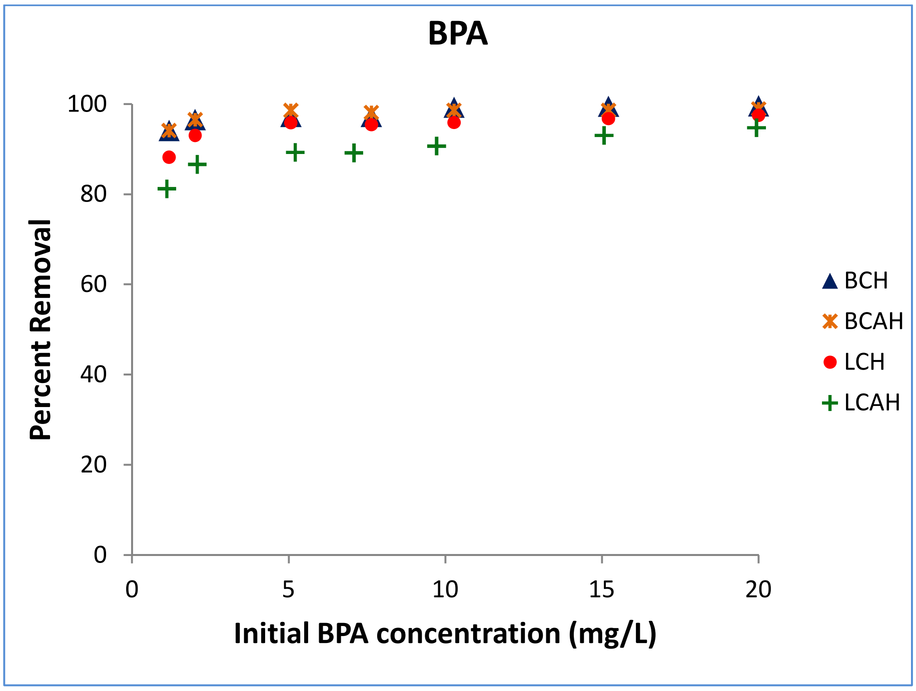

Figure 3.2.9. Removal of BPA by the hybrid materials as a function of initial BPA concentration.

3.2.2.3. EE2

The concentration dependence removal of EE2 was performed with the initial concentration range of 1.0 mg/L to 10.0 mg/L, at constant pH ~7.0, with a solid dose of 2 g/L. The results obtained are shown in Tables 3.2.10 (a–d) and Figure 3.2.10. The figure and tables reveal that increasing the initial EE2 concentration in the studied concentration range insignificantly affects the very high percent uptake of EE2 from aqueous solutions. The results point to the strong affinity of hybrid materials towards the attenuation of EE2. For the LCAH solid, the percent removal of EE2 is lower compare to the other solids possibly due to the less loading of HDTMA. Moreover, a decrease percent removal of EE2 is observed at the lower concentrations. It is observe from the table that increasing the EE2 concentration from 1.03 mg/L to 10.17 mg/L, the corresponding increase in percent uptake obtained is from 83.38% to 93.22% for BCH, from 83.33% to 89.83% for BCAH, from 83.33% to 93.22% for LCH and from 66.67% to 83.05% for LCAH solid, respectively.

Table 3.2.10 (a). Effect of EE2 initial concentration on the removal by BCH.

Initial conc. (mg/L)	Final conc. (mg/L)	% Removal
1.03	0.17	83.38
2.24	0.17	92.32
5.34	0.34	93.55
7.24	0.52	92.86
10.17	0.69	93.22

Table 3.2.10 (b). Effect of EE2 initial concentration on the removal by LCH.

Initial conc. (mg/L)	Final conc. (mg/L)	% Removal
1.03	0.17	83.33
2.24	0.17	92.31
5.34	0.52	90.32
7.24	0.69	90.48
10.17	0.69	93.22

Table 3.2.10 (c). Effect of EE2 initial concentration on the removal by BCAH.

Initial conc. (mg/L)	**Final conc. (mg/L)**	**% Removal**
1.03	0.17	83.33
2.24	0.34	84.62
5.34	0.34	93.55
7.24	0.69	90.48
10.17	1.03	89.83

Table 3.2.10 (d). Effect of EE2 initial concentration on the removal by LCAH.

Initial conc. (mg/L)	**Final conc. (mg/L)**	**% Removal**
1.03	0.34	66.67
2.24	0.52	76.92
5.34	0.86	83.87
7.24	1.03	85.71
10.17	1.72	83.05

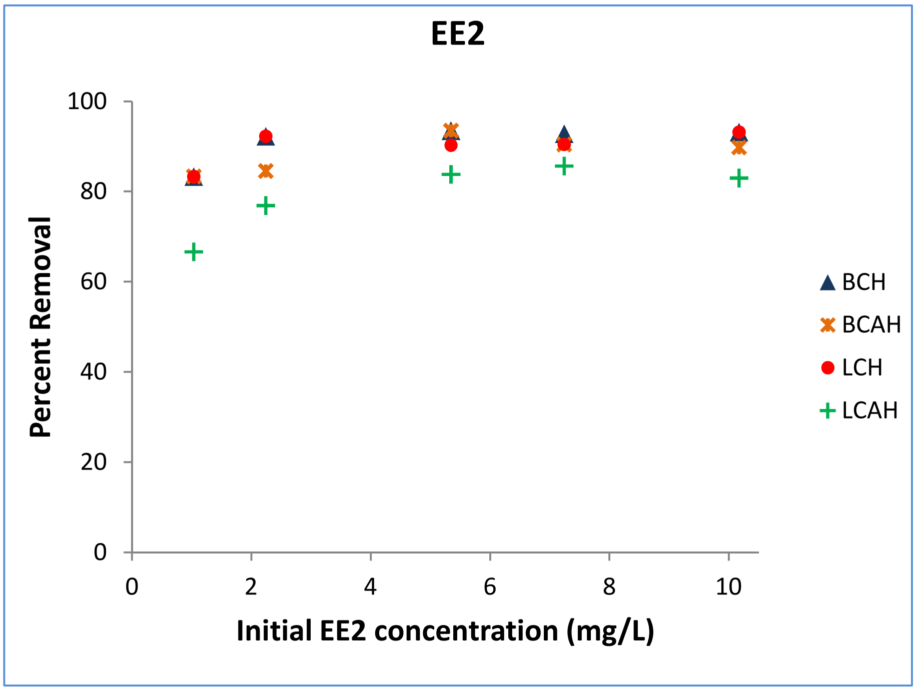

Figure 3.2.10. Removal of EE2 by the hybrid materials as a function of initial EE2 concentration.

3.2.2.4. DFS

The concentration dependence removal of DFS was assessed for the initial diclofenac concentration of *Ca*. 1.0 mg/L to 20.0 mg/L, at constant pH ~7.0, with a solid dose of 2 g/L. The results obtained are tabulated in Table 3.2.11 (a–d) and then presented graphically in Figure 3.2.11. The figure clearly indicates that increasing the concentration of DFS from 1.0 to 20.0 mg/L could not notably affect the percent removal of DFS from aqueous solutions. These results show a strong affinity of hybrid materials towards the sorbing species of DFS. However, a lower removal of DFS is observed (i.e., around 85%) with the LCAH solid, which is due to the less loading of HDTMA with the clay solid and the lower specific pore volume and pore size. More quantitatively, on increasing the DFS concentration from 1.16 mg/L to 20.00 mg/L, the corresponding increase in percent removal obtained is from 97.14% to 98.68% for BCH solid and from 94.29% to 98.68% for BCAH solids, respectively. Similarly, increasing the DFS concentration from 1.19 mg/L to 19.97 mg/L, the corresponding increase in percent uptake is from 94.44% to 97.36% for LCH solid and from 80.56% to 86.61% for LCAH solids.

Table 3.2.11 (a). Effect of DFS initial concentration on the removal by BCH.

Initial conc. (mg/L)	Final conc. (mg/L)	% Removal
1.16	0.03	97.14
2.11	0.07	96.88
5.02	0.03	99.34
6.83	0.13	98.07
10.26	0.13	98.71
14.85	0.17	98.89
20.00	0.26	98.68

Table 3.2.11 (b). Effect of DFS initial concentration on the removal by LCH.

Initial conc. (mg/L)	Final conc. (mg/L)	% Removal
1.19	0.07	94.44
2.34	0.10	95.77
5.22	0.10	98.10
7.43	0.17	97.78
10.26	0.23	97.75
15.38	0.40	97.43
19.97	0.53	97.36

Table 3.2.11 (c). Effect of DFS initial concentration on the removal by BCAH.

Initial conc. (mg/L)	Final conc. (mg/L)	% Removal
1.16	0.07	94.29
2.11	0.07	96.88
5.02	0.10	98.03
6.83	0.17	97.58
10.26	0.17	98.39
14.85	0.20	98.67
20.00	0.26	98.68

Table 3.2.11 (d). Effect of DFS initial concentration on the removal by LCAH.

Initial conc. (mg/L)	Final conc. (mg/L)	% Removal
1.19	0.23	80.56
2.34	0.33	85.92
5.21	0.73	86.08
7.43	0.92	87.56
10.26	1.32	87.14
15.38	2.01	86.91
19.97	2.67	86.61

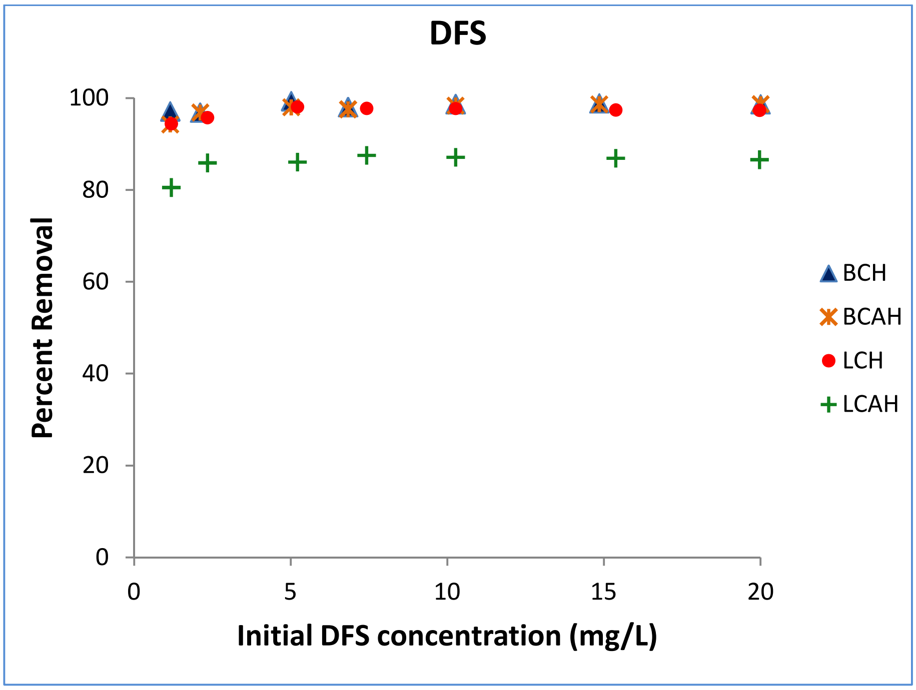

Figure 3.2.11. Removal of DFS by the hybrid materials as a function of initial DFS concentration.

3.2.2.5. TC

The concentration dependence removal of TC was studied varying the initial TC concentrations from 1.0 mg/L to 20.0 mg/L, at constant pH ~7.0, and with a solid dose of 2 g/L. The results are shown in Table 3.2.12 (a–d) and also presented graphically in Figure 3.2.12. Increasing the concentration of TC from 1.0 to 20.0 mg/L, insignificantly affects the percent uptake of TC within the studied concentration range. Again, relatively slightly less uptake of TC is obtained by the LCAH solid. These results are in consistent with the pH dependence study. However, slightly less percent uptake is observed on increasing the initial TC concentration. The high percent removal achieves at varied initial TC concentrations indicates the strong affinity of the hybrid materials towards the remediation of TC from aqueous solution.

Table 3.2.12 (a). Effect of TC initial concentration on the removal by BCH.

Initial conc. (mg/L)	Final conc. (mg/L)	% Removal
0.95	0.00	100.00
2.22	0.00	100.00
5.34	0.00	100.00
7.19	0.18	97.48
10.00	0.36	96.38
14.98	0.63	95.77
19.82	1.18	94.06

Table 3.2.12 (b). Effect of TC initial concentration on the removal by LCH.

Initial conc. (mg/L)	Final conc. (mg/L)	% Removal
0.95	0.00	100.00
2.22	0.05	97.97
5.34	0.09	98.31
7.20	0.14	98.11
10.00	0.14	98.64
14.98	0.32	97.88
19.82	0.54	97.26

Table 3.2.12 (c). Effect of TC initial concentration on the removal by BCAH.

Initial conc. (mg/L)	Final conc. (mg/L)	% Removal
0.95	0.00	100.00
2.22	0.00	100.00
5.34	0.09	98.31
7.20	0.23	96.86
10.00	0.36	96.38
14.98	0.63	95.77
19.82	1.13	94.29

Table 3.2.12 (d). Effect of TC initial concentration on the removal by LCAH.

Initial conc. (mg/L)	Final conc. (mg/L)	% Removal
0.95	0.00	100.00
2.22	0.00	100.00
5.34	0.23	95.77
7.20	0.41	94.34
10.00	0.95	90.50
14.98	1.67	88.82
19.82	2.40	87.90

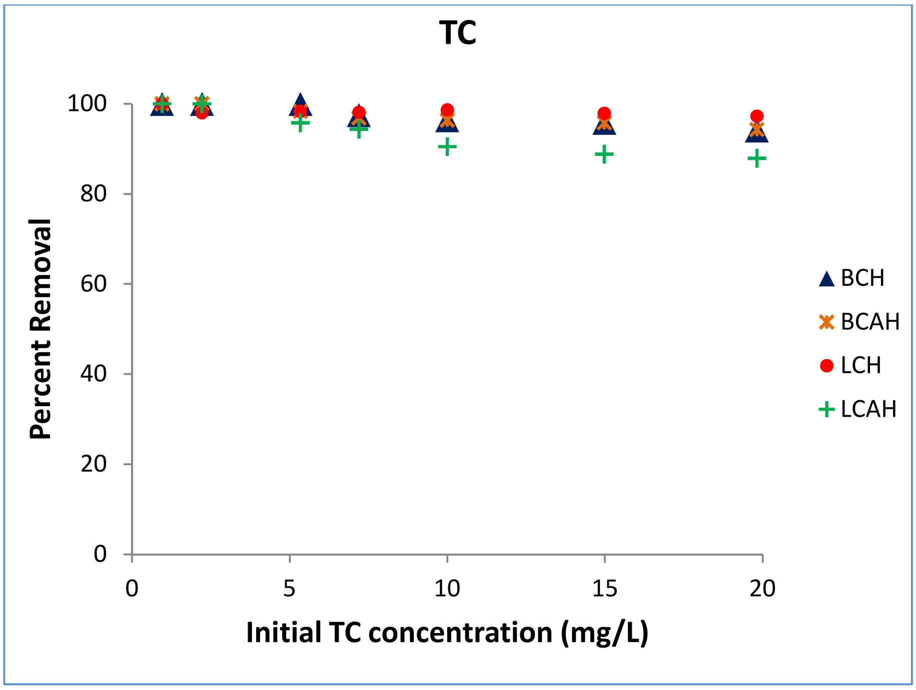

Figure 3.2.12. Removal of TC by the hybrid materials as a function of initial TC concentration.

3.2.3. Adsorption isotherm modeling

The equilibrium state concentration dependence sorption data of EDCs showed very high and almost constant percent removal in the studied concentration ranges. Since no significant effect on the percent uptake on increasing the EDCs concentration is obtained, therefore, this restricts to perform the adsorption isotherm modeling studies. The concentration dependence sorption data of As(III) and As(V) (*cf.* Section 3.2.2.1), are utilized in isotherm modeling studies using the standard Freundlich and Langmuir adsorption isotherm models (*cf.* Section 2.3.8, Eq. 2.3 and 2.4), in their linearize form, and the results are represented in Figure 3.2.13 to 3.2.16. Modeling studies indicate that Freundlich adsorption isotherm is not fitted well with the equilibrium state data since the R^2 values obtained are very low. However, the data are fitted well to the Langmuir adsorption model. Therefore, the Langmuir constants are evaluated and returned in Table 3.2.13. The results indicate that the Langmuir monolayer capacity for As(V) by the BCAH and LCAH solids is extremely high compare to the corresponding BCH and LCH solids. However, the hybrid materials, i.e., BCH, LCH, BCAH and LCAH possess an almost similar sorption capacity for As(III). These results are in line with our previous observation on the pH dependence studies. Further, Langmuir constant 'b' is obtained for these systems which reflects the strength and affinity of these solids towards the adsorbing species (Gupta et al., 2005).

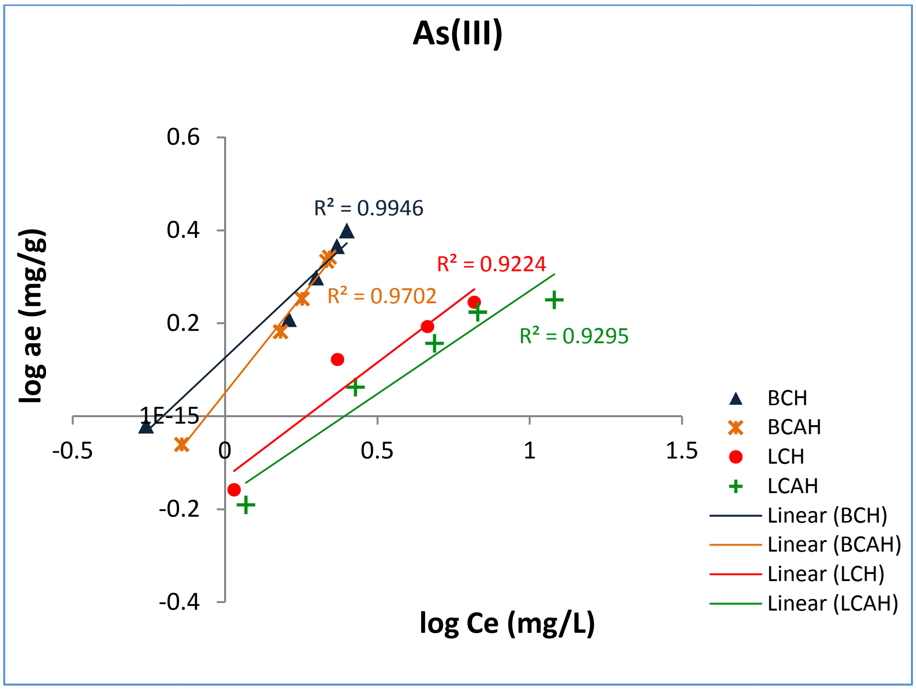

Figure 3.2.13. Freundlich adsorption isotherm for the removal of As(III).

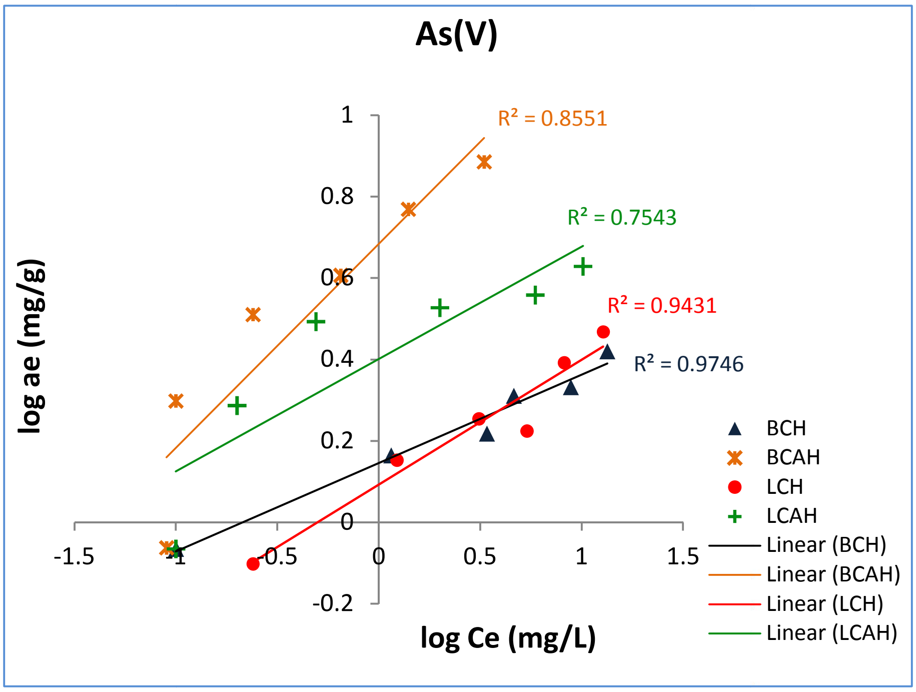

Figure 3.2.14. Freundlich adsorption isotherm for the removal of As(V).

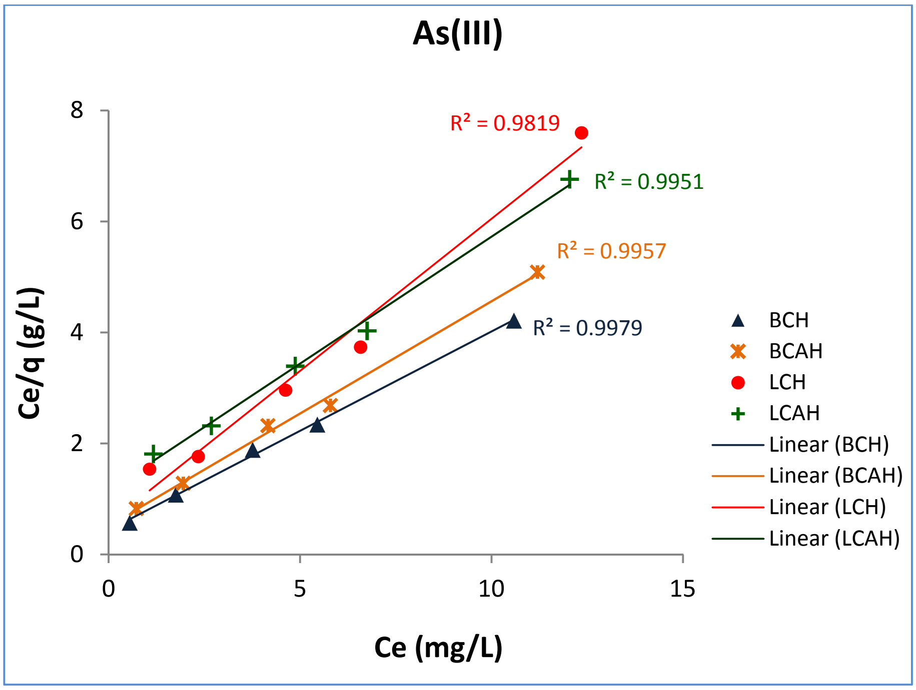

Figure 3.2.15. Langmuir adsorption isotherm for the removal of As(III).

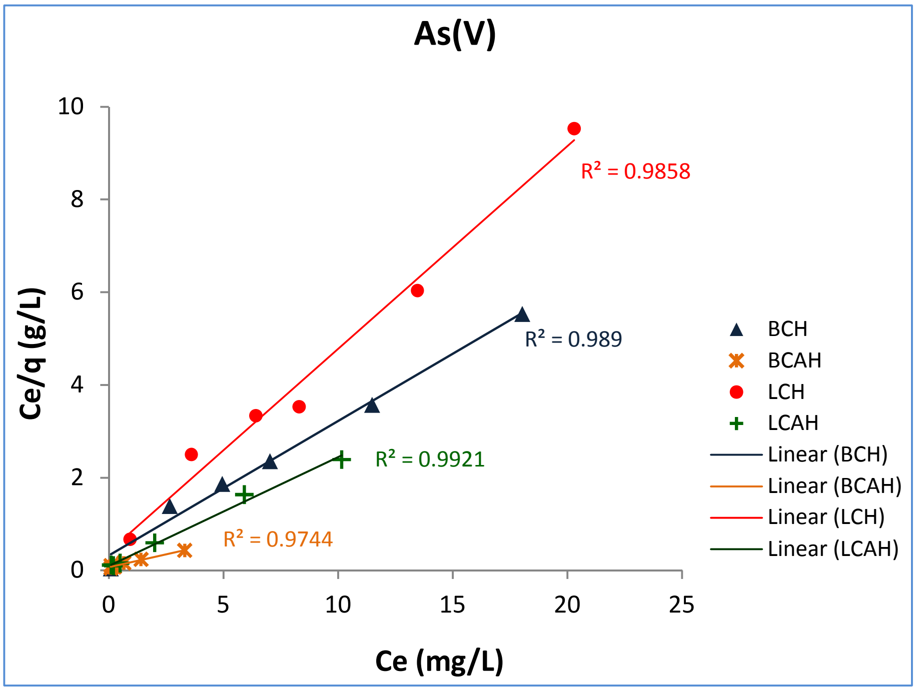

Figure 3.2.16. Langmuir adsorption isotherm for the removal of As(V).

Table 3.2.13. Langmuir constants estimated for the sorption of As(III) and As(V) by the hybrid materials.

Hybrid materials	As(III)			As(V)		
	Langmuir monolayer capacity (q_o) (mg/g)	b (L/g)	R^2	Langmuir monolayer capacity (q_o) (mg/g)	b (L/g)	R^2
BCH	2.793	0.816	0.998	3.449	0.896	0.989
LCH	1.824	0.971	0.982	2.287	1.074	0.986
BCAH	2.471	0.787	0.996	8.937	1.634	0.974
LCAH	2.184	0.399	0.995	4.255	2.495	0.992

3.2.4. Effect of background electrolyte concentration

3.2.4.1. As(III) and As(V)

The specific and non-specific sorption of As(III) or As(V) onto these hybrid materials is studied by obtaining the sorption data at varied background electrolyte concentrations. It is reported that the sorption through the outer–sphere complexation sensitive to the variation of background electrolyte concentration, since: (i) the background electrolyte ions might compete with the non–specific sorbed ions toward the solid surface, and (ii) the activity of the adsorbing species is to be greatly influenced by the variation of the interfacial potential because of the change in ionic strength as the outer sphere complexes are located at the same plane in the generalized triple layer model with the adsorbed background electrolyte ions. On the other hand, the inner sphere complexes are not influenced by the change in background electrolyte concentrations since the adsorbed ions are residing at the plane, which is closer to surface where usually background electrolyte ions are not located (Hayes et al., 1988).

Therefore, the study was extended to observe the change in background electrolyte concentration, i.e., $NaNO_3$ for the sorption of As(III) and As(V) by these solids at constant pH 4.5. The background electrolyte concentration was increased from 0.001 to 0.1 mol/L of $NaNO_3$ (100 times) and the corresponding percent removal of As(III)/or As(V) was obtained. The results are shown in Table 3.2.14 (a–d) and 3.2.15 (a–d); and then graphically in Figure 3.2.17 and 3.2.18, respectively, for As(III) and As(V).

It is observed from Figure 3.2.17 that on increasing the background electrolyte concentration from 0.001 to 0.1 mol/L $NaNO_3$, the corresponding decrease in percent uptake of As(III) is from 47.10% to 20.60% for BCH, from 60.46% to 27.30 % for BCAH, from 45.50% to 14.2 % for LCH and from 55.36% to 25.13% for LCAH. It is evident that the increase in background electrolyte concentrations cause considerably a mark decrease in percent uptake of As(III) by these solids. This clearly indicates the sorption of As(III) by these solids is primarily with a weak van der Waals forces and, possibly, forming an outer sphere complexes onto the solid surface. These are in accordance to the mechanism proposed with the pH dependence studies. Previously, it was demonstrated that the sorption of As(III) or even As(V) by the iron hydroxides was somewhat suppressed in the presence of coexisting solutes studied for ground waters of Bangladesh (Meng et al., 2002). Similarly, the organo–modified sericite samples showed a similar outer sphere complexation for As(III) (Lee and Tiwari, 2014).

Further, Figure 3.2.18 shows that increase in background electrolyte concentrations from 0.001 mol/L to 0.1 mol/L $NaNO_3$ caused to decrease the As(V) sorption from 34.88% to 26.44% for BCH, from 87.49% to 78.20% for BCAH, from 24.00% to 21.69% for LCH and from 89.51% to 86.18% for LCAH solids. These results clearly show that the presence of background electrolytes even at 0.1 mol/L of $NaNO_3$ could not affect significantly the sorption of As(V) by these solids. Therefore, the sorption of As(V) is predominantly of chemisorptive type and As(V) possibly forming a strong chemical bond at the surface active sites and residing on the inner sphere plane. Similar results were reported previously for the organo–inorgano–modified sericite (Tiwari and Lee, 2012). However, the removal of As(V) by the titanium dioxide showed a mixed mechanism, i.e., inner and outer–sphere complexation (Liu et al., 2008).

Table 3.2.14 (a). Effect of background electrolyte ($NaNO_3$) concentration on the removal of As(III) by BCH.

$NaNO_3$ (mol/L)	Initial conc. (mg/L)	Final conc. (mg/L)	% Removal
0.001	7.84	3.13	47.10
0.005	7.84	4.04	38.00
0.01	7.84	4.31	35.30
0.05	7.84	4.73	31.10
0.1	7.84	5.78	20.60

Table 3.2.14 (b). Effect of background electrolyte ($NaNO_3$) concentration on the removal of As(III) by LCH.

$NaNO_3$ (mol/L)	Initial conc. (mg/L)	Final conc. (mg/L)	% Removal
0.001	7.84	3.29	45.50
0.005	7.84	4.41	34.30
0.01	7.84	4.61	32.30
0.05	7.84	5.38	24.60
0.1	7.84	6.42	14.20

Table 3.2.14 (c). Effect of background electrolyte ($NaNO_3$) concentration on the removal of As(III) by BCAH.

$NaNO_3$ (mol/L)	Initial conc. (mg/L)	Final conc. (mg/L)	% Removal
0.001	7.84	3.10	60.46
0.005	7.84	3.55	54.72
0.01	7.84	4.45	43.24
0.05	7.84	4.58	41.58
0.1	7.84	5.70	27.30

Table 3.2.14 (d). Effect of background electrolyte ($NaNO_3$) concentration on the removal of As(III) by LCAH.

$NaNO_3$ (mol/L)	Initial conc. (mg/L)	Final conc. (mg/L)	% Removal
0.001	7.84	3.50	55.36
0.005	7.84	4.05	48.34
0.01	7.84	4.55	41.96
0.05	7.84	4.77	39.16
0.1	7.84	5.87	25.13

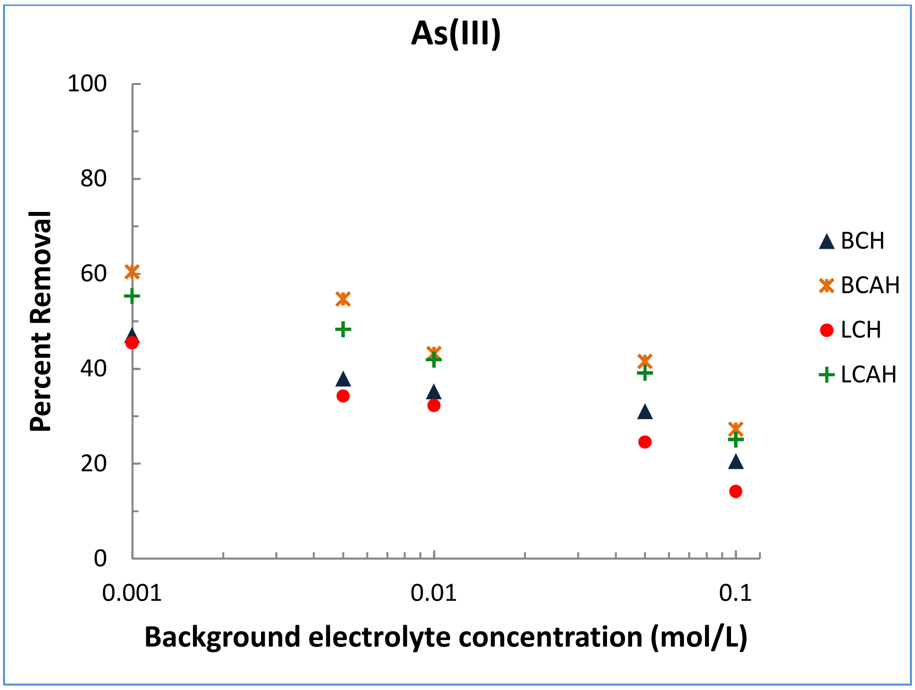

Figure 3.2.17. Removal of As(III) by the hybrid materials as a function of background electrolyte concentration.

Table 3.2.15 (a). Effect of background electrolyte ($NaNO_3$) concentration on the removal of As(V) by BCH.

$NaNO_3$ (mol/L)	Initial conc. (mg/L)	Final conc. (mg/L)	% Removal
0.001	9.91	7.00	34.88
0.005	9.91	7.58	27.95
0.01	9.91	7.93	26.16
0.05	9.91	7.99	27.23
0.1	9.91	7.90	26.44

Table 3.2.15 (b). Effect of background electrolyte ($NaNO_3$) concentration on the removal of As(V) by LCH.

$NaNO_3$ (mol/L)	Initial conc. (mg/L)	Final conc. (mg/L)	% Removal
0.001	9.91	8.17	24.00
0.005	9.91	8.12	22.81
0.01	9.91	8.07	24.86
0.05	9.91	8.32	24.23
0.1	9.91	8.41	21.69

Table 3.2.15 (c). Effect of background electrolyte ($NaNO_3$) concentration on the removal of As(V) by BCAH.

$NaNO_3$ (mol/L)	Initial conc. (mg/L)	Final conc. (mg/L)	% Removal
0.001	9.91	1.24	87.49
0.005	9.91	1.46	85.27
0.01	9.91	2.19	77.90
0.05	9.91	2.15	78.30
0.1	9.91	2.16	78.20

Table 3.2.15 (d). Effect of background electrolyte ($NaNO_3$) concentration on the removal of As(V) by LCAH.

$NaNO_3$ (mol/L)	Initial conc. (mg/L)	Final conc. (mg/L)	% Removal
0.001	9.91	1.04	89.51
0.005	9.91	1.49	84.96
0.01	9.91	1.57	84.16
0.05	9.91	1.81	81.74
0.1	9.91	1.37	86.18

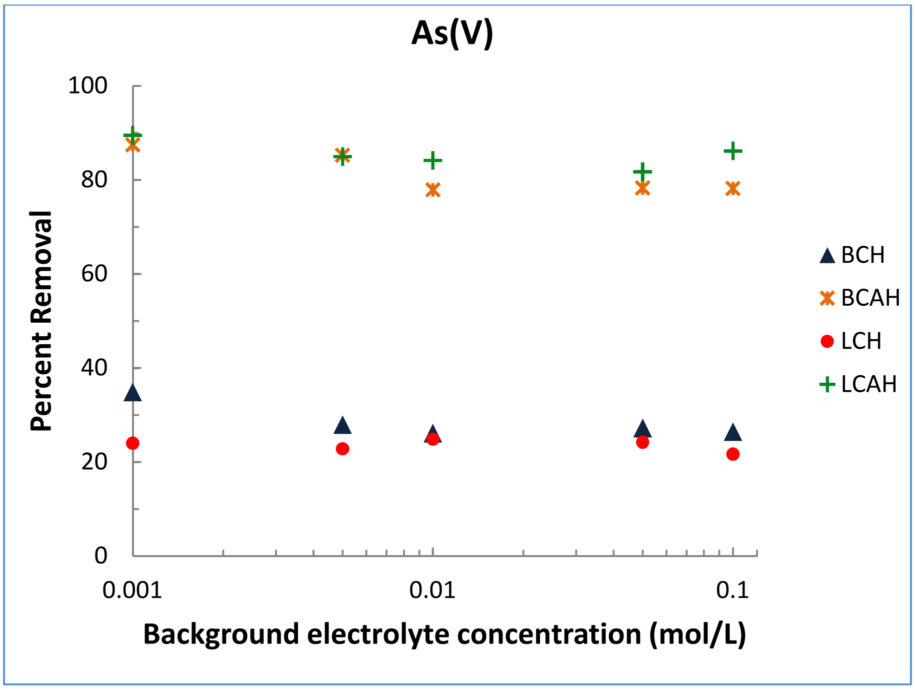

Figure 3.2.18. Removal of As(V) by the hybrid materials as a function of background electrolyte concentration.

3.2.4.2. BPA

The effect of background electrolyte on the sorption of BPA by the hybrid materials was assessed employing a wide range of background electrolyte (NaCl) concentrations from 0.0001 mol/L to 0.1 mol/L; keeping initial BPA concentration of 10.0 mg/L, at pH~7.0, and with a solid dose of 2 g/L. The experiments were conducted as discussed in Chapter 2.3.7.3. The data are returned in Table 3.2.16 (a–d) and the percent removal of BPA is presented as a function of background electrolyte concentrations in Figure 3.2.19. Figure clearly shows that increasing the background electrolyte concentrations from 0.0001 to 0.1 mol/L (1000 times) could not affect significantly the percent uptake of BPA by these solids employed. Therefore, this again points to the strong affinity of the solids towards BPA. It is further observed that increasing the background electrolyte concentration slightly causes to increase the percent removal of BPA by LCAH solid. It is attributed mainly due to the salting-out effect of the electrolytes which refers to the reduced solubility of organic compounds in aqueous salt solutions (Xie et al., 1997). Na^+ may reduce the water solubility of BPA (i.e., salting-out effect), which leads to an increase in BPA removal. A similar observation was reported by Zhou et al., (2012). They observed that the sorption of BPA onto the modified peat showed negligible ionic strength-dependence, and the increased in ionic strength to 1.0 mol/L NaCl or $CaCl_2$ induced a slight increased in modified peat sorption capacity by approximately 5%. They further reported that strong hydrophobic interaction between the hydrophobic phenyl groups of BPA and the grafted HTAB groups played an important role during the sorption process.

Table 3.2.16 (a). Effect of background electrolyte (NaCl) concentration on the removal of BPA by BCH.

NaCl (mol/L)	Initial conc. (mg/L)	Final conc. (mg/L)	% Removal
0.0001	10.35	0.14	98.66
0.001	10.42	0.21	98.00
0.01	10.63	0.28	97.38
0.1	10.56	0.42	96.05

Table 3.2.16 (b). Effect of background electrolyte (NaCl) concentration on the removal of BPA by LCH.

NaCl (mol/L)	Initial conc. (mg/L)	Final conc. (mg/L)	% Removal
0.0001	10.35	0.21	97.99
0.001	10.42	0.28	97.33
0.01	10.63	0.28	97.38
0.1	10.56	0.35	96.71

Table 3.2.16 (c). Effect of background electrolyte (NaCl) concentration on the removal of BPA by BCAH.

NaCl (mol/L)	Initial conc. (mg/L)	Final conc. (mg/L)	% Removal
0.0001	10.35	0.14	98.66
0.001	10.42	0.14	98.67
0.01	10.63	0.28	97.38
0.1	10.56	0.56	94.73

Table 3.2.16 (d). Effect of background electrolyte (NaCl) concentration on the removal of BPA by LCAH.

NaCl (mol/L)	Initial conc. (mg/L)	Final conc. (mg/L)	% Removal
0.0001	10.21	0.42	95.91
0.001	10.14	0.49	95.21
0.01	10.14	0.49	95.21
0.1	10.07	0.76	92.41

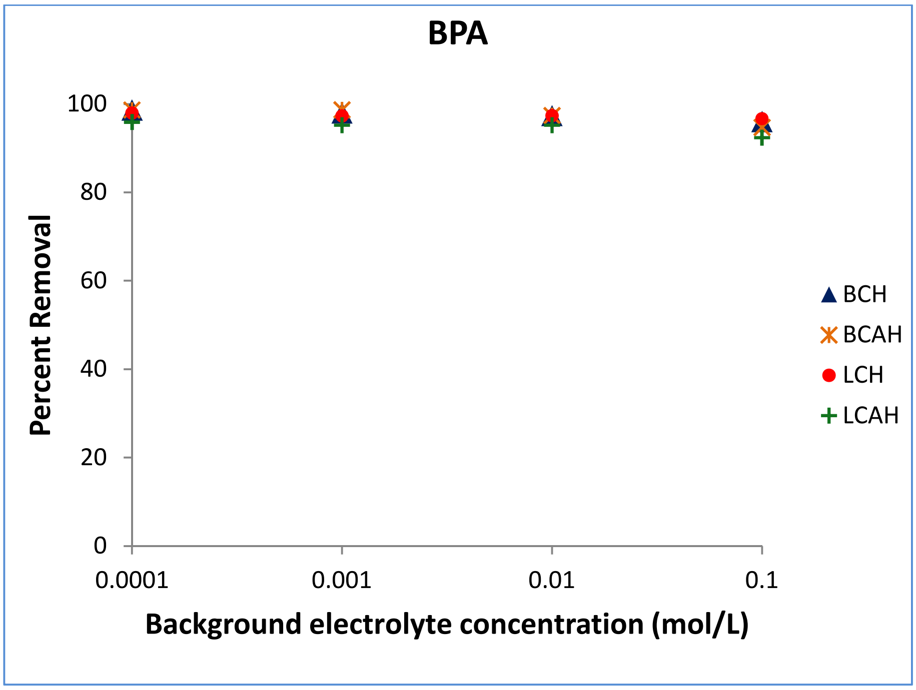

Figure 3.2.19. Removal of BPA by the hybrid materials as a function of background electrolyte concentration.

3.2.4.3. EE2

The effect of background electrolytes in the removal of EE2 by the materials was assessed varying the background electrolyte concentrations from 0.0001 mol/L to 0.1 mol/L NaCl, at an initial EE2 concentration of ~5.0 mg/L and at pH ~7.0. The results are returned in Table 3.2.17 (a–d) and then the percent removal of EE2 is presented as a function of background electrolyte concentrations in Figure 3.2.20. Figure clearly shows that increasing the background electrolyte concentrations from 0.0001 mol/L to 0.1 mol/L (1000 times) affects remarkably the sorption of EE2 by these hybrid materials. This again infers the strong affinity of modified solids towards EE2. It is observed that the increase in ionic strength causes a little enhancement in the percent sorption of EE2 by LCAH solid, possibly, due to the decrease in EE2 solubility resulting from the salting-out effect of the electrolytes (Xie et al., 1997; Joseph et al, 2011). Joseph et al (2011) reported that increase in NaCl concentration from 0 to 320 mM could not affect significantly the adsorption of either BPA or EE2 by the SWCNTs, in both young and old landfill leachate solutions. The adsorption of BPA and EE2 from young leachate by SWCNTs was also not affected by increase in the concentration of Ca^{2+}. Further, they pointed that in case of old leachate conditions, an increase in the Ca^{2+}concentration from 0 to 150 mM increased the adsorption of BPA and EE2 by 12% and 19%, respectively.

Table 3.2.17 (a). Effect of background electrolyte (NaCl) concentration on the removal of EE2 by BCH.

NaCl (mol/L)	Initial conc. (mg/L)	Final conc. (mg/L)	% Removal
0.0001	5.52	0.52	90.63
0.001	5.34	0.69	87.10
0.01	5.34	0.69	87.10
0.1	5.52	0.86	84.38

Table 3.2.17 (b). Effect of background electrolyte (NaCl) concentration on the removal of EE2 by LCH.

NaCl (mol/L)	Initial conc. (mg/L)	Final conc. (mg/L)	% Removal
0.0001	5.52	0.52	90.63
0.001	5.34	0.52	90.32
0.01	5.34	0.86	83.87
0.1	5.52	1.03	81.25

Table 3.2.17 (c). Effect of background electrolyte (NaCl) concentration on the removal of EE2 by BCAH.

NaCl (mol/L)	Initial conc. (mg/L)	Final conc. (mg/L)	% Removal
0.0001	5.52	0.34	93.75
0.001	5.34	0.34	93.55
0.01	5.34	0.69	87.10
0.1	5.52	0.69	87.50

Table 3.2.17 (d). Effect of background electrolyte (NaCl) concentration on the removal of EE2 by LCAH.

NaCl (mol/L)	Initial conc. (mg/L)	Final conc. (mg/L)	% Removal
0.0001	5.52	0.69	87.50
0.001	5.34	0.86	83.87
0.01	5.34	1.03	80.65
0.1	5.52	1.21	78.13

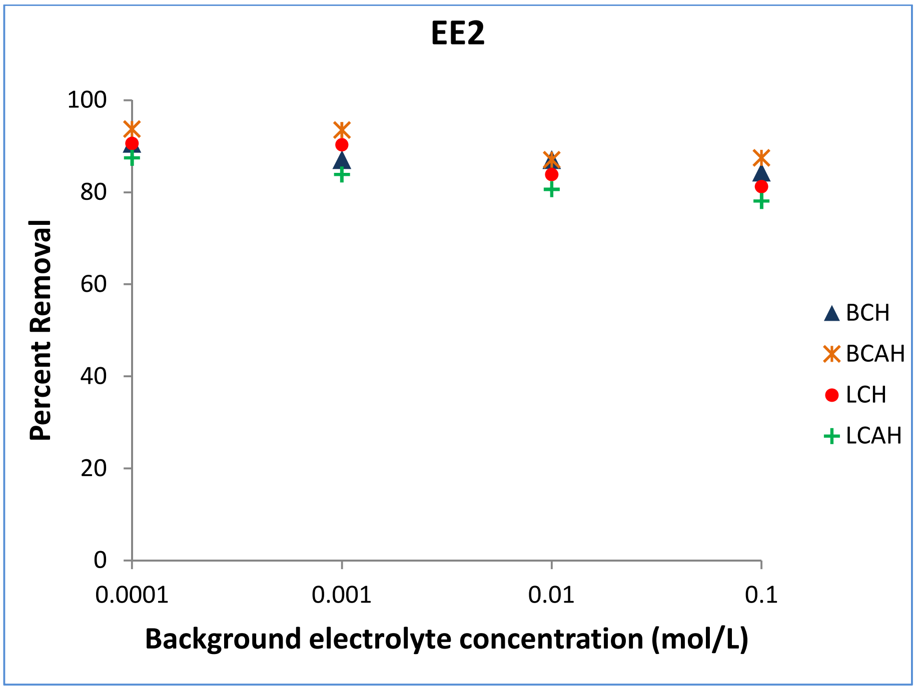

Figure 3.2.20. Removal of EE2 by the hybrid materials as a function of background electrolyte concentration.

3.2.4.4. DFS

Effect of background electrolytes in the sorptive removal of DFS by the hybrid materials could enabled to explain the mechanism involved at solid/solution interfaces (Hayes et al., 1988). The sorption of diclofenac sodium by BCH, BCAH, LCH and LCAH was assessed by increasing the background electrolyte concentrations from 0.0001 mol/L to 0.1 mol/L NaCl, at an initial DFS concentration of ~10.0 mg/L, at a constant pH ~7.0, and at the solid dose of 2 g/L. The data are presented in Tables 3.2.18 (a–d) and then shown graphically in Figure 3.2.21. Figure clearly indicates that increasing the background electrolyte concentrations even up to 1000 times could not affect significantly the percent uptake of DFS by these solids employed, however, a minor enhancement in the percent sorption by LCAH solid is observed. Therefore, this infers the strong affinity of solids towards DFS. Also, this implies that the partitioned DFS is bound with relatively stronger forces. In another report, the uptake of DFS by the anion exchange polymer resin was not notably affected in the presence of citrate or phosphate from aqueous solutions (Landry and Boyer, 2013).

Table 3.2.18 (a). Effect of background electrolyte (NaCl) concentration on the removal of DFS by BCH.

NaCl (mol/L)	Initial conc. (mg/L)	Final conc. (mg/L)	% Removal
0.0001	9.97	0.17	98.34
0.001	9.90	0.20	98.00
0.01	10.07	0.20	98.03
0.1	10.10	0.33	96.73

Table 3.2.18 (b). Effect of background electrolyte (NaCl) concentration on the removal of DFS by LCH.

NaCl (mol/L)	Initial conc. (mg/L)	Final conc. (mg/L)	% Removal
0.0001	9.97	0.30	97.02
0.001	10.03	0.30	97.04
0.01	9.97	0.33	96.69
0.1	9.93	0.50	95.02

Table 3.2.18 (c). Effect of background electrolyte (NaCl) concentration on the removal of DFS by BCAH.

NaCl (mol/L)	Initial conc. (mg/L)	Final conc. (mg/L)	% Removal
0.0001	9.97	0.17	98.34
0.001	9.90	0.20	98.00
0.01	10.07	0.30	97.05
0.1	10.10	0.40	96.08

Table 3.2.18 (d). Effect of background electrolyte (NaCl) concentration on the removal of DFS by LCAH.

NaCl (mol/L)	Initial conc. (mg/L)	Final conc. (mg/L)	% Removal
0.0001	9.97	0.30	97.02
0.001	10.03	0.33	96.71
0.01	9.97	0.36	96.36
0.1	9.93	0.73	92.69

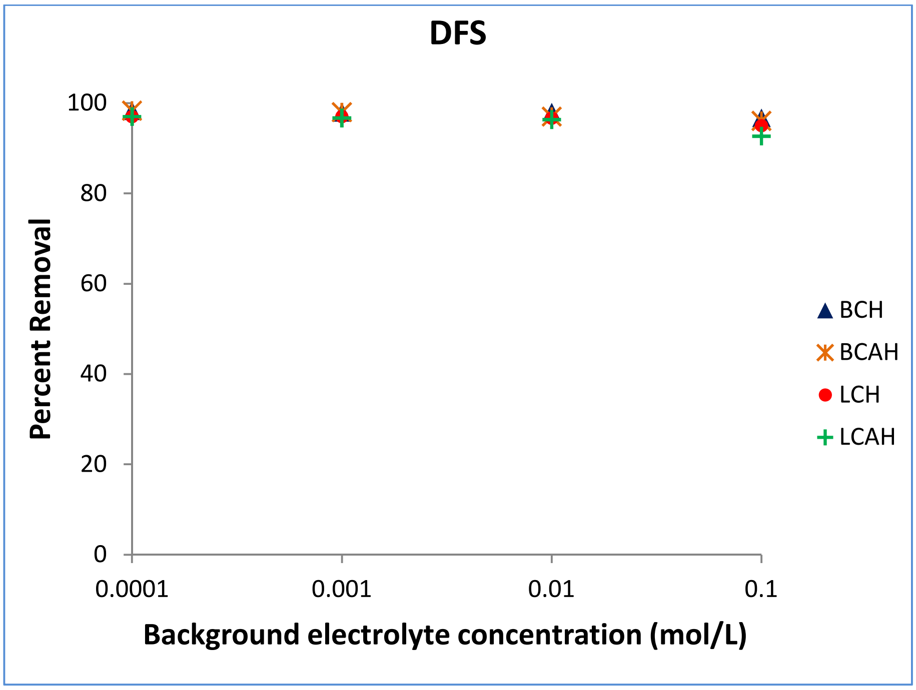

Figure 3.2.21. Removal of DFS by the hybrid materials as a function of background electrolyte concentration.

3.2.4.5. TC

The sorption of tetracycline by BCH, BCAH, LCH and LCAH was assessed with the background electrolyte concentrations ranging from 0.0001 mol/L to 0.1 mol/L NaCl, at an initial TC concentration of ~10.0 mg/L, at constant pH ~7.0, and with a solid dose of 2 g/L. The data obtained are given in Table 3.2.19 (a–d) and the percent removal of TC is presented as a function of background electrolyte concentrations, graphically in Figure 3.2.22. Figure clearly shows that increasing the background electrolyte concentrations even up to 1000 times could not affect the percent uptake of TC by these solids employed. Therefore, this indicates the strong affinity of solids towards TC. It is observed that the increase in ionic strength causes to a feeble enhancement in the percent sorption of TC by the BCAH and LCAH solids. This is due to the salting-out effect of the electrolytes. Previously, Zhang et al. (2011) reported that increasing the ionic strength of NaCl hardly affected the adsorption of

TC by multi-walled carbon nanotubes. In other report, Zhao et al. (2012) observed that the presence of humic acid favored greatly the adsorption of TC onto montmorillonite.

Table 3.2.19 (a). Effect of background electrolyte (NaCl) concentration on the removal of TC by BCH.

NaCl (mol/L)	Initial conc. (mg/L)	Final conc. (mg/L)	% Removal
0.0001	10.09	0.50	95.06
0.001	10.05	0.59	94.15
0.01	10.05	1.00	90.09
0.1	10.14	1.13	88.84

Table 3.2.19 (b). Effect of background electrolyte (NaCl) concentration on the removal of TC by LCH.

NaCl (mol/L)	Initial conc. (mg/L)	Final conc. (mg/L)	% Removal
0.0001	10.09	0.23	97.76
0.001	10.05	0.32	96.85
0.01	10.05	0.63	93.69
0.1	10.14	1.13	88.84

Table 3.2.19 (c). Effect of background electrolyte (NaCl) concentration on the removal of TC by BCAH.

NaCl (mol/L)	Initial conc. (mg/L)	Final conc. (mg/L)	% Removal
0.0001	10.09	0.54	94.62
0.001	10.05	0.50	95.05
0.01	10.05	0.36	96.40
0.1	10.14	0.18	98.21

Table 3.2.19 (d). Effect of background electrolyte (NaCl) concentration on the removal of TC by LCAH.

NaCl (mol/L)	Initial conc. (mg/L)	Final conc. (mg/L)	% Removal
0.0001	10.09	1.45	85.65
0.001	10.05	1.31	86.94
0.01	10.05	0.95	90.54
0.1	10.14	0.86	91.52

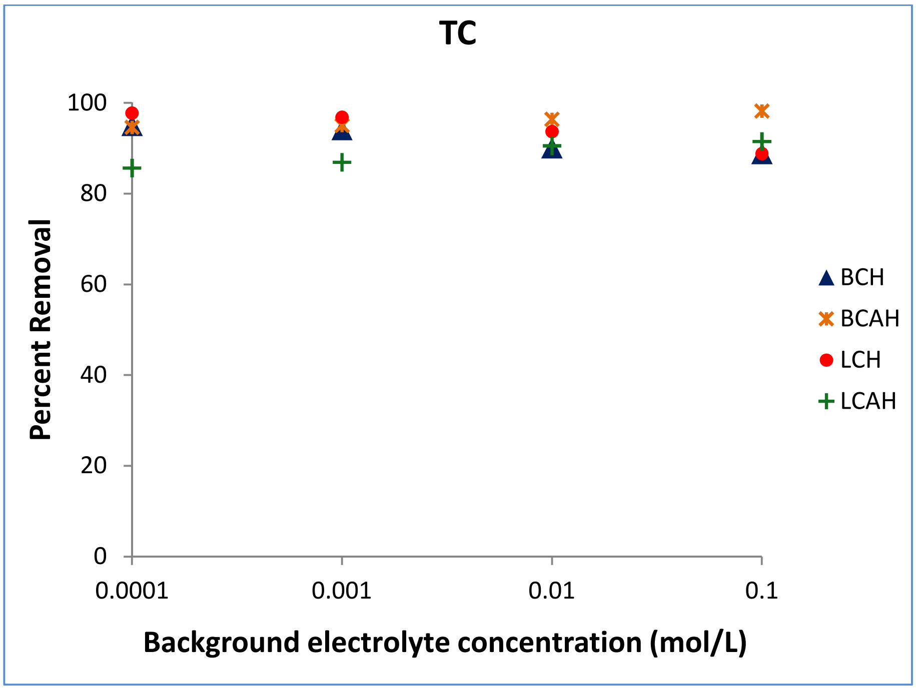

Figure 3.2.22. Removal of TC by the hybrid materials as a function of background electrolyte concentration.

3.2.5. Effect of contact time

3.2.5.1. As(III) and As(V)

The time dependence sorption of As(III) and As(V) by these hybrid materials was conducted as detailed before in Chapter 2.3.7.4, and the results are presented in Table 3.2.20 (a–d) and 3.2.21 (a–d); and shown graphically in Figure 3.2.23 and 3.2.24, respectively for As(III) and As(V). It is observed from the figures that a sharp initial uptake of arsenic is occurring onto the surface of solids which slow down with the lapse of time and reach to a saturation value within *Ca*. 180 mins of contact. It is noted that within the initial 60 mins of contact most of the arsenic species are aggregated onto the solid surface. This indicates that the sorption of arsenic is relatively fast and efficient onto these solids. Comparing these two oxyanions, the uptake of As(III) is relatively faster than As(V).

Table 3.2.20 (a). Effect of contact time on the removal of As(III) by BCH.

Contact Time (min.)	Initial conc. (mg/L)	Final conc. (mg/L)	% Removal
5	11.82	8.51	28.00
10	11.82	8.37	29.19
20	11.82	7.73	34.60
30	11.82	7.55	36.13
60	11.82	7.04	40.44
120	11.82	6.95	41.20
180	11.82	6.95	41.20
300	11.82	6.92	41.46
720	11.82	6.90	41.62

Table 3.2.20 (b). Effect of contact time on the removal of As(III) by LCH.

Contact Time (min.)	Initial conc. (mg/L)	Final conc. (mg/L)	% Removal
5	11.82	9.24	21.83
10	11.82	8.86	25.04
20	11.82	8.68	26.57
30	11.82	8.48	28.26
60	11.82	8.24	30.29
120	11.82	8.13	31.22
180	11.82	8.02	32.15
300	11.82	7.68	35.03
720	11.82	7.26	38.58

Table 3.2.20 (c). Effect of contact time on the removal of As(III) by BCAH.

Contact Time (min.)	Initial conc. (mg/L)	Final conc. (mg/L)	% Removal
5	10.59	9.60	9.35
10	10.59	8.85	16.43
20	10.59	8.64	18.41
30	10.59	8.28	21.81
60	10.59	8.02	24.27
120	10.59	7.17	32.29
180	10.59	7.05	33.43
300	10.59	7.00	33.90
720	10.59	6.97	34.18

Table 3.2.20 (d). Effect of contact time on the removal of As(III) by LCAH.

Contact Time (min.)	Initial conc. (mg/L)	Final conc. (mg/L)	% Removal
5	10.93	9.79	10.43
10	10.93	9.54	12.72
20	10.93	9.46	13.45
30	10.93	8.94	18.21
60	10.93	8.54	21.87
120	10.93	8.37	23.42
180	10.93	8.14	25.53
300	10.93	7.91	27.63
720	10.93	7.67	29.83

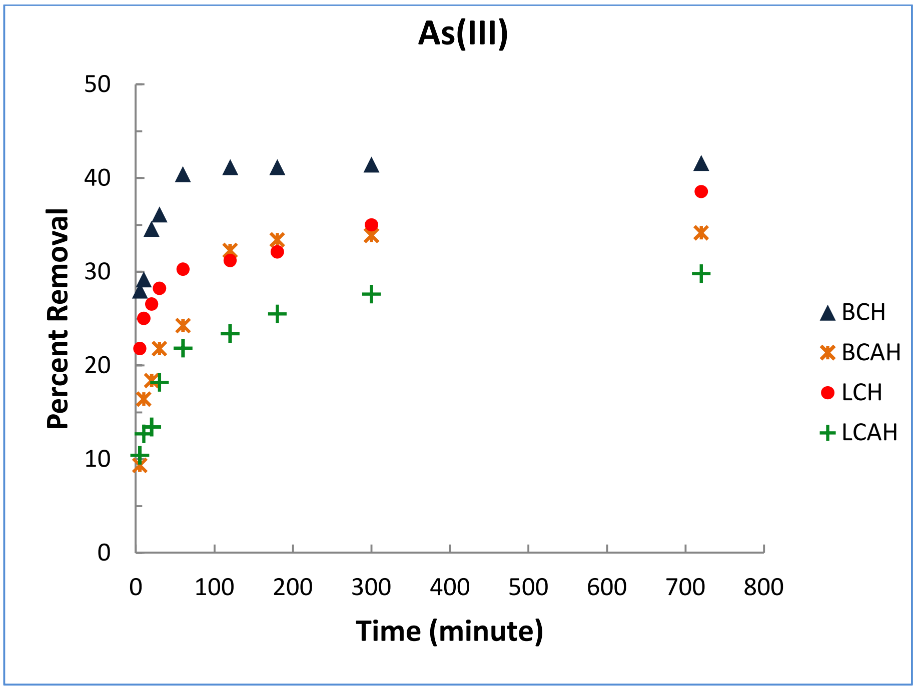

Figure 3.2.23. Removal of As(III) by the hybrid materials as a function of contact time.

Table 3.2.21 (a). Effect of contact time on the removal of As(V) by BCH.

Contact Time (min.)	Initial conc. (mg/L)	Final conc. (mg/L)	% Removal
5	10.89	8.55	21.49
10	10.89	7.33	32.69
20	10.89	6.81	37.47
30	10.89	6.70	38.48
60	10.89	6.61	39.30
120	10.89	6.16	43.43
180	10.89	6.06	44.35
300	10.89	6.01	44.81
720	10.89	5.73	47.38

Table 3.2.21 (b). Effect of contact time on the removal of As(V) by LCH.

Contact Time (min.)	Initial conc. (mg/L)	Final conc. (mg/L)	% Removal
5	10.89	9.73	10.65
10	10.89	9.13	16.16
20	10.89	8.88	18.46
30	10.89	8.57	21.30
60	10.89	8.45	22.41
120	10.89	8.07	25.90
180	10.89	8.05	26.08
300	10.89	7.93	27.18
720	10.89	7.43	31.77

Table 3.2.21 (c). Effect of contact time on the removal of As(V) by BCAH.

Contact Time (min.)	**Initial conc. (mg/L)**	**Final conc. (mg/L)**	**% Removal**
5	10.53	5.08	51.76
10	10.53	4.74	54.99
20	10.53	4.17	60.40
30	10.53	3.94	62.58
60	10.53	2.92	72.27
120	10.53	2.06	80.44
180	10.53	1.51	85.66
300	10.53	0.63	94.02
720	10.53	0.44	95.82

Table 3.2.21 (d). Effect of contact time on the removal of As(V) by LCAH.

Contact Time (min.)	**Initial conc. (mg/L)**	**Final conc. (mg/L)**	**% Removal**
5	10.53	6.64	36.94
10	10.53	6.11	41.98
20	10.53	5.54	47.39
30	10.53	4.68	55.56
60	10.53	4.14	60.68
120	10.53	3.21	69.52
180	10.53	3.08	70.75
300	10.53	3.06	70.94
720	10.53	2.95	71.98

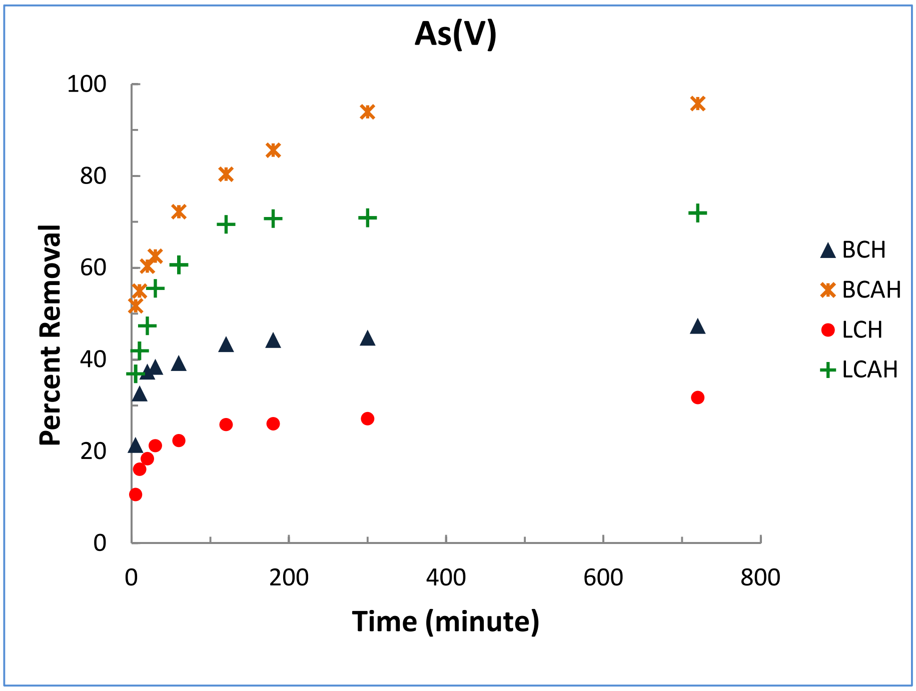

Figure 3.2.24. Removal of As(V) by the hybrid materials as a function of contact time.

3.2.5.2. BPA

The removal behaviour of the hybrid materials towards BPA as a function of time was assessed at different intervals of contact time for sorption, taking the initial BPA concentration of 10.0 mg/L, at pH~7, and with a solid dose of 2 g/L. The data obtained are returned in Table 3.2.22 (a–d) and also presented graphically in Figure 3.2.25. It is observed from the figure that the hybrid materials show efficient removal of BPA from aqueous solutions since within 10 minutes of contact, almost an apparent equilibrium is achieved. This indicates that the sorption of BPA is very fast and efficient onto these onto these hybrid materials. This again reaffirms the affinity of these solids towards BPA. Previously, Zheng et al. (2013) reported that the removal of BPA by the organoclays (Ca-montmorillonite modified with DDTMA and HDTMA) reached an apparent equilibrium within around 5 minutes of contact. The fast removal rate implied strong adsorption interaction between the organoclay surface and the hydrophobic compound.

Table 3.2.22 (a). Effect of contact time on the removal of BPA by BCH.

Contact Time (min.)	Initial conc. (mg/L)	Final conc. (mg/L)	% Removal
1	10.63	1.94	81.70
2	10.63	1.39	86.93
3	10.63	1.18	88.88
4	10.63	0.83	92.16
5	10.21	0.35	92.81
10	10.21	0.21	94.12
15	10.21	0.14	94.77
20	10.63	0.21	98.04
30	10.63	0.28	97.39

Table 3.2.22 (b). Effect of contact time on the removal of BPA by LCH.

Contact Time (min.)	Initial conc. (mg/L)	Final conc. (mg/L)	% Removal
1	10.21	2.85	72.11
2	10.21	2.36	76.87
5	10.21	1.18	88.43
10	10.21	0.69	93.20
15	10.21	0.49	95.24
30	10.21	0.42	95.91

Table 3.2.22 (c). Effect of contact time on the removal of BPA by BCAH.

Contact Time (min.)	Initial conc. (mg/L)	Final conc. (mg/L)	% Removal
1	10.21	1.60	81.05
2	10.21	0.83	88.24
3	10.63	0.76	92.81
4	10.63	0.63	94.12
5	10.63	0.49	95.43
10	10.63	0.56	94.77
15	10.63	0.49	95.43
20	10.63	0.28	97.38
30	10.63	0.14	98.69

Table 3.2.22 (d). Effect of contact time on the removal of BPA by LCAH.

Contact Time (min.)	Initial conc. (mg/L)	Final conc. (mg/L)	% Removal
1	10.21	4.03	60.54
2	10.21	2.99	70.75
5	10.21	2.01	80.27
10	10.21	1.25	87.75
15	10.21	0.97	90.48
30	10.21	0.90	91.15

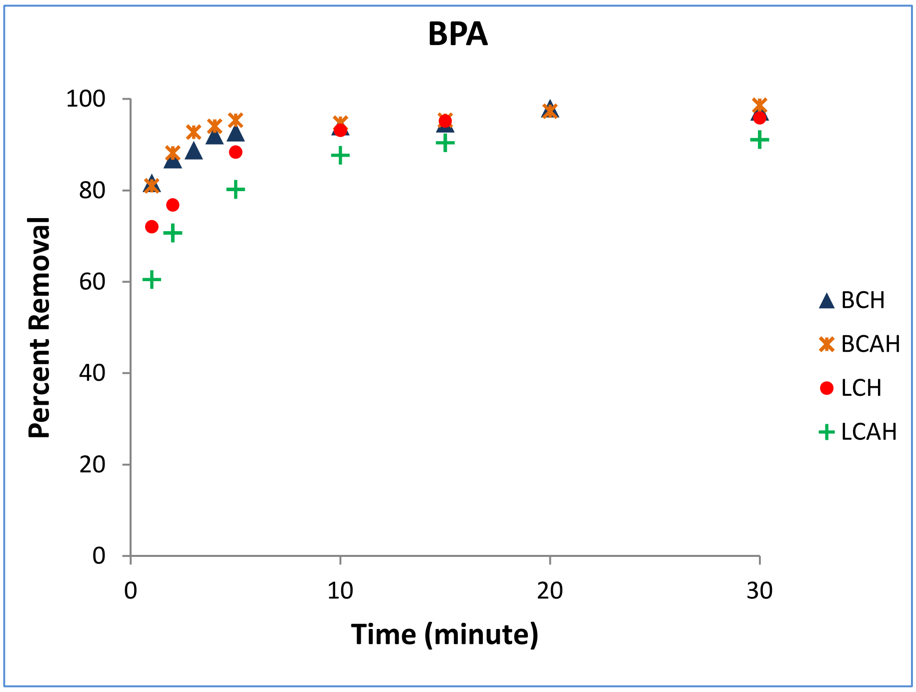

Figure 3.2.25. Removal of BPA by the hybrid materials as a function of contact time.

3.2.5.3. EE2

Time dependence removal data of EE2 obtained is presented in Table 3.2.23 (a–d) and the amount of EE2 removed as a function of time is shown graphically in Figure 3.2.26. It is clearly seen from the figure that the materials show efficient sorption of EE2 from aqueous solutions since within 15 minutes of contact almost a saturation value is achieved. The sorption of EE2 is relatively fast and this indicates the affinity of the materials towards EE2. Feng et al. (2010) also reported that the amount of EE2 adsorbed at the end of 15 minutes of contact by the inactivated sludge was reached to 83.8% and 87.9% at the initial EE2 concentrations of 1.0 and 5.0 mg/L, respectively using a solid dose of 1.0 g/L.

Table 3.2.23 (a). Effect of contact time on the removal of EE2 by BCH.

Contact Time (min.)	Initial conc. (mg/L)	Final conc. (mg/L)	% Removal
1	5.69	2.41	57.58
2	5.69	1.90	66.67
3	5.69	1.55	72.73
5	5.69	1.38	75.76
10	5.69	1.03	81.82
15	5.69	0.86	84.85
30	5.69	0.52	90.91
45	5.69	0.52	90.91
60	5.69	0.34	93.94

Table 3.2.23 (b). Effect of contact time on the removal of EE2 by LCH.

Contact Time (min.)	Initial conc. (mg/L)	Final conc. (mg/L)	% Removal
1	5.69	2.59	54.55
2	5.69	2.24	60.61
3	5.69	1.90	66.67
5	5.69	1.55	72.73
10	5.69	1.21	78.79
15	5.69	1.03	81.82
30	5.69	0.86	84.85
45	5.69	0.69	87.88
60	5.69	0.52	90.91

Table 3.2.23 (c). Effect of contact time on the removal of EE2 by BCAH.

Contact Time (min.)	Initial conc. (mg/L)	Final conc. (mg/L)	% Removal
1	5.69	2.93	48.48
2	5.69	2.59	54.55
3	5.69	2.24	60.61
5	5.69	1.90	66.67
10	5.69	1.38	75.76
15	5.69	1.21	78.79
30	5.69	0.69	87.88
45	5.69	0.69	87.88
60	5.69	0.52	90.91

Table 3.2.23 (d). Effect of contact time on the removal of EE2 by LCAH.

Contact Time (min.)	Initial conc. (mg/L)	Final conc. (mg/L)	% Removal
1	5.69	3.62	36.36
2	5.69	3.28	42.42
3	5.69	2.93	48.48
5	5.69	2.41	57.58
10	5.69	1.90	66.67
15	5.69	1.55	72.73
30	5.69	1.38	75.76
45	5.69	1.21	78.79
60	5.69	1.03	81.82

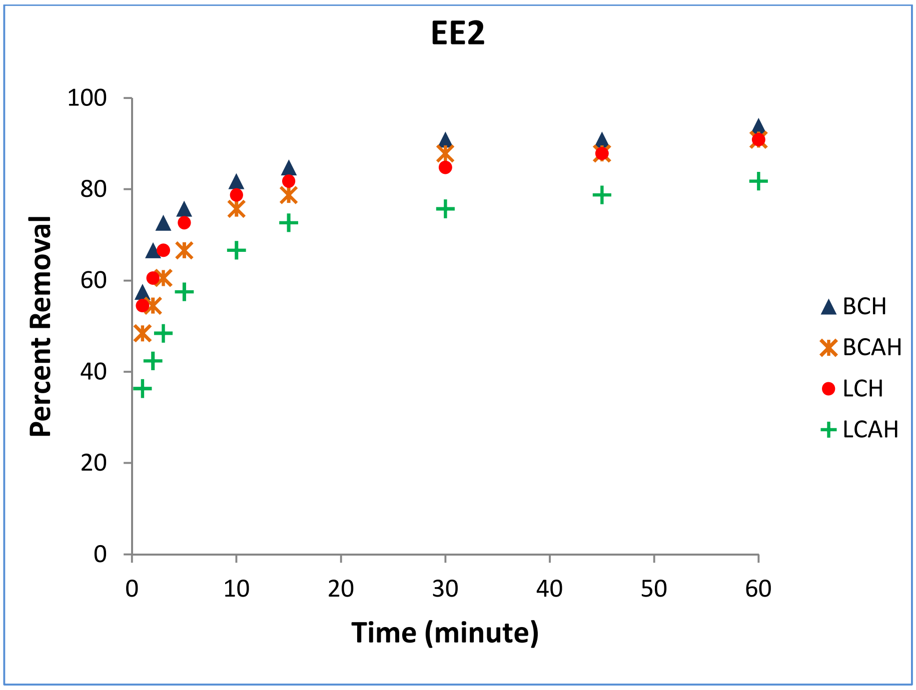

Figure 3.2.26. Removal of EE2 by the hybrid materials as a function of contact time.

3.2.5.4. DFS

Time dependence removal of DFS was studied varying the contact time, and the results are presented in Table 3.2.24 (a–d) and then in Figure 3.2.27. It is clear from the figure that the materials BCH and BCAH show extremely efficient removal behaviour, in particular, the removal of DFS from aqueous solutions since within 2–5 minutes of contact almost an apparent equilibrium is achieved. This indicates the affinity and efficiency of these solids towards DFS. However, the uptake of DFS onto the LCH and LCAH solids show comparatively slow and apparent solid solution equilibrium is achieved within 15 mins of contact.

Table 3.2.24 (a). Effect of contact time on the removal of DFS by BCH.

Contact Time (min.)	Initial conc. (mg/L)	Final conc. (mg/L)	% Removal
1	10.03	2.01	79.94
2	10.03	1.06	89.47
5	10.03	0.46	95.40
7	10.03	0.40	96.05
10	10.03	0.26	97.37
15	10.03	0.10	99.01
30	10.03	0.13	98.68

Table 3.2.24 (b). Effect of contact time on the removal of DFS by LCH.

Contact Time (min.)	Initial conc. (mg/L)	Final conc. (mg/L)	% Removal
1	10.10	5.84	42.15
2	10.10	5.22	48.36
3	10.10	4.46	55.89
4	10.10	4.19	58.50
5	10.10	3.80	62.42
7	10.10	3.07	69.61
10	10.10	1.49	85.30
15	10.10	0.76	92.48
20	10.10	0.50	95.10
25	10.10	0.33	96.73
30	10.10	0.30	97.06

Table 3.2.24 (c). Effect of contact time on the removal of DFS by BCAH.

Contact Time (min.)	Initial conc. (mg/L)	Final conc. (mg/L)	% Removal
1	10.03	1.29	87.17
2	10.03	0.46	95.40
5	10.03	0.26	97.37
7	10.03	0.30	97.04
10	10.03	0.26	97.37
15	10.03	0.20	98.03
30	10.03	0.13	98.68

Table 3.2.24 (d). Effect of contact time on the removal of DFS by LCAH.

Contact Time (min.)	Initial conc. (mg/L)	Final conc. (mg/L)	% Removal
1	10.20	6.11	40.13
2	10.20	5.31	47.89
3	10.20	4.75	53.40
4	10.20	4.29	57.93
5	10.20	3.37	66.99
7	10.20	2.41	76.38
10	10.20	1.55	84.79
15	10.20	1.16	88.67
20	10.20	1.16	88.67
25	10.20	1.16	88.67
30	10.20	1.16	88.67

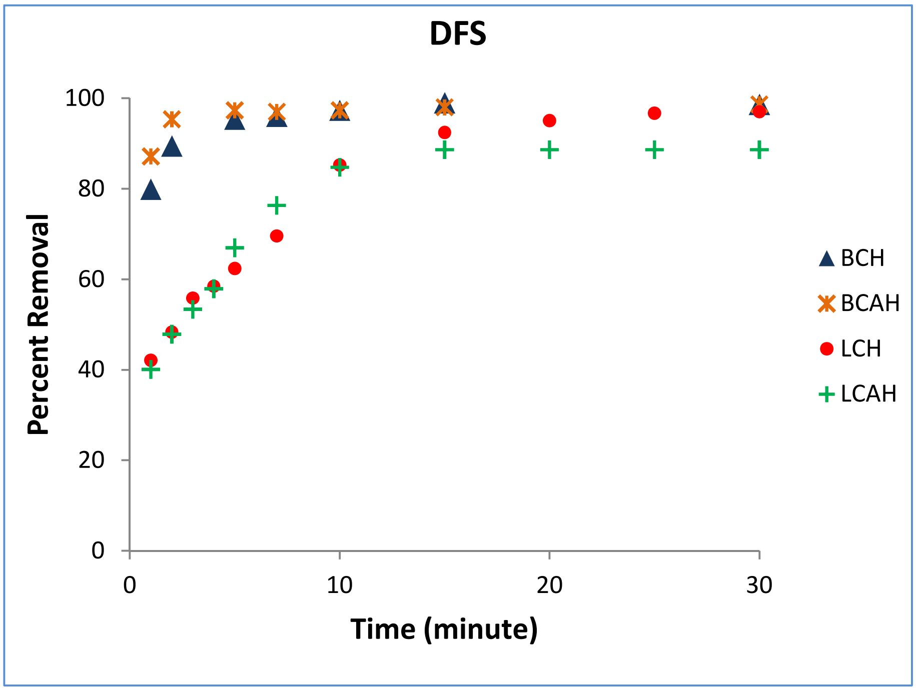

Figure 3.2.27. Removal of DFS by the hybrid materials as a function of contact time.

3.2.5.5. TC

Similarly, removal behavior of the hybrid materials for TC as a function of time is presented in Table 3.2.25 (a–d) and Figure 3.2.28. The time dependence sorption was assessed as detailed before in Chapter 2.3.7.4. It is observed from the figure that the hybrid materials show relatively efficient removal of TC from aqueous solutions. Within 120 minutes of contact, almost an apparent equilibrium is achieved, which again indicates the affinity of these solids towards TC.

Table 3.2.25 (a). Effect of contact time on the removal of TC by BCH.

Contact Time (min.)	Initial conc. (mg/L)	Final conc. (mg/L)	% Removal
1	9.82	6.52	33.64
2	9.82	5.93	39.63
3	9.82	5.29	46.08
5	9.82	4.57	53.46
10	9.82	3.67	62.67
15	9.82	3.12	68.20
30	9.82	2.58	73.73
60	9.82	1.86	81.11
120	9.82	1.40	85.71
180	9.82	1.54	84.33
240	9.82	1.09	88.94

Table 3.2.25 (b). Effect of contact time on the removal of TC by LCH.

Contact Time (min.)	Initial conc. (mg/L)	Final conc. (mg/L)	% Removal
1	9.82	8.96	8.76
2	9.82	8.64	11.99
3	9.82	8.46	13.83
5	9.82	7.87	19.82
10	9.82	7.01	28.57
15	9.82	6.11	37.78
30	9.82	4.84	50.69
60	9.82	3.26	66.82
120	9.82	2.67	72.81
180	9.82	1.95	80.18
240	9.82	0.81	91.71

Table 3.2.25 (c). Effect of contact time on the removal of TC by BCAH.

Contact Time (min.)	Initial conc. (mg/L)	Final conc. (mg/L)	% Removal
1	9.82	6.52	33.64
2	9.82	5.66	42.40
3	9.82	4.98	49.31
5	9.82	4.75	51.61
10	9.82	4.03	58.99
15	9.82	3.58	63.59
30	9.82	3.21	67.28
60	9.82	2.81	71.43
120	9.82	2.13	78.34
180	9.82	1.86	81.11
240	9.82	1.49	84.79

Table 3.2.25 (d). Effect of contact time on the removal of TC by LCAH.

Contact Time (min.)	Initial conc. (mg/L)	Final conc. (mg/L)	% Removal
1	9.82	8.37	14.75
3	9.82	8.19	16.59
5	9.82	7.78	20.74
10	9.82	7.24	26.27
15	9.82	6.34	35.48
30	9.82	5.57	43.32
60	9.82	4.43	54.84
120	9.82	3.71	62.21
180	9.82	2.94	70.05
240	9.82	2.26	76.96

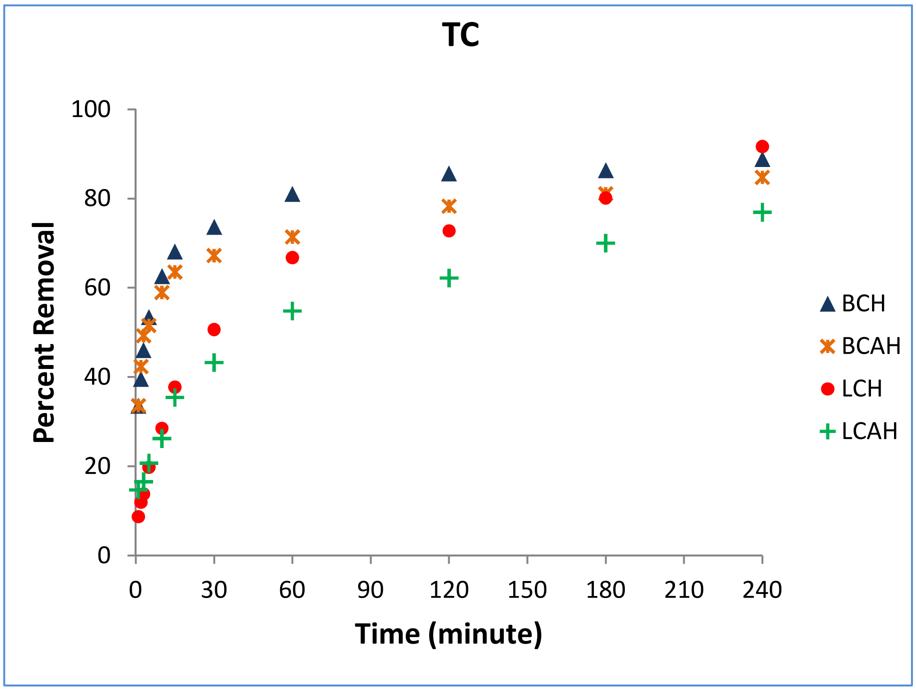

Figure 3.2.28. Removal of TC by the hybrid materials as a function of contact time.

3.2.6. Kinetic modeling studies

The uptake of BPA and EE2 by these hybrid materials, along with DFS by BCH and BCAH is found extremely fast, since an apparent equilibrium is achieved within 2–3 minutes of contact. This apparently restricts to perform further the kinetic modeling studies. The other systems however, are utilized to conduct the kinetic modeling for three different kinetic models, *viz*., pseudo-first order (PFO) (Azizian, 2004), pseudo-second order (PSO) (Ho and McKay, 1998) and fractal-like-pseudo-second order (FL-PSO) (Haerifar and Azizian, 2012) models using the non-linear equations (*cf.* Eq. 2.5, 2.6 and 2.7). A non–linear least square fitting method is conducted for the estimation of unknown parameters thereof.

3.2.6.1. As(III) and As(V)

The kinetic data of As(III) and As(V) are utilized for kinetic modeling and the results are presented graphically in Figure 3.2.29 to 3.2.34. The estimated values of the rate constants along with the least square sum are returned in Table 3.2.26. The table reveals that the kinetic simulation data are better fitted to the PSO and FL-PSO models compare to the PFO model since reasonably low least square sum is obtained for these two models. The results again show that BCH or LCH materials possess relatively higher removal capacity for As(III) whereas BCAH and LCAH hybrid materials show a significantly higher removal capacity for As(V) compare to the BCH and LCH materials. Moreover, the fair applicability of the PSO model pointed that the arsenic species are bound onto the surface of solid material by strong forces. Earlier, it was mentioned that the adsorption of divalent metal cations onto the *sphagnum* moss peat followed the second-order rate laws. Therefore, it was concluded that metal cations were bound with strong chemical forces that occurred between the peat surface active groups and divalent metal ions by the sharing or exchange of electrons (Ho and McKay, 2000).

Table 3.2.26. Kinetic data obtained for the sorption of As(III) and As(V) by the hybrid materials.

Systems	PFO Model			PSO Model			FL–PSO Model			
	q_e	k_1	s^2	q_e	k_2	s^2	q_e	k	α	s^2
BCH–As(III)	2.241	0.209	0.194	2.427	0.137	0.059	3.159	0.172	0.396	0.019
LCH–As(III)	1.712	0.251	0.055	1.831	0.237	0.011	2.079	0.355	0.503	0.002
BCAH–As(III)	1.488	0.063	0.137	1.740	0.043	0.063	3.587	0.025	0.471	0.032
LCAH–As(III)	1.419	0.047	0.214	1.542	0.043	0.089	1.973	0.081	0.522	0.022
BCH–As(V)	2.340	0.131	0.177	2.483	0.081	0.061	2.499	0.089	0.947	0.060
LCH–As(V)	1.437	0.075	0.189	1.552	0.068	0.070	1.880	0.123	0.528	0.028
BCAH–As(V)	4.284	0.117	3.210	4.618	0.035	1.413	8.973	0.030	0.247	0.137
LCAH–As(V)	3.526	0.093	1.059	3.750	0.039	0.302	4.162	0.072	0.599	0.102

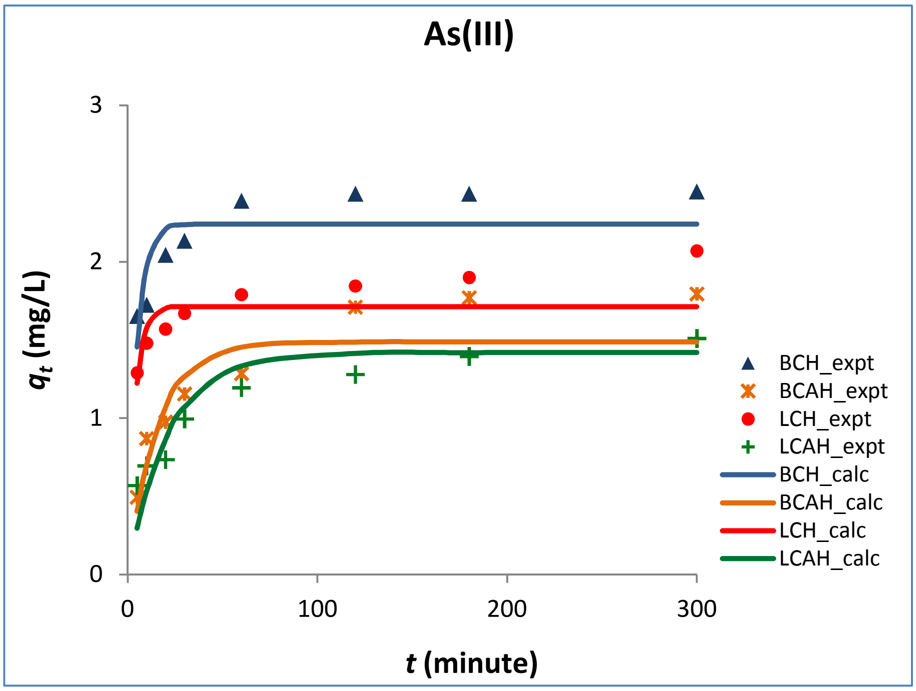

Figure 3.2.29. Plot of PFO model for the sorption of As(III) by the solids.

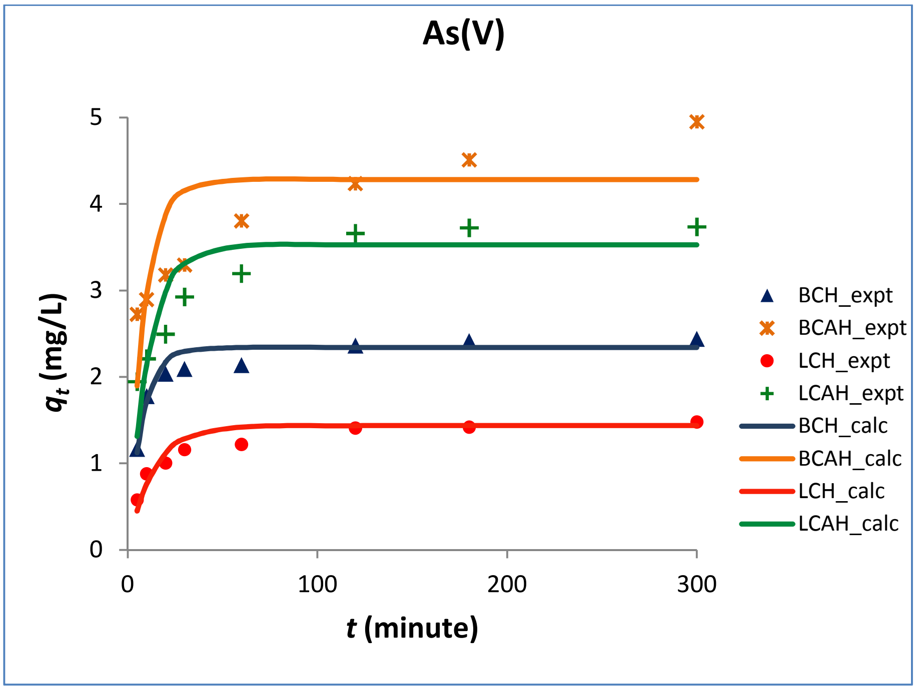

Figure 3.2.30. Plot of PFO model for the sorption of As(V) by the solids.

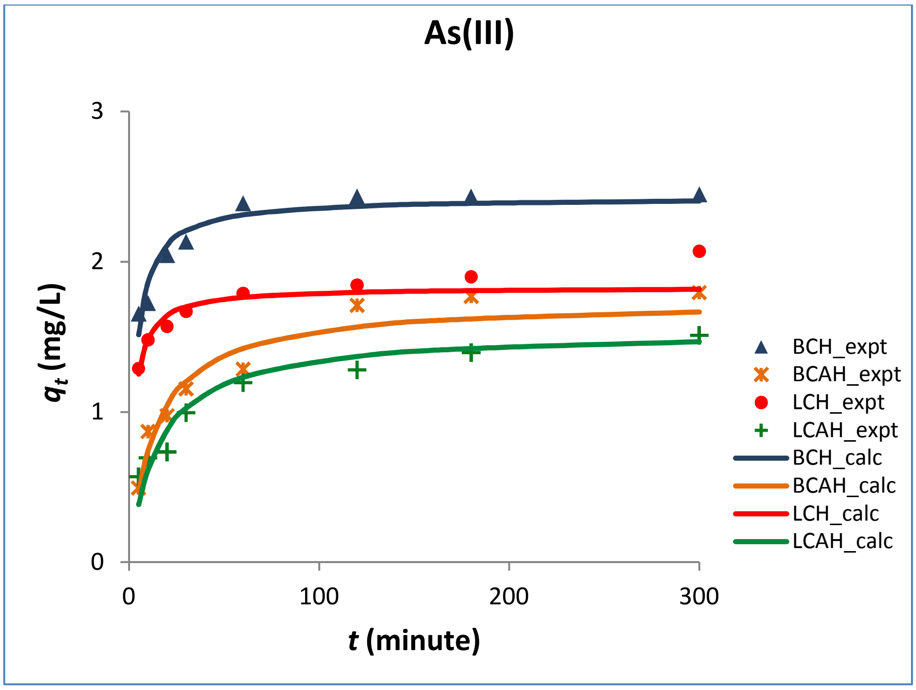

Figure 3.2.31. Plot of PSO model for the sorption of As(III) by the solids.

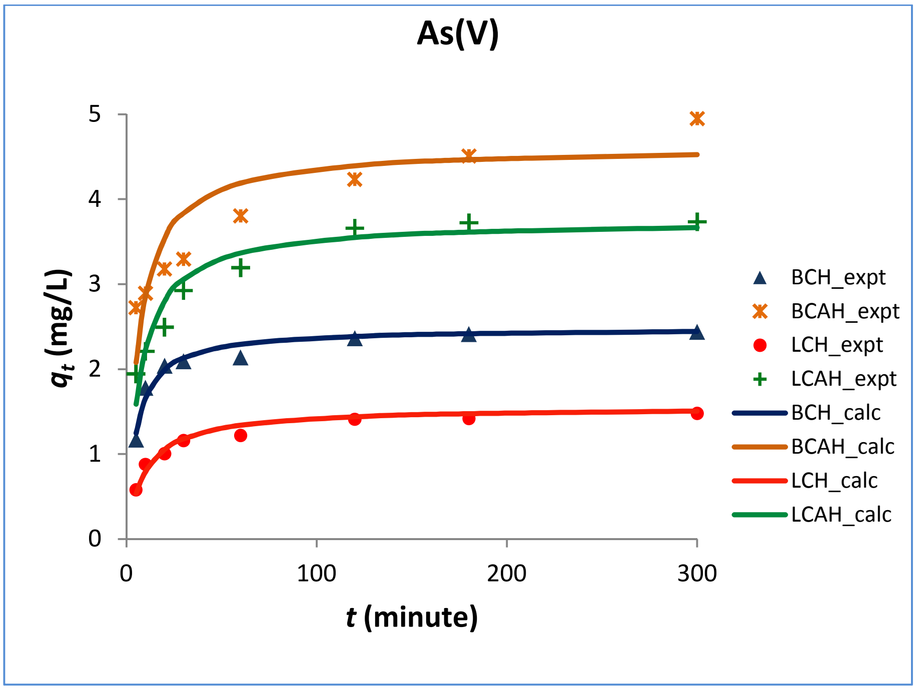

Figure 3.2.32. Plot of PSO model for the sorption of As(V) by the solids.

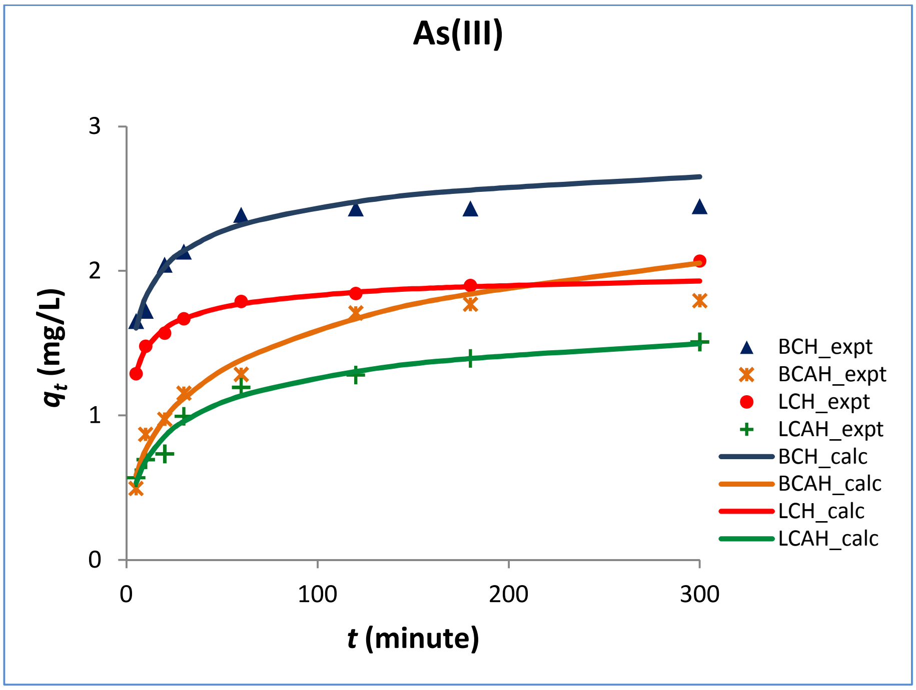

Figure 3.2.33. Plot of FL–PSO model for the sorption of As(III) by the solids.

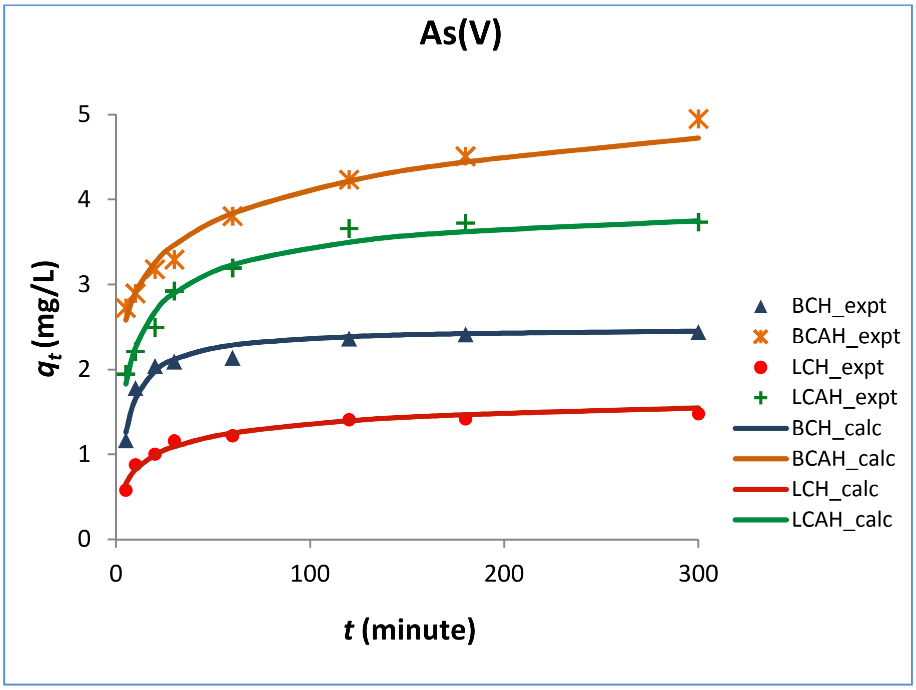

Figure 3.2.34. Plot of FL–PSO model for the sorption of As(V) by the solids.

3.2.6.2. DFS

The kinetic data of DFS are utilized in the kinetic modeling to estimate the rate constants along with the removal capacity of the solids. Since the uptake process of DFS by the LCH and LCAH is relatively slow, and hence is utilized for modeling studies (Figure 3.2.35 to 3.2.37). The estimated values of the unknown parameters along with the least square sum are returned in Table 3.2.27. It is observed that the results are more fitted to the PSO and FL-PSO models compare to the PFO model. Table also shows that comparing to LCAH, LCH possess relatively high removal capacity at least for the DFS. Moreover, the applicability of the PSO model indicates that the sorbate species are bound onto the surface of solid materials by strong chemical forces.

Table 3.2.27. Kinetic parameters estimated using various kinetic models along with the least square sum (s^2) for the removal of DFS by LCH and LCAH solids.

Systems	**PFO Model**			**PSO Model**			**FL–PSO Model**			
	q_e	k_1	s^2	q_e	k_2	s^2	q_e	k	α	s^2
BCH–DFS	3.292	0.443	0.486	3.676	0.164	0.132	4.780	0.104	0.552	0.014
BCAH–DFS	3.010	0.608	0.311	3.311	0.265	0.059	3.770	0.211	0.641	0.017
LCH–DFS	4.698	0.284	1.740	5.282	0.074	0.804	8.091	0.039	0.497	0.311
LCAH–DFS	4.432	0.344	0.882	4.939	0.100	0.432	5.363	0.096	0.776	0.352

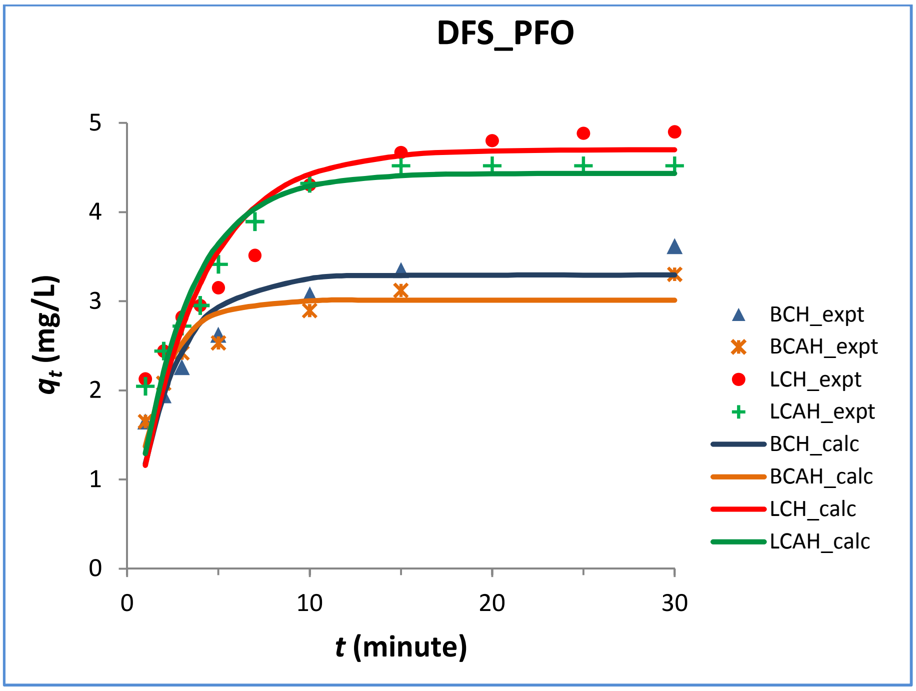

Figure 3.2.35. Plot of PFO model for the sorption of DFS.

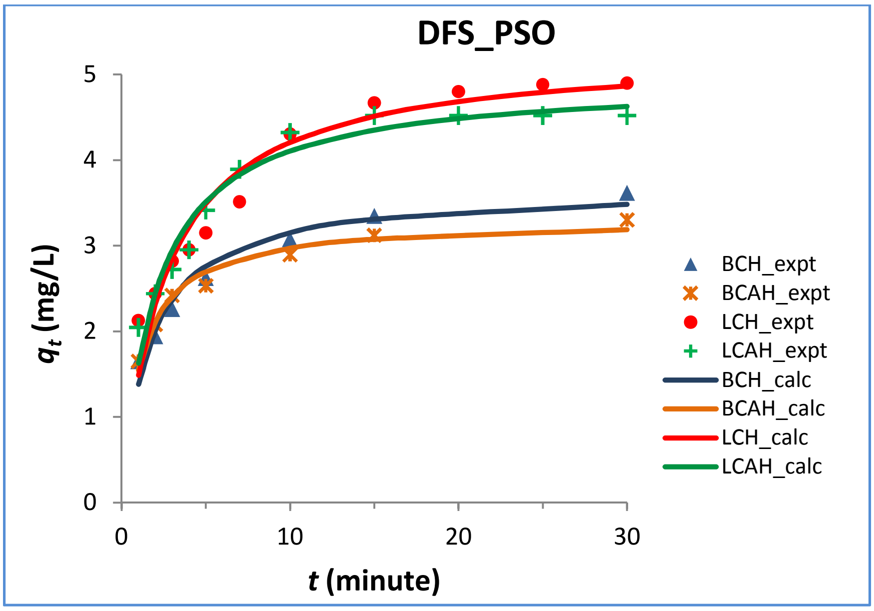

Figure 3.2.36. Plot of PSO model for the sorption of DFS.

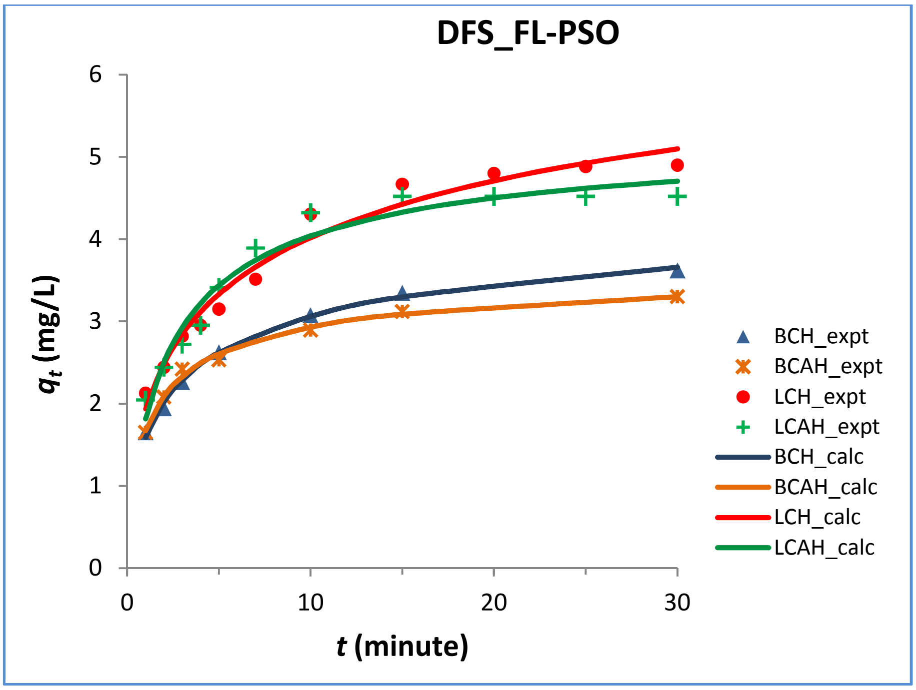

Figure 3.2.37. Plot of FL–PSO model for the sorption of DFS.

3.2.6.3. TC

The time dependence sorption data of TC are utilized to conduct the kinetic modeling for three different kinetic models and a non-linear least square fitting is conducted for the estimation of unknown parameters. The plots are shown in Figure 3.2.38 to 3.2.40. The estimated values of the rate constants along with the least square sum are returned in Table 3.2.28. The results show that the non-linear PSO and FL-PSO models very well represent the kinetics of TC sorption onto the hybrid materials compared to the PFO model. Table also shows that comparing to the Al-pillared solids, organo-clays possessed higher removal capacity except in the FL-PSO model for LCH and LCAH solids. Moreover, BCH and LCH exhibit a comparable removal capacity; and LCAH shows a little lower removal capacity comparing to the other solids except in the FL-PSO model. Further, the applicability of the PSO model indicates that the sorbate species are bound onto the surface of material by strong forces.

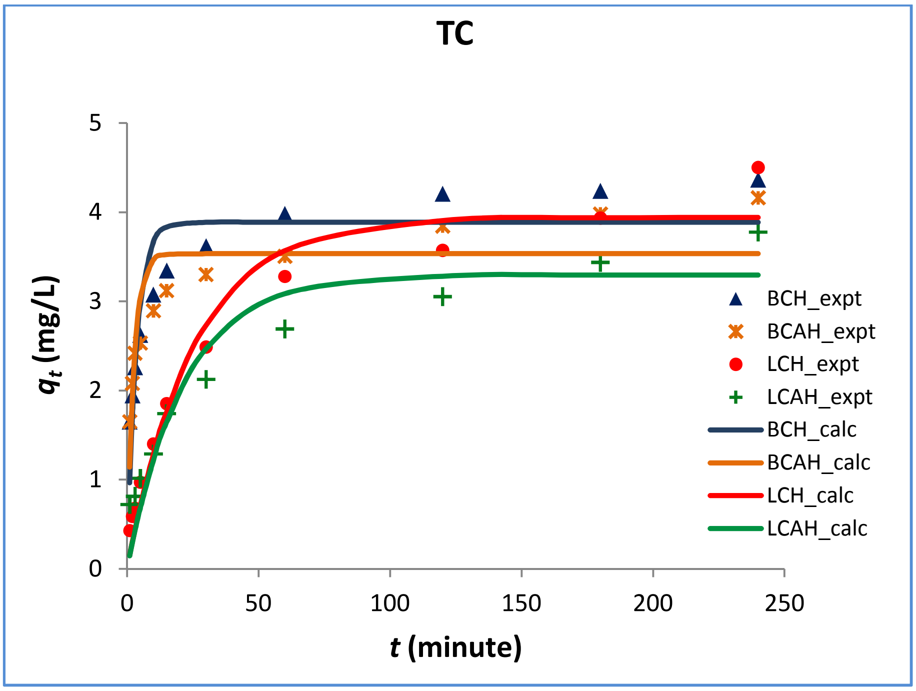

Figure 3.2.38. Plot of PFO model for the sorption of TC by the solids.

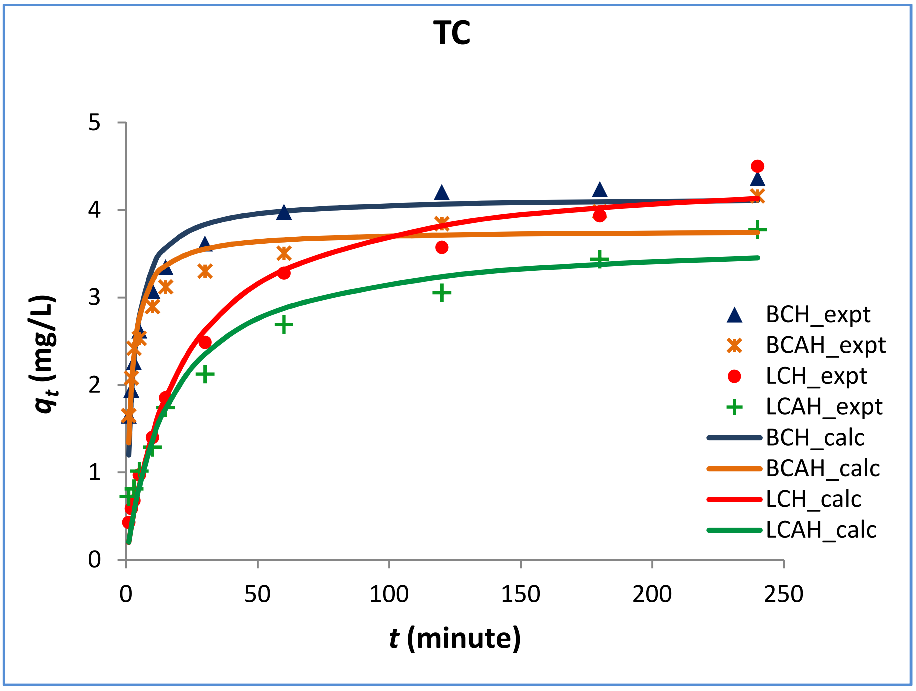

Figure 3.2.39. Plot of PSO model for the sorption of TC by the solids.

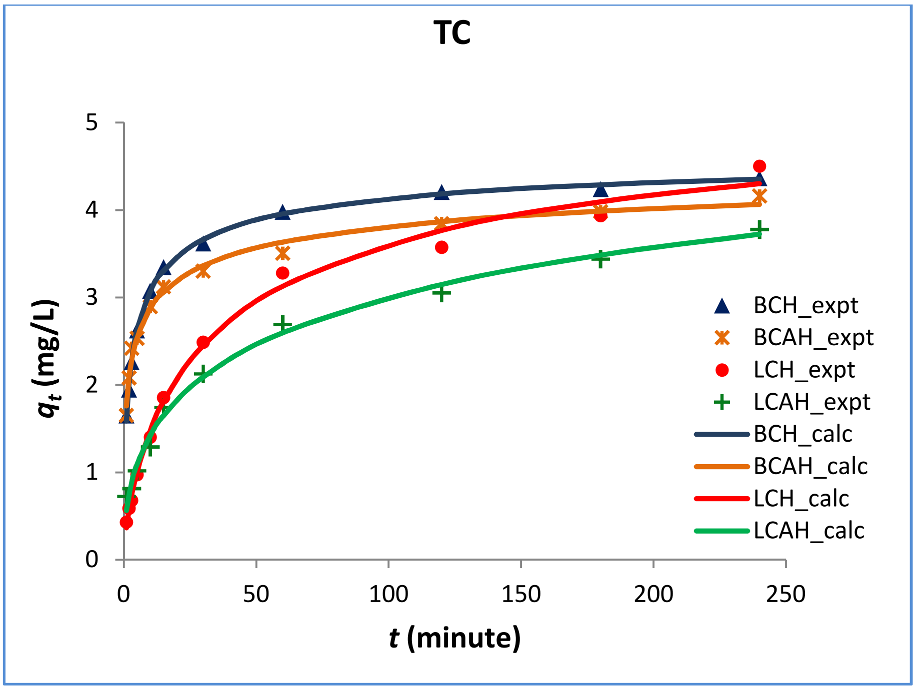

Figure 3.2.40. Plot of FL–PSO model for the sorption of TC by the solids.

Table 3.2.28. Kinetic parameters estimated using various kinetic models along with the least square sum (s^2) for the removal of TC by the solids.

Systems	**PFO Model**			**PSO Model**			**FL–PSO Model**			
	q_e	k_1	s^2	q_e	k_2	s^2	q_e	k	α	s^2
BCH–TC	3.783	0.308	1.481	4.150	0.098	0.503	4.763	0.105	0.558	0.018
BCAH–TC	3.533	0.390	1.766	3.769	0.146	0.656	4.810	0.120	0.410	0.064
LCH–TC	3.940	0.039	0.883	4.506	0.010	0.350	5.536	0.013	0.712	0.043
LCAH–TC	3.296	0.046	1.192	3.701	0.016	0.608	7.404	0.011	0.457	0.088

3.2.7. Effect of phenol on arsenic removal

The hybrid materials were utilized to assess the As(III) and As(V) removal at varying concentrations of phenol, i.e., *Ca*. 2.0 to 15.0 mg/L keeping the arsenic concentration 10.0 mg/L and pH 4.5 as constant. Results were evaluated as the percent removal of arsenic as a function of initial phenol concentration and also the amount of phenol removed as a function of initial phenol concentration as given in Table 3.2.29 (a–d) to 3.2.32 (a–d). Results are also presented graphically as percent removal of arsenic as a function of phenol concentrations in Figure 3.2.41 for As(III) and 3.2.43 for As(V); and also the amount of phenol removed as a function of phenol concentration in Figure 3.2.42 for As(III) and 3.2.44 for As(V). It is to be noted that the percent removal of As(III) is significantly decrease with the increase in phenol concentration (*cf.* Fig. 3.2.41), whereas the similar increase in phenol concentration significantly increases the amount of phenol removed (*cf.* Fig. 3.2.42). The results clearly demonstrate that there is a competition between phenol and As(III) toward the available active sites and phenol is preferentially sorbed onto the solid surface. The increase in extent of phenol removal is due to the preferential partitioning of phenol that is taking place at the HDTMA hydrophobic core and this suppresses the weakly bound As(III). It was previously reported that the alkylammonium molecule preferentially resides at the surface layer of clay, leaving the organic tail radiating away from the surface and providing a strong hydrophobic core (Alexandre and Dubois, 2000; Zanetti et al., 2000), which possibly causes to increase of phenol sorption.

On the other hand, it is observed that the increase in phenol concentration from *Ca.* 2.0 to 15.0 mg/L is not affected, significantly, the uptake of As(V) (*cf.* Fig. 3.2.43). However, the amount of phenol removed is increased by a small extent (*cf.* Fig. 3.2.44). These results fully differed from the results obtained for the As(III) removal in the presence of phenol. However, the results favoured the assumption that the binding sites are different for these two different types of sorbing species. As proposed, the As(V) is specifically bound with the aluminol or the silanol group and forming a strong chemical bond. However, the introduced HDTMA molecule is providing a strong hydrophobic core which enabled to partition phenol by the van der Waals forces. Therefore, there is no apparent change in the percent uptake of As(V) even at an increase of phenol concentration from *Ca.* 2 to 15 mg/L. However, the uptake of phenol is increased by a small amount with the increase in phenol concentrations. Earlier it was reported that the inorgano-organo-clay, i.e., bentonite modified with Fe–polycations and cetyltrimethylammonium bromide materials showed fairly good applicability in the simultaneous removal of phosphate and phenanthrene from aqueous solutions. They further pointed that the hybrid material possessed two different active sites capable to sequester different types of pollutants, i.e., organic and inorganic pollutants from aqueous solutions simultaneously (Ma and Zhu, 2006). Similarly, the aluminium pillared and HDTMA modified sericite showed similar results and found suitable for the simultaneous removal of phenol and arsenic from aqueous solutions (Tiwari and Lee, 2012).

Table 3.2.29 (a). Effect of phenol concentration on the removal of As(III) by BCH.

Initial phenol conc. (ppm)	Initial As(III) conc. (mg/L)	Final As(III) conc. (mg/L)	% Removal
2.24	12.57	6.88	45.27
5.37	12.53	7.05	43.74
8.84	13.06	8.36	35.99
12.55	12.41	9.53	23.21
16.83	12.44	9.51	23.56

Table 3.2.29 (b). Effect of phenol concentration on the removal of As(III) by LCH.

Initial phenol conc. (ppm)	Initial As(III) conc. (mg/L)	Final As(III) conc. (mg/L)	% Removal
2.24	12.57	7.95	36.75
5.37	12.53	8.47	32.40
8.84	13.06	10.06	22.97
12.55	12.41	10.72	13.62
16.83	12.44	10.69	14.07

Table 3.2.29 (c). Effect of phenol concentration on the removal of As(III) by BCAH.

Initial phenol conc. (ppm)	Initial As(III) conc. (mg/L)	Final As(III) conc. (mg/L)	% Removal
2.24	12.57	7.64	39.22
5.37	12.53	7.81	37.67
8.84	13.06	8.33	36.22
12.55	12.41	8.95	27.88
16.83	12.44	10.21	17.93

Table 3.2.29 (d). Effect of phenol concentration on the removal of As(III) by LCAH.

Initial phenol conc. (ppm)	Initial As(III) conc. (mg/L)	Final As(III) conc. (mg/L)	% Removal
2.24	12.57	9.04	28.08
5.37	12.53	8.92	28.81
8.84	13.06	10.12	22.51
12.55	12.41	10.57	14.83
16.83	12.44	11.52	7.40

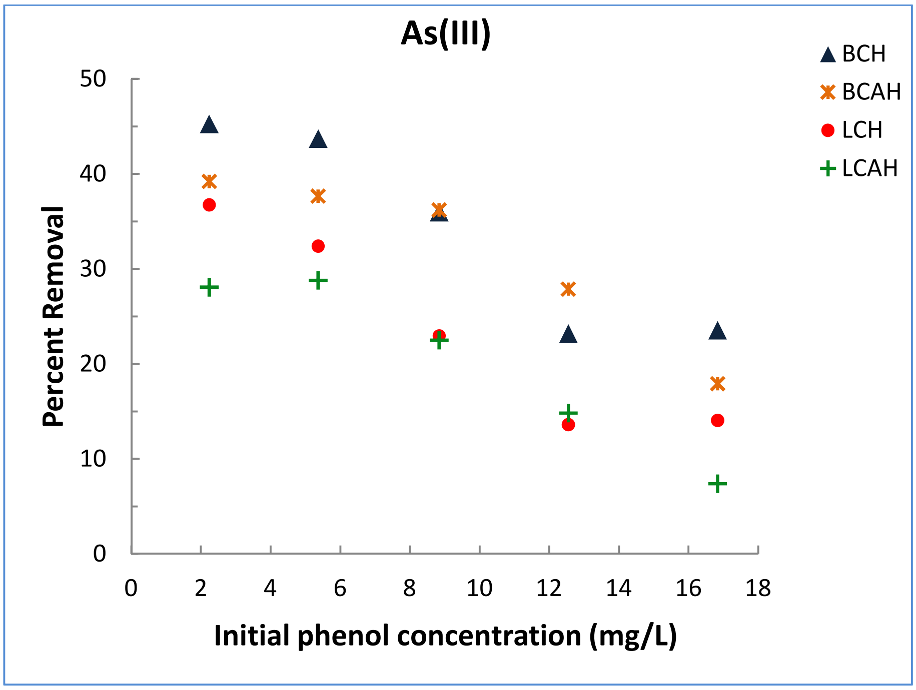

Figure 3.2.41. Removal of As(III) by the hybrid materials as a function of phenol concentration.

Table 3.2.30 (a). Removal of phenol by BCH in presence of As(III) as a function of phenol concentration.

As(III) conc. (ppm)	Initial phenol conc. (mg/L)	Final phenol conc. (mg/L)	Amount Removed (mg/g)
12.57	2.24	0.73	0.75
12.53	5.37	3.20	1.08
13.06	8.84	6.41	1.22
12.41	12.55	9.50	1.53
12.44	16.83	14.44	1.58

Table 3.2.30 (b). Removal of phenol by LCH in presence of As(III) as a function of phenol concentration.

As(III) conc. (ppm)	Initial phenol conc. (mg/L)	Final phenol conc. (mg/L)	Amount Removed (mg/g)
12.57	2.24	0.54	0.85
12.53	5.37	3.67	0.85
13.06	8.84	7.30	0.77
12.41	12.55	10.62	0.97
12.44	16.83	14.63	1.10

Table 3.2.30 (c). Removal of phenol by BCAH in presence of As(III) as a function of phenol concentration.

As(III) conc. (ppm)	Initial phenol conc. (mg/L)	Final phenol conc. (mg/L)	Amount Removed (mg/g)
12.57	2.24	0.77	0.73
12.53	5.37	3.47	0.95
13.06	8.84	6.60	1.12
12.41	12.55	9.81	1.37
12.44	16.83	13.44	1.70

Table 3.2.30 (d). Removal of phenol by LCAH in presence of As(III) as a function of phenol concentration.

As(III) conc. (ppm)	Initial phenol conc. (mg/L)	Final phenol conc. (mg/L)	Amount Removed (mg/g)
12.57	2.24	0.85	0.69
12.53	5.37	3.86	0.75
13.06	8.84	7.34	0.75
12.41	12.55	11.16	0.69
12.44	16.83	14.98	0.93

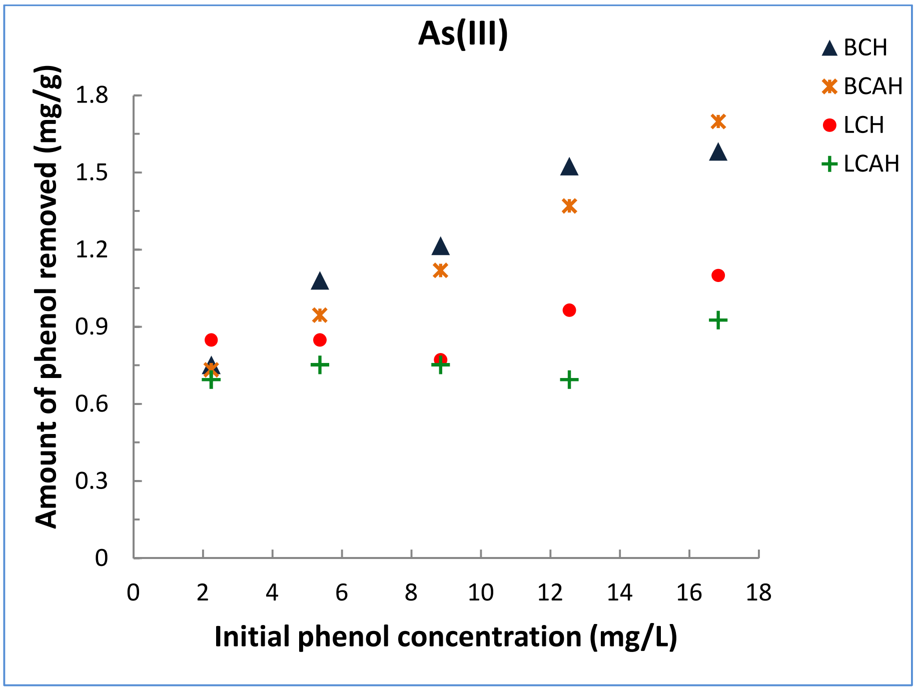

Figure 3.2.42. Removal of phenol as a function of initial phenol concentration.

Table 3.2.31 (a). Effect of phenol concentration on the removal of As(V) by BCH.

Initial phenol conc. (ppm)	Initial As(V) conc. (mg/L)	Final As(V) conc. (mg/L)	% Removal
2.44	9.11	4.54	50.16
4.85	8.89	4.62	48.03
8.11	8.76	4.85	44.63
11.63	8.85	4.37	50.62
14.69	8.82	4.60	47.85

Table 3.2.31 (b). Effect of phenol concentration on the removal of As(V) by LCH.

Initial phenol conc. (ppm)	Initial As(V) conc. (mg/L)	Final As(V) conc. (mg/L)	% Removal
2.44	9.11	6.31	30.74
4.85	8.89	6.40	28.01
8.11	8.76	6.43	26.60
11.63	8.85	7.03	20.56
14.69	8.82	6.96	21.09

Table 3.2.31 (c). Effect of phenol concentration on the removal of As(V) by BCAH.

Initial phenol conc. (ppm)	Initial As(V) conc. (mg/L)	Final As(V) conc. (mg/L)	% Removal
2.44	9.11	0.12	98.68
4.85	8.89	0.39	95.61
8.11	8.76	0.36	95.89
11.63	8.85	0.30	96.61
14.69	8.82	0.42	95.24

Table 3.2.31 (d). Effect of phenol concentration on the removal of As(V) by LCAH.

Initial phenol conc. (ppm)	Initial As(V) conc. (mg/L)	Final As(V) conc. (mg/L)	% Removal
2.44	9.11	1.81	80.13
4.85	8.89	2.54	71.43
8.11	8.76	2.55	70.89
11.63	8.85	2.35	73.45
14.69	8.82	2.89	67.23

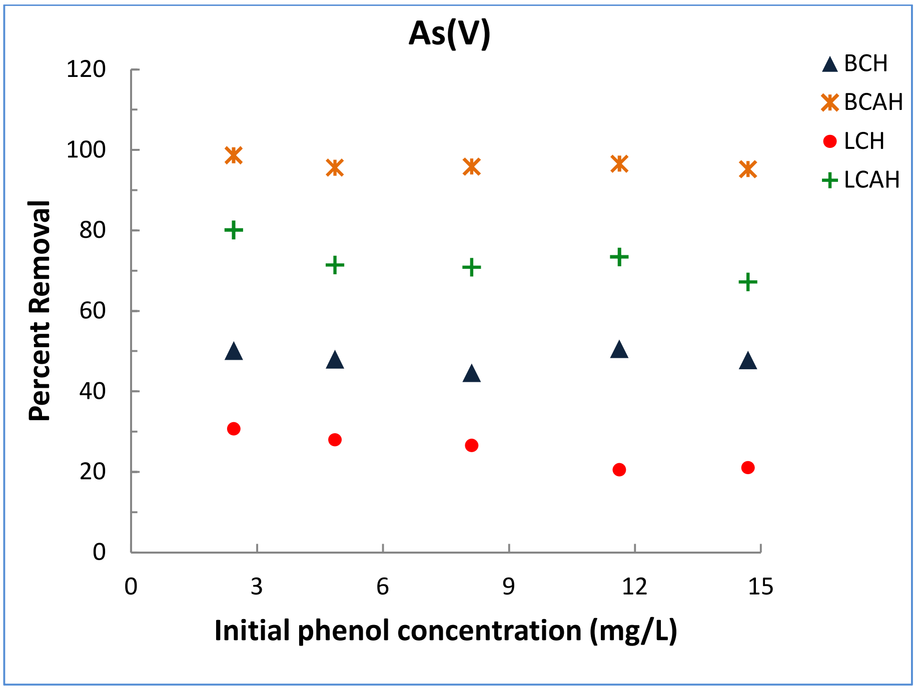

Figure 3.2.43. Removal of As(V) by the hybrid materials as a function of phenol concentration.

Table 3.2.32 (a). Removal of phenol by BCH in presence of As(V) as a function of phenol concentration.

As(V) conc. (ppm)	Initial phenol conc. (mg/L)	Final phenol conc. (mg/L)	Amount Removed (mg/g)
9.11	2.44	1.01	0.72
8.89	4.85	3.29	0.78
8.76	8.11	6.45	0.83
8.85	11.63	9.41	1.11
8.82	14.69	11.07	1.03

Table 3.2.32 (b). Removal of phenol by LCH in presence of As(V) as a function of phenol concentration.

As(V) conc. (ppm)	Initial phenol conc. (mg/L)	Final phenol conc. (mg/L)	Amount Removed (mg/g)
9.11	2.44	1.17	0.64
8.89	4.85	3.58	0.64
8.76	8.11	6.84	0.64
8.85	11.63	10.20	0.72
8.82	14.69	13.29	0.70

Table 3.2.32 (c). Removal of phenol by BCAH in presence of As(V) as a function of phenol concentration.

As(V) conc. (ppm)	Initial phenol conc. (mg/L)	Final phenol conc. (mg/L)	Amount Removed (mg/g)
9.11	2.44	1.07	0.68
8.89	4.85	3.32	0.77
8.76	8.11	6.19	0.96
8.85	11.63	9.80	0.91
8.82	14.69	13.00	0.85

Table 3.2.32 (d). Removal of phenol by LCAH in presence of As(V) as a function of phenol concentration.

As(V) conc. (ppm)	Initial phenol conc. (mg/L)	Final phenol conc. (mg/L)	Amount Removed (mg/g)
9.11	2.44	1.07	0.68
8.89	4.85	3.36	0.75
8.76	8.11	6.64	0.73
8.85	11.63	10.16	0.73
8.82	14.69	13.09	0.80

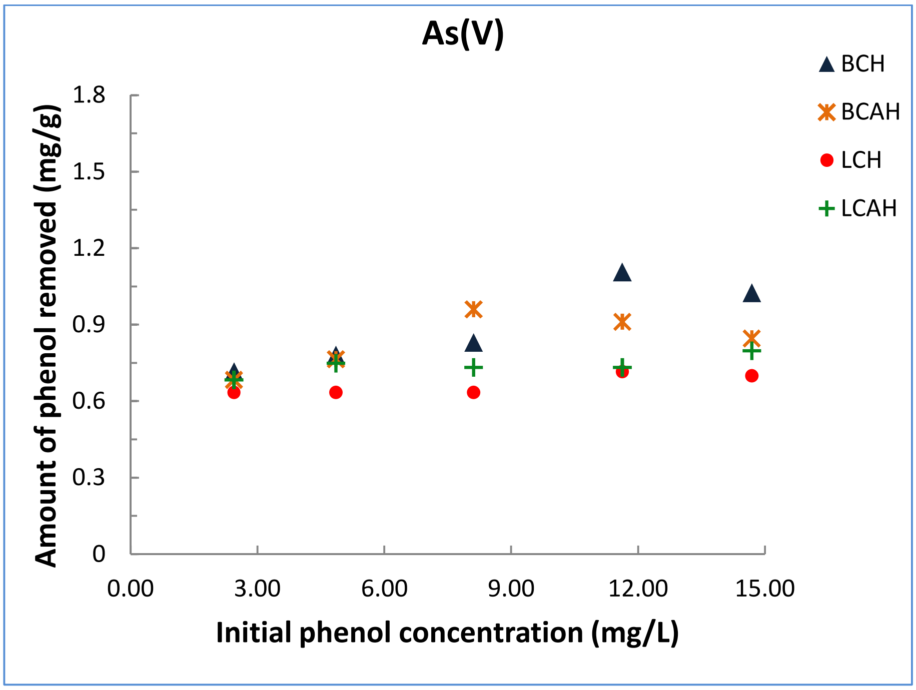

Figure 3.2.44. Removal of phenol as a function of initial phenol concentration.

3.2.8. Effect of co-ions on arsenic removal

Further, the sorption of As(III) and As(V) was conducted in presence of several cations and anions separately, keeping the arsenic concentration 10.0 mg/L and pH 4.5 as constant, with a solid dose of 2 g/L. The co-ion concentration was taken as 50.0 mg/L. The cations chosen were Cd(II), Cu(II) and Mn(II) ions; whereas the anions taken were glycinate, iminodiacetate (IDA), sulfate, oxalate, phosphate and ethylenediaminetetraacetate (EDTA) ions. The results are presented in Table 3.2.33 to 3.2.36 and shown graphically in Figure 3.2.45 to 3.2.48.

Figure 3.2.45 shows that the presence of these cations, in general, caused to decrease the percent removal of As(III). However, the sorption of As(III) by the solids BCAH and LCAH is not affected significantly by the presence of Cd(II). The presence of anions, at least for BCH and LCH solids, is caused to decrease significantly the percent removal of As(III) (*cf.* Fig. 3.2.46). However, BCAH and LCAH solids possess almost identical percent removal of As(III) as compare to the blank sorption data. Therefore, the solids BCAH and LCAH are selective sorbing materials for the removal of As(III) even in the presence of several anions. Earlier, it was reported that the presence of several anions NO_3^-, Cl^-, SO_4^{2-}, HCO_3^- and CO_3^{2-} showed a marked decrease in As(III) sorption by the hybrid material, i.e., zirconium(IV) oxide-ethanolamine (ZrO–EA). However, the presence of CO_3^{2-} and HCO_3^- caused practically negligible removal of As(III) (Mandal et al., 2011).

Table 3.2.33 (a). Effect of cations on the removal of As(III) by BCH.

Cations	Initial As(III) conc. (ppm)	Final As(III) conc. (ppm)	% Removal
Cd(II)	10.32	7.00	32.17
Cu(II)	9.98	7.24	27.46
Mn(II)	9.93	6.83	31.22
Blank	10.00	5.84	41.62

Table 3.2.33 (b). Effect of cations on the removal of As(III) by LCH.

Cations	Initial As(III) conc. (ppm)	Final As(III) conc. (ppm)	% Removal
Cd(II)	10.32	7.34	28.88
Cu(II)	9.98	7.65	23.35
Mn(II)	9.93	7.24	27.09
Blank	10.00	6.14	38.57

Table 3.2.33 (c). Effect of cations on the removal of As(III) by BCAH.

Cations	Initial As(III) conc. (ppm)	Final As(III) conc. (ppm)	% Removal
Cd(II)	10.32	6.93	32.85
Cu(II)	9.98	7.20	27.86
Mn(II)	9.93	7.18	27.69
Blank	10.00	6.58	34.18

Table 3.2.33 (d). Effect of cations on the removal of As(III) by LCAH.

Cations	Initial As(III) conc. (ppm)	Final As(III) conc. (ppm)	% Removal
Cd(II)	10.32	7.11	31.10
Cu(II)	9.98	7.55	24.35
Mn(II)	9.93	7.19	27.59
Blank	10.00	7.12	28.81

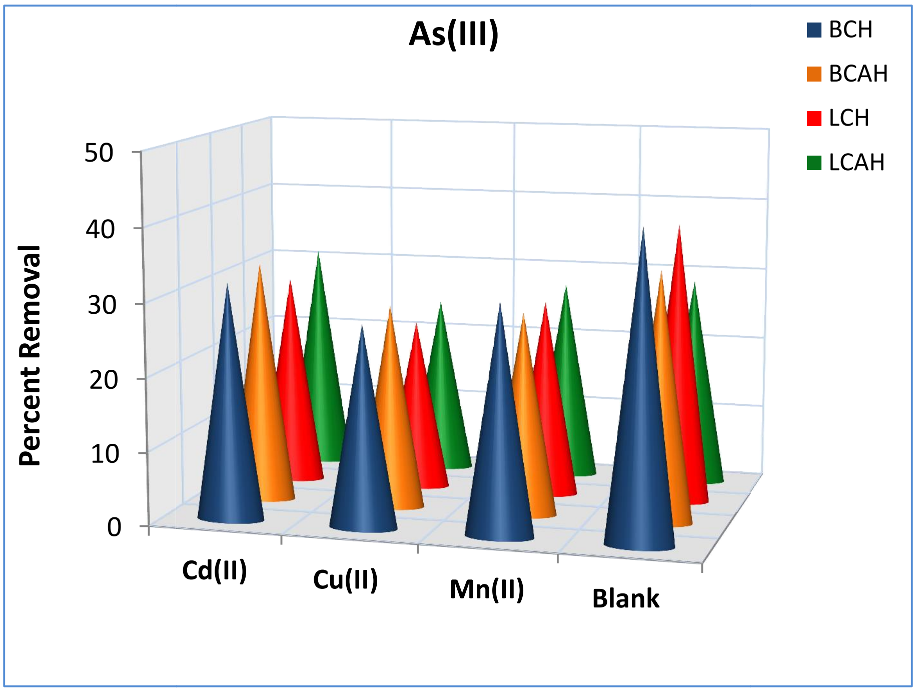

Figure 3.2.45. Removal of As(III) by the hybrid materials in presence of cations.

Table 3.2.34 (a). Effect of anions on the removal of As(III) by BCH.

Cations	Initial As(III) conc. (ppm)	Final As(III) conc. (ppm)	% Removal
Glycinate	10.55	7.57	28.25
IDA	11.32	7.65	32.42
Sulfate	9.46	7.08	25.16
Oxalate	11.27	6.95	38.33
Phosphate	9.47	7.32	22.70
EDTA	10.66	7.35	31.05
Blank	10.5	6.13	41.62

Table 3.2.34 (b). Effect of anions on the removal of As(III) by LCH.

Cations	Initial As(III) conc. (ppm)	Final As(III) conc. (ppm)	% Removal
Glycinate	10.55	8.27	21.61
IDA	11.32	8.16	27.92
Sulfate	9.46	7.61	19.56
Oxalate	11.27	7.68	31.85
Phosphate	9.47	7.84	17.21
EDTA	10.66	8.32	21.95
Blank	10.5	6.45	38.57

Table 3.2.34 (c). Effect of anions on the removal of As(III) by BCAH.

Cations	Initial As(III) conc. (ppm)	Final As(III) conc. (ppm)	% Removal
Glycinate	10.55	7.36	30.24
IDA	11.32	7.23	36.13
Sulfate	9.46	6.96	26.43
Oxalate	11.27	6.98	38.07
Phosphate	9.47	7.15	24.50
EDTA	10.66	7.22	32.27
Blank	10.5	6.9111	34.18

Table 3.2.34 (d). Effect of anions on the removal of As(III) by LCAH.

Cations	Initial As(III) conc. (ppm)	Final As(III) conc. (ppm)	% Removal
Glycinate	10.55	7.55	28.44
IDA	11.32	8.11	28.36
Sulfate	9.46	7.16	24.31
Oxalate	11.27	7.74	31.32
Phosphate	9.47	7.44	21.44
EDTA	10.66	7.78	27.02
Blank	10.5	7.47495	28.81

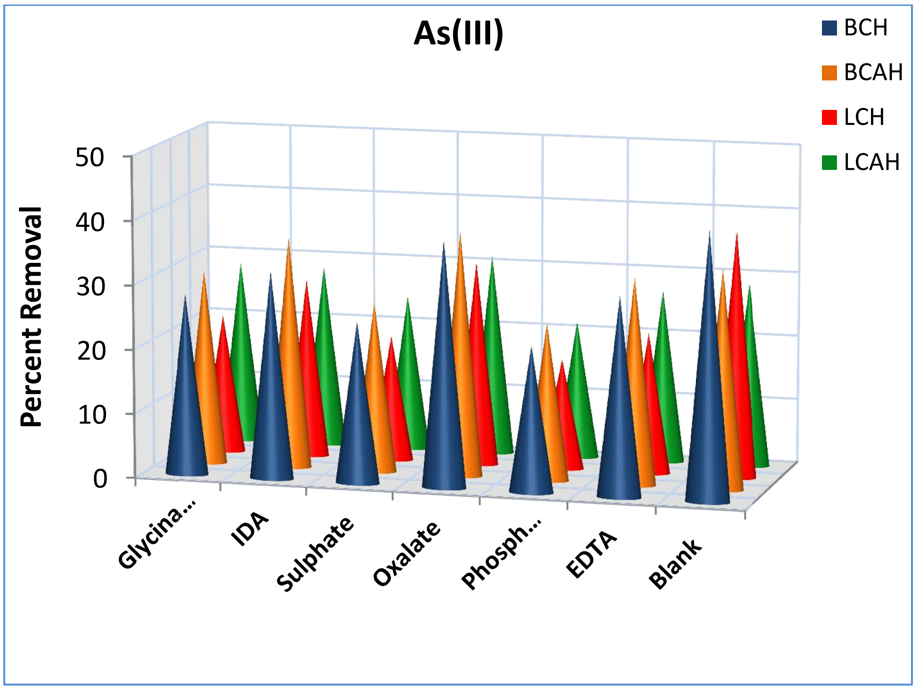

Figure 3.2.46. Removal of As(III) by the hybrid materials in presence of anions.

Unlike As(III), the uptake of As(V) is almost unaffected in the presence of Cd(II), Cu(II) or Mn(II) for solids BCAH and LCAH (*cf.* Fig. 3.2.47). Moreover, for the solids BCH and LCH, the presence of Cu(II) and Mn(II) could not affect significantly the attenuation of

As(V); whereas the presence of Cd(II), definitely, causes to decrease the uptake of As(V) for the solids BCH and LCH. Previously, it was reported that the presence of Ca^{2+} or Mg^{2+} enhanced the arsenate sorption whereas Fe^{2+} caused to decrease the removal of arsenate by the iron based sorbing materials (Zhu et al., 2009a).

Similarly, the presence of glycinate, IDA, oxalate and EDTA could not affect the uptake of As(V) by the solids BCAH and LCAH (*cf.* Fig. 3.2.48). However, the presence of phosphate, to some extent, decreases the uptake of As(V). The presence of these anions, in general, could affect the removal of As(V) by the BCH and LCH solids from aqueous solutions. These results again show the greater applicability of the aluminium pillared HDTMA modified clay samples in the effective and selective removal of arsenic from ground water samples. Previously, it was also reported that the presence of phosphate suppressed the arsenic removal by the ferrous based red mud sludge, however, carbonate showed no effect in arsenic removal (Li et al., 2010b). Further, it is suggested that since phosphorous and arsenic elements are lying in the same group, and arsenate and phosphate are having similar molecular structures which caused for competitive sorption onto the same surface active sites. The other report indicated that the anions such as arsenate, phosphate, or even silicate readily formed inner-sphere complexes with the surfaces of iron oxides (or nano zero valent iron supported on activated carbon) and a competitive sorption occurred for the binding sites and hence decreased the sorption of arsenic. The sulfate ions were sorbed both specifically and non-specifically and the bond strength with iron (hydr)oxide was much weaker than that of arsenate and hence, it affected insignificantly the uptake of arsenic (Zhu et al., 2009a; Jia and Demopoulos, 2005). Similarly, the presence of co-ions such as chloride, nitrate, sulfate, chromate, and acetate was not interfered with the sorption of As(V), whereas phosphate greatly influenced the sorption by the aluminium–loaded Shirasu–zeolite (Xu et al., 2002).

Table 3.2.35 (a). Effect of cations on the removal of As(V) by BCH.

Cations	Initial As(V) conc. (ppm)	Final As(V) conc. (ppm)	% Removal
Cd(II)	10.55	7.58	28.15
Cu(II)	12.85	6.48	49.57
Mn(II)	13.01	6.65	48.89
Blank	10.50	5.53	47.38

Table 3.2.35 (b). Effect of cations on the removal of As(V) by LCH.

Cations	Initial As(V) conc. (ppm)	Final As(V) conc. (ppm)	% Removal
Cd(II)	10.55	9.37	11.18
Cu(II)	12.85	9.29	27.70
Mn(II)	13.01	9.80	24.67
Blank	10.50	7.16	31.77

Table 3.2.35 (c). Effect of cations on the removal of As(V) by BCAH.

Cations	Initial As(V) conc. (ppm)	Final As(V) conc. (ppm)	% Removal
Cd(II)	10.55	0.13	98.77
Cu(II)	12.85	0.14	98.91
Mn(II)	13.01	0.79	93.93
Blank	10.50	0.17	98.51

Table 3.2.35 (d). Effect of cations on the removal of As(V) by LCAH.

Cations	Initial As(V) conc. (ppm)	Final As(V) conc. (ppm)	% Removal
Cd(II)	10.55	2.69	74.50
Cu(II)	12.85	2.39	81.40
Mn(II)	13.01	1.03	92.08
Blank	10.50	2.67	74.54

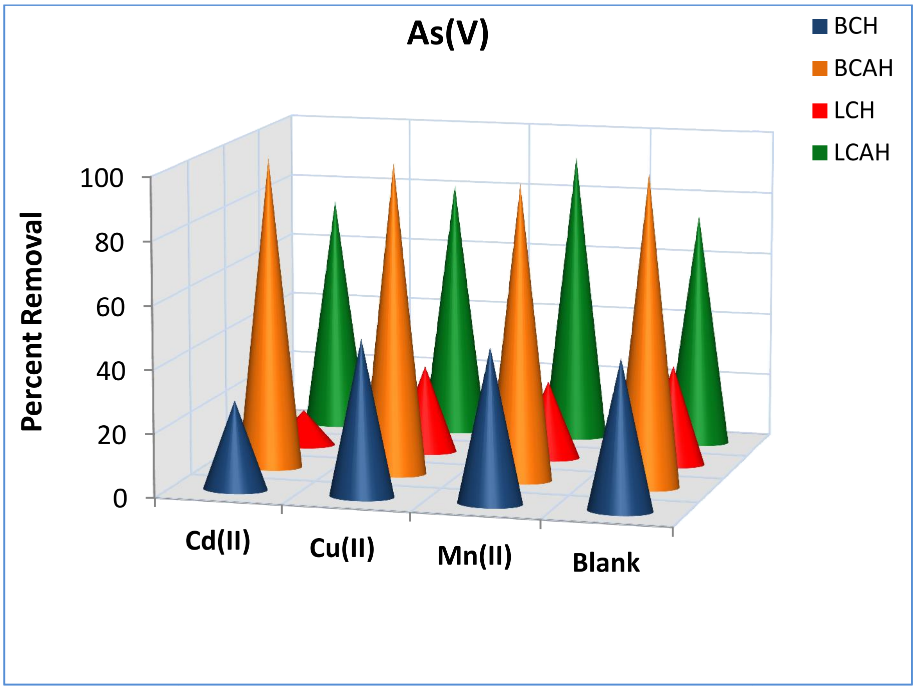

Figure 3.2.47. Removal of As(V) by the hybrid materials in presence of cations.

Table 3.2.36 (a). Effect of anions on the removal of As(V) by BCH.

Anions	Initial As(V) conc. (ppm)	Final As(V) conc. (ppm)	% Removal
Glycinate	11.03	5.14	53.40
IDA	10.88	7.97	26.75
Sulfate	11	8.24	25.09
Oxalate	11.46	8.53	25.57
Phosphate	11.52	8.53	25.95
EDTA	11.88	8.23	30.72
Blank	10.55	5.55	47.38

Table 3.2.36 (b). Effect of anions on the removal of As(V) by LCH.

Anions	Initial As(V) conc. (ppm)	Final As(V) conc. (ppm)	% Removal
Glycinate	11.03	8.68	21.31
IDA	10.88	8.83	18.84
Sulfate	11	9.37	14.82
Oxalate	11.46	9.67	15.62
Phosphate	11.52	9.88	14.24
EDTA	11.88	10.03	15.57
Blank	10.55	7.20	31.77

Table 3.2.36 (c). Effect of anions on the removal of As(V) by BCAH.

Anions	Initial As(III) conc. (ppm)	Final As(III) conc. (ppm)	% Removal
Glycinate	11.03	0.19	98.28
IDA	10.88	0.34	96.88
Sulfate	11.00	0.48	95.64
Oxalate	11.46	1.18	89.70
Phosphate	11.52	1.97	82.90
EDTA	11.88	0.02	98.15
Blank	10.55	0.16	98.51

Table 3.2.36 (d). Effect of anions on the removal of As(V) by LCAH.

Anions	Initial As(III) conc. (ppm)	Final As(III) conc. (ppm)	% Removal
Glycinate	11.03	1.16	89.48
IDA	10.88	1.72	84.19
Sulfate	11.00	2.25	79.55
Oxalate	11.46	3.33	70.94
Phosphate	11.52	6.66	42.19
EDTA	11.88	2.38	79.97
Blank	10.55	2.69	74.54

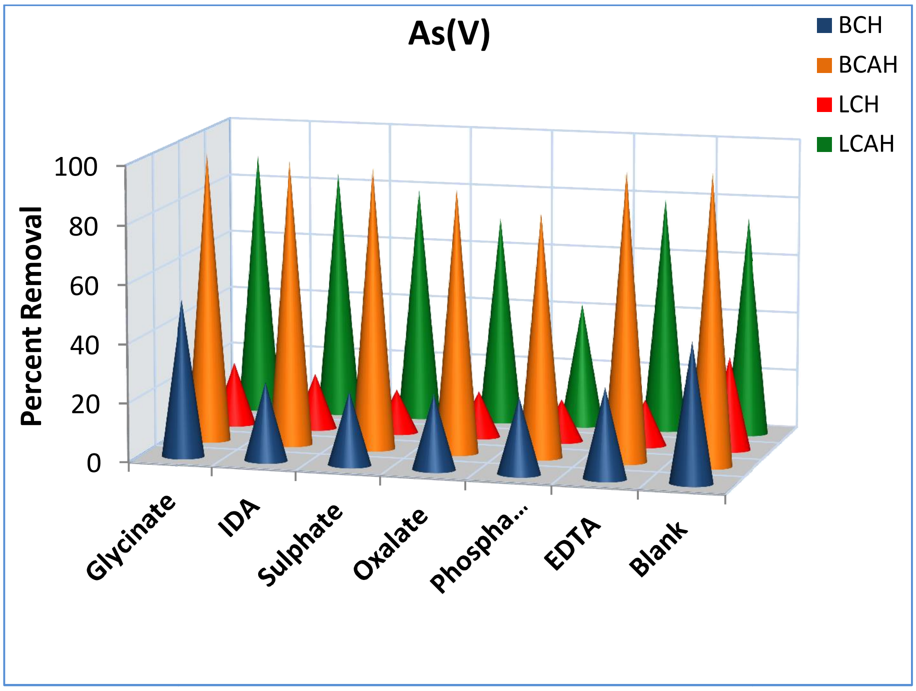

Figure 3.2.48. Removal of As(V) by the hybrid materials in presence of anions.

3.2.9. Effect of co-existing ions on EDCs removal

The sorption of EDCs by the hybrid materials was conducted in presence of several cations and anions separately, keeping the EDCs concentration 5.0 mg/L for EE2 and 10.0 mg/L for BPA, DFS and TC, at pH ~7.0, and with a solid dose of 2.0 g/L. The co-existing ion concentration was taken as 50.0 mg/L. The cations chosen were Cd(II), Cu(II) and Mn(II); whereas the anions taken were nitrate, phosphate, glycinate, iminodiacetate (IDA) and ethylenediaminetetraacetate (EDTA). The results are presented in Tables 3.2.37 to 3.2.44 and also shown graphically in Figures 3.2.49 to 3.2.56.

The presence of these cations, *viz*., Cd(II), Cu(II) and Mn(II), in general, cause insignificant change in the percent removal of EDCs. In presence of cations, the solids possess almost identical percent removal of the four EDCs, *viz*., BPA, EE2, DFS and TC as compared to the blank sorption data. However, the sorption of the four EDCs by the solid LCAH is insignificantly enhanced by about 1−2% by the presence of these cations. Therefore, these results further indicated the efficiency and selectivity of the hybrid materials in the removal of these EDCs even in presence of studied cations.

Similarly, the presence of nitrate, phosphate, glycinate, IDA and EDTA, in general, could not affect the uptake of the four EDCs by the solids comparing to the blank sorption data. These results further enhances the applicability of the hybrid clay samples in the effective and selective removal of EDCs from aqueous solutions. Previously Senturk et al. (2009) showed that the presence of 0.01 and 0.5 mol/L of NaCl and Na_2SO_4 could not significantly affect the adsorption of phenol onto organobentonite. Bagherifam et al. (2014) observed that the presence of Cl^-, CO_3^{2-} and SO_4^{2-} anions showed negligible effect on perchlorate uptake capacity using the HDPy-montmorillonite suggesting a high selectivity in the removal of perchlorate from aqueous solutions. Similarly, El-Nahhal and Safi (2004) indicated that adsorption of phenanthrene onto organo-clay (benzyltrimethylammonium modified montmorillonite) caused to increase from 0.85 to 0.96 mg/g as the concentration of NaCl increased was increased from the 0 to 150.0 g NaCl/L. Further, Berhane et al. (2015) reported that no significant difference in sorption of carbamazepine by palygorskite-montmorillonite (PM) was observed between ionic strength of 1.0 and 10.0 mmol/L of $CaCl_2$, but elevated level of carbamazepine sorption was observed at a solution ionic strength of 100 mmol/L. They further reported that higher Ca^{2+} concentration could affect the aqueous solubility of carbamazepine by decreasing its hydrophilicity and salting-out effect while enhanced sorption onto the PM surface was found to be diffusion controlled.

Table 3.2.37 (a). Effect of cations on the removal of BPA by BCH.

Cations	Initial BPA conc. (ppm)	Final BPA conc. (ppm)	% Removal
Blank	9.92	0.02	99.81
Cd	9.92	0.06	99.37
Cu	9.92	0.13	98.66
Mn	9.92	0.01	99.90

Table 3.2.37 (b). Effect of cations on the removal of BPA by LCH.

Cations	Initial BPA conc. (ppm)	Final BPA conc. (ppm)	% Removal
Blank	9.92	0.17	98.33
Cd	9.92	0.32	96.80
Cu	9.92	0.14	98.61
Mn	9.92	0.16	98.35

Table 3.2.37 (c). Effect of cations on the removal of BPA by BCAH.

Cations	Initial BPA conc. (ppm)	Final BPA conc. (ppm)	% Removal
Blank	9.92	0.06	99.40
Cd	9.92	0.05	99.50
Cu	9.92	0.09	99.09
Mn	9.92	0.04	99.63

Table 3.2.37 (d). Effect of cations on the removal of BPA by LCAH.

Cations	Initial BPA conc. (ppm)	Final BPA conc. (ppm)	% Removal
Blank	9.92	0.49	95.09
Cd	9.92	0.30	97.02
Cu	9.92	0.31	96.86
Mn	9.92	0.28	97.15

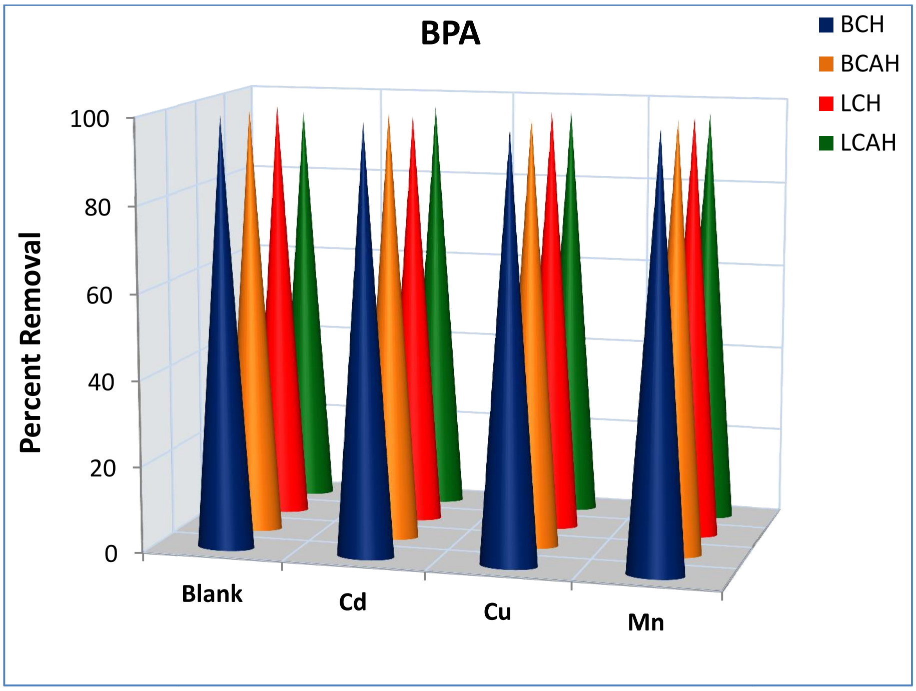

Figure 3.2.49. Removal of BPA by the hybrid materials in presence of cations.

Table 3.2.38 (a). Effect of cations on the removal of EE2 by BCH.

Cations	Initial BPA conc. (ppm)	Final BPA conc. (ppm)	% Removal
Blank	5.01	0.23	95.40
Cd	5.03	0.19	96.28
Cu	5.05	0.26	94.82
Mn	5.04	0.07	98.70

Table 3.2.38 (b). Effect of cations on the removal of EE2 by LCH.

Cations	Initial BPA conc. (ppm)	Final BPA conc. (ppm)	% Removal
Blank	5.01	0.26	94.89
Cd	5.03	0.30	94.06
Cu	5.05	0.32	93.60
Mn	5.04	0.18	96.46

Table 3.2.38 (c). Effect of cations on the removal of EE2 by BCAH.

Cations	Initial BPA conc. (ppm)	Final BPA conc. (ppm)	% Removal
Blank	5.01	0.22	95.64
Cd	5.03	0.19	96.18
Cu	5.05	0.20	95.95
Mn	5.04	0.19	96.28

Table 3.2.38 (d). Effect of cations on the removal of EE2 by LCAH.

Cations	Initial BPA conc. (ppm)	Final BPA conc. (ppm)	% Removal
Blank	5.01	0.47	90.57
Cd	5.03	0.43	91.40
Cu	5.05	0.42	91.60
Mn	5.04	0.43	91.48

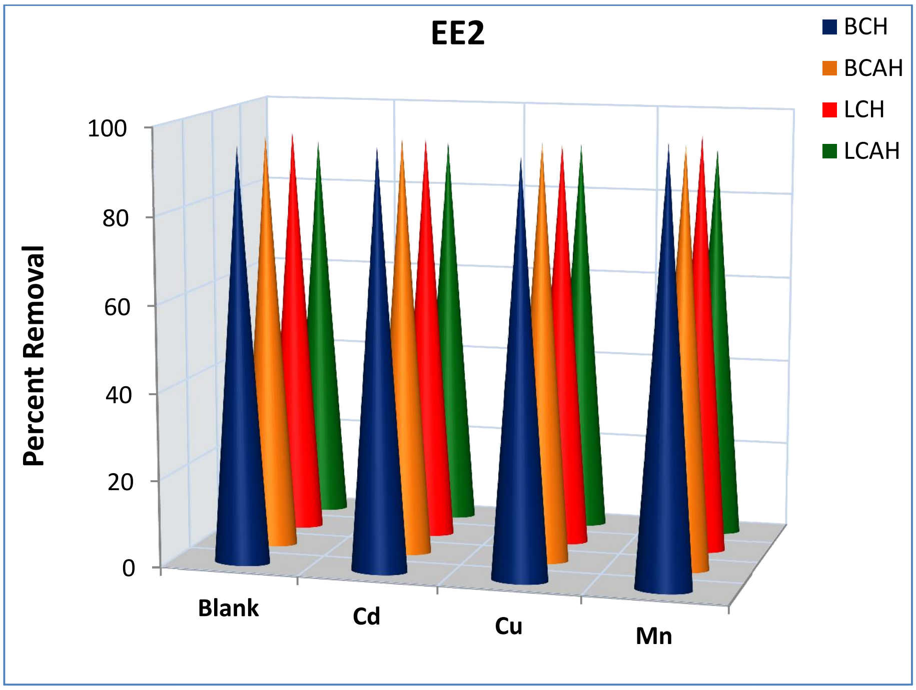

Figure 3.2.50. Removal of EE2 by the hybrid materials in presence of cations.

Table 3.2.39 (a). Effect of cations on the removal of DFS by BCH.

Cations	Initial BPA conc. (ppm)	Final BPA conc. (ppm)	% Removal
Blank	10.00	0.01	99.88
Cd	10.02	0.03	99.74
Cu	10.02	0.00	99.96
Mn	10.01	0.01	99.86

Table 3.2.39 (b). Effect of cations on the removal of DFS by LCH.

Cations	Initial BPA conc. (ppm)	Final BPA conc. (ppm)	% Removal
Blank	10.00	0.24	97.58
Cd	10.02	0.04	99.58
Cu	10.02	0.02	99.80
Mn	10.01	0.04	99.61

Table 3.2.39 (c). Effect of cations on the removal of DFS by BCAH.

Cations	Initial BPA conc. (ppm)	Final BPA conc. (ppm)	% Removal
Blank	10.00	0.05	99.50
Cd	10.02	0.01	99.88
Cu	10.02	0.00	99.96
Mn	10.01	0.01	99.86

Table 3.2.39 (d). Effect of cations on the removal of DFS by LCAH.

Cations	Initial BPA conc. (ppm)	Final BPA conc. (ppm)	% Removal
Blank	10.00	0.93	90.74
Cd	10.02	0.67	93.35
Cu	10.02	0.66	93.40
Mn	10.01	0.66	93.41

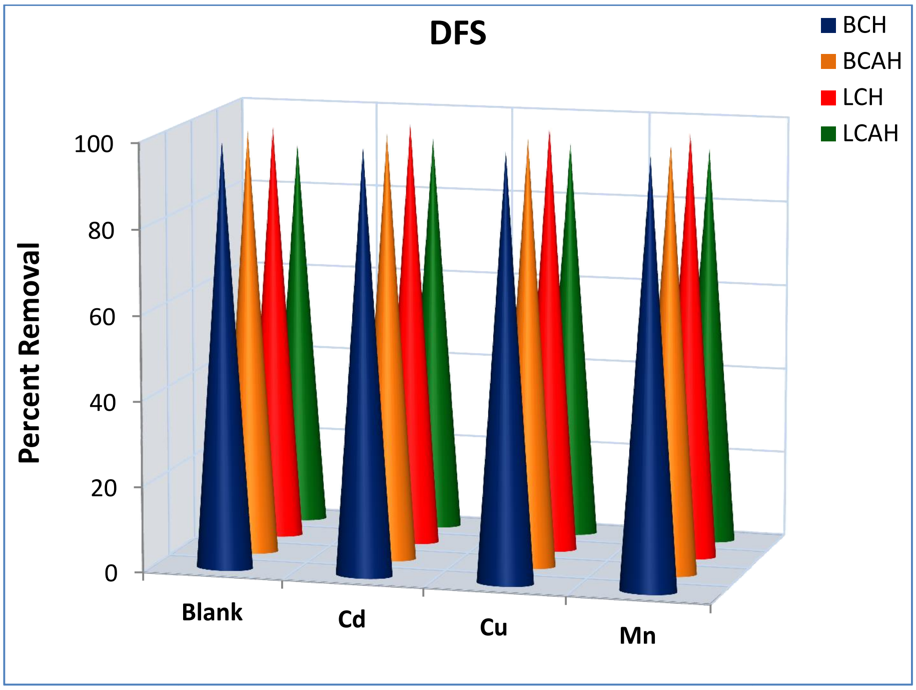

Figure 3.2.51. Removal of DFS by the hybrid materials in presence of cations.

Table 3.2.40 (a). Effect of cations on the removal of TC by BCH.

Cations	Initial BPA conc. (ppm)	Final BPA conc. (ppm)	% Removal
Blank	10.11	0.07	99.35
Cd	10.11	0.09	99.12
Cu	10.11	0.07	99.32
Mn	10.11	0.07	99.34

Table 3.2.40 (b). Effect of cations on the removal of TC by LCH.

Cations	Initial BPA conc. (ppm)	Final BPA conc. (ppm)	% Removal
Blank	10.11	0.07	99.29
Cd	10.11	0.09	99.06
Cu	10.11	0.11	98.92
Mn	10.11	0.06	99.37

Table 3.2.40 (c). Effect of cations on the removal of TC by BCAH.

Cations	Initial BPA conc. (ppm)	Final BPA conc. (ppm)	% Removal
Blank	10.11	0.05	99.48
Cd	10.11	0.07	99.35
Cu	10.11	0.08	99.19
Mn	10.11	0.05	99.46

Table 3.2.40 (d). Effect of cations on the removal of TC by LCAH.

Cations	Initial BPA conc. (ppm)	Final BPA conc. (ppm)	% Removal
Blank	10.11	0.70	93.13
Cd	10.11	0.51	94.95
Cu	10.11	0.47	95.37
Mn	10.11	0.47	95.30

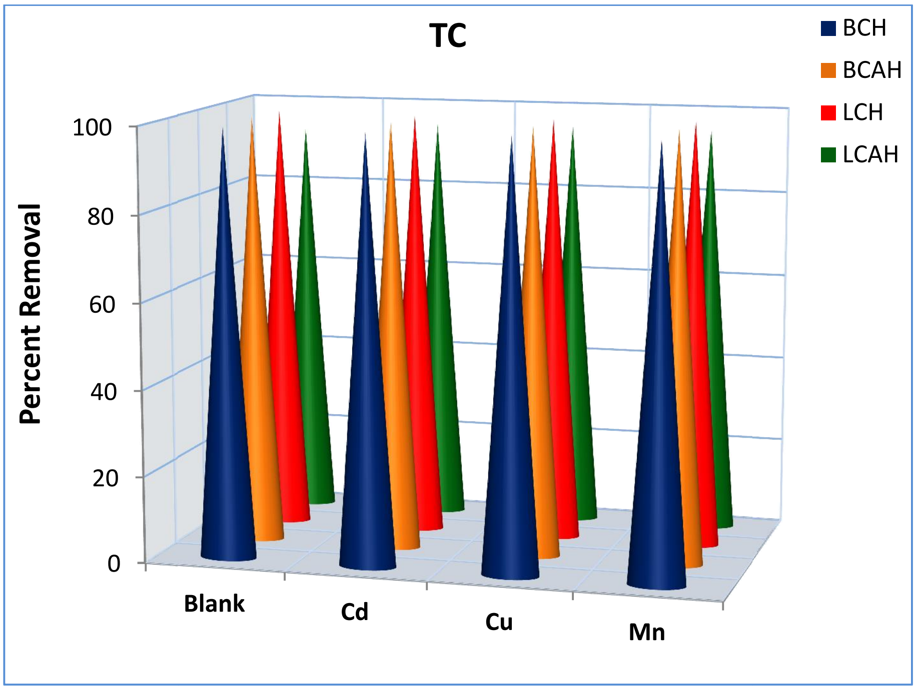

Figure 3.2.52. Removal of TC by the hybrid materials in presence of cations.

Table 3.2.41 (a). Effect of anions on the removal of BPA by BCH.

Anions	Initial BPA conc. (ppm)	Final BPA conc. (ppm)	% Removal
Blank	9.92	0.02	99.81
Nitrate	9.92	0.07	99.25
Phosphate	9.92	0.03	99.68
Glycinate	9.92	0.03	99.66
IDA	9.92	0.02	99.77
EDTA	9.92	0.04	99.62

Table 3.2.41 (b). Effect of anions on the removal of BPA by LCH.

Anions	Initial BPA conc. (ppm)	Final BPA conc. (ppm)	% Removal
Blank	9.92	0.17	98.33
Nitrate	9.92	0.14	98.58
Phosphate	9.92	0.15	98.50
Glycinate	9.92	0.16	98.34
IDA	9.92	0.07	99.28
EDTA	9.92	0.07	99.28

Table 3.2.41 (c). Effect of anions on the removal of BPA by BCAH.

Anions	Initial BPA conc. (ppm)	Final BPA conc. (ppm)	% Removal
Blank	9.92	0.06	99.40
Nitrate	9.92	0.08	99.23
Phosphate	9.92	0.04	99.61
Glycinate	9.92	0.06	99.38
IDA	9.92	0.03	99.68
EDTA	9.92	0.05	99.54

Table 3.2.41 (d). Effect of anions on the removal of BPA by LCAH.

Anions	Initial BPA conc. (ppm)	Final BPA conc. (ppm)	% Removal
Blank	9.92	0.49	95.09
Nitrate	9.92	0.32	96.75
Phosphate	9.92	0.28	97.13
Glycinate	9.92	0.47	95.30
IDA	9.92	0.47	95.22
EDTA	9.92	0.29	97.07

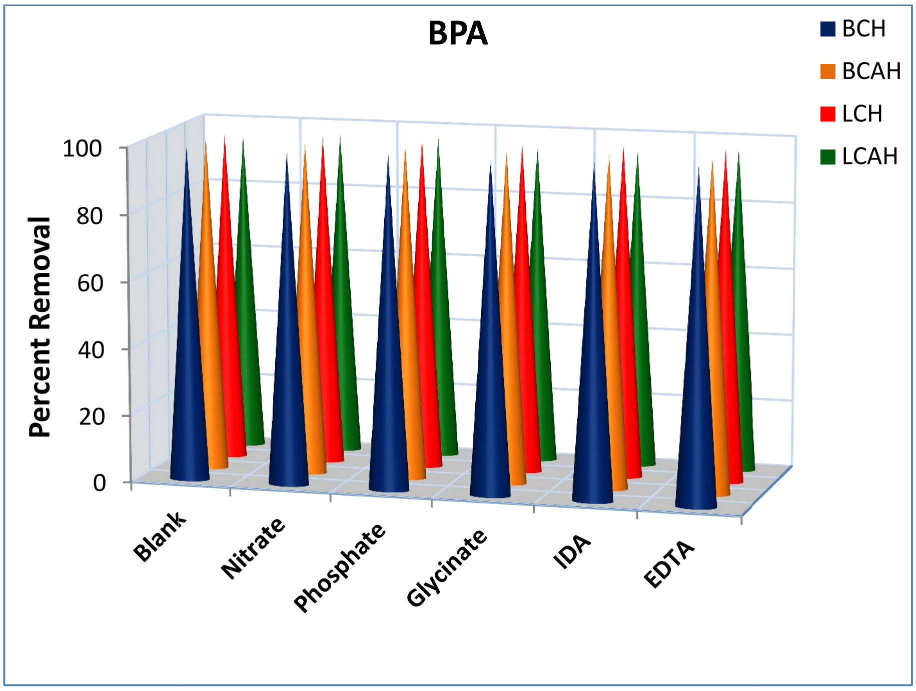

Figure 3.2.53. Removal of BPA by the hybrid materials in presence of anions.

Table 3.2.42 (a). Effect of anions on the removal of EE2 by BCH.

Anions	Initial BPA conc. (ppm)	Final BPA conc. (ppm)	% Removal
Blank	5.01	0.23	95.40
Nitrate	5.02	0.20	95.94
Phosphate	5.06	0.18	96.43
Glycinate	5.05	0.24	95.28
IDA	5.02	0.24	95.21
EDTA	5.02	0.24	95.26

Table 3.2.42 (b). Effect of anions on the removal of EE2 by LCH.

Anions	Initial BPA conc. (ppm)	Final BPA conc. (ppm)	% Removal
Blank	5.01	0.26	94.89
Nitrate	5.02	0.26	94.85
Phosphate	5.06	0.24	95.20
Glycinate	5.05	0.24	95.19
IDA	5.02	0.25	95.07
EDTA	5.02	0.24	95.19

Table 3.2.42 (c). Effect of anions on the removal of EE2 by BCAH.

Anions	Initial BPA conc. (ppm)	Final BPA conc. (ppm)	% Removal
Blank	5.01	0.22	95.64
Nitrate	5.02	0.21	95.82
Phosphate	5.06	0.18	96.30
Glycinate	5.05	0.18	96.41
IDA	5.02	0.18	96.36
EDTA	5.02	0.19	96.27

Table 3.2.42 (d). Effect of anions on the removal of EE2 by LCAH.

Anions	Initial BPA conc. (ppm)	Final BPA conc. (ppm)	% Removal
Blank	5.01	0.47	90.57
Nitrate	5.02	0.46	90.81
Phosphate	5.06	0.51	89.75
Glycinate	5.05	0.46	90.73
IDA	5.02	0.48	90.34
EDTA	5.02	0.50	90.05

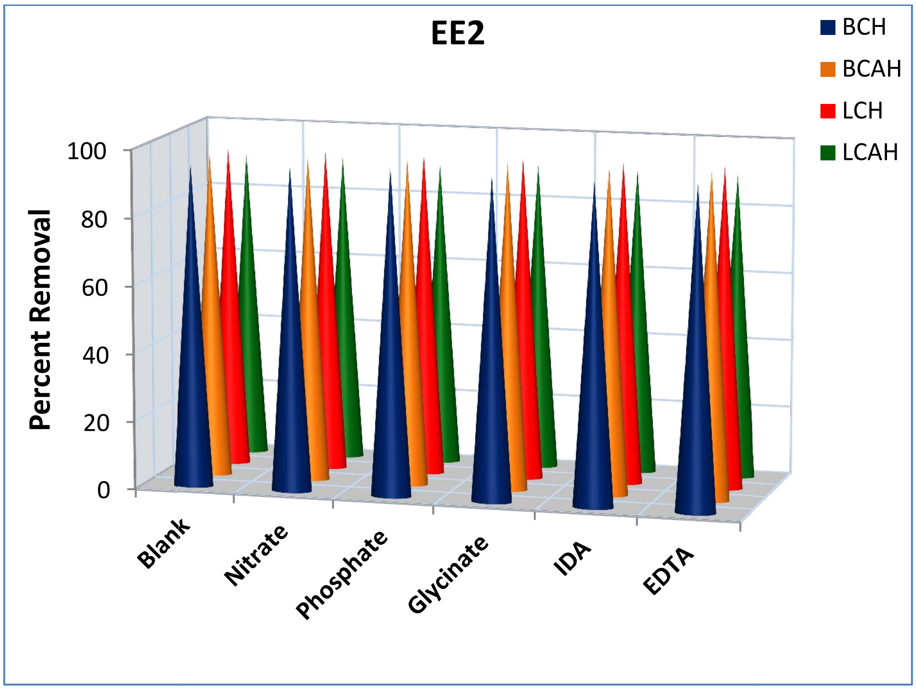

Figure 3.2.54. Removal of EE2 by the hybrid materials in presence of anions.

Table 3.2.43 (a). Effect of anions on the removal of DFS by BCH.

Anions	Initial BPA conc. (ppm)	Final BPA conc. (ppm)	% Removal
Blank	10.00	0.01	99.88
Nitrate	10.01	0.06	99.42
Phosphate	10.02	0.15	98.45
Glycinate	10.01	0.06	99.37
IDA	10.01	0.00	99.97
EDTA	10.00	0.16	98.44

Table 3.2.43 (b). Effect of anions on the removal of DFS by LCH.

Anions	Initial BPA conc. (ppm)	Final BPA conc. (ppm)	% Removal
Blank	10.00	0.24	97.58
Nitrate	10.01	0.08	99.22
Phosphate	10.02	0.48	95.22
Glycinate	10.01	0.17	98.32
IDA	10.01	0.01	99.87
EDTA	10.00	0.02	99.79

Table 3.2.43 (c). Effect of anions on the removal of DFS by BCAH.

Anions	Initial BPA conc. (ppm)	Final BPA conc. (ppm)	% Removal
Blank	10.00	0.05	99.50
Nitrate	10.01	0.03	99.73
Phosphate	10.02	0.05	99.55
Glycinate	10.01	0.06	99.35
IDA	10.01	0.12	98.84
EDTA	10.00	0.05	99.49

Table 3.2.43 (d). Effect of anions on the removal of DFS by LCAH.

Anions	Initial BPA conc. (ppm)	Final BPA conc. (ppm)	% Removal
Blank	10.00	0.93	90.74
Nitrate	10.01	0.68	93.21
Phosphate	10.02	0.95	90.47
Glycinate	10.01	0.82	91.84
IDA	10.01	0.90	90.98
EDTA	10.00	0.84	91.58

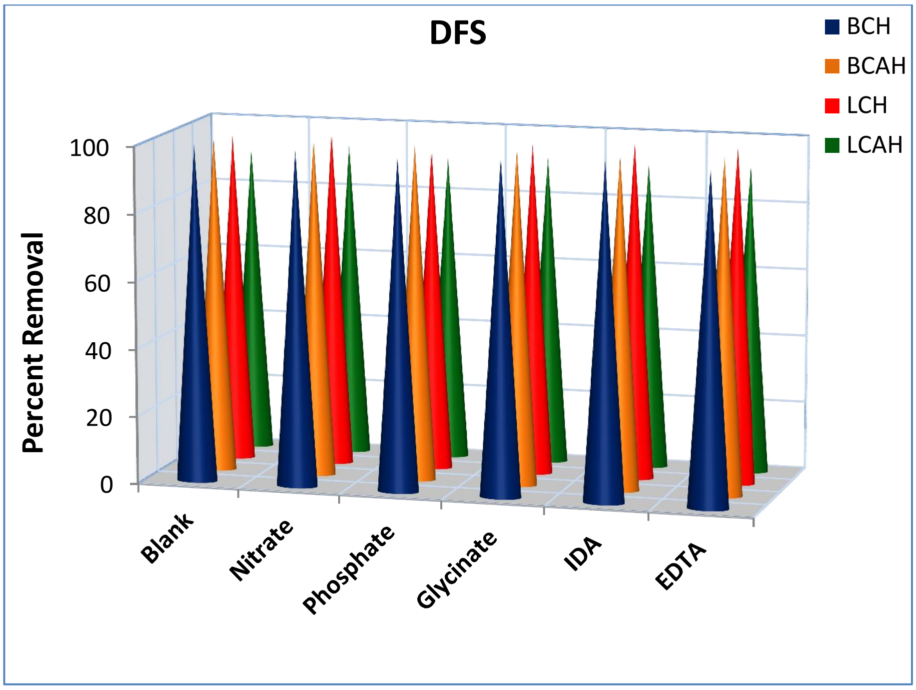

Figure 3.2.55. Removal of DFS by the hybrid materials in presence of anions.

Table 3.2.44 (a). Effect of anions on the removal of TC by BCH.

Anions	Initial BPA conc. (ppm)	Final BPA conc. (ppm)	% Removal
Blank	10.11	0.07	99.35
Nitrate	10.11	0.07	99.28
Phosphate	10.11	0.15	98.54
Glycinate	10.12	0.09	99.11
IDA	10.11	0.08	99.19
EDTA	10.12	0.15	98.49

Table 3.2.44 (b). Effect of anions on the removal of TC by LCH.

Anions	Initial BPA conc. (ppm)	Final BPA conc. (ppm)	% Removal
Blank	10.11	0.07	99.29
Nitrate	10.11	0.12	98.78
Phosphate	10.11	0.39	96.17
Glycinate	10.12	0.29	97.16
IDA	10.11	0.01	99.88
EDTA	10.12	0.09	99.15

Table 3.2.44 (c). Effect of anions on the removal of TC by BCAH.

Anions	Initial BPA conc. (ppm)	Final BPA conc. (ppm)	% Removal
Blank	10.11	0.05	99.48
Nitrate	10.11	0.04	99.59
Phosphate	10.11	0.18	98.21
Glycinate	10.12	0.06	99.37
IDA	10.11	0.15	98.57
EDTA	10.12	0.05	99.50

Table 3.2.44 (d). Effect of anions on the removal of TC by LCAH.

Anions	Initial BPA conc. (ppm)	Final BPA conc. (ppm)	% Removal
Blank	10.11	0.70	93.13
Nitrate	10.11	0.47	95.34
Phosphate	10.11	0.73	92.75
Glycinate	10.12	0.52	94.82
IDA	10.11	0.54	94.63
EDTA	10.12	0.72	92.86

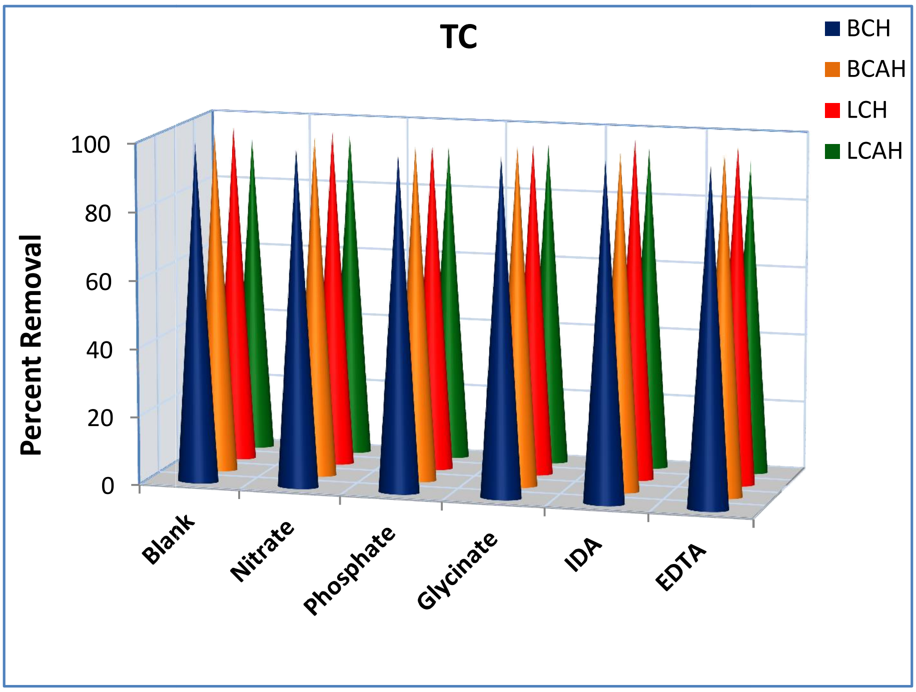

Figure 3.2.56. Removal of TC by the hybrid materials in presence of anions.

3.3. COLUMN REACTOR STUDIES

3.3.1. BPA

The column reactor operations were performed to assess the removal/loading capacity of employed hybrid materials, *viz*., BCH, BCAH, LCH and LCAH for BPA under the dynamic conditions. The fixed bed column experiments were conducted using 0.5 g of hybrid materials and ~10.0 mg/L of solution at pH ~7.0. Other column conditions were same as stated previously (*cf.* Section 2.3.10). The breakthrough curves obtained are presented graphically in Figure 3.3.1. The figure reveals that relatively high breakthrough volume is obtained for BPA using these hybrid materials. A complete breakthrough volume is achieved at the throughput volume of 3.90 L, 2.16 L, 1.50 L and 0.78 L, respectively, for BCH, BCAH, LCH and LCAH solids. Relatively high breakthrough volume obtained for BPA indicates a strong affinity of these solids towards BPA under the fixed bed column conditions. It is reported previously that a fixed-bed process is having an additional advantage of continuous contact of sorbed species with solid surface which results in better exhaustion capacity than batch reactor operation (Adak et al., 2006).

Further, the non-linear least square fitting is performed using the breakthrough column data employing the Thomas equation (Eq. 2.8). The fitting is conducted to simulate two unknown parameters i.e., Thomas constants K_T and q_o. Values of Thomas constants along with the least square sum are evaluated and returned in Table 3.3.1. The data indicate that a high loading capacity is achieved for BPA by these solids under the dynamic conditions. Relatively, BCH shows relatively a higher sorption capacity comparing to the BCAH solid. Similarly, LCH solid possesses relatively higher removal capacity for BPA than LCAH solids. This infers that Al-pillared samples possess less loading of HDTMA, hence causes to decrease the BPA partitioning. The removal capacity is in the order: BCH > BCAH > LCH > LCAH. The higher removal capacity of BC based samples is perhaps due to the higher smectite content contained by the BC compared to the LC based samples. BC based solids also show higher specific pore volume and pore size which is also responsible for the higher removal capacity compared to the LC based hybrid materials. Although LCH sample possesses relatively less loading capacity of BPA, it is highly comparable to the bentonite based hybrid materials. These results are similar to the findings of batch reactor experiments. Also, these results are in line to the other report in which the Thomas equation was utilized to demonstrate the loading capacity of different sorbents (Tiwari and Lee, 2011; Tiwari et al., 2014).

Table 3.3.1. Thomas constants estimated for the removal of BPA by hybrid materials.

Materials	**Thomas constants**		**Least square sum (s^2)**
	q_o (mg/g)	**K_T (L/min/mg)**	
BCH	50.976	$2.15\text{x}10^{-4}$	1.40
BCAH	30.477	$4.30\text{x}10^{-4}$	0.83
LCH	19.588	$4.34\text{x}10^{-4}$	0.05
LCAH	10.086	$7.85\text{x}10^{-4}$	0.07

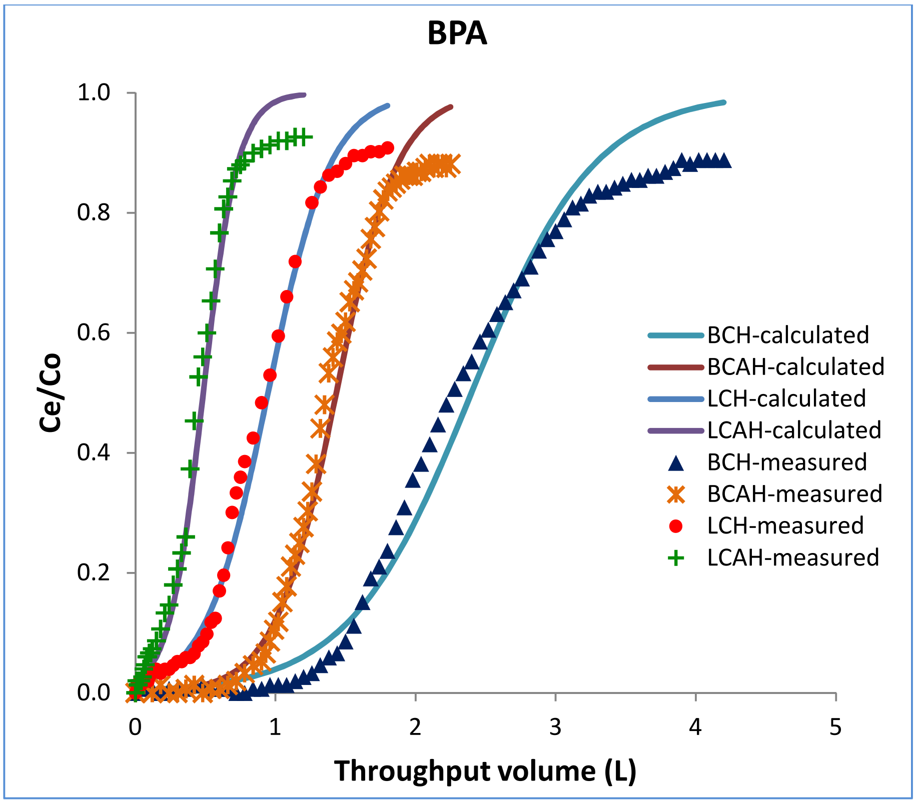

Figure 3.3.1. Breakthrough curves obtained for the removal of BPA by the hybrid materials.

3.3.2. EE2

The column experiments were performed to assess the loading capacity of hybrid materials for EE2 under the dynamic conditions, using 0.25 g of modified clay and *Ca*. 5.0 mg/L of EE2, at pH ~7.0, under the same column conditions as stated before. The breakthrough curves are returned in Figure 3.3.2. Figure reveals that relatively high breakthrough volume is obtained for EE2 by these solids. A complete breakthrough is attained at the throughput volume of 8.04 L, 6.54 L, 6.48 L and 5.04 L, respectively, for BCH, BCAH, LCH and LCAH solids. This indicates a strong affinity of these solids towards EE2 under the fixed bed column conditions.

Further, a non-linear least square fitting is conducted using the breakthrough column data employing the Thomas equation (Eq. 2.8). Values of Thomas constants along with the least square sum are evaluated and returned in Table 3.3.2. The data indicate that a high loading capacity is achieved for EE2 by these solids under the dynamic conditions. BCH shows relatively higher removal capacity comparing to the BCAH, LCH and LCAH solids. Moreover, LCAH and BCAH solids possess with relatively less removal capacity of EE2 comparing to their respective organo-modified solids i.e., BCH and LCH. This is due to the fact that the BCAH and LCAH solids contained with less HDTMA loading and causing less partitioning of EE2 from aqueous solutions. The loading capacity decreases in the order: BCH > BCAH > LCH > LCAH. The bentonite based samples show higher sorption capacity compared to the local clay based samples, which is due to the higher smectite content of BC, and the higher specific pore volume and pore size of BC based hybrid materials compared to the hybrid materials precursor to the LC. However, it is interesting to note that local clay based hybrid materials also possess fairly a good and comparable loading capacity comparing to the BCH and BCAH solids at least for the EE2 removal. Similar application of Thomas equation to demonstrate the loading capacity of sericite for Cu(II) and Pb(II) was reported previously by Tiwari et al. (2007).

Table 3.3.2. Thomas constants estimated for the removal of EE2 by hybrid materials.

Materials	Thomas constants		Least square sum (s^2)
	q_o (mg/g)	K_T (L/min/mg)	
BCH	111.979	1.59 x10^{-4}	10.0
BCAH	97.987	1.70 x10^{-4}	11.0
LCH	86.965	1.88 x10^{-4}	11.0
LCAH	64.996	2.30 x10^{-4}	10.0

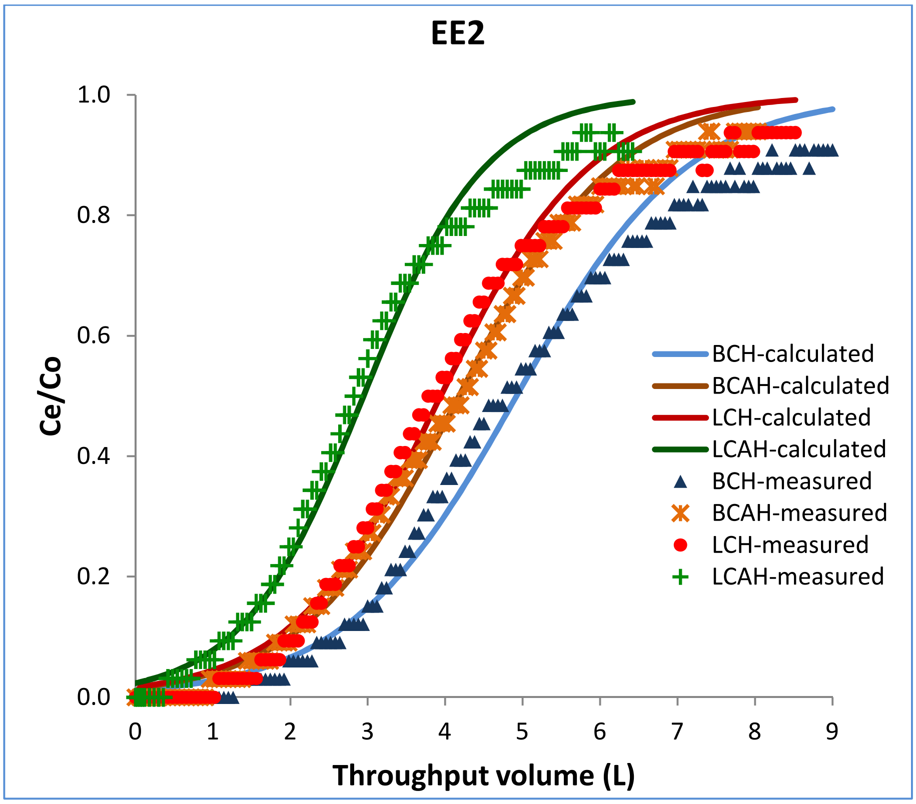

Figure 3.3.2. Breakthrough curves obtained for the removal of EE2 by the hybrid materials.

3.3.3. DFS

The fixed bed column experiments were conducted with 0.5 g of modified clay and *Ca*. 10.0 mg/L of DFS at pH ~7.0 having the other column conditions as stated before. The breakthrough curves are presented in Figure 3.3.3. A complete breakthrough volume is achieved at the throughput volume of 1.56 L, 1.32 L, 0.62 L and 0.51 L, respectively, for BCH, BCAH, LCH and LCAH solids. Relatively high breakthrough volume obtained for DFS indicates a strong affinity of these solids towards diclofenac sodium under the fixed bed column conditions. The non-linear least square fitting is conducted using the breakthrough column data employing the Thomas equation. Values of Thomas constants along with the least square sum are returned in Table 3.3.3. The data indicate that a high loading capacity is achieved for diclofenac by these solids under the dynamic conditions. BCH and LCH possess relatively higher removal capacity compare to their corresponding Al–pillared samples (BCAH and LCAH). This is perhaps due to the less loading of HDTMA which decreases the portioning of DFS by these solids.

Table 3.3.3. Thomas constants estimated in the removal of DFS by hybrid materials.

Materials	**Thomas constants**		**Least square sum (s^2)**
	q_o (mg/g)	**K_T (L/min/mg)**	
BCH	18.987	$5.09\text{x}10^{-4}$	3.20
BCAH	13.992	$5.65\text{x}10^{-4}$	5.60
LCH	7.986	$1.19\text{x}10^{-3}$	0.99
LCAH	5.490	$1.57\text{x}10^{-3}$	3.50

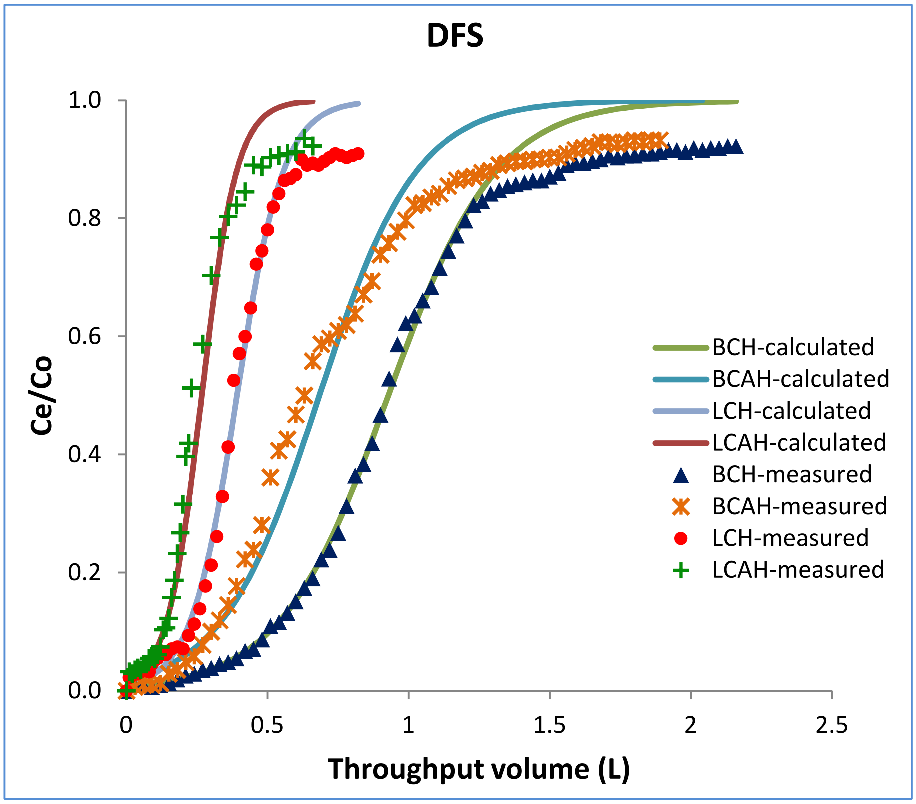

Figure 3.3.3. Breakthrough curves obtained for the removal of DFS by the hybrid materials.

3.3.4. TC

Similarly, the column experiments were carried out with 0.25 g of modified clay and *Ca*. 10.0 mg/L of TC, at pH ~7.0, with the other column conditions as mentioned previously. The breakthrough curves are shown in Figure 3.3.4. A complete breakthrough volume is achieved at the throughput volume of 1.39 L, 1.12 L, 1.09 L and 0.94 L, respectively, for BCH, BCAH, LCH and LCAH solids. The non-linear least square fitting is performed using the breakthrough column data employing the Thomas equation. The fitting is conducted to simulate two unknown parameters, i.e., Thomas constants K_T and q_o; and the values of Thomas constants along with the least square sum are returned in Table 3.3.4. The removal capacity follows the trend: BCH > BCAH > LCH > LCAH. The bentonite based samples show higher sorption capacity comparing to the local clay based samples, which is due to the higher smectite content of BC, and the higher specific pore volume and pore size of BC based hybrid materials. Al-pillared samples possess comparatively less loading capacity than their corresponding organo-modified solids due to lower HDTMA loading. The data indicate that a high loading capacity is achieved for TC by these solids under the dynamic conditions; which indicates the possible applicability of these modified materials in the attenuation of TC from aqueous solutions. These results are in conformity to the batch reactor studies. Similar results were also reported previously in which Thomas equation was utilized to demonstrate the loading capacity of manganese-coated sand (Lee et al., 2009).

Table 3.3.4. Thomas constants estimated for the removal of TC by hybrid materials.

Materials	**Thomas constants**		**Least square sum (s^2)**
	q_o (mg/g)	**K_T (L/min/mg)**	
BCH	34.976	4.89 x10^{-4}	12.0
BCAH	29.963	6.09 x10^{-4}	12.0
LCH	26.956	6.59 x10^{-4}	12.0
LCAH	23.478	7.09 x10^{-4}	11.0

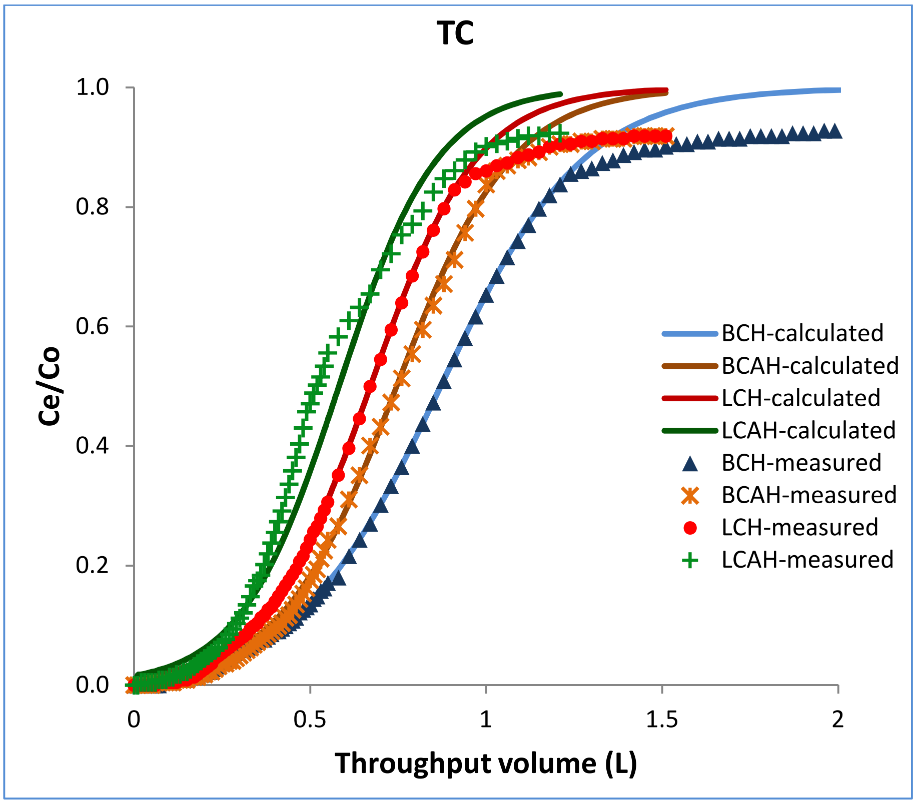

Figure 3.3.4. Breakthrough curves obtained for the removal of TC by the hybrid materials.

CHAPTER 4

CONCLUSIONS

4. CONCLUSIONS

The natural bentonite and locally collected clay samples were fully exploited in the preparation of various hybrid materials, and further these materials were employed in the remediation of aquatic environment contaminated with the arsenic and micro-pollutants under the batch and column reactor operations. Bentonite clay was procured from a commercial supplier. It was mined near Bhuj, Gujarat, India. The bentonite was washed with distilled water and dried at 90^{o}C in a drying oven prior to further use for preparation in hybrid materials. Local clay was collected from the field of Phullen Village, Mizoram, India. Since it contained with several impurities, therefore it was thoroughly separated using the standard ISRIC (International Soil Reference and Information Centre) method. The cation exchange capacity (CEC) of pristine bentonite and local clay was found to be 69.35 and 46.38 meq/100 g of clay, respectively. The XRF analysis of the bentonite and local clay showed that both the clay samples possessed mainly the silicon, aluminium and iron oxides. Moreover, the composition of various metal oxides for both the clay samples was found to be almost identical. The hybrid materials, namely, BCH and LCH were prepared successfully from the bentonite and local clay by the introduction of hexadecyltrimethylammonium bromide (HDTMA) organo-cation onto the clay by the simple wet cation exchange process. Similarly, the aluminium pillared and HDTMA modified hybrid materials (BCAH and LCAH) were obtained by the simple process conducted in aqueous medium.

The hybrid materials along with the pristine clay samples were characterized with the FE-SEM (Field-Emission Scanning Electron Microscopic), FT-IR (Fourier Transform Infrared) spectroscopy and XRD (X-ray Diffraction) analytical methods. The IR data showed that the organic molecule (HDTMA) was well introduced within the clay network. The XRD data were matched with the standard ICDD (International Centre for Diffraction Data) reference pattern and enabled the presence of quartz, smectite, illite and kaolinite minerals in both the bentonite and local clay materials. Quantitatively, it was evaluated that bentonite is having 43.71%, 23.17%, 1.73% and 31.39% of quartz, smectite, kaolinite and illite, respectively. Similarly, local clay contained with 79.35%, 6.20%, 0.45% and 14.01%, respectively of quartz, smectite, kaolinite and illite. SEM images of these solids showed a disordered structure of HDTMA-modified clay materials (BCH and LCH) whereas Al-pillared solids showed that fine particles of aluminium oxides were also aggregated onto the clay surface. The pH_{PZC} values of these solids were found to be 9.8, 8.2, 6.1, 5.8, 5.1 and 5.1 for the samples BC, BCH, BCAH, LC, LCH and LCAH, respectively. BET analysis indicated that very high BET specific surface was obtained for the unmodified BC having low pore volume and pore size compared to the LC. The BC based hybrid materials showed a remarkable decrease of specific surface area and an increase in pore size (diameter) and pore volume of the materials. On the other hand, the introduction of HDTMA or Al-HDTMA onto LC caused relative increase in the specific surface area as well as a decrease in pore diameter of the solids.

The hybrid materials along with the pristine clay were employed for the removal of As(III) and As(V) from aqueous solutions under various physico-chemical parametric studies. Both As(III) and As(V) showed relatively higher percent sorption at a pH range 4.0-7.0. BCAH and LCAH solids were possessed much enhanced percent removal of As(V) compared to the BCH or LCH solids, whereas BCH, LCH, BCAH and LCAH possessed almost identical removal percent for As(III). The modified solids showed significantly higher percent removal for both As(III) and As(V) species compared to the virgin clay. The increase in sorptive concentration greatly favoured the removal of As(III) and As(V) by these hybrid solids. The increase in background electrolyte concentrations from 0.001 to 0.1 mol/L $NaNO_3$

insignificantly affected the percent removal of As(V) by the hybrid materials whereas the As(III) removal was decreased significantly. This indicated that the As(V) was bound with strong chemical forces and forming an 'inner sphere complexes' at the solid surfaces; whereas As(III) was sorbed with weak van der Waals forces and forming an 'outer sphere complexes' at the solid surface. Similarly, increase in phenol concentration was caused a significant decrease of As(III) removal, but at the same time the phenol removal was increased significantly. On the other hand, As(V) removal was unaffected by the increase in phenol concentration, whereas the phenol removal was increased slightly. This implied that there was a competition between phenol and As(III) toward the available active sites and phenol was preferentially sorbed onto the solid surface. The hybrid materials, perhaps, possessed different active sites capable to sequester different types of pollutants, i.e., organic (phenol) and inorganic (As(V)) pollutants from aqueous solutions simultaneously which caused for As(V) and phenol removal as unaffected. The uptake of As(III) and As(V) by these hybrid materials was rapid and followed the pseudo-second-order and fractal like pseudo-second-order rate kinetics. The presence of several cations, *viz.*, Cd(II), Cu(II) and Mn(II); and anions, *viz.*, glycine, IDA, sulphate, oxalate, phosphate and EDTA were examined. The BCAH and LCAH were overall highly selective at least for As(V).

Similarly, the materials were successfully utilized in the remediation of some of EDCs, *viz.*, BPA, EE2, DFS and TC from aqueous solutions under the batch and column reactor operations. The pH dependence sorption of EDCs by the hybrid materials indicated that very high percent uptake of EDCs were obtained for all the modified solids, and this was almost independent to the change in solution pH from 4 to 10, however a slightly decreased removal at very high pH was observed in most of the cases. Al pillared HDTMA modified local clay showed slightly less uptake of EDCs possibly due to less loading of the HDTMA cation which reduced the hydrophobic core within the clay structure. Further, it was noted that the pristine bentonite and local clay showed very insignificant uptake of EDCs which was further decreased with increasing the solution pH. In the case of TC, virgin bentonite and local clay showed a high percent removal at very low pH values, which was, however, decreased significantly with increasing the solution pH.

The concentration dependence removal study revealed that increasing the EDCs concentration could not affect the percent removal of EDCs from aqueous solution in the studied concentration range. The results again pointed strong affinity of hybrid materials towards the attenuation of EDCs. However, a slightly lower removal of EDCs was shown by the LCAH solid which was due to the less loading of HDTMA within the clay network. Increasing background electrolyte concentrations (1000 times) from 0.0001 mol/L to 0.1 mol/L NaCl could not affect the specific sorption of EDCs by the modified solids employed. This implied that the partitioned of EDC was bound with relatively stronger forces. However, in some case, slightly enhanced sorption of EDC in the presence of background electrolyte was observed at least for the LCAH solid. The presence of diverse ions insignificantly affected the removal of EDCs, which again indicated the efficiency and selectivity of the hybrid materials. Time dependence removal studies indicated that a very fast uptake of EDCs was occurred on the modified materials. This reaffirmed the affinity of the solids towards the studied EDCs. Kinetic modeling performed on few data indicated that results were best fitted to the PSO and FL-PSO models compared to the PFO model. Moreover, the applicability of the PSO model indicated that the sorbate species were bound onto the surface of hybrid material by strong forces.

The column reactor operations revealed that very high breakthrough volume were obtained for the attenuation of EDCs using the modified solids. Further, the non-linear least square fitting were performed employing the Thomas equation. Results indicated that very high loading capacity of these EDCs was achieved by the hybrid materials under the dynamic conditions; which again indicated the affinity of the modified solids towards the studied EDCs. The loading capacity for the EDCs was in the order: BCH > BCAH > LCH > LCAH. The bentonite based solids showed relatively higher removal capacity compared to the local clay based solids which is due to the higher content of smectite contained by the bentonite than the local clay. Bentonite based solids also showed higher specific pore volume and pore size which enabled higher removal capacity of micro-pollutants compared to the LC based hybrid materials. The organo-clays possessed relatively higher removal capacity for the studied EDCs which was due to higher HDTMA loading compared to the inorgano-organo-clays. Although LCH sample possessed relatively less loading capacity for EDCs, but it was highly comparable to the bentonite based samples. This further indicated applicability of the local clay by modification with suitable organic cations in the possible attenuation of wastewater contaminated with organic pollutants. Therefore, the hybrid materials were found to be useful and effective in the removal of As(III), As(V) and the studied EDCs from aqueous solutions. The BCAH and LCAH solids showed somewhat lesser attenuation capacity for the EDCs from aqueous solution comparing to the corresponding HDTMA modified solids (BCH and LCH) however, it provided an enhanced settling capacity which made easy and viable separation from aqueous solutions. Overall, the hybrid materials are found to be useful alternatives for the efficient, effective and selective remediation of water contaminated with variety of micro-pollutants. The laboratory scale studies is, therefore, useful input data to be implemented or implicated towards the large scale or pilot plant scale treatment of wastewater or even ground water contaminated with these micro-pollutants.

REFERENCES

REFERENCES

Aarab, N., Lemaire–Gony, S., Unruh, E., Hansen, P.D., Larsen, B.K., Andersen, O.K., Narbonne, J.F., (2006). Preliminary study of responses in mussel (*Mytilus edulis*) exposed to bisphenol A, diallyl phthalate and tetrabromodiphenyl ether. *Aquat. Toxicol.*, **78**(S.1): S86–S92.

Abhyankar, L.N., Jones, M.R., Guallar, E., Navas–Acien, A., (2012). Arsenic exposure and hypertension: a systematic review. *Environ. Health Perspect.*, **120**: 494–500.

Adak, A., Bandyopadhyay, M., Pal, A., (2006). Fixed bed column study for the removal of crystal violet (C.I. Basic Violet 3) dye from aquatic environment by surfactant–modified alumina. *Dyes Pigm.*, **69**: 245–251.

Adams, C., Wang, Y., Loftin, K., Meyer, M., (2002). Removal of antibiotics from surface and distilled water in conventional water treatment process. *J. Environ. Eng.*, **128**: 253–260.

Adamson, A.W., (1982). *Physical Chemistry of Surfaces*, 4th ed., John Wiley & Sons, New York.

Aguinaco, A., Beltrán, F.J., García–Araya, J.F., Oropesa, A., (2012). Photocatalytic ozonation to remove the pharmaceutical diclofenac from water: influence of variables. *Chem. Eng. J.*, **189–190**: 275–282.

Ahmaruzzaman, M., (2008). Adsorption of phenolic compounds on low–cost adsorbents: A review. *Adv. Colloid Interf. Sci.*, **143**: 48–67.

Ahmed, M.F., (2002). Alternative Water Supply Options for Arsenic Affected Areas of Bangladesh, ITN–Bangladesh, Centre for Water Supply and Waste Management Civil Engineering Building, BUET, Dhaka, Bangladesh. http://www.physics.harvard.edu/~wilson/arsenic/conferences/Feroze_Ahmed/Sec_3.htm.

Ai, L., Zhang, C., Liao, F., Wang, Y., Li, M., Meng, L., Jiang, J., (2011). Removal of methylene blue from aqueous solution with magnetite loaded multi–wall carbon nanotube: Kinetic, isotherm and mechanism analysis. *J. Hazard. Mater.*, **198**: 282–290.

Ainger, C., Butler, D., Caffor, I., Crawford–Brown, D., Helm, D., Stephenson, T., (2009). *A Low Carbon Water Industry in 2050* – Report: SC070010/R3, Environment Agency, Bristol.

Al–Degs, Y., Khraisheh, M.A.M., Allen, S.J., Ahmad, M.N., (2000). Effect of carbon surface chemistry on the removal of reactive dyes from textile effluents. *Water Res.*, **34**: 927–935.

Alexandre, M., Dubois, P., (2000). Polymer–layered silicate nano–composites: preparation, properties and uses of a new class of materials. *Mater. Sci. Eng. Res.*, **28**: 1–63.

Alkaram, U.F., Mukhlis, A.A., Al–Dujaili, A.H., (2009). The removal of phenol from aqueous solutions by adsorption using surfactant–modified bentonite and kaolinite. *J. Hazard. Mater.*, **169**: 324–332.

Al–Khateeb, L.A., Obaid, A.Y., Asiri, N.A., Salam, M.A., (2014). Adsorption behavior of estrogenic compounds on carbon nanotubes from aqueous solutions: Kinetic and thermodynamic studies. *J. Ind. Eng. Chem.*, **20**: 916–924.

Alo, R., Facciolo, R.M., Madeo, M., Guisi, G., Carelli, A., Canonaco, M., (2005). Effects of the xenoestrogen bisphenol A in dicephalic regions of the teleost fish *Coris julis* occur preferentially via distinct somatostatin receptor subtypes. *Brain Res. Bull.*, **65**: 267–273.

Alther, G.R., (2002). Using organo clays to enhance carbon filtration. Waste Man., (Elsevier, Amsterdam, Neth.), **22**: 507–513.

Altundogan, H.S., Altundogan, S., Tumen, F., Bildik, M., (2000). Arsenic removal from aqueous solutions by adsorption on red mud. *Waste Manage.*, **20**: 761–767.

Altundogan, H.S., Altundogan, S., Tumen, F., Bildik, M., (2002). Arsenic adsorption for aqueous solution by activated red mud. *Waste Manage*., **22**: 357–363.

Alvarez–Puebla, R.A., dos Santos Jr., D.S., Blanco, C., Echeverri, J.C., Garrido, J.J., (2005). Particle and surface characterization of a natural illite and study of its copper retention. *J. Colloid Interf. Sci*., **285**: 41–49.

Amin, M.N., Kaneco, S., Kitagawa, T., Begum, A., Katsumata, H., Suzuki, T., Ohta, K., (2006). Removal of arsenic in aqueous solutions by adsorption onto waste rice husk. *Ind. Eng. Chem. Res.*, (*ACS*), **45**: 8105–8110.

Andersen, H., Siegrist, H., Bent, H.S., Ternes, T.A., (2003). Fate of estrogens in a municipal sewage treatment plant. *Environ. Sci. Technol*., **37**: 4021–4026.

Aposhian, H.V., Aposhian, M.M., (2006). Arsenic toxicology: five questions. *Chem. Res. Toxicol*., **19**: 1–15.

Aris, A.Z., Shamsuddin, A.S., Praveena S.M., (2014). Occurrence of 17α–ethynylestradiol (EE2) in the environment and effect on exposed biota: a review. *Environ. Inter*., **69**: 104–119.

Aroke, U.O., El–Nafaty, U.A., (2014). XRF, XRD and FTIR properties and characterization of HDTMA–Br surface modified organo–kaolinite clay. *Inter. J. Emerg. Technol. Adv. Eng.*, **4**: 817–825.

Asfour, H.M., Fadali, O.A., Nasser, M.M., El–Geundi, M.S., (1985). Equilibrium studies on adsorption of basic dyes on hardwood. *J. Chem. Technol. Biotechnol*., **35**: 21–27.

Asha, K.K., Sankar, T.V., Nair, P.G., (2007). Effect of tetracycline on pancreas and liver function of adult male albino rats. *J. Pharm. Pharmacol*., **59**: 1241–1248.

Atia, A.A., (2008). Adsorption of chromate and molybdate by cetylpyridinium bentonite. *Appl. Clay Sci.*, **41**: 73–84.

Atkinson, S.K., Marlatt, V.L., Kimpe, L.E., Lean, D.R.S., Trudeau, V.L., Blais, J.M., (2012). The occurrence of steroidal estrogens in south–eastern Ontario wastewater treatment plants. *Sci. Total Environ.*, **430**: 119–125.

Azizian, S., (2004). Kinetic models of sorption: a theoretical analysis. *J. Colloid Interf. Sci.*, **276**: 47–52.

Bagherifam, S., Komarneni, S., Lakzian, A., Fotovat, A., Khorasani, R., Huang, W., Ma, J., Hong, S., Cannon, F.S., Wang, Y., (2014). Highly selective removal of nitrate and perchlorate by organoclay. *Appl. Clay Sci.*, **95**: 126–132

Bailey, S.E., Olin, T.J., Bricka, R.M., Adrian, D.D., (1999). A review of potentially low–cost sorbents for heavy metals. *Water Res.*, **33**: 2469–2479.

Barceló, D., (2003). Emerging pollutants in water analysis. *TrAC Trend. Anal. Chem.*, **22**: xiv–xvi.

Baron, P.C., Wang, Z., Pinnavaia, T.J., (1999). Polymer–layered silicate nano–composites: an overview. *Appl. Clay Sci.*, **15**: 11–29.

Bartholow, M., (2011). *Top 200 Drugs of 2010.* http://www.pharmacytimes.com/publications/issue/2011/may2011/top–200–drugs–of–2010.

Bazrafshan, E., Mostafapour, F.K., Hosseini, A.R., Khorshid, A.R., Mahvi, A.H., (2013). Decolorisation of reactive red 120 dye by using single–walled carbon nanotubes in aqueous solutions. *J. Chem.*, Article ID: 938374, http://dx.doi.org/10.1155/2013/938374.

Berhane , T.M., Levy, J., Krekeler, M.P.S., Danielson, N.D., Stalcup, A., (2015). Sorption–desorption of carbamazepine by palygorskite–montmorillonite (PM) filter medium. *J. Hazard. Mater.*, **282**: 183–193.

Bhatnagar, A., Sillanpää, M., (2010). Utilization of agro–industrial and municipal waste materials as potential adsorbents for water treatment—A review. *Chem. Eng. J.*, **157**: 277–296.

Bhattacharyya, K.G., Gupta, S.S., (2008). Adsorption of a few heavy metals on natural and modified kaolinite and montmorillonite: A review. *Adv. Colloid Interf. Sci.*, **140**: 114–131.

Birdi, K.S., (2009). *Handbook of Surface and Colloid Chemistry*, Third Ed., CRC Press, Taylor & Francis Group, LLC, p.166.

Bissen, M., Frimmel, F.H., (2003). Arsenic—a review. Part I: Occurrence, toxicity, speciation, and mobility. *Acta Hydrochim. Hydrobiol.*, **31**: 9–18.

Bolong, N., Ismail, A.F., Salim, M.R., Matsuura, T., (2009). A review of the effects of emerging contaminants in wastewater and options for their removal. *Desalination*, **239**: 229–246.

Bouras, O., Bollinger, J.C., Baudu, M., Khalaf, H., (2007). Adsorption of diuron and its degradation products from aqueous solution by surfactant modified pillared clays. *Appl. Clay Sci.*, **37**: 240–250.

Bouras, O., Houari, M., Khalaf, H., (2001). Using of surfactant modified Fe–pillared bentonite for the removal of pentachlorophenol from aqueous stream. *Environ. Technol.*, **22**: 69–74.

Bowman, R.S., Li, Z., Roy, S.J., Burt, T., Johnson, R.S., Johnson, R.L., (2002). Pilot test of a surfactant–modified zeolite permeable barrier for groundwater remediation. J.A. Smith, S. Burns (Eds.), Physical and Chemical Remediation of Contaminated Aquifers, Kluwer Academic Pub., p.161–185.

Boyd, S.A., Mortland, M.M., Chiou, C.T., (1988). Sorption characteristics of organic compounds on hexadecyltrimethylammonium–smectite. *Soil Sci. Soc. Am. J.*, **52**: 652–657.

Bradl, H.B., (2004). Adsorption of heavy metal ions on soils and soils constituents. *J. Colloid Interf. Sci.*, **277**: 1–18.

Braga, O., Smythe, G.A., Schafer, A.I., Feitz, A.J., (2005). Fate of steroid estrogens in Australian inland and coastal wastewater treatment plants. *Environ. Sci. Technol.*, **39**: 3351–3359.

Bras, I.P., Santos, L., Alves, A., (1999). Organochlorine pesticides removal by pinus bark sorption. *Environ. Sci. Technol.*, **33**: 631–634.

Brierley, C.L., (1990). Bioremediation of metal–contaminated surface and groundwater. *Geomicrobiol. J.*, **8**: 201–223.

Brum, M.C., Capitaneo, J.L., Oliveira, J.F., (2010). Removal of hexavalent chromium from water by adsorption onto surfactant modified montmorillonite. *Miner. Eng.*, **23**: 270–272.

Cabrera–Lafaurie, W.A., Román, F.R., Hernández–Maldonado, A.J., (2012). Transition metal modified and partially calcined inorganic–organic pillared clays for the adsorption of salicylic acid, clofibric acid, carbamazepine, and caffeine from water. *J. Colloid Interf. Sci.*, **386**: 381–391.

Cabrera–Lafaurie, W.A., Román, F.R., Hernández–Maldonado, A.J., (2015). Single and multi–component adsorption of salicylic acid, clofibric acid, carbamazepine and caffeine from water onto transition metal modified and partially calcined inorganic–organic pillared clay fixed beds. *J. Hazard. Mater.*, **282**: 174–182.

Cai, K., Phillips, D.H., Elliott, C.T., Muller, M., Scippo, M.–L., Connolly, L., (2013). Removal of natural hormones in dairy farm wastewater using reactive and sorptive materials. *Sci. Total Environ.*, **461–462**: 1–9.

Campbell, C.G., Borglin, S.E., Green, F.B., Grayson, A., Wozei, E., Stringfellow, W.T., (2006). Biologically directed environmental monitoring, fate, and transport of estrogenic endocrine disrupting compounds in water: a review. *Chemosphere*, **65**: 1265–1280.

Cao, F., Bai, P., Li, H., Ma, Y., Deng, X., Zhao, C., (2009). Preparation of polyethersulfone–organophilic montmorillonite hybrid particles for the removal of bisphenol A. *J. Hazard. Mater.*, **162**: 791–798.

Cargouët, M., Perdiz, D., Mouatassim–Souali, A., Tamisier–Karolak, S., Levi, Y., (2004). Assessment of river contamination by estrogenic compounds in Paris area (France). *Sci. Total Environ.*, **324**: 55–66.

Carrizosa, M.J., Hermosin, M.C., Koskinen, W.C., Cornejo, J., (2003). Use of organosmectites to reduce leaching losses of acidic herbicides. *Soil Sci. Soc. Am. J.*, **67**: 511–517.

Carrizosa, M.J., Koskinen, W.C., Hermosin, M.C., Cornejo, J., (2001). Dicamba adsorption – desorption on organoclays. *Appl. Clay Sci.*, **18**: 223–231.

Centeno, J.A., Mullick, F.G., Martinez, L., Page, N.P., Gibb, H., Longfellow, D., Thompson, D., Ladich, E.R., (2002). Pathology related to chronic arsenic exposure. *Environ. Health Perspect.*, **110**: 883–886.

Chae, J.–P., Park, M.S., Hwang, Y.–S., Min, B.–H., Kim, S.–H., Lee, H.–S., Park, M.–J., (2015). Evaluation of developmental toxicity and teratogenicity of diclofenac using *Xenopus* embryos. *Chemosphere*, **120**: 52–58.

Chang, H.–S., Choo, K.–H., Lee, B., Choi, S.–J., (2009). The methods of identification, analysis, and removal of endocrine disrupting compounds (EDCs) in water– Review. *J. Hazard. Mater.*, **172**: 1–12.

Chantawong, V., Harvey, N.W., Bashkin, V.N., (2001). Adsorption of lead nitrate on Thai kaolin and ballclay. *Asian J. Energy Environ.*, **2**: 33–48.

Chen, C.C., Chung, Y.C., (2006). Arsenic removal using a biopolymer chitosan sorbent. J. Environ. Sci. Health Part A: Toxic/Hazard. Subst. Environ. Eng., **41**: 645–658.

Chen, C., Zhou, W., Yang, Q., Zhu, L., Zhu, L., (2014). Sorption characteristics of nitrosodiphenylamine (NDPhA) and diphenylamine (DPhA) onto organo–bentonite from aqueous solution. *Chem. Eng. J.*, **240**: 487–493.

Chiban, M., Zerbet, M., Carja, G., Sinan, F., (2012). Application of low–cost adsorbents for arsenic removal: A review. *J. Environ. Chem. Ecotoxicol.*, **4**: 91–102.

Choong, T.S.Y., Chuah, T., Robiah, Y., Koay, F.G., Azni, I., (2007). Arsenic toxicity, health hazards and removal techniques from water: an overview. *Desalination*, **217**: 139–166.

Cleuvers, M., (2003). Aquatic ecotoxicity of pharmaceuticals including the assessment of combination effects. *Toxicol. Lett.*, **142**: 185–194.

Crain, D.A., Eriksen, M., Iguchi, T., Jobling, S., Laufer, H., LeBlanc, G.A., Guillette, L. J., (2007). An ecological assessment of bisphenol–A: evidence from comparative biology. *Reprod. Toxicol.*, **24**: 225–239.

Cundy, A.B., Hopkinson, L., Whitby, R.L.D., (2008). Use of iron–based technologies in contaminated land and groundwater remediation: a review. *Sci. Total Environ.*, **400**: 42–51.

Dabrowski, A., (2001). Adsorption –from theory to practice. *Adv. Colloid Interf. Sci.*, **93**: 135–224.

Dambies, L., Roze, A., Guibal, E., (2000). As(V) sorption on molybdate–impregnated chitosan gel beads (MICB), *Adv. Chitin Sci.*, **4**: 302–309.

Dawodu, F.A., Akpomie, K.G., (2014). Kinetic, equilibrium, and thermodynamic studies on the adsorption of cadmium (II) ions using "Aloji kaolinite" mineral. *The Pacific J. Sci. Technol.*, **15**: 268–276.

de Paiva, L.B., Morales, A.R., Diaz, F.R.V., (2008). Organoclays: properties, preparation and applications. *Appl. Clay Sci.*, **42**: 8–24.

Delclos, K.B., Weis, C.C., Bucci, T.J., Olson, G., Mellick, P., Sadovova, N., Latendresse J.R., Thorn B., Newbold, R.R., (2009). Overlapping but distinct effects of genistein and ethinylestradiol (EE2) in female Sprague–Dawley rats in multigenerational reproductive and chronic toxicity studies. *Reprod. Toxicol.*, **27**: 117–132.

DeLorenzo, M.E., Fleming, J., (2008). Individual and mixture effects of selected pharmaceuticals and personal care products on the marine phytoplankton species *Dunaliella tertiolecta*. *Arch. Environ. Contam. Toxicol.*, **54**: 203–210.

Denizli, A., Cihangir, N., Rad, A.Y., Taner, M., Alsancak, G., (2004). Removal of chlorophenols from synthetic solutions using *Phanerochaete chrysosporium*. *Process Biochem.*, **39**: 2025–2030.

Dentel, S.K., Jamrah, A.I., Sparks, D.L., (1998). Sorption and cosorption of 1,2,4–trichlorobenzene and tannic acid by organo–clays. *Water Res.*, **32**: 3689–3697.

Devesa, V., Del Razo, L.M., Adair, B., Drobná, Z., Waters, S.B., Hughes, M.F., Styblo M., Thomas. D.J., (2004). Comprehensive analysis of arsenic metabolites by pH–specific hydride generation atomic absorption spectrometry. *J. Anal. At. Spectrom.*, **19**: 1460–1467.

Díaz, E., Ordóñez, S., Vega, A., Coca, J., (2004). Adsorption characterisation of different volatile organic compounds over alumina, zeolites and activated carbon using inverse gas chromatography. *J. Chromat. A*, **1049**: 139–146.

Douillet, C., Currier, J., Saunders, J., Bodnar, W.M., Matoušek, T., Stýblo M., (2013). Methylated trivalent arsenicals are potent inhibitors of glucose stimulated insulin secretion by murine pancreatic islets. *Toxicol. Appl. Pharmacol.*, **267**: 11–15.

Dussault, È.B., Balakrishnan, V.K., Borgmann, U., Solomon, K.R., Sibley, P.K., (2009). Bioaccumulation of the synthetic hormone 17α–ethinylestradiol in the benthic invertebrates *Chironomus tentans* and *Hyalella azteca*. *Ecotoxicol. Environ. Saf.*, **72**: 1635–1641.

EFSA, (2014). European Food Safety Authority, Mandate for a scientific opinion on the risk assessment of dietary bisphenol A. (http://www.efsa.europa.eu/en/topics/topic/bisphenol.htm).

Eisazadeh, A., Kassim, K.A., Nur, H., (2012). Solid–state NMR and FTIR studies of lime stabilized montmorillonitic and lateritic clays. *App. Clay Sci.*, **67–68**: 5–10.

El–Nahhal, Y.Z., Safi, J.M., (2004). Stability of an organoclay complex: effects of high concentrations of sodium chloride. *Appl. Clay Sci.*, **24**: 129–136.

Faria, P.C.C., Órfão, J.J.M., Pereira, M.F.R., (2004). Adsorption of anionic and cationic dyes on activated carbons with different surface chemistries. *Water Res.*, **38**: 2043–2052.

Farombi, E.O., Ugwuezunmba, M.C., Ezenwadu, T.T., Oyeyemi, M.O., Ekor, M., (2008). Tetracycline–induced reproductive toxicity in male rats: Effects of vitamin C and *N*–acetylcysteine. *Experim. Toxicol. Pathol.*, **60**: 77–85.

Faust, S.D., Aly, O.M., (1987). *Adsorption Process for Water Treatment*, Butterworths Publishers, Stoneham.

Feng, Y., Zhang, Z., Gao, P., Su, H., Yu, Y., Ren, N., (2010). Adsorption behavior of EE_2 (17α–ethinylestradiol) onto the inactivated sewage sludge: Kinetics, thermodynamics and influence factors. *J. Hazard. Mater.*, **175**: 970–976.

Fent, K., Weston, A.A., Caminada, D., (2006). Ecotoxicology of human pharmaceuticals. *Aquat. Toxicol.*, **76**: 122–159.

Flint, S., Markle, T., Thompson, S., Wallace, E., (2012). Bisphenol A exposure, effects, and policy: A wildlife perspective. *J. Environ. Manage.*, **104**: 19–34.

Foo, K.Y., Hameed, B.H., (2010). Insights into the modeling of adsorption isotherm systems, *Chem. Eng. J.*, **156**: 2–10.

Fosshage, M., (2014). A new wastewater treatment technology for developing countries. *Filtr. Sep.*, **51**: 14–17.

Franz, M., Arafat, H.A., Pinto, N.G., (2000). Effect of chemical surface heterogeneity on the adsorption mechanism of dissolved aromatics on activated carbon. *Carbon*, **38**: 1807–1819.

Freneaux, E., Labbe, G., Letteron, P., Dinh, T.L., Degott, C., Geneve, J., Larrey, D., Pessayre, D., (1988). Inhibition of the mitochondrial oxidation of fatty acids by tetracycline in mice and in man: possible role in microvesicular steatosis induced by this antibiotic. *Hepatology*, **8**: 1056–1062.

Fromenty, B., Pessayre, D., (1995). Inhibition of mitochondrial beta–oxidation as a mechanism of hepatotoxicity. *Pharmacol. Ther.*, **67**: 101–154.

Fu, F., Dionysiou, D.D., Liu, H., (2014). The use of zero–valent iron for groundwater remediation and wastewater treatment: A review. *J. Hazard. Mater.*, **267**: 194–205.

Furuya, M., Sasaki, F., Hassanin, A.M.A., Kuwahara, S., Tsukamoto, Y., (2002). Effects of bisphenol–A on the growth of comb and testes of male chicken. *Can. J. Vet. Res.*, **67**: 68–71.

Gao, P., Munir, M., Xagoraraki, I., (2012). Correlation of tetracycline and sulfonamide antibiotics with corresponding resistance genes and resistant bacteria in a conventional municipal wastewater treatment plant. *Sci. Total Environ.*, **173**: 421–422.

Garg, V.K., Amita, M., Kumar, R., Gupta, R., (2004). Basic dye (methylene blue) removal from simulated wastewater by adsorption using Indian Rosewood sawdust: a timber industry waste. *Dyes Pigm.*, **63**: 243–250.

Ghobarkar, H., Schäf, O., Guth, U., (1999). Zeolites – from kitchen to space. *Prog. Solid State Chem.*, **27**: 29–73.

Ghurye, G., Clifford, D., Tripp, A., (2004). Iron coagulation and direct microfiltration to remove arsenic from groundwater. *J. Am. Water Works Assoc.*, **96**: 143–152.

Gieseking, J.E., (1939). The mechanism of cation exchange in the montmorillonite–beidellite–nontronite type of clay minerals. *Soil Sci.*, **47**: 1–14.

Gleick, P.H., (1993). *Water in Crisis: A Guide to the World's Freshwater Resources*. Oxford University Press Inc., 198 Madison Avenue, Now York.

Gokcimen, A., Ragbetli, M.C., Bas, O., Tunc, A.T., Aslan, H., Yazici, A.C., Kaplan, S., (2007). Effect of prenatal exposure to an anti–inflammatory drug on neuron number in cornu ammonis and dentate gyrus of the rat hippocampus: a stereological study. *Brain Res*., **1127**: 185–192.

Greenlee, L.F., Lawler, D.F., Freeman, B.D., Marrot, B., Moulin, P., (2009). Reverse osmosis desalination: Water sources, technology, and today's challenges. *Water Res*., **43**: 2317–2348.

Groisman, L., Rav–Acha, C., Gerstl, Z., Mingelgrin, U., (2004). Sorption of organic compounds of varying hydrophobicities from water and industrial wastewater by long– and short–chain organoclays. *Appl. Clay Sci*., **24**: 159–166.

Guégan, R., Giovanela, M., Warmont, F., Motelica–Heino, M., (2015). Nonionic organoclay: A 'Swiss Army knife' for the adsorption of organic micro–pollutants? *J. Colloid Interf. Sci.*, **437**: 71–79.

Gugenheim, S., Martin, R.T., (1995). Definition of clay and clay mineral: Joint report of the AIPEA nomenclature and CMS nomenclature committees. *Clays Clay Miner*., **43**: 255–256.

Gupta, V.K., Saini, V.K., Jain, N., (2005). Adsorption of As(III) from aqueous solutions by iron oxide–coated sand. *J. Colloid Interf. Sci.*, **288**: 55–60.

Gupta, V.K., Ali, I., Saini, V.K., (2004). Removal of chlorophenols from wastewater using red mud: an aluminum industry waste. *Environ. Sci. Technol*., **38**: 4012–4018.

Haap, T., Triebskorn, R., Köhler, H.–R., (2008). Acute effects of diclofenac and DMSO to Daphnia magna: immobilisation and hsp70–induction. *Chemosphere*, **73**: 353–359.

Haerifar, M., Azizian, S., (2012). Fractal–like adsorption kinetics at the solid/solution interface. *J. Phys. Chem. C*, **116**: 13111–13119.

Han, J., Qiu, W., Cao, Z., Hu, J., Gao, W., (2013). Adsorption of ethinylestradiol (EE2) on polyamide 612: Molecular modeling and effects of water chemistry. *Water Res*., **47**: 2273–2284.

Hao, J., Han, M.J., Wang, C., Meng, X., (2009). Enhanced removal of arsenite from water by a mesoporous hybrid material – thiol–functionalized silica coated activated alumina. *Micro. Meso. Mater*., **124**: 1–7.

Hassard, F., Biddle, J., Cartmell, E., Jefferson, B., Tyrrel, S., Stephenson. T., (2014). Rotating biological contactors for wastewater treatment–A review. *Proc. Saf. Environ. Protect*., Available online 4 August 2014, DOI: 10.1016/j.psep.2014.07.003.

Hayes, K.F., Papelis, C., Leckie, J.O., (1988). Modeling ionic strength effects on anion adsorption at hydrous oxide/solution interfaces. *J. Colloid Interf. Sci.*, **125**: 717–726.

He, H., Ma, Y., Zhu, J., Yuan, P., Qing, Y., (2010). Organo clays prepared from montmorillonites with different cation exchange capacity and surfactant configuration. *Appl. Clay Sci.*, **48**: 67–72.

Heaton, P.C., Fenwick, S.R., Brewer, D.E., (2007). Association between tetracycline or doxycycline and hepatotoxicity: a population–based case–control study. *J. Clin. Pharm. Ther.*, **32**: 483–487.

Hecker, M., Hollert, H., Cooper, R., Vinggaard, A.M., Akahori, Y., Murphy, M., Nellemann, C., Higley, E., Newsted, J., Wu, R., Lam, P., Laskey, J., Buckalew, A., Grund, S., Nakai, M., Timm, G., Giesy, J., (2007). The OECD validation program of the H295R steroidogenesis assay for the identification of in vitro inhibitors and inducers of testosterone and estradiol production. Phase 2: Inter–laboratory pre–validation studies. *Environ. Sci. Pollut. Res.*, **14**: 23–30.

Hermosin, M.C., Calderon, M.J., Aguer, J.P., Cornejo, J., (2001). Organoclays for controlled release of the herbicide fenuron. *Pest. Manage. Sci.*, **57**: 803–809.

Ho, Y.S., (2006). Review of second–order models for adsorption systems. *J. Hazard. Mater.*, **136**: 681–689.

Ho, Y.S., Mckay, G., (1998). A comparison of chemisorption kinetic models applied to pollutant removal on various sorbents. *Process Saf. Environ. Protect.*, **76**: 332–340.

Ho, Y.S., McKay, G., (1999a). Batch Lead (II) removal from aqueous solution by peat: equilibrium and kinetics. *Process Saf. Environ. Protect.*, **77**: 165–173.

Ho, Y.S., McKay, G., (1999b). Pseudo–second order model for sorption processes. *Process Biochem.*, **34**: 451–465.

Ho, Y.S., Mckay, G., (2000). The kinetics of sorption of divalent metal ions onto *sphagnum* moss peat. *Water Res.*, **34**: 735–742.

Hoeger, B., Köllner, B., Dietrich, D.R., Hitzfeld, B., (2005). Water–borne diclofenac affects kidney and gill integrity and selected immune parameters in brown trout (*Salmo trutta f. fario*). *Aquat. Toxicol.*, **75**: 53–64.

Höll, W.H., (2010). Mechanisms of arsenic removal from water. *Environ. Geochem. Health.*, **32**: 287–290.

Hollas, J.M., (2005). *Modern Spectroscopy*. 4th Edition, John Wiley and Sons Ltd., USA, p. 262.

Hong, H., Jiang, W.–T., Zhang, X., Tie, L., Li, Z., (2008). Adsorption of Cr(VI) on STAC–modified rectorite. *Appl. Clay Sci.*, **42**: 292–299.

Hsu, Y.H., Wang, M.K., Pai, C.W., Wang, Y.S., (2000). Sorption of 2,4–dichlorophenoxy propionic acid by organo–clay complexes. *Appl. Clay Sci.*, **16**: 147–159.

Huang, J., Wang, X., Jin, Q., Liu, Y., Wang, Y., (2007). Removal of phenol from aqueous solution by adsorption of phenol from aqueous solution by adsorption onto OTMAC–modified attapulgite. *J. Environ. Manage.*, **84**: 229–236.

Huang, Y.Q., Wong, C.K., Zheng, J.S., Bouwman, H., Barra, R., Wahlstrom, B., Neretin, L., Wong, M.H., (2012). Bisphenol A (BPA) in China: a review of sources, environmental levels, and potential human health impacts. *Environ. Inter.*, **42**: 91–99.

Hughes, M.F., Beck, B.D., Chen, Y., Lewis, A.S., Thomas, D.J., (2011). Arsenic exposure and toxicology: a historical perspective. *Toxicol. Sci.*, **123**: 305–332.

Iesana, C.M., Capat, C., Ruta, F., Udrea, I., (2008). Evaluation of a novel hybrid inorganic/organic polymertype material in the arsenic removal process from drinking water. *Water. Res.*, **42**: 4327–4333.

ISRIC, (2002). International Soil Reference and Information Centre (ISRIC), Procedures for soil analysis, 6th Edition, L.P. van Reeuwijk Ed., F.A.O., United Nations, Wageningen, Netherlands. (http://www.isric.org/isric/webdocs/docs/ISRIC_TechPap09_2002.pdf).

IUPAC, (1971). Manual of symbols and terminology for physicochemical quantities and units, Appendix II: Definitions, Terminology and Symbols in Colloid and Surface Chemistry, Part I, Prepared by D. H. Everett, Butterworths, London, p.11.

IUPAC, (1997). Compendium of Chemical Terminology, 2nd ed. (the "Gold Book"). Compiled by A. D. McNaught and A. Wilkinson. Blackwell Scientific Publications, Oxford.

Jain, C.K., Singh, R.D., (2012). Technological options for the removal of arsenic with special reference to South East Asia–Review. *J. Environ. Manage.*, **107**:1–18.

Jaynes, W., Boyd, S., (1990). Trimethylphenylammonium–smectite as an effective adsorbent of water soluble aromatic hydrocarbons. *J. Air Waste Manage. Assoc.*, **40**: 1649–1653.

Jia, Y., Demopoulos, G.P., (2005). Adsorption of arsenate onto ferrihydrite from aqueous solution: Influence of media (sulfate vs. nitrate), added gypsum, and pH alteration. *Environ. Sci. Technol.*, **39**: 9523–9527.

Jiang, M.–Q., Jin, X.–Y., Lu, X.–Q., Chen, Z.–L., (2010). Adsorption of Pb(II), Cd(II), Ni(II) and Cu(II) onto natural kaolinite clay. *Desalination*, **252**: 33–39.

Johnson, A.C., Belfroid, A., Di Corcia, A., (2000). Estimating steroid oestrogen inputs into activated sludge treatment works and observations on their removal from the effluent. *Sci. Total Environ.*, **256**: 163–173.

Jordan, J.W., (1949). Organophilic bentonites I. Swelling in organic liquids. *J. Phys. Chem.*, **53**: 294–306.

Joseph, L., Boateng, L.K., Flora, J.R.V., Park, Y.–G., Son, A., Badawy, M., Yoon, Y., (2013). Removal of bisphenol A and 17α–ethinyl estradiol by combined coagulation and adsorption using carbon nanomaterials and powdered activated carbon. *Sep. Purif. Technol.*, **107**: 37–47.

Joseph, L., Zaib, Q., Khan, I.A., Berge, N.D., Park, Y.G., Saleh, N.B., Yoon, Y., (2011). Removal of bisphenol A and 17α–ethinyl estradiol from landfill leachate using single–walled carbon nanotubes. *Water Res.*, **45**: 4056–4068.

Jović–Jovičić, N., Milutinović–Nikolić, A., Banković, P., Dojčinović, B., Nedić, B., Gržetić, I., Jovanović, D., (2010). Synthesis, characterization and adsorptive properties of organobentonites. *Acta Phy. Pol. A.*, **117**: 849–854.

Juang, L.C., Wang, C.C., Lee, C.K., Hsu, T.C., (2007). Dyes adsorption onto organoclay and MCM–41. *J. Environ. Eng. Manage.*, **17**: 29–38.

Kartinen Jr., E.O., Martin, C.J., (1995). An overview of arsenic removal processes. *Desalination*, **103**: 79–88.

Khalaf, H., Bouras, O., Perrichon, V., (1997). Synthesis and characterization of Al–pillared and cationic surfactant modified Al–pillared Algerian bentonite. *Micro. Mater.*, **8**: 141–150.

Khan, S.A., Rehman, R., Khan, M.A., (1995). Sorption of strontium on bentonite. *Waste Manage.*, **15**: 641–650.

Khormaei, M., Nasernejad, B., Edrisi, M., Eslamzadeh, T., (2007). Copper biosorption from aqueous solutions by sour orange residue. *J. Hazard. Mater.*, **149**: 269–274.

Kikkawa, R., Fujikawa, M., Yamamoto, T., Hamada, Y., Yamada, H., Horii I., (2006). In vivo hepatotoxicity study of rats in comparison with in vitro hepatotoxicity screening system. *J. Toxicol. Sci.*, **31**: 23–34.

Kim, H.Y., Jeon, J., Hollender, J., Yu, S., Kim, S.D., (2014). Aqueous and dietary bioaccumulation of antibiotic tetracycline in *D. magna* and its multigenerational transfer. *J. Hazard. Mater.*, **279**: 428–435.

Ko, C.H., Fan, C., Chiang, P.N., Wang, M.K., Lin, K.C., (2007). p–Nitrophenol, phenol and aniline sorption by organo–clays. *J. Hazard. Mater.*, **149**: 275–282.

Konta, J., (1995). Clay and man: clay raw materials in the service of man. *Appl. Clay Sci.* **10**: 275–335.

Krishna, B.S., Murty, D.S.R., Prakash, B.S.J., (2000). Thermodynamics of chromium(VI) anionic species sorption onto surfactant–modified montmorillonite clay. *J. Colloid Interf. Sci*., **229**: 230–236.

Krishnan, K., Gagné, M., Nong, A., Aylward, L.L., Hays, S.M., (2010). Biomonitoring Equivalents for bisphenol A (BPA). *Regu. Toxicol. Pharmacol*., **58**: 18–24.

Kuleyin, A., (2007). Removal of phenol and 4–chlorophenol by surfactant–modified natural zeolite. *J. Hazard. Mater.*, **144**: 307–315.

Kumar, S., (2008). *Spectroscopy of Organic Compounds*. Guru Nanak Dev University, Amritsar. http://nsdl.niscair.res.in/jspui/handle/123456789/793.

Kundu, S., Gupta, K.A., (2006). Investigation on the adsorption efficiency of iron oxide coated cement (IOCC) towards As(V)– kinetics, equilibrium and thermodynamics studies. *Colloids Surf. A*: *Physicochem. Eng. Aspects*, **273**: 121–128.

Labadie, P., Budzinski, H., (2006). Alteration of steroid hormone balance in juvenile turbot (*Psetta maxima*) exposed to nonylphenol, bisphenol A, tetrabromodiphenyl ether 47, diallylphthalate, oil, and oil spiked with alkylphenols. *Arch. Environ. Contam. Toxicol*., **50**: 552–561.

Ladeira, A.C.Q., Ciminelli, V.S.T., Nepomuceno, A.L., (2002). Seleção de solos para a imobilização de arsênio. Rem: Rev. Esc. Minas., **55**: 215–221.

Lagaly, G., (1984). Clay–Organic interaction. In: P.B. Tanke (Ed.), Clay minerals: Their structure, behaviour and use. Proc. Royal Society discussion meeting on November, 1983, A311, The Royal Society, London. p.315–332.

Lagaly, G., (1986). Interaction of alkylamines with different types of layered compounds. *Solid State Ion*., **22**: 43–51.

Lalhmunsiama, Tiwari, D., Lee, S.–M., (2012). Activated carbon and manganese coated activated carbon precursor to dead biomass in the remediation of arsenic contaminated water. *Environ. Eng. Res.*, **17**: S41–S48.

Landry, K.A., Boyer, T.H., (2013). Diclofenac removal in urine using strong–base anion exchange polymer resins. *Water Res*., **47**: 6432–6444.

Larcher, S., Delbès, G., Robaire, B. Yargeau, V., (2012). Degradation of 17α–ethinylestradiol by ozonation – Identification of by–products and assessment of their estrogenicity and toxicity. *Environ. Inter*., **39**: 66–72.

Larcher, S., Yargeau, V., (2013). Biodegradation of 17α–ethinylestradiol by heterotrophic bacteria. *Environ. Pollut*., **173**: 17–22.

Lee, J.F., Mortland, M.M., Boyd, S.A., Chiou, C.T., (1989). Shape–selective adsorption of aromatic compounds from water by tetramethylammonium–smectite. *J. Chem. Soc., Faraday Trans. I*, **85**: 2953–2962.

Lee, S.M., Kim, W.G., Laldawngliana, C., Tiwari, D., (2010). Removal behavior of surface modified sand for Cd(II) and Cr(VI) from aqueous solutions. *J. Chem. Eng. Data*, **55**: 3089–3094.

Lee, S.M., Tiwari, D., (2012). Organo and inorgano–organo–modified clays in the remediation of aqueous solutions: an overview. *Appl. Clay Sci.*, **59–60**: 84–102.

Lee, S.M., Tiwari, D., (2014). Organo–modified sericite in the remediation of an aquatic environment contaminated with As(III) or As(V). *Environ. Sci. Pollut. Res.*, **21**: 407–418.

Lee, S.M., Tiwari, D., Choi, K.M., Yang, J.K., Chang, Y.Y., Lee, H.D., (2009). Removal of Mn(II) from aqueous solutions using manganese–coated sand samples. *J. Chem. Eng.Data*, **54**: 1823–1828.

Lemic, J., Tomasevic–Canovic, M., Adamovic, M., Kovacevic, D., Milacevic, S., (2007). Competitive adsorption of polycyclic aromatic hydrocarbons on organo–zeolites. *Micro. Meso. Mater.*, **105**: 317–323.

Lepper, M.H., Wolfe, C.K., Zimmerman, H.J., Caldwell Jr, E.R., Spies, H.W., Dowling, H.F., (1951). Effect of large doses of aureomycin on human liver. *AMA Arch. Inter. Med.*, **88**: 271–283.

Li, J., Jiang, L., Liu, X., Lv, J., (2013). Adsorption and aerobic biodegradation of four selected endocrine disrupting chemicals in soil – water system. *Inter. Biodeterior. Biodegrad.*, **76**: 3–7.

Li, Y., Chen, B., Zhu L., (2010a). Enhanced sorption of polycyclic aromatic hydrocarbons from aqueous solution by modified pine bark. *Biores. Technol.*, **101**: 7307–7313.

Li, Y., Wang, J., Luan, Z., Liang, Z., (2010b). Arsenic removal from aqueous solution using ferrous based red mud sludge. *J. Hazard. Mater.*, **177**: 131–137.

Li, Y., Zhang, F.–S., Xiu, F.–R., (2009). Arsenic(V) removal from aqueous system using adsorbent developed from a high iron–containing fly ash. *Sci. Total Environ.*, **407**: 5780–5786.

Li, Z., Bowman, R.S., (1997). Counter ion effects on the sorption of cationic surfactant and chromate on natural clinoptilonite. *Environ. Sci. Technol.*, **31**: 2407–2412.

Li, Z., Bowman, R.S., (2001). Retention of inorganic oxyanions by organo–kaolinite. *Water Res.*, **35**: 3771–3776.

Litter, M.I., Morgada, M.E., Bundschuh, J., (2010). Possible treatments for arsenic removal in Latin American waters for human consumption– Review. *Environ. Poll.*, **158**: 1105–1118.

Liu, G.J., Zhang, X.R., McWilliams, L., Talley, J.W., Neal, C.R., (2008). Influence of ionic strength, electrolyte type, and NOM on As(V) adsorption onto TiO_2. *J. Environ. Sci. Health Part A*, **43**: 430–436.

Liu, Z.–h., Kanjo, Y., Mizutani S., (2009). Removal mechanisms for endocrine disrupting compounds (EDCs) in wastewater treatment — physical means, biodegradation, and chemical advanced oxidation: A review. *Sci. Total Environ.*, **407**: 731–748.

Liu, N., Wang, M.–X., Liu, M.–M., Liu, F., Weng, L., Koopal, L.K., Tan, W.–F., (2012). Sorption of tetracycline on organo–montmorillonites. *J. Hazard. Mater.*, **225–226**: 28–35.

Lu, L., Gao, M., Gu, Z., Yang, S., Liu, Y., (2014). A comparative study and evaluation of sulfamethoxazole adsorption onto organo–montmorillonites. *J. Environ. Sci.*, **26**: 2535–2545.

Ma, J., Zhu, L., (2006). Simultaneous sorption of phosphate and phenanthrene to inorgano–organo–bentonite from water. *J. Hazard. Mater.*, **136**: 982–988.

MacEwan, D.M.C., (1944). Identification of the montmorillonite group of minerals by X–rays. *Nature*, **154**: 577–578.

Malek, A., Farooq, S., (1996). Comparison of isotherm models for hydrocarbon adsorption on activated carbon, *AIChE J.,* **42**: 3191–3201.

Mandal, B.K., Suzuki, K.T., (2002). Arsenic around the world: a review. *Talanta*, **58**: 201–235.

Mandal, S., Padhi, T., Patel, R.K., (2011). Studies on the removal of arsenic (III) from water by a novel hybrid material. *J. Hazard. Mater.*, **192**: 899–908.

Mazellier, P., Méité, L., De Laat, J., (2008). Photodegradation of the steroid hormones 17β–estradiol (E2) and 17α–ethinylestradiol (EE2) in dilute aqueous solution. *Chemosphere*, **73**: 1216–1223.

McBride, M.B., Pinnavaia, T.J., Mortland, M.M., (1975). Adsorption of aromatic molecules by clays in aqueous suspension. Preprints of papers, Presented at the national meeting of the American Chemical Society, Div. of Environ. Chemistry. **15**: 44–46.

Meloun, M., Bordovska, S., Galla, L., (2007). The thermodynamic dissociation constants of four non–steroidal anti–inflammatory drugs by the least–squares nonlinear regression of multiwavelength spectrophotometric pH–titration data. *J. Pharm. Biomed. Anal.*, **45**: 552–564.

Meng, X., Korfiatis, G.P., Bang, S., Bang, K.W., (2002). Combined effects of anions on arsenic removal by iron hydroxides. *Toxicol. Lett.*, **133**: 103–111.

Middleton, H., Moore, M.R., Chapman, H., Leusch, F., Tan, B., Drew, R., Frangos, J., Khan, S., Leslie, G., Shaw, G., (2008). Australian Guidelines for Water Recycling: Recycled Water Quality – A Guide to Determining, Monitoring and Achieving Safe Concentrations of Chemicals in Recycled Water. Environmental Protection and Heritage Council, National Water Commission, Queensland Government, Canberra, ACT, Australia.

Miranda, K., Pereira–Filho, E.R., (2009). Potentialities of thermospray flame furnace atomic absorption spectrometry (TS–FF–AAS) in the fast sequential determination of Cd,Cu, Pb and Zn. *Anal. Methods*, **1**: 215–219.

Mohan, D., Pittman Jr., C.U., (2007). Arsenic removal from water/wastewater using adsorbents—A critical review. *J. Hazard. Mater.*, **142**: 1–53.

Mondal, P., Bhowmic, S., Chatterjee, D., Figoli, A., Van der Bruggen, B., (2013). Remediation of inorganic arsenic in groundwater for safe water supply: A critical assessment of technological solutions–Review. *Chemosphere*, **92**: 157–170.

Mook, W.T., Aroua, M.K., Issabayeva. G., (2014). Prospective applications of renewable energy based electrochemical systems in wastewater treatment: A review. *Renew. Sust. Ener. Rev.*, **38**: 36–46.

Moreno–Castilla, C., (2004). Adsorption of organic molecules from aqueous solutions on carbon materials. *Carbon*, **42**: 83–94.

Mortland, M.M., Shaobai, S., Boyd, S.A., (1986). Clay–organic complexes as adsorbents for phenol and chlorophenols. *Clays Clay Miner.*, **34**: 581–585.

Muller, M., Combalbert, S., Delgenès, N., Bergheaud, V., Rocher, V., Benoît, P., Delgenès J.P., Patureau, D., Hernandez–Raquet, G., (2010). Occurrence of estrogens in sewage sludge and their fate during plant–scale anaerobic digestion. *Chemosphere*, **81**: 65–71.

Mustaqeem, M., Bagwan, M.S., Patil, P.R., (2013). Evaluation of removal efficiency of Ni(II) from aqueous solution by natural leaves. *Rasayan J. Chem*., **6**: 307 – 314.

Nabi, D., Aslam, I., Qazi, I.A., (2009). Evaluation of the adsorption potential of titanium dioxide nanoparticles for arsenic removal. *J. Environ. Sci.*, **21**: 402–408.

Naidoo, V., Duncan, N., Bekker, L., Swan, G., (2007). Validating the domestic fowl as a model to investigate the pathophysiology of diclofenac in gyps vultures. *Environ. Toxicol. Pharmacol.*, **24**: 260–266.

Nassef, M., Kim, S.G., Seki, M., Kang, I.J., Hano, T., Shimasaki, Y., Oshima, Y., (2010). In ovo nanoinjection of triclosan, diclofenac and carbamazepine affects embryonic development of medaka fish (*Oryzias latipes*). *Chemosphere*, **79**: 966–973.

Navarro, P., Alguacil, F.J., (2002). Adsorption of antimony and arsenic from a copper electrorefining solution onto activated carbon. *Hydrometallurgy*, **66**: 101–105.

Navas–Acien, A., Silbergeld, E.K., Streeter, R.A., Clark, J.M., Burke, T.A., Guallar, E., (2006). Arsenic exposure and type 2 diabetes: a systematic review of the experimental and epidemiologic evidence. *Environ. Health Perspect.*, **114**: 641–648.

Newcombe, R.L., Möller, G., (2008). Arsenic removal from drinking water: A review. Blue Water Technologies Inc., Hayden, ID: 2006. http://www.blueh2o.net/docs/asreview%20080305.pdf.

Ng, J.C., (2005). Environmental contamination of arsenic and its toxicological impact on humans. *Environ. Chem.*, **2**: 146–160.

Ng, L.E., Halliwell, B., Wong, K.P., (2008). Nephrotoxic cell death by diclofenac and meloxicam. *Biochem. Biophys. Res. Comm.*, **369**: 873–877.

Nieminen, P., Lindstrom–Seppa, P., Mustonen, A., Mussalo–Rauhamaa, H., Kukkonen, J.V.K., (2002). Bisphenol A affects endocrine physiology and biotransformation enzyme activities of the field vole (Microtus agrestis). *Gen. Comp. Endocrinol.*, **126**: 183–189.

Niu, J., Ding, S., Zhang, L., Zhao, J., Feng, C., (2013). Visible–light–mediated Sr–Bi_2O_3 photocatalysis of tetracycline: Kinetics, mechanisms and toxicity assessment. *Chemosphere*, **93**: 1–8.

Nzengung, V.A., Voudrias, E.A., Nkedi–Kizza, P., Wampler, J.M., Weaver, C.E., (1996). Organic cosolvent effects on sorption equilibrium of hydrophobic organic chemicals by organoclays. *Environ. Sci. Technol.*, **30**: 89–96.

Oaks, J.L., Gilbert, M., Virani, M.Z., Watson, R.T., Meteyer, C.U., Rideout, B.A., Shivaprasad, H.L., Ahmed, S., Chaudhry, M.J., Arshad, M., Mahmood, S., Ali, A., Khan, A.A., (2004). Diclofenac residues as the cause of vulture population decline in Pakistan. *Nature*, **427**: 630–633.

Oehlmann, J., Schulte–Oehlmann, U., Tillmann, M., Markert, B., (2000). Effects of endocrine disruptors on prosobranch snails (Mollusca: Gastropoda) in the laboratory. Part 1: bisphenol A and octylphenol as xeno–estrogens. *Ecotoxicology*, **9**: 383–397.

Oller, I., Malato, S., Sánchez–Pérez, J.A., (2011). Combination of advanced oxidation processes and biological treatments for wastewater decontamination – A review. *Sci. Total Environ.*, **409**: 4141–4166.

Oscarson, D.W., Hume, H.B., King, F., (1994). Sorption of cesium on compacted bentonite. *Clays Clay Miner*., **42**, 731–736.

Parfitt, G.D., Rochester, C.H., (1983). *In Adsorption from Solution at the Solid–Liquid Interface*, Academic Press, New York, p.3.

Park, Y., Ayoko, G.A., Frost R.L., (2011a). Characterisation of organoclays and adsorption of p–nitrophenol: Environmental application. *J. Colloid Interf. Sci.*, **360**: 440–456.

Park, Y., Ayoko, G.A., Kristof, J., Horvath, E., Frost, R.L., (2012). A thermoanalytical assessment of an organoclay. *J. Ther. Anal. Calorim*., **107**: 1137–1142.

Park, Y., Ayoko, G.A., Frost. R.L., (2011b). Application of organoclays for the adsorption of recalcitrant organic molecules from aqueous media. *J. Colloid Interf. Sci*., **354**: 292–305.

Park, Y., Sun, Z., Ayoko, G.A., Frost, R.L., (2014). Bisphenol A sorption by organo–montmorillonite: Implications for the removal of organic contaminants from water. *Chemosphere*, **107**: 249–256.

Parolo, M.E., Savini, M.C., Vallés, J.M., Baschini, M.T., Avena, M.J., (2008). Tetracycline adsorption on montmorillonite: pH and ionic strength effects. *Appl. Clay Sci.*, **40**: 179–186.

Pauwels, B., Wille, K., Noppe, H., De Brabandar, H., de Wiele, T.V., Verstraete, W., Boon, N., (2008). 17α–ethinylestradiol cometabolism by bacteria degrading estrone, 17β– estradiol and estriol. *Biodegradation*, **19**: 683–693.

Petrick, J.S., Ayala–Fierro, F., Cullen, W.R., Carter, D.E., Vasken, A.H., (2000). Monomethylarsonous acid ((MMA)(III)) is more toxic than arsenite in Chang human hepatocytes. *Toxicol. Appl. Pharmacol*., **163**: 203–207.

Plappally, A.K., Lienhard V, J.H., (2012). Energy requirements for water production, treatment, end use, reclamation, and disposal. Renew. *Sust. Ener. Rev*., **16**: 4818–4848.

Polubesova, T., Zadaka, D., Groisman, L., Nir, S., (2006). Water remediation by micelle–clay system: Case study for tetracycline and sulfonamide antibiotics. *Water Res*., **40**: 2369–2374.

Pradas, E.G., Sanchez, M.V., Cruz, F.C., Viciana, M.S., Perez, M.F., (1994). Adsorption of cadmium and zinc from aqueous solution on natural and activated bentonite. *J. Chem. Tech. Biotechnol.*, **59**: 289–295.

Pusch, R., (1992). Use of bentonite for isolation of radioactive waste products. *Clay Miner*. **27**: 353–361.

Qu, X., Alvarez, P.J.J., Li, Q., (2013). Applications of nanotechnology in water and wastewater treatment. *Water Res*., **47**: 3931–3946.

Raab, A., Wright, S.H., Jaspars, M., Meharg, A.A., Feldmann, J., (2007). Pentavalent arsenic can bind to biomolecules. *Angew. Chem. Inter. Ed.*, **46**: 2594–2597.

Rahardjo, A.K., Susanto, M.J.J., Kurniawan, A., Indraswati, N., Ismadji, S., (2011). Modified Ponorogo bentonite for the removal of ampicillin from wastewater. *J. Hazard. Mater.*, **190**: 1001–1008.

Rawajfih, Z., Nsour, N., (2006). Characteristics of phenol and chlorinated phenols sorption onto surfactant–modified bentonite. *J. Colloid Interf. Sci.*, **298**: 39–49.

Rhee, J.S., Jung, M.W., Paeng, K.J., (1998). Evaluation of chitin and chitosan as a sorbent for the preconcentration of phenol and chlorophenols in water. *Anal. Sci.*, **14**: 1089–1094.

Richards, S., Bouazza, A., (2007). Phenol adsorption in organo–modified basaltic clay and bentonite. *Appl. Clay Sci.*, **37**: 133–142.

Rmalli, S.W.A., Harrington, C.F., Ayub, M., Haris, P.I., (2005). A biomaterial based approach for arsenic removal from water. *J. Environ. Monit.*, **7**: 279–282.

Rodríguez–Cruz, M.S., Andrades, M.S., Sánchez–Martín, M.J., (2008). Significance of the long–chain organic cation structure in the sorption of the penconazole and metalaxyl fungicides by organo clays. *J. Hazard. Mater.*, **160**: 200–207.

Rodríguez–Cruz, M.S., Sánchez–Martín, M.J., Andrades, M.S., Sánchez–Camazano, M., (2007). Modification of clay barriers with a cationic surfactant to improve the retention of pesticides in soils. *J. Hazard. Mater.*, **139**: 363–372.

Ross, D.S., Ketterings, Q., (2011). Recommended methods for determining soil cation exchange capacity, *Coop. Bulletin No*. 493, Chapter 9, p. 75. http://extension.udel.edu/lawngarden/files/2012/10/CHAP9.pdf

Sanchez–Martin, M.J., Rodriguez–Cruz, M.S., Andrades, M.S., Sanchez–Camazano, M., (2006). Efficiency of different clay minerals modified with a cationic surfactant in the adsorption of pesticides: influence of clay type and pesticide hydrophobicity. *Appl. Clay Sci.*, **31**: 216–228.

Santos, L.H.M.L.M., Araújo, A.N., Fachini, A., Pena, A., Delerue–Matos, C., Montenegro, M.C.B.S.M., (2010). Ecotoxicological aspects related to the presence of pharmaceuticals in the aquatic environment – Review. *J. Hazard. Mater.*, **175**: 45–95.

Saravanan, M., Karthika, S., Malarvizhi, A., Ramesh, M., (2011). Ecotoxicological impacts of clofibric acid and diclofenac in common carp (*Cyprinus carpio*) fingerlings: hematological, biochemical, ionoregulatory and enzymological responses. *J. Hazard. Mater.*, **195**: 188–194.

Scheidegger, A.M., Fendorf, M., Sparks, D.L., (1996). Mechanisms of nickel sorption on pyrophyllite: Macroscopic and microscopic approaches. Soil Sci. Soc. Am. J., **60**: 1763–1772.

Schmidt, W., O'Rourke, K., Hernan, R., Quinn, B., (2011). Effects of the pharmaceuticals gemfibrozil and diclofenac on the marine mussel (*Mytilus spp*.) and their comparison with standardized toxicity tests. *Marine Poll. Bull*., **62**: 1389–1395.

Schmitt–Jansen, M., Bartels, P., Adler, N., Altenburger, R., (2007). Phytotoxicity assessment of diclofenac and its phototransformation products. *Anal. Bioanal. Chem*., **387**: 1389–1396.

Sehar, S., Aamir, R., Naz, I., Ali, N., Ahmed, S., (2013). Reduction of contaminants (physical, chemical, and microbial) in domestic wastewater through hybrid constructed wetland. *ISRN Microbiol*., **2013**:350260. http://dx.doi.org/10.1155/2013/350260.

Senturk, H.B., Ozdes, D., Gundogdu, A., Duran, C., Soylak, M., (2009). Removal of phenol from aqueous solutions by adsorption onto organo modified Tirebolu bentonite: Equilibrium, kinetic and thermodynamic study. *J. Hazard. Mater*., **172**: 353–362.

Sharma, V.K., Sohn, M., (2009). Aquatic arsenic: toxicity, speciation, transformations, and remediation. *Environ. Inter*., **35**: 743–759.

Shen, C., Meng, Q., Schmelzer, E., Bader, A., (2009). Gel entrapment culture of rat hepatocytes for investigation of tetracycline–induced toxicity. *Toxicol. App. Pharmacol*., **238**: 178–187.

Sheng, G., Xu, S., Boyd, S.A., (1996). Cosorption of organic contaminants from water by contaminants from water by exchanged clays. *Water Res*., **30**: 1483–1489.

Silva, C.P., Otero, M., Esteves, V., (2012). Processes for the elimination of estrogenic steroid hormones from water: A review. *Environ. Poll*., **165**: 38–58.

Singh, B.K., Nayak, P.S. (2004): Sorption equilibrium studies of toxic nitro–substituted phenols on fly ash. – *Adsorp. Sci. Technol*., **22**: 295–309.

Singh, T.S., Pant, K.K., (2004). Equilibrium, kinetics and thermodynamic studies for adsorption of As(III) on activated alumina. *Sep. Purif. Technol*., **36**: 139–147.

Skoog, D.A., Crouch, S.R., Holler, F.J., (2007). *Principles of Instrumental Analysis*. 6th ed. Belmont, CA: Thomson Brooks/Cole, p.169–173.

Slimani, M.S., Ahlafi, H., Moussout, H., Boukhlifi, F., Zegaoui, O., (2014). Adsorption of hexavalent chromium and phenol onto bentonite modified with hexadecyltrimethylammonium bromide (HDTMABr). *J. Adv. Chem*., **8**: 1602–1611.

Smith, A.H. Hopenhayn, C. Bates, M.N. Goeden, H.M. Picciotto, I.H. Duggan, H.M., Wood R., Kosnett M.J., *Smith* M.T., (1992). Cancer risks from arsenic in drinking water. *Environ. Health Perspect*., **97**: 259–267.

Smith, C.R., (1934). Base exchange reactions of bentonite and salts of organic bases. *J. Am. Chem. Soc*., **56**: 1561–1563.

Snyder, S.A., Westerhoff, P., Yoon, Y., Sedlak, D.L., (2003). Pharmaceuticals, personal care products, and endocrine disruptors in water: implications for the water industry. *Environ. Eng. Sci.*, **20**: 449–469.

Socías–Viciana, M.M., Hermosin, M.C., Cornejo, J., (1998). Removing prometrone from water by clays and organic clays. *Chemosphere*, **37**: 289–300.

Sohoni, P., Tyler, C.R., Hurd, K., Caunter, J., Hetheridge, M., Williams, T., Woods, C., Evans, M., Toy, R., Gargas, M., Sumpter, J.P., (2001). Reproductive effects of long term exposure to bisphenol A in the fathead minnow (Pimephales promelas). *Environ. Sci. Technol*., **35**: 2917–2925.

Srinivasan, K.R., Fogler, S.H., (1990). Use of inorgano–organo clays in the removal of priority pollutants from industrial wastewaters: adsorption of benzo(α)–pyrene and chlorophenols from aqueous solutions. *Clays Clay Miner.*, **38**: 287–293.

Srivastava, S.K., Tyagi, R., Pant, N., Pal, N., (1989). Studies on the removal of some toxic metal ions. Part II. Removal of lead and cadmium by montmorillonite and kaolinite. *Environ. Technol. (Lett.)*, **10**: 275–282.

Su, J., Huang, H.G., Jin, X.Y., Lu, X.Q., Chen, Z.L., (2011). Synthesis, characterization and kinetic of a surfactant–modified bentonite used to remove As(III) and As(V) from aqueous solution. *J. Hazard. Mater.*, **185**: 63–70.

Sun, H.–J., Rathinasabapathi, B., Wu, B., Luo, J., Pu, L.–P., Ma, L.Q., (2014). Arsenic and selenium toxicity and their interactive effects in humans –Review. *Environ. Inter*., **69**: 148–158.

Tabak, A., Yilmaz, N., Eren, E., Caglar, B., Afsin, B., Sarihan, A., (2011). Structural analysis of naproxen–intercalated bentonite (Unye). *Chem. Eng. J.*, **174**: 281–288.

Tang, X., Naveedullah, Hashmi, M.Z., Zhang, H., Qian, M., Yu, C., Shen, C., Qin, Z., Huang, R., Qiao, J., Chen, Y., (2013). A preliminary study on the occurrence and dissipation of estrogen in livestock wastewater. *Bull. Environ. Contam. Toxicol*., **90**: 391–396.

Teng, W.T., Khor, E., Tan, T.K., Lim, L.Y., Tan, S.C., (2001). Concurrent production of chitin from shrimp shells and Fungi. *Carbo. Res*., **332**: 305–316.

Thomas, H.C., (1944). Heterogeneous ion exchange in a flowing system, *J. Am. Chem. Soc*., **66**: 1664–1666.

Thomas, F., Schouller, E., Bottero, J.Y., (1995). Adsorption of salicylate and polyacrylate on mesoporous aluminas. *Colloids Surf. A: Physicochem. Eng. Aspects*, **95**: 271–279**.**

Tiwari, D., Kim, W., Kim, M., Prasad, S.K., Lee, S.M., (2015). Organo–modified sericite in the remediation of phenol–contaminated waters. *Desal. Water Treat*., **53**: 446–451.

Tiwari, D., Laldawngliana, C., Lee, S.M., (2014). Immobilized small sized manganese dioxide sand in the remediation of arsenic contaminated water. *Environ. Eng. Res*., **19**: 107–113.

Tiwari, D., Lee, S.M., (2011). Biomass derived materials in the remediation of heavy–metal contaminated water: removal of Cd(II) and Cu(II) from aqueous solutions. *Water Environ. Res*., **83**: 874–881.

Tiwari, D., Lee, S.M., (2012). Novel hybrid materials in the remediation of ground waters contaminated with As(III) and As(V). *Chem. Eng. J.*, **204–206**: 23–31.

Tiwari, D., Kim, H.U., Lee, S.M., (2007). Removal behavior of sericite for Cu(II) and Pb(II) from aqueous solutions: Batch and column studies. *Sep. Purif. Technol*., **57**: 11–16.

Tyrovola, K., Nikolaidis, N.P., Veranis, N., Kallithrakas–Kontos, N., Koulouridakis, P.E., (2006). Arsenic removal from geothermal waters with zero–valent iron – effect of temperature, phosphate and nitrate. *Water Res*., **40**: 2375–2386.

Undabeytia, T., Nir, S., Sanchez–Verdejo, T., Villaverde, J., Maqueda, C., Morillo, E., (2008). A clay–vesicle system for water purification from organic pollutants. *Water Res.*, **42**: 1211–1219.

Unuabonah, E.I., Taubert, A., (2014). Clay–polymer nanocomposites (CPNs): Adsorbents of the future for water treatment–Review. *Appl. Clay Sci*., **99:** 83–92.

USEPA, (1997). U.S. Environmental Protection Agency, Special report on environmental endocrine disruption: an effects assessment and analysis. EPA/630/R–96/012.

USEPA, (2000a). U.S. Environmental Protection Agency, Technologies and Costs for Removal of Arsenic from Drinking water, EPA report 815–R–00–028, International Consultants, Author: Malcolm Pirnie, INC, 4134 Linden Avenue, Dayton, Ohio, 45432.

USEPA, (2000b). U.S. Environmental Protection Agency, Regulations on the Disposal of Arsenic Residuals from Drinking Water Treatment Plants. Office of Research and Development, U.S. EPA, EPA/600/R–00/025.

USEPA, (2003). U.S. Environmental Protection Agency, Arsenic Treatment Technology Evaluation Handbook for Small Systems. U.S. EPA 816–R–03–014.

USEPA, (2010). U.S. Environmental Protection Agency, Bisphenol A Action Plan, CASRN 80–05–7, Washington D.C., USA.

USFDA, (2011). United States Food and Drug Administration. http://www.accessdata.fda.gov/drugsatfda_docs/label/2011/021234s005lbl.pdf.

USFDA, (2012). U.S. Food and Drug Administration (USFDA) and National Center for Toxicological Research (NCTR), Endocrine Disruptor Knowledge Base (EDKB). http://www.fda.gov/scienceresearch/bioinformaticstools/endocrinedisruptorknowledgebase/default.htm.

Vaishya, R.C., Gupta, S.K., (2004). Modelling arsenic(III) adsorption from water by sulfate modified iron–oxide coated sand (SMIOCS). *Sep. Sci. Technol.*, **39**: 645–666.

Vallee, B.L., Ulmer, D.D., Wacker, W.E., (1960). Arsenic toxicology and biochemistry. *A.M.A. Arch. Ind. Health*, **21**: 132–151.

Vidal, N.C., Volzone, C., (2009). Analysis of tetramethylammonium–montmorillonite and retention of toluene from aqueous solution. *Appl. Clay Sci.*, **45**: 227–231.

Vogna, D., Marotta, R., Napolitano, A., Andreozzi, R., d'Ischia, M., (2004). Advanced oxidation of the pharmaceutical drug diclofenac with UV/H_2O_2 and ozone. *Water Res.*, **38**: 414–422.

Vosges, M., Braguer, J.–C., Combarnous Y., (2008). Long–term exposure of male rats to low–dose ethinylestradiol (EE2) in drinking water: Effects on ponderal growth and on litter size of progeny. *Reprod. Toxicol.*, **25**: 161–168.

Walsh, A., (1955). The application of atomic absorption spectra to chemical analysis. *Spectrochim. Acta*, **7**: 108 – 117.

Wang, K.H., Choi, M.H., Koo, C.M., Choi, C.M. Chung, I.J., (2001). Synthesis and characterization of maleated polyethylene/clay nano–composites. *Polymer*, **42**: 9819–9826.

Wang, S., Peng, Y., (2010). Natural zeolites as effective adsorbents in water and wastewater treatment. *Chem. Eng. J.*, **156**: 11–24.

Wang, Y., Liu, H., Liu, G., Xie, Y., (2014). Oxidation of diclofenac by aqueous chlorine dioxide: Identification of major disinfection byproducts and toxicity evaluation. *Sci. Total Environ.*, **473–474**: 437–445.

Wang, Y.H., Zhang, J.C., Song, L.F., Hu, J.Y., Ong, S.L., Ng, W.J., (2005). Adsorption removal of phenol in water and simultaneous regeneration by catalytic oxidation. *Environ. Eng. Sci.*, **22**: 608–614.

Westerhoff, P., Yoon, Y., Snyder, S., Wert, E., (2005). Fate of endocrine–disrupter, pharmaceuticals and personal care product chemicals during simulated drinking water treatment process. *Environ. Sci. Technol.*, **39**: 6649–6663.

Xi, Y., Mallavarapu, M., Naidu, R., (2009). Preparation, chracterization of surfactants modified clay minerals and nitrate adsorption. *Appl. Clay Sci*., **48**: 92–96.

Xie, W.H., Shiu, W.Y., Mackay, D., (1997). A review of the effect of salts on the solubility of organic compounds in seawater. *Mar. Environ. Res*., **44**: 429–444.

Xu, J.J., Henstock, P.V., Dunn, M.C., Smith, A.R., Chabot, J.R., de Graaf, D., (2008). Cellular imaging predictions of clinical drug–induced liver injury. *Toxicol. Sci*., **105**: 97–105.

Xu, Y., Nakajima, T., Ohki, A., (2002). Adsorption and removal of arsenic(V) from drinking water by aluminium–loaded zeolite Shirasu. *J. Hazard. Mater.*, **92**: 275–287.

Yan, L., Shan, X., Wen, B., Zhang, S., (2007a). Effect of lead on the sorption of phenol onto montmorillonites and organo–montmorillonites. *J. Colloid Interf. Sci*., **308**: 11–19.

Yan, L.G., Wang, J., Yu, H.Q., Wei, Q., Du, B., Shan, X.Q., (2007b). Adsorption of benzoic acid by CTAB exchanged montmorillonite. *Appl. Clay Sci*., **37**: 226–230.

Yan, Z., Lu, G., Liu, J., Jin, S., (2012). An integrated assessment of estrogenic contamination and feminization risk in fish in Taihu Lake, China. *Ecotoxicol. Environ. Saf*., **84**: 334–340.

Yang, W., Tang, Z., Zhou, F., Zhang, W., Song, L., (2013). Toxicity studies of tetracycline on *Microcystis aeruginosa* and *Selenastrum capricornutum. Environ. Toxicol. Pharmacol.*, **35**: 320–324.

Yildiz, N., Gonulsen, R., Koyuncu, H., Calimli, A., (2005). Adsorption of benzoic acid and hydroquinone by organically modified bentonites. *Colloids Surf. A: Physicochem. Eng. Aspects*, **260**: 87–94.

Ying, G.G., Kookana, R., Waite, T., (2004). Endocrine Disrupting Chemicals (EDCs) and Pharmaceuticals and Personal Care Products (PPCPs) in Reclaimed Water in Australia. Australian Water Conservation and Reuse Research Program, Australian Water Association, CSIRO Land & Water, Adelaide and Sydney, Australia.

Yoon, Y., Westerhoff, P., Snyder, S.A., Esparza, M., (2003). HPLC–fluorescence detection and adsorption of bisphenol A, 17β–estradiol, and 17α–ethynyl estradiol on powdered activated carbon. *Water Res*., **37**: 3530–3537.

Zanetti, M., Lomakin, S., Camino, G., (2000). Polymer layered silicate nano–composites. *Macro. Mater. Eng*., **279**: 1–9.

Zangwill, A., (1988). *Physics at Surfaces*. Cambridge Univ. Press, New York, Chapter 14.

Zhang, Y., Geißen, S.U., Gal, C., (2008). Carbamazepine and diclofenac: removal in wastewater treatment plants and occurrence in water bodies. *Chemosphere*, **73**: 1151–1161.

Zhang, L., Song, X., Liu, X., Yang, L., Pan, F., Lv, J., (2011). Studies on the removal of tetracycline by multi–walled carbon nanotubes. *Chem. Eng. J*., **178**: 26–33.

Zhao, H., Jaynes, W.F., Vance, G.F., (1996). Sorption of the ionizable organic compound, DICAMBA (3,6–dichloro–2–methoxy benzoic acid), by organo–clays. *Chemosphere*, **33**: 2089–2100.

Zhao, Y., Gu, X., Gao, S., Geng, J., Wang, X., (2012). Adsorption of tetracycline (TC) onto montmorillonite: Cations and humic acid effects. *Geoderma*, **183–184**: 12–18.

Zheng, S., Sun, Z., Park, Y., Ayoko, G.A., Frost, R.L., (2013). Removal of bisphenol A from wastewater by Ca–montmorillonite modified with selected surfactants. *Chem. Eng. J.*, **234**: 416–422.

Zheng, Y.M., Zou, S.W., Nanayakkara, K.G.N., Matsuura, T., Chen, J.P., (2011). Adsorptive removal of arsenic from aqueous solution by a PVDF/zirconia blend flat sheet membrane. *J. Membrane Sci.* **374**: 1–11.

Zhou, Y., Lu, P., Lu, J., (2012). Application of natural biosorbent and modified peat for bisphenol A removal from aqueous solutions. *Carb. Polym.*, **88**: 502–508.

Zhu, H., Jia, Y., Wua, X., Wang, H., (2009a). Removal of arsenic from water by supported nano zero–valent iron on activated carbon. *J. Hazard. Mater.*, **172**: 1591–1596.

Zhu, L., Chen, B., Shen, X., (2000). Sorption of phenol, p–nitrophenol, and aniline to dual cation organobentonites from water. *Environ. Sci. Technol.*, **34**: 468–475.

Zhu, L., Zhu, R., (2007). Simultaneous sorption of organic compounds and phosphate to inorganic–organic bentonites from water. *Sep. Purif. Technol.*, **54**: 71–76.

Zhu, R., Zhu, L., Zhu, J., Ge, F., Wang, T., (2009b). Sorption of naphthalene and phosphate to the CTMAB–Al_{13} intercalated bentonites. *J. Hazard. Mater.*, **168**: 1590–1594.

LIST OF PUBLICATIONS

APPENDIX

PUBLISHED JOURNAL PAPERS

LIST OF PUBLICATIONS

A. Journals

1. **Thanhmingliana**, Seung–Mok Lee, Diwakar Tiwari. Use of hybrid materials in the decontamination of bisphenol A from aqueous solutions. *RSC Advances*, 2014, 4, p 43921–43930. [IF: 3.840]

2. **Thanhmingliana**, Diwakar Tiwari, Seung–Mok Lee. Hybrid materials in the remediation of arsenic contaminated waters: a physico–chemical study. *Desalination and Water Treatment,* Available online (5 Nov. 2014).
   DOI: 10.1080/19443994.2014.979241. [IF: 1.173]

3. **Thanhmingliana**, Diwakar Tiwari. Efficient use of hybrid materials in the remediation of aquatic environment contaminated with micro–pollutant diclofenac sodium. *Chemical Engineering Journal*, 263 (2015) 364–373. [IF: 4.321]

4. Seung–Mok Lee, Lalhmunsiama, **Thanhmingliana**, Diwakar Tiwari. Porous hybrid materials in the remediation of water contaminated with As(III) and As(V). *Chemical Engineering Journal*, 270 (2015) 496-507. [IF: 4.321]

5. **Thanhmingliana**, Seung Mok Lee, Diwakar Tiwari, Shailesh K. Prasad. Efficient attenuation of 17α-ethynylestradiol (EE2) and tetracycline using novel hybrid materials: batch and column reactor studies. *RSC Advances*, 2015, 5, 46834–46842. [IF: 3.840]

B. Conference / Seminar

1. **Thanhmingliana**, Diwakar Tiwari, Seung–Mok Lee. Novel organo–modified–sericite in the treatment of arsenic contaminated water: Batch and column reactor studies. Second International Conference on 'Advanced Oxidation Processes' (AOP–2012), from 5th – 8th October 2012, M.G University, Kottayam, Kerala, India.

2. **Thanhmingliana**, Seung–Mok Lee, Diwakar Tiwari. Organo–modified–sericite in the treatment of bisphenol–A from aqueous solutions: Batch and column reactor studies. International Conference on 'Harnessing Natural Resources for Sustainable Development', from 29th – 31st January 2014, Cotton College, Guwahati, Assam, India.

3. C. Lalhriatpuia, **Thanhmingliana**, Diwakar Tiwari. Hybrid materials in the remediation of wastewaters contaminated with diclofenac sodium: Batch and column reactor operations. National Seminar on 'Management of Natural Resources for Sustainable Development: Challenges and Opportunities', from 6th – 7th March 2014. Organized by Department of Geography and Resource Management, School of Earth Sciences, Mizoram University, Aizawl, Mizoram, India.

4. **Thanhmingliana**, Diwakar Tiwari. Efficient use of hybrid materials in the decontamination of diclofenac sodium from aqueous solutions. Orientation Workshop on 'Radiation–Its Applications in Chemical, Physical and Life Sciences' from 29th – 31st October 2014, at Mizoram University, Aizawl, Mizoram, Organized by: UGC–DAE Consortium for Scientific Research, Kolkata Centre & Chemistry Department, Mizoram University, Aizawl, Mizoram, India.

5. **Thanhmingliana**, Diwakar Tiwari. Hybrid clay materials in the decontamination of bisphenol–A from aqueous solutions: Batch and column reactor studies. North East Regional Seminar on 'Trends in Colloid and Interface Science' (NERSTCIS – 2014), from 27th –28th November 2014. Organized by Centre for Advanced Studies in Chemistry, Department of Chemistry, North–Eastern Hill University, Shillong, Meghalaya, India; under the auspices of North Eastern Chapter of Indian Society for Surface Science and Technology.

6. **Thanhmingliana**, Diwakar Tiwari, Seung Mok Lee. Attenuation of tetracycline from aqueous solutions using hybrid materials precursor to clay: batch and column reactor studies. The 10th Asia Pacific Conference on Sustainable Energy & Environmental Technologies (APCSEET 2015), University of Seoul, Seoul, South Korea. Organized by R & D Center of Core Technologies for Water Treatment, Department of Energy and Environmental System Engineering, University of Seoul, Seoul, South Korea.

Publishing
Journals, books and databases

ROYAL SOCIETY OF CHEMISTRY

RSC Advances

2014, 4, Issue 83, Page 43815 to 44321

An international journal to further the chemical sciences

Impact Factor 3.840 Indexed in Web of Science

ISSN (Online): 2046-2069

About the journal

RSC Advances is an international, peer-reviewed journal covering all of the chemical sciences, including multidisciplinary and emerging areas. The criteria for publication are that the work must be high quality, well conducted and add to the development of the field. Articles submitted to the journal are evaluated by international referees for the overall quality and accuracy of the science presented.

RSC Advances publishes communications, papers and reviews. For more details on the scope of the journal read about our advanced topic modelling technology which assigns articles into 12 main topics and over 100 further sub-categories.

Subject categories

Advanced topic modelling technology with 12 main topics and over 100 sub-categories.

Editor

RSC Advances is supported by international Editorial and Advisory Boards, led by **Professor Mike Ward** (University of Sheffield, UK), which input into the development and strategy of the journal.

Contact the Journal

RSC Advances
Royal Society of Chemistry, Thomas Graham House, Science Park, Milton Road, Cambridge CB4 0W
Tel: +44 (0) 1223 420066
Fax: +44 (0) 1223 420247
Email: RSC Advances

RSC Advances

PAPER

Cite this: *RSC Adv.*, 2014, **4**, 43921

Use of hybrid materials in the decontamination of bisphenol A from aqueous solutions

Thanhmingliana,[a] Seung Mok Lee[b] and Diwakar Tiwari*[a]

Hybrid materials were obtained by modifying natural sericite. The sericite was modified with hexadecyltrimethylammonium bromide (HS) and alkyldimethylbenzylammonium chloride (AS) to obtain organo-modified sericites, together with aluminum-H-sericite (AHS) and aluminum-A-sericite (AAS) as inorgano–organo-modified sericite hybrid materials. The hybrid materials were characterized by FT-IR spectrometry, XRD and SEM. The pH_{PZC} values of the solid hybrid materials were obtained by acid–base titration. The Brunauer–Emmett–Teller surface area and pore size of the hybrid materials were also determined. The resulting materials were used in the remediation of waste waters contaminated with bisphenol A (BPA) using batch and column reactor operations. The batch experiments showed that an increase in pH from 2.0 to 10.0 did not affect the percentage uptake of BPA by these hybrid materials, but at pH > 10.0 the percentage uptake of BPA decreased significantly for the AHS and AAS hybrid materials. An increase in the concentration of BPA (1.0–20 mg L^{-1}) and the background electrolyte concentration (0.0001–0.1 mol L^{-1} NaCl) did not affect the percentage removal of BPA by these hybrid materials. The time dependence adsorption data showed that BPA was quickly taken up onto these hybrid materials as most of the BPA was trapped within the first few minutes of contact. The kinetic data fitted well to a pseudo-second-order and fractal-like pseudo-second-order model rather a pseudo-first-order model. The results of pseudo-second-order fitting showed that the removal capacities of the AS, HS, AAS and AHS hybrid materials for BPA were 4.816, 5.047, 4.874 and 4.856 mg g^{-1}, respectively. In addition, AAS and AHS were used for dynamic studies in column experiments. The breakthrough curves were then used for the non-linear fitting of the Thomas equation. The loading capacity of the column for BPA using the AHS and AAS hybrid materials was estimated.

Received 8th July 2014
Accepted 2nd September 2014

DOI: 10.1039/c4ra06793b

www.rsc.org/advances

1. Introduction

Endocrine-disrupting chemicals can disturb the human nervous and endocrine systems and weaken the immune and reproductive systems by mimicking biological activity and reproductive hormones.[1,2] Bisphenol A (BPA) is an important micro-pollutant and a potential endocrine disrupter. BPA mimics the female estrogen 17-β-estradiol. BPA can alter the normal hormonal system of animals and has various biochemical effects, *e.g.* morphological alterations and interference in sex differentiation; it can also reduce fertility.[3,4] BPA has been shown to cause the proliferation of MCF-7 human breast cancer cells[5] and exert a mutagenic action on human RSa cells.[6] Several other *in vitro* and *in vivo* assays have confirmed that BPA may increase infertility, genital tract abnormalities and even breast cancer.[7,8]

BPA is widely used as a monomer in the synthesis of polycarbonate plastics and the epoxy resins used as dental sealants and liners in food packaging, flame retardants and other speciality products.[9–11] These products contain minute amounts of unreacted BPA, which may leach from the materials and enter the aquatic environment and biosphere.[12,13] The maximum concentration of BPA detected in leachates from landfill sites is 17.2 mg L^{-1}.[14] Significant levels of BPA have been reported in urine samples.[11,15–17] The European Commission Scientific Committee on Food recommended a tolerable daily intake of 0.05 mg kg^{-1} body weight per day for BPA in the context of food stored in contact with plastics.[18] Similarly, the United States Environmental Protection Agency recommended a safety level of a maximum acceptable or reference dose of 0.05 mg kg^{-1} body weight/day.[19,20]

Various methods, including physical,[21] chemical[22] and biological[23] techniques, have been used to treat waters contaminated with BPA. An effective way to remove BPA from waste water is *via* adsorption onto various adsorptive materials. However, the moderately hydrophobic nature of BPA (octanol–water partition coefficient $K_{ow} = 10^{3.4}$), which has a low polarity due to the presence of only two hydroxyl groups,[24] has restricted

---

[a] *Department of Chemistry, School of Physical Sciences, Mizoram University, Aizawl-796004, India. E-mail: diw_tiwari@yahoo.com; Fax: +91-389-2330834; Tel: +91-389-2301806*

[b] *Department of Environmental Engineering, Catholic Kwandong University, 522 Naegok-dong, Gangneung, 210-701, Korea*

the use of several adsorbent materials in the treatment of waters contaminated with BPA. Carbonaceous materials have been found to be effective for the removal of BPA.[25] However, the uptake of BPA is reduced with an increase in temperature or ionic strength. Various minerals, activated carbon precursors and even coconut-based biomass have been studied and the results of these experiments suggest that activated carbon has a significantly higher capacity than minerals to remove BPA from aqueous solutions.[26] Waters from various sources contaminated with endocrine-disrupting chemicals were treated with single- and multi-walled carbon nanotubes in addition to powdered activated carbon.[27] A mesoporous carbon sample with a high specific surface area (920 m^2 g^{-1}) was obtained with hexagonal SBA-15 mesoporous silica and was used in the rapid and efficient removal of BPA. The sorption followed a pseudo-second-order kinetic model and was unaffected in the pH range 3–9.[28]

The green algae *Monoraphidium braunii* has been studied for the remediation of BPA in the presence and absence of natural organic matter (NOM) and the results showed that NOM did not affect the active uptake of BPA by this algae.[3] However, when single-walled carbon nanotube ultra-filtration membranes were assessed for the attenuation of BSA and 17-β-estradiol in the presence of NOM, it was shown that NOM fouls the membrane by blocking the pores and forming a cake or gel, which ultimately decreases the transport of the endocrine-disrupting chemicals.[29] Multi-walled carbon nanotubes showed a very high uptake capacity for BPA in aqueous wastes and hydrogen bonding and hydrophobic action are the leading mechanisms involved in the attenuation of BPA by this solid.[30] Natural dead biomass (*e.g.* peat, rice husks, bagasse and sawdust) and hexadecyltrimethylammonium bromide (HDTMA)-modified peat have been used to remove BPA from aqueous solutions by passive adsorption. The results indicate that modified peat is an effective adsorbent material in the removal of BPA and a hydrophobic interaction between the solid/solution interface was proposed.[31,32]

BPA immobilized on granular activated carbon was exposed to a dielectric barrier discharge plasma to decompose the BPA in an integrated treatment process.[33] A molecular level simulation was performed using the molecular mechanics Poisson–Boltzmann surface area approach for the removal of BPA and 17-α-ethinyl estradiol by adsorption onto graphene, single-walled carbon nanotubes and multi-walled carbon nanotubes. The simulation results were consistent with the experimental findings and an increase in ionic strength did not significantly affect the immobilization of BPA and 17-α-ethinyl estradiol.[34]

Clay minerals (phyllosilicates) are composed, with a few exceptions, of crystal structures consisting of sheets packed firmly in structural layers. The individual structural layers consist of two, three or four sheets. The sheets are formed from tetrahedral $[SiO_4]^{4-}$ (T) and octahedral $[AlO_3(OH)_3]^{6-}$ (O). The interiors of the tetrahedrons and octahedrons contain smaller metal cations and their apices are occupied by oxygen atoms, some of which are connected to protons to form –OH. These fundamental structural elements are arranged to form a hexagonal network within each sheet. Depending on the number and ratio of the sheets in the fundamental structural unit, the substitution of cations within the octahedrons and tetrahedrons determines the charge in these layers. Silicate layers have a tendency to organize themselves to form stacks with a regular van der Waals gap between them: an 'interlayer'. The electrostatic negativity of the structural layer is naturally compensated by cations within this interlayer space. The most common exchangeable cations are K^+, Na^+, Ca^{2+}, Mg^{2+} and H^+. A simple treatment of the clay minerals allows any of these cations to be exchanged with another cation. The removal of ions from the octahedral or tetrahedral sheets is energetically more demanding and produces a material with a new microstructure and larger pore volumes.[35–37] The electrical charge, the micro- to meso-level porosity, the available surface functional groups and the presence of exchangeable cations within the interlayer space make clay minerals useful natural adsorbents that can be used for the removal/attenuation of several toxic heavy metal ions from aqueous solutions. However, these materials have a low selectivity towards, and low removal capacity for, several non-polar or less polar organic contaminants. Clay minerals can, however, be modified with an appropriate organic surfactant molecule or even a pillared inorgano–organo-clay to make them effective materials for the attenuation of organic impurities.[38–40] This modification makes the clay structure more organophilic and enhances the hydrophobicity.[35,41,42] Dodecyltrimethylammonium bromide and HDTMA surfactants have been used in a sequential treatment to modify montmorillonite or Ca-montmorillonite for use in the removal of BPA from aqueous solutions. The hydrophobicity introduced by loading the surfactant molecules contributes a partitioning phase, which strongly interacts with the BPA molecule through hydrophobic interactions.[43,44] Polyethersulfone was introduced to HDTMA-modified montmorillonite by a liquid–liquid phase separation technique. The resultant hybrid material was then used as a molecular sieve to remove BPA from aqueous solutions. Moreover, the BPA-loaded polyethersulfone–HDTMA-modified montmorillonite could be regenerated by washing with ethanol.[45]

Sericite is a natural clay mineral found widely in Korea, China and Japan. The crystal structure of sericite has a very compact layer structure and is generally known as 'white powders of muscovite'. The chemical formula of muscovite is $KSi_3Al_3O_{10}(OH)_2$ and it has a layer charge density close to ≤ 2 e^- per unit cell. The unit cell is composed of 2 : 1 T : O phyllosilcate layers.[35,37,46] The high unit charge of sericite results in a strong electrostatic attractive force that holds the aluminosilicate layers and the cations in the interlayer space tightly together. Muscovite therefore does not swell in water and the cation-exchange capacity (CEC) is low compared with other common clays. However, muscovite has very varied properties, such as a molecularly smooth surface and resistivity to acids, and is used in fireproofing and electrical insulation.[46] The interlayer spacing of the (002) plane is 10 Å. Sericite has been used for the removal of Cu(II), Pb(II), Ni(II) and Cs(I) from aqueous solution.[47–49] Sericite can also be modified with HDTMA and alkyldimethylbenzylammonium chloride (AMBA) to obtain organo-modified sericite; this has been used in the removal of arsenic and phenol from aqueous solution.[50,51]

Similarly, aluminum-pillared sericite subsequently modified with HDTMA or AMBA has been synthesized and used in the attenuation of As(III) and As(V) from aqueous solution.[52] The work reported here extends the use of organo- or inorgano–organo-modified sericite hybrid materials in the remediation of waters contaminated with BPA using batch and column reactor procedures.

2. Materials and methods

2.1 Materials

Sericite was obtained from the Keumnam deposit, Gagokmyun, Samcheok City, Kangwon Province, Korea. The sample was crushed in a mortar and sieved to obtain 200–300 British Standard Sieve particles. The powdered sericite was washed with purified water and dried at 90 °C in a drying oven. The CEC of sericite was determined using the standard United States Environmental Protection Agency method 9080 (http://www.epa.gov/osw/hazard/testmethods/sw846/pdfs/9080.pdf) and was 8.85 mEquiv./100 g of sericite. Sericite contained various metal oxides, as reported previously.[47] HDTMA [$CH_3(CH_2)_{15}N(CH_3)_3Br$)] was obtained from Sigma-Aldrich (St Loius, MO, USA) and AMBA (total assay $C_{22}H_{40}NCl$) 50% solution and aluminum(III) chloride were obtained from Junsei Chemical Co. Ltd (Japan). BPA ($C_{15}H_{16}O_2$) was obtained from Sigma-Aldrich and was used without further purification (Scheme 1). Sodium chloride (Extrapure) was obtained from HiMedia, India. The other chemicals used were of analytical-reagent or equivalent grade. The deionized water was further purified (18 MΩ cm) using a Millipore water purification system (Milli-Q+).

2.2 Methodology

2.2.1 Preparation of HDTMA sericite or AMBA sericite. HDTMA- or AMBA-modified sericite was obtained by the wet cation-exchange method reported previously.[50] In brief, 20 g of sericite was taken into 1 L of HDTMA or AMBA solution to give a CEC of 1 for sericite. The mixture was refluxed for 48 h at 60 °C with constant stirring. The slurries were filtered and the solid washed with purified water. Any excess or free surfactant was cleaned by Soxhlet extraction. The organo-modified sericite samples were then dried at 90 °C and stored in an airtight polyethylene bottle until further use. The HDTMA sericite and AMBA sericite are referred to as the HS and AS samples, respectively.

2.2.2 Preparation of inorgano–organo-sericite. Aluminum-pillared and HDTMA- or AMBA-modified sericites were obtained by the wet cation-exchange method reported previously.[52] In brief, the pillaring aluminum solution was prepared by mixing 100 mL of 0.4 mol L^{-1} NaOH solution with 100 mL of 0.2 mol L^{-1} $AlCl_3$ solution with vigorous and constant stirring. The mixture was stored for 7 days at room temperature to age. A known amount of HDTMA or AMBA solution was then added to this solution with continuous stirring; the HDTMA or AMBA was taken as equivalent to a 1 : 1 CEC of sericite. Sericite powder (4 g) was taken separately into 300 mL of water. The HDTMA or AMBA mixed aluminum solution was added to this dispersed mixture with vigorous stirring. The mixture was stirred for about 5 h at room temperature and then stored at room temperature for another 2 days. The dispersion was separated carefully and the solid was washed with purified water. The obtained solids [Al-HDTMA-sericite (AHS) and Al-AMBA-sericite (AAS)] were dried at 50 °C and gently ground in a mortar.

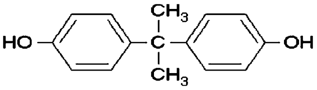

Scheme 1 Chemical structure of bisphenol A.

2.2.3 Characterization and surface morphology of hybrid materials. The surface morphologies of these hybrid materials and sericite were obtained by scanning electron microscopy using a Model FE-SEM SU-70 scanning electron microscope (Hitachi, Japan). X-ray diffraction (XRD) data were collected by a Model X'Pert PRO MPD X-ray diffractometer (PANalytical, the Netherlands). The diffraction data were recorded at a scan rate of 0.034 of 2θ illumination at an applied voltage of 45 kV with a measured current of 35 mA. The Cu K_α radiation used had a wavelength of 1.5418 Å. The solid materials were characterized by FT-IR spectrometry using the KBr disk method (Tensor 27, Bruker, USA).

2.2.4 pH_{PZC} measurements. The pH_{PZC} (point of zero charge) of the materials was obtained by the previously reported method.[53,54] The pH_{PZC} value is taken as the point at which the curve crossed the line at which $pH_{final} = pH_{initial}$. The Brunauer–Emmett–Teller (BET) surface area was obtained using the N_2 adsorption method with a BET surface area analyzer (Model-1201, Macsorb HM, Japan).

2.2.5 Batch reactor experiments. A stock solution of 100 mg L^{-1} BPA was prepared by dissolving an appropriate amount of BPA in purified water. The solubility is greatly enhanced by sonicating the solution for 5 min. The required BPA concentrations were then obtained by the successive dilution of stock solutions. A 50 mL aliquot of 10.0 mg L^{-1} of BPA solution was taken into polyethylene bottles and the pH was adjusted by adding concentrated HCl/NaOH solution dropwise. The pH was measured using an Orion 2 Star pH Benchtop pH meter (Thermoscientific, USA). AS, HS, AHS, or AAS solid (0.1 g) was then added into these bottles. The bottles were kept in an automatic incubator shaker (TM Weiber, ACMAS Technologies Pvt Ltd, India) for 24 h at 25 ± 1 °C. The samples were then removed from the shaker and filtered with a 0.45 μm syringe filter; the pH was then checked again and recorded. The filtrates are subjected to measure the absorbance of solutions using a UV-visible spectrophotometer (Model UV1, Thermo Electron Corporation, USA) at 276 nm. A calibration graph was obtained using standard BPA solutions with concentrations of 1.0, 5.0, 10.0, 20.0 and 25.0 mg L^{-1}.

The effect of the BPA concentration on adsorption was studied by varying the BPA concentration from 1.0 to 20.0 mg L^{-1} at a constant pH of about 6.5 and a constant temperature of 25 ± 1 °C. The sorption process was carried out as reported previously. The results are reported in terms of the initial BPA concentration (mg L^{-1}) against the percentage of BPA removed.

The dependence of the adsorption of BPA on the background electrolyte concentration was determined by varying the background electrolyte concentration from 0.0001 to 0.1 mol L^{-1} NaCl in the sorptive solution. The solution pH (about 6.5) and temperature (25 ± 1 °C) were kept constant throughout. The results are presented as the percentage of BPA removed against the background electrolyte concentration.

The time dependence of the adsorption of BPA by these hybrid materials was also determined. The initial BPA concentration was held at 10.0 mg L^{-1} with the hybrid materials at a constant dose of 2.0 g L^{-1} at a pH of about 6.5 and a temperature of 25 ± 1 °C. The results are reported as the amount of BPA removed (mg g^{-1}) as a function of time (min). The time dependent adsorption data were also used to fit various known kinetic models, *e.g.* the pseudo-first-order (PFO), pseudo-second-order (PSO) and fractal-like pseudo-second-order (FL-PSO) models.

2.2.6 Column experiments. A glass column (1 cm inner diameter) packed with 0.5 g of hybrid materials (in the middle of the column) was used for the column experiments. About 1.5 g of 14–16 British Standard Sieve size clean sand particles were placed above and below the hybrid materials and the column was packed with glass beads. A BPA 10.0 mg L^{-1} solution with a constant pH of 6.5 was pumped up from the bottom of the column using a peristaltic pump (KrosFlo Research I Peristaltic Pump, Spectrum Laboratories Inc., CA, USA) at a constant flow-rate of 1.0 mL min^{-1}. The effluent samples were collected using a fraction collector (Spectra/Chrom CF-2 Fraction Collector, Spectrum Laboratories). The liquid samples collected were filtered using a 0.45 μm syringe filter and the total bulk sorptive concentration was measured using UV-vis spectrophotometry.

The breakthrough data were used to optimize the loading capacity of the solids under dynamic conditions using the Thomas equation (eqn (1)):[55]

$$\frac{C_e}{C_o} = \frac{1}{1 + e^{(K_T(q_o m - C_o V))/Q}} \tag{1}$$

where C_e and C_o are the concentrations (mg L^{-1}) of the effluent and influent BPA solutions, respectively, K_T is the Thomas rate constant (L min^{-1} mg^{-1}), q_o is the maximum amount of BPA loaded (mg g^{-1}) under the specified column conditions, m is the mass (g) of hybrid materials used, V is the throughput volume (L) and Q is the flow-rate of the pumped sorptive solution (L min^{-1}). A non-linear regression calculation was performed using the column data by the least-squares fitting method for two unknown parameters (K_T and q_o).

3. Results and discussion

3.1 Characterization of hybrid materials

The hybrid materials (AS, HS, AHS and AAS) were characterized by FT-IR spectrometry and XRD and their surface morphology was studied using SEM. The results have been reported previously.[50,52] The pH_{PZC} values were 6.89, 5.10, 6.20, 6.20 and 6.30 for sericite, HS, AS, AAS and AHS, respectively. The specific BET surface areas were 2.06, 5.72, 6.60, 0.93 and 1.71 m^2 g^{-1} for sericite, AS, HS, AAS and AHS, respectively. The BET results show that the modified samples HS and AS have a significantly higher specific surface area than unmodified sericite. This may be a result of the introduction of the HDTMA or AMBA molecules within the interlayer space, which acts to prop up the interlayer space. In contrast, the AAS and AHS hybrid materials have a decreased specific surface area, perhaps because the pores are occupied by small aluminum oxide particles.

3.2 Batch reactor operations

3.2.1 Effect of pH. The mechanism involved at the solid–solution interface was investigated by studying the dependence of the adsorption of BPA on pH. This was obtained by varying the solution pH from about pH 2.0 to 12.0. The percentage uptake of BPA is presented as a function of pH in Fig. 1. Fig. 1 clearly shows that the very high percentage uptake of BPA (90%) by these hybrid materials is almost unaffected in the pH range 2.0–10.0. BPA has two hydrogens that can be dissociated. The values of pK_{a1} and pK_{a2} have been reported to be 9.9 and 10.2, respectively.[56] The anionic species BPA^- and BPA^{2-} are therefore dominant at pH > 9.9 (Reaction (1)). However, in the pH range 2.0–9.0, BPA predominantly exists as a neutral molecule. All these solids have a net negative charge above about pH 6, depending on their pH_{PZC} values (Reaction (2)). It is interesting to note that the uptake of BPA is not affected by the variation in the charge carried by these solids. Therefore the high uptake of BPA can be attributed to the fact that the HDTMA- or AMBA-modified sericite has a high hydrophobicity and strong organophilic behavior, which effectively partitions the BPA molecule. This indicates that partitioning is a driving force in this pH range for the attenuation of BPA by AS, HS, AAS and AHS hybrid materials. These hybrid materials are therefore effective molecular sieves for the removal of BPA from aqueous solutions.

Chiou *et al.*[57,58] previously reported that non-ionic organic compounds are adsorbed onto a soil phase by partitioning between water and the soil organic phase and that this largely depends on the solubility of the organic component. Benzene, toluene and phenol were sequentially partitioned by organo-

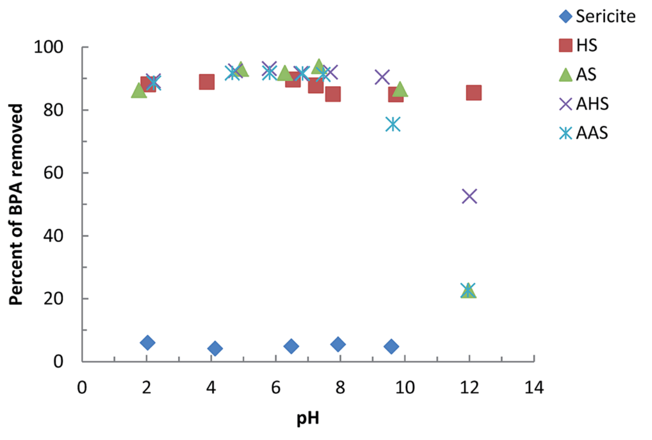

Fig. 1 pH dependence of the adsorption of BPA by sericite, AS, HS, AHS and AAS.

modified zeolites.[59] An enhanced π–π dispersion interaction was suggested in the pH range in which the surface and BPA carry no net charge.[25] Similarly, a strong π–π interaction between the benzene ring of BPA and the hydrophobic benzene ring of the solid surface can be demonstrated. This leads to hydrogen bonding of the phenolic group of BPA with the $Al(OH)_4$ on the surface of the sorbent.[1]

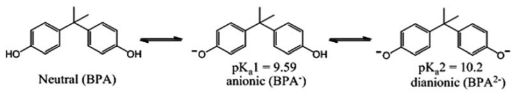

Reaction 1 (2)

$$\equiv SOH_2^+ \rightarrow \quad \equiv SOH^0 \quad \rightarrow \quad \equiv SO^-$$

Reaction 2

$$pH_{PZC} \qquad (3)$$

With a further increase in pH beyond about pH 10.0, a sharp decrease in the percentage uptake of BPA occurred with the AS and AAS hybrid materials. This may be because the surface of these solids and BPA both carry a net negative charge, which greatly enhances the repulsive electrostatic forces. The solute is therefore prevented from entering the interlayer space, hence restricting the partitioning or sorption of BPA by these solids. Similar findings have been reported previously for the adsorption of BPA by ordered mesoporous carbon[28] or multi-walled carbon nanotubes.[30] However, the removal of BPA by the HS or AHS hybrid materials was either not affected, or insignificantly affected, at pH 12.0, which shows the high affinity of BPA towards the solid surfaces of HS and AHS. This high affinity means that there is little effect on the immobilization of BPA. This may be attributed to the fact that HDTMA is an aliphatic organic cation, whereas AMBA is an aromatic cation ring. Aliphatic chain compounds are flat and form a stable monolayer within the interlayer space of sericite, whereas aromatic compounds have a less stable structure. Similar results have been reported previously for the adsorption of As(III) and As(V) from organo-modified sericite[50] and aluminum-HDTMA- or aluminum-AMBA-modified sericites.[52]

Fig. 1 also compares the properties of the modified sericite with unmodified sericite. Unmodified sericite removes an almost negligible percentage of BPA. This again indicates that the introduction of an organic molecule within the sericite network greatly enhances its hydrophobicity and organophilic nature and hence favors the partitioning of BPA between the solid and aqueous medium, providing useful sieving of BPA from aqueous solutions at the molecular level.

3.2.2 Effect of BPA concentration. The dependence of adsorption by AS, HS, AAS and AHS on the concentration of BPA was determined by varying the concentration of BPA from about 1.0 to 20.0 mg L^{-1} at pH 6.5 and 25 ± 1 °C (Fig. 2). Fig. 2 clearly shows that increasing the initial concentration of BPA from 1.53 to 19.51 mg L^{-1} did not significantly affect the percentage of BPA removed from aqueous solutions. These results suggest that these materials have an enhanced affinity towards BPA and that they may be useful molecular sieves that could be used to remove BPA from aqueous solutions. As the high uptake of BPA onto these solids was unaffected by the initial concentration of BPA, adsorption isotherm studies were not carried out.

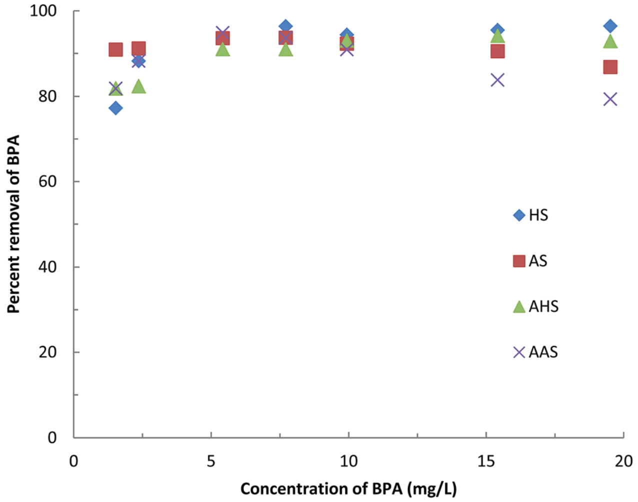

Fig. 2 Effect of concentration of BPA on its removal from aqueous solution by AS, HS, AHS and AAS.

3.2.3 Effect of background electrolyte concentrations. The effect of the background electrolyte concentration on the adsorption of BPA by the hybrid materials could help to explain the mechanism taking place at the solid/solution interfaces.[60] The specific adsorption is not affected by changes in the background electrolyte concentrations, but the non-specific adsorption is greatly affected by such changes. The adsorption of BPA was therefore investigated at various background electrolyte concentrations (NaCl from 0.0001 to 0.1 mol L^{-1}). The initial BPA concentration was kept constant at 10.0 mg L^{-1} at

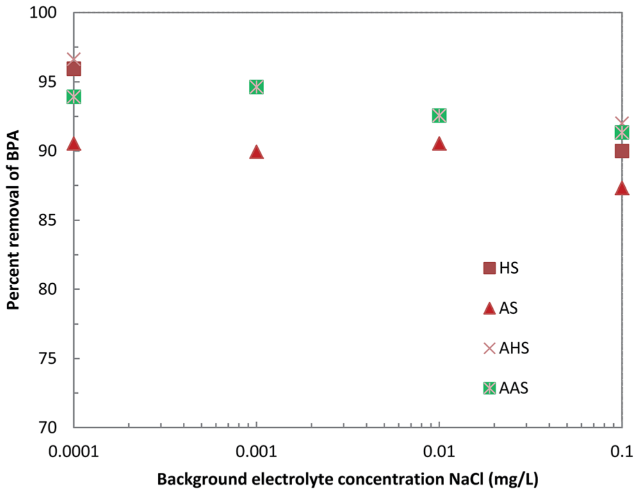

Fig. 3 Effect of background electrolyte concentration (NaCl) on the removal of BPA by AS, HS, AAS and AHS.

pH 6.5. Fig. 3 shows the results as a function of the percentage removal of BPA against the background electrolyte concentrations. Increasing the background electrolyte concentration from 0.0001 to 0.1 mol L^{-1} NaCl caused a decrease in the removal of BPA as follows: AS, a 3.21% decrease (90.54–87.33%); HS, a 3.38% decrease (95.95–92.57%); AAS, 2.59% decrease (93.92–91.33%); and AHS, a 4.62% decrease (96.62–92.00%). These results indicate that a 1000-fold increase in the background electrolyte concentration of NaCl causes an insignificant decrease in the removal of BPA by these hybrid materials. Therefore it is inferred that BPA is immobilized by strong forces and is likely to bind specifically on these hybrid materials. It has been reported previously that As(V) was adsorbed specifically onto γ-Al_2O_3 in the pH range 3.0–9.2, whereas As(III) was not adsorbed specifically in the pH range 4.5–9.0.[61,62] Similarly, when using an anion-exchange polymer resin the uptake of diclofenac from aqueous solutions was not significantly affected in the presence of citrate or phosphate.[63] Other studies have suggested that the adsorption of BPA onto activated carbon is slightly enhanced at very high ionic strengths (0.5 mol L^{-1} NaCl), possibly because screening of the surface charge and the favoring of π–π interactions enhanced the adsorption of BPA along with the salting-out effect.[25,64,65]

3.2.4 Kinetic studies. The time dependence of the adsorption of BPA by the hybrid materials was investigated by varying the time of contact from 5 to 180 min. The initial BPA concentration was kept constant at 10.0 mg L^{-1} (pH 6.5). Fig. 4 shows that the immobilization of BPA on these hybrid materials is fairly fast. Within the initial few minutes of contact most of the BPA is aggregated by the solids and an apparent equilibrium is achieved within 60 min of contact. The fast initial uptake of BPA results in a higher affinity of these hybrid materials towards BPA.

The time dependence data was used in kinetic studies to determine the rate constant and the capacity of these solids to remove BPA. The following non-linear PFO,[66] pseudo-second-order (PSO)[67] and fractal-like pseudo-second-order (FL-PSO)[68] kinetic models were used:

$$q_t = q_e(1 - \exp(-k_1 t)) \quad (4)$$

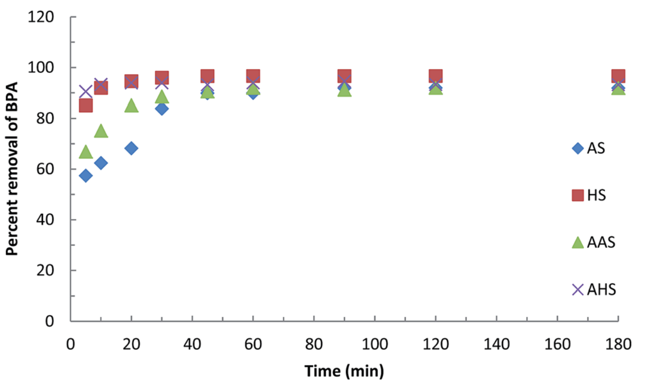

Fig. 4 Time dependence of the adsorption of BPA by AS, HS, AHS and AAS.

$$q_t = \frac{k_2 q_e{}^2 t}{1 + k_2 q_e t} \quad (5)$$

$$q_t = \frac{k q_e{}^2 t^\alpha}{1 + k q_e t^\alpha} \quad (6)$$

where q_t and q_e are the amounts of BPA adsorbed at time t and the adsorption capacity at equilibrium, respectively. k_1 and k_2 are the PFO and PSO rate constants, respectively. The constants k and α are the rate constant and the fractal constant, respectively. A non-linear least-squares fitting was carried out to estimate the unknown parameters and the results are shown in Fig. 5a–c for the PFO, PSO and FL-PSO kinetic models, respectively. Table 1 gives the estimated values of the unknown parameters and the least-squares sum. The results are better fitted to the PSO and FL-PSO models than to the PFO model. The adsorption capacity obtained by these models was comparable, except for AS using the FL-PSO model. The theoretical studies indicate that the rate coefficient of PSO model (k_2) is a complex function of the initial concentration of the adsorbate species.[66] However, the FL-PSO model is based on the fact that different paths of adsorption take place and the adsorption rate coefficient is a function of time.[69] The PFO kinetic model, which was derived by Lagergren method, could show the properties of the Langmuir rate at initial times of adsorption or close to equilibrium.[66,70] The applicability of the PSO model indicates that the adsorbate species are bound onto the surface of the solids by strong forces. It has been reported previously that the adsorption of divalent metal cations onto *sphagnum* moss peat follows second-order rate laws.[71,72] They further indicated that the metal cations are forming strong chemical forces with the surface active groups of peat.[71,72]

3.3 Column studies

Fixed-bed column studies were carried out using the column conditions described earlier. Breakthrough curves were obtained for AHS and AAS (as a reference material) for the removal of BPA (Fig. 6). A relatively high breakthrough volume was obtained for BPA using AAS and AHS. Quantitatively, complete breakthrough was obtained at a BPA throughput of 0.12 and 0.20 L for AAS and AHS, respectively. The relatively high breakthrough volume obtained for BPA indicates the strong affinity of these solids towards BPA under dynamic conditions.[73,74] It was reported previously that fixed-bed processes have the additional advantage of continuous contact of the adsorbing species with the solid surface, which results in better exhaustion of adsorbent solids.[75]

A non-linear least-squares analysis was performed using the breakthrough column data to simulate the two unknown constants K_T and q_o (Fig. 6). Table 2 gives the values of the Thomas constants and the least-squares sum obtained for these systems. The data clearly show that a relatively high loading capacity is achieved for BPA by these solids, even under dynamic conditions. This demonstrates the useful practical application of the solids in the removal of BPA from aqueous solutions. These results are similar to the findings of batch

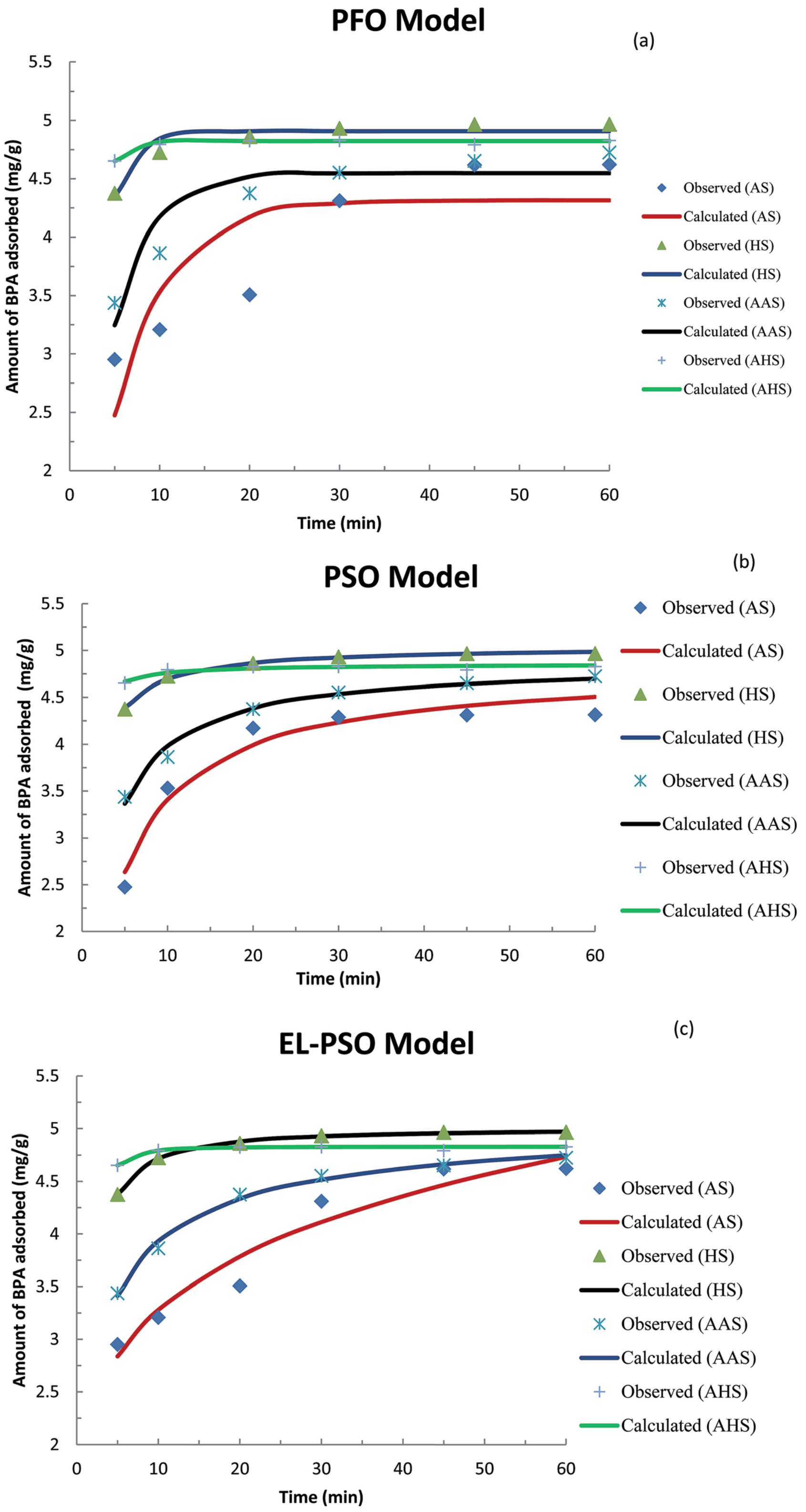

Fig. 5 Fitting of different models for the adsorption of BPA by AS, HS, AAS and AHS hybrid materials: (a) PFO model; (b) PSO model; and (c) FL-PSO model.

reactor experiments in which the Thomas equation was fitted to demonstrate the loading capacity of different sorbents.[52,76] The lower removal capacity obtained with column reactor operation compared with the corresponding batch reactor operation is a result of the insufficient time of contact available for the adsorption of BPA by these solids.[47]

Table 1 Estimated kinetic parameters for the PFO, PSO and FL-PSO kinetic models in the sorption of BPA by AS, HS, AAS and AHS hybrid materials[a]

		System			
Model	Constant evaluated	AS	HS	AAS	AHS
PFO	q_e (mg g^{-1})	4.315	4.908	4.547	4.823
	k_1 (min^{-1})	0.170	0.434	0.250	0.667
	s^2	0.9614	0.0242	0.1968	0.0030
PSO	q_e (mg g^{-1})	4.816	5.047	4.874	4.856
	k_2	0.050	0.265	0.091	1.037
	s^2	0.4360	0.0015	0.0204	0.0039
FL-PSO	q_e	7.851	5.003	5.166	4.830
	k	0.037	0.190	0.120	0.132
	α	0.396	1.237	0.710	2.309
	S^2	0.1964	0.0005	0.0089	0.0023

[a] AS = AMBA-sericite; HS = HDTMA-sericite; AAS = aluminum-HDTMA-sericite; and AHS = aluminum-HDTMA-sericite; s^2 = least-squares sum.

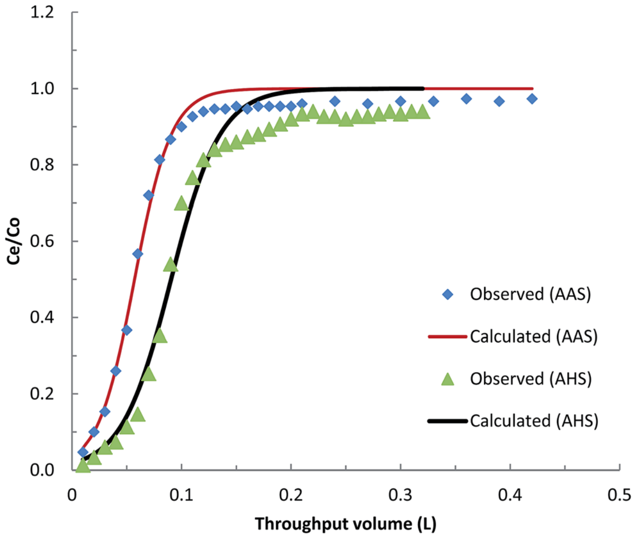

Fig. 6 Breakthrough curves for the removal of BPA by AAS and AHS.

Table 2 Thomas constants estimated for the removal of BPA by AAS and AHS solids[a]

	Thomas constant		
System	q_o	K_T	Least-square sum (s^2)
BPA-AAS	1.285	5.27×10^{-3}	3.2×10^{-2}
BPA-AHS	2.035	3.95×10^{-3}	1.2×10^{-1}

[a] AAS = aluminum-HDTMA-sericite; AHS: aluminum-HDTMA-sericite.

4. Conclusions

Sericite, a natural mica-type clay, was modified with HDTMA (H) and AMBA (A) to obtain organo-modified sericites (HS and AS) and aluminum-H-sericite (AHS) and aluminum-A-sericite (AAS) inorgano–organo-modified sericite hybrid materials. These materials were characterized by FT-IR spectrometry and XRD and the surface morphology was studied using SEM. The pH_{PZC} values for these solids were 6.89, 5.10, 6.20, 6.20 and 6.30 for sericite, HS, AS, AAS and AHS, respectively. These hybrid materials were used as effective and efficient molecular sieves for the removal of BPA from aqueous solutions. Batch experiments were performed to determine various physico-chemical parameters. Data for the effect of pH (2.0–12.0) on the uptake of BPA showed that the adsorption of BPA is almost independent of pH in the range 2.0–10.0, but above this pH it is significantly decreased, at least for AS and AAS. The concentration of BPA (1.0–20 mg L^{-1}) and the background electrolyte concentration (NaCl 0.0001–0.1 mol L^{-1}) do not significantly affect the percentage uptake of BPA by these hybrid materials. The kinetic data show that BPA is rapidly immobilized by the hybrid materials and the kinetic data fits well to the PSO and FL-PSO models. The overall capacity for the removal of BPA was 4.816, 5.047, 4.874 and 4.856 mg g^{-1} for the AS, HS, AAS and AHS hybrid materials, respectively. The materials were used under dynamic conditions in column reactor operations. The breakthrough curves could be used for non-linear fitting to the Thomas equation. The breakthrough data fits the Thomas equation well. The loading capacity for BPA was 1.285 and 2.035 for the AAS and HAS hybrid materials, respectively. These results indicate that these hybrid materials have the potential to be used as effective molecular sieves for the removal of BPA from aqueous solutions.

Acknowledgements

One of the authors (D.T.) acknowledges the CSIR, New Delhi for financial support in the form of Research Project no. 01 (2567)/12/EMR-II.

References

1 M. Zhou, Y. Wu, J. Qiao, J. Zhang, A. McDonald, G. Li and F. Li, *J. Colloid Interface Sci.*, 2013, **405**, 157–163.

2 R. H. Waring and R. M. Harris, *Mol. Cell. Endocrinol.*, 2005, **244**, 2–9.

3 C. E. Gattullo, H. Bährs, C. E. W. Steinberg and E. Loffredo, *Sci. Total Environ.*, 2012, **416**, 501–506.

4 D. A. Crain, M. Eriksen, T. Iguchi, S. Jobling, H. Laufer and G. A. LeBlanc, *Reprod. Toxicol.*, 2007, **24**, 225–239.

5 A. V. Krishnan, P. Stathis, S. F. Permuth, L. Tokes and D. Feldman, *Endocrinology*, 1993, **132**, 2279.

6 S. Takahashi, X. J. Chi, Y. Yamaguchi, H. Suzuki, S. Sugaya and K. Kita, *Mutat. Res.*, 2001, **490**, 199–207.

7 M. M. Munoz de Toro, C. M. Markey, P. R. Wadia, E. H. Luque, B. S. Rubin, C. Sonnenschein and A. M. Soto, *Endocrinology*, 2005, **146**, 4138–4147.

8 K. L. Howdeshell, A. K. Hotchkiss, K. A. Thayer, J. G. Vandenbergh and F. S. vom Saal, *Nature*, 1999, **401**, 763–764.

9 J. Chen, X. Huang and D. Lee, *Process Biochem.*, 2008, **43**, 451–456.

10 C. A. Staples, P. B. Dorn, G. M. Klecka, S. T. O'Block and L. R. Harris, *Chemosphere*, 1998, **36**, 2149–2173.

11 J. G. Teeguarden and S. Hanson-Drury, *Food Chem. Toxicol.*, 2013, **62**, 935–948.

12 T. Geens, T. G. Apelbaum, L. Goeyens, H. Neels and A. Covaci, ntake of bisphenol A from canned beverages and foods on the Belgian market, *Food Addit. Contam., Part A*, 2010, **27**, 1627–1637.

13 J. Yonekubo, K. Hayakawa and J. Sajiki, *J. Agric. Food Chem.*, 2008, **56**, 2041–2047.

14 T. Yamamoto, A. Yasuhara, H. Shiraishi and O. Nakasugi, *Chemosphere*, 2001, **42**, 415–418.

15 T. Bushnik, D. Haines, P. Levallois, J. Levesque, J. Van Oostdam and C. Viau, *Health Reports*, 2010, **21**, 7–18.

16 A. M. Calafat, X. Ye, L. Y. Wong, J. A. Reidy and L. L. Needham, *Environ. Health Perspect.*, 2008, **116**, 39–44.

17 J. S. Lakind, J. Levesque, P. Dumas, S. Bryan, J. Clarke and D. Q. Naiman, *J. Exposure Sci. Environ. Epidemiol.*, 2012, **22**, 219–226.

18 Commission of the European Communities, Opinion of the Scientific Committeeon Food on Bisphenol SCF/CS/PM/3936, (2002).

19 A WWF European Toxics Programme Report, Bisphenol A: A Known Endocrine Disruptor, Registered Charity No. 20170 (2000).

20 S. Yüksel, N. Kabay and M. Yüksel, *J. Hazard. Mater.*, 2013, **263**, 307–310.

21 Y. H. Kim, B. Lee, K. H. Choo and S. J. Choi, *Microporous Mesoporous Mater.*, 2011, **138**, 184–190.

22 C. Y. Wang, H. Zhang, F. Li and L. Y. Zhu, *Environ. Sci. Technol.*, 2010, **44**, 6843–6848.

23 A. Svenson, A. S. Allard and M. Ek, *Water. Res.*, 2003, **37**, 4433–4443.

24 Chemistry and Analytical Methods for Determination of Bisphenol A in Food and Biological Samples FAO/WHO Expert Meeting on Bisphenol A (BPA) Ottawa, Canada, 2–5 November (2010). Report Prepared by Xu-Liang Cao, (http://www.who.int/foodsafety/chem/chemicals/1_chemistry_analytical_methods.pdf).

25 G. Liua, J. Mab, X. Li and Q. Qin, *J. Hazard. Mater.*, 2009, **164**, 1275–1280.

26 W.-T. Tsai, C.-W. Lai and T.-Y. Su, *J. Hazard. Mater.*, 2006, **B134**, 169–175.

27 L. Joseph, L. K. Boateng, J. R. V. Flora, Y.-G. Park, A. Son, M. Badawy and Y. Yoon, *Sep. Purif. Technol.*, 2013, **107**, 37–47.

28 Q. Sui, J. Huang, Y. Liu, X. Chang, G. Ji, S. Deng, T. Xie and G. Yu, *J. Environ. Sci.*, 2011, **23**, 177–182.

29 J. Heo, J. R. V. Flora, N. Her, Y.-G. Park, J. Cho, A. Son and Y. Yoon, *Sep. Purif. Technol.*, 2012, **90**, 39–52.

30 L. Zhang, F. Pan, X. Liu, L. Yang, X. Jiang, J. Yang and W. Shi, *Chem. Eng. J.*, 2013, **218**, 238–246.

31 Y. Zhou, P. Lu and J. Lu, *Carbohydr. Polym.*, 2012, **88**, 502–508.

32 Y. Zhou, L. Chen, P. Lu, X. Tang and J. Lu, *Sep. Purif. Technol.*, 2011, **81**, 184–190.

33 S. Tang, N. Lu, J. Li and Y. Wu, *Thin Solid Films*, 2012, **521**, 257–260.

34 L. K. Boateng, J. Heo, J. R. V. Flora, Y.-G. Park and Y. Yoon, *Sep. Purif. Technol.*, 2013, **116**, 471.

35 S. M. Lee and D. Tiwari, *Appl. Clay Sci.*, 2012, **59–60**, 84.

36 S. W. Bailey, in *Crystal Structure of Clay Minerals and Their X-Ray Identification*, ed. G. W. Brndley and G. Brown, Mineralogical Society London, 1980, pp. 1–113.

37 J. Konta, *Appl. Clay Sci.*, 1995, **10**, 275–335.

38 G. R. Alther, *Waste Manag.*, 2002, **22**, 507–513.

39 J. Q. Jiang, C. Cooper and S. Ouki, *Chemosphere*, 2002, **47**, 711–716.

40 J. Smith, S. Bartlett-Hunt and S. Burns, *J. Hazard. Mater.*, 2003, **B96**, 91–97.

41 R. S. Bowman, Z. Li, S. J. Roy, T. Burt, T. L. Johnson and R. L. Johnson, in *Physical and Chemical Remediation of Contaminated Aquifers*, ed. J. A. Smith and S. Burns, Kluwer Academic Pulishers, 2002, pp. 161–163.

42 Z. Li and R. S. Bowman, *Water. Res.*, 2001, **35**, 3771–3776.

43 Y. Park, Z. Sun, G. A. Ayoko and R. L. Frost, *Chemosphere*, 2014, **107**, 249–256.

44 S. Zheng, Z. Sun, Y. Park, G. A. Ayoko and R. L. Frost, *Chem. Eng. J.*, 2013, **234**, 416–422.

45 F. Cao, P. Bai, H. Li, Y. Ma, X. Deng and C. Zhao, *J. Hazard. Mater.*, 2009, **162**, 791–798.

46 Y. J. Shih and Y. H. Shen, *Appl. Clay Sci.*, 2009, **43**, 282–288.

47 D. Tiwari, H. U. Kim and S. M. Lee, *Sep. Purif. Technol.*, 2007, **57**, 11–16.

48 C. Jeon and T. N. Kwon, *J. Ind. Eng. Chem.*, 2013, **19**, 68–72.

49 J. O. Kim, S. M. Lee and C. Jeon, *Chem. Eng. Res. Des.*, 2014, **92**, 368–374.

50 S. M. Lee and D. Tiwari, *Environ. Sci. Pollut. Res.*, 2014, **21**, 407–418.

51 D. Tiwari, W. Kim, M. Kim, S. K. Prasad and S.-M. Lee, *Desalin. Water Treat.*, 2013, DOI: 10.1080/19443994.2013.846562.

52 D. Tiwari and S. M. Lee, *Chem. Eng. J.*, 2012, **204–206**, 23–31.

53 J. Rivera-Utrilla, I. Bautista-Toledo, M. A. Ferro-Garcia and C. Moreno-Castilla, *J. Chem. Technol. Biotechnol.*, 2001, **76**, 1209–1215.

54 L. S. M. Lee and D. Tiwari, *Chem. Eng. J.*, 2013, **225**, 128–137.

55 H. C. Thomas, *J. Am. Chem. Soc.*, 1944, **66**, 1664–1666.

56 C. Tian, J. T. Wang and X. L. Song, *Water, Air, Soil Pollut.*, 2009, **199**, 301–310.

57 C. T. Chiou, L. J. Peters and V. H. Freed, *Science*, 1979, **206**, 831–832.

58 C. T. Chiou, P. E. Porter and D. W. Schmedding, *Environ. Sci. Technol.*, 1983, **17**, 227–231.

59 M. Ghiaci, A. Abbaspur, R. Kia and F. Seyedeyn-Azad, *Sep. Purif. Technol.*, 2004, **40**, 217–229.

60 K. F. Hayes, C. Papelis and J. O. Leckie, *J. Colloid Interface Sci.*, 1988, **125**, 717–726.

61 Y. Arai, E. J. Elzinga and D. L. Sparks, *J. Colloid Interface Sci.*, 2001, **235**, 80–88.

62 Z. Li, T. Burt and R. S. Bowman, *Environ. Sci. Technol.*, 2000, **34**, 3756–3760.

63 K. A. Landry and T. H. Boyer, *Water. Res.*, 2013, **47**, 6432–6444.

64 V. Lopez-Ramon, C. Moreno-Castilla, J. Rivera-Utrilla and L. R. Radovic, *Carbon*, 2002, **41**, 2009–2025.

65 G. Newcombe and M. Drikas, *Carbon*, 1997, **35**, 1239–1250.

66 S. Azizian, *J. Colloid Interface Sci.*, 2004, **276**, 47–52.

67 Y. S. Ho and G. Mckay, *Process Saf. Environ. Prot.*, 1998, **76**, 332–340.

68 M. Haerifar and S. Azizian, *Chem. Eng. J.*, 2013, **215–216**, 65–71.

69 M. Haerifar and S. Azizian, *J. Phys. Chem. C*, 2012, **116**, 13111–13119.

70 Y. Liu and L. Shen, *Langmuir*, 2008, **24**, 11625–11630.

71 Y. S. Ho, *J. Hazard. Mater.*, 2006, **B136**, 681–689.

72 Y. S. Ho and G. McKay, *Water. Res.*, 2000, **34**, 735–742.

73 J. T. Matheickal and Q. Yu, *Bioresour. Technol.*, 1999, **69**, 223–229.

74 M. A. Stylianou, M. P. Hadjiconstantinou, V. J. Inglezakis, K. G. Moustakas and M. D. Loizidou, *J. Hazard. Mater.*, 2007, **143**, 575–581.

75 A. Adak, M. Bandyopadhyay and A. Pal, *Dyes Pigm.*, 2006, **69**, 245–251.

76 A. Singh, D. Kumar and J. P. Gaur, *Water. Res.*, 2012, **46**, 779–788.

Desalination and Water Treatment

Published in cooperation with Balaban Publishers

ISSN
1944-3994 (Print), 1944-3986 (Online)

2014 Impact Factor: 1.173

Publication Frequency
52 issues per year

Hybrid materials in the remediation of arsenic contaminated waters: a physico-chemical study

DOI: 10.1080/19443994.2014.979241

Thanhmingliana[a*], Diwakar Tiwari[a*] & Seung-Mok Lee[b*]

Publishing models and article dates explained

- Received: 3 May 2014
- Accepted: 12 Oct 2014
- Published online: 05 Nov 2014

Author affiliations

[a] Department of Chemistry, School of Physical Sciences, Mizoram University, Aizawl 796004, India, Tel. +91 389 2301806; Fax: +91 389 2330834

[b] Department of Health and Environment, Kwandong University, Gangneung, Gangwondo 210710, Korea

This article was downloaded by: [Diwakar Tiwari]
On: 07 November 2014, At: 13:37
Publisher: Taylor & Francis
Informa Ltd Registered in England and Wales Registered Number: 1072954 Registered office: Mortimer House, 37-41 Mortimer Street, London W1T 3JH, UK

Desalination and Water Treatment
Publication details, including instructions for authors and subscription information:
http://www.tandfonline.com/loi/tdwt20

Hybrid materials in the remediation of arsenic contaminated waters: a physico-chemical study

Thanhmingliana[a], Diwakar Tiwari[a] & Seung-Mok Lee[b]

[a] Department of Chemistry, School of Physical Sciences, Mizoram University, Aizawl 796004, India, Tel. +91 389 2301806; Fax: +91 389 2330834

[b] Department of Health and Environment, Kwandong University, Gangneung, Gangwondo 210710, Korea

Published online: 05 Nov 2014.

To cite this article: Thanhmingliana, Diwakar Tiwari & Seung-Mok Lee (2014): Hybrid materials in the remediation of arsenic contaminated waters: a physico-chemical study, Desalination and Water Treatment, DOI: 10.1080/19443994.2014.979241

To link to this article: http://dx.doi.org/10.1080/19443994.2014.979241

PLEASE SCROLL DOWN FOR ARTICLE

Taylor & Francis makes every effort to ensure the accuracy of all the information (the “Content”) contained in the publications on our platform. However, Taylor & Francis, our agents, and our licensors make no representations or warranties whatsoever as to the accuracy, completeness, or suitability for any purpose of the Content. Any opinions and views expressed in this publication are the opinions and views of the authors, and are not the views of or endorsed by Taylor & Francis. The accuracy of the Content should not be relied upon and should be independently verified with primary sources of information. Taylor and Francis shall not be liable for any losses, actions, claims, proceedings, demands, costs, expenses, damages, and other liabilities whatsoever or howsoever caused arising directly or indirectly in connection with, in relation to or arising out of the use of the Content.

This article may be used for research, teaching, and private study purposes. Any substantial or systematic reproduction, redistribution, reselling, loan, sub-licensing, systematic supply, or distribution in any form to anyone is expressly forbidden. Terms & Conditions of access and use can be found at http://www.tandfonline.com/page/terms-and-conditions

Desalination and Water Treatment
www.deswater.com
doi: 10.1080/19443994.2014.979241

(2014) 1–11

Taylor & Francis
Taylor & Francis Group

Hybrid materials in the remediation of arsenic contaminated waters: a physico-chemical study

Thanhmingliana[a], Diwakar Tiwari[a,*], Seung-Mok Lee[b]

[a]*Department of Chemistry, School of Physical Sciences, Mizoram University, Aizawl 796004, India,*
email: thantea13@gmail.com (Thanhmingliana), Tel. +91 389 2301806; Fax: +91 389 2330834;
email: diw_tiwari@yahoo.com (D. Tiwari)
[b]*Department of Health and Environment, Kwandong University, Gangneung, Gangwondo 210710, Korea,*
email: leesm@kd.ac.kr (S.-M. Lee)

Received 3 May 2014; Accepted 12 October 2014

ABSTRACT

Hybrid materials are obtained by the organic modification of sericite using the organic cations viz. tetramethylammonium chloride (TMA or T) and dimethyldioctadecylammonium chloride as (DDDMA or D) by a simple wet cation exchange process. Surface morphology of these solids is discussed with the Scanning Electron Microscopic images. Moreover, the materials are characterized by the X-ray diffraction and Fourier Transform-Infrared analytical techniques. Removal behavior of these organo-modified sericite samples is assessed for arsenite and arsenate from aqueous solutions under the batch and column reactor operations. The batch reactor experiments show that increasing the sorptive concentration (1–20 mg/L) and pH (2–10) is caused to decrease the percent uptake of arsenite and arsenate significantly. Increasing the background electrolyte concentrations from 0.0001 to 0.1 mol/L $NaNO_3$ causes a significant decrease in percent removal of As(III) which infers that As(III) is sorbed onto the solid surface, primarily, by weak electrostatic or by van der Waals forces hence, forming an outer-sphere complexes at the solid surface. On the other hand As(V) uptake is insignificantly affected in presence of background electrolyte concentrations. This indicates that As(V) is sorbed by a strong chemical force and forming an inner sphere complexes onto the solid surface. The equilibrium state modeling shows that the data is fitted well to the Freundlich and Langmuir adsorption isotherms. The sorption capacities of these solids are calculated under these equilibrium conditions which indicate that organo-modified-sericite samples possess significantly higher removal capacity comparing to the virgin sericite. The leaching of the organic molecules (T or D) are also conducted in the sorption process of As(III) or As(V) and shows that almost negligible amount of T or D leaches in the bulk solutions since the Total Organic Carbon value of the bulk solution is not increased. Further, the breakthrough curves are obtained for these oxyanions under the column experimentations and the data is fitted well to the Thomas equation hence, the maximum loading capacity for arsenic is estimated under the dynamic conditions.

Keywords: Hybrid materials; Arsenite; Arsenate; Batch operation; Fixed-bed column; Sorption

---

*Corresponding author.

1. Introduction

Arsenic is a ubiquitous element available in all segments of environment. It enters and mobilizes into the natural environment mainly through a combination of natural processes such as weathering reactions, biological activity and volcanic emission as well as through several anthropogenic activities. Additionally, the mining activities, combustion of fossil fuels, the use of arsenic containing pesticides, herbicides and crop desiccants are reportedly releasing the arsenic into the environment. Arsenic has received a greater concern in the South East Asia (major part of Bangladesh and West Bengal, India); where arsenic contaminated soil causes contamination of underground waters which is reported to be a major source of drinking water [1]. It is further reported that more than six million people are on great risk; drinking the water having arsenic level above 50 μg/L in that region [2,3]. Arsenic poisoning is associated with various biological disorders including with skin, lung, bladder and kidney cancer, pigmentation changes, skin thickening (hyperkeratosis), neurological disorder, muscular weakness, loss of appetite, nausea etc. [4,5]. The acute toxicity may cause even the mortality [6]. Keeping in view the World Health Organization (WHO) in 1993 and the United States Environmental Protection Agency (US-EPA) in 2001 have reduced the limit of arsenic in drinking water from 50 to 10 μg/L [7,8].

Various materials such as zeolites, clays, activated carbon, bio-materials, metal oxides, zero-valent iron and neutralized red mud are suggested, previously, a good sorbing materials to remove arsenic from the arsenic contaminated waters [9]. Clay and minerals are natural materials and perhaps viable materials for the arsenic decontamination. However, the sorption capacity of these materials is reportedly insignificant for arsenic. Additionally, these materials possess low settling capacities hence, limiting its practical implication in such purposes [10]. Initial studies of using surfactant-modified clays in the environmental remediation are mainly focused on removal of hydrophobic organic contaminants from water [11,12]. Moreover, it is reported that if the surfactant loading on clays and zeolite is exceeded to its cation exchange capacity (CEC) or external CEC, the modified mineral could reverse their surface charge and show strong affinities for anions such as chromate, nitrate, sulfate [13–15] and iodide [16]. Li and Bowman [17] used kaolinite intercalated with hexadecyltrimethylammonium bromide (HDTMA) as an effective adsorbent for arsenate removal, and reported that the adsorption capacity of As(V) onto the organo-kaolinite is at least two times greater than the un-modified kaolinite. Kaolinite and zeolite modified by HDTMA causes to enhance the As(V) adsorption significantly, whereas the As(III) adsorption is almost unaffected [18]. Organo-bentonites are prepared by modification of bentonite with various cationic surfactants, and are used to remove As(V) and As(III) from aqueous solutions [9]. The results show that the adsorption capacities of bentonite modified with octadecyl benzyl dimethyl ammonium is significantly higher than the un-modified bentonite. The adsorption kinetics is fitted well to the pseudo-second-order rate model. The adsorption of As(V) and As(III) is strongly dependent to solution pH. Moreover, the presence of anions could not affect, significantly, the adsorption of As (III), but it clearly suppresses the As(V) sorption. Hybrid zirconiumpolyacrylamide material (ZrPACM-43) is synthesized by the sol–gel pathway and further the materials are applied in the removal of arsenic(III) from aqueous solutions [19]. Similarly, amino functionalized magnetic graphene composites are synthesized using the graphene sheets and further the material is useful in decontamination of several heavy metal toxic ions from aqueous solutions [20].

Sericite is a mica based natural clay, having abundance in Korea is used in the removal/speciation of several inorganic cations viz. Cu(II), Pb(II), Ni(II), Cs(I) etc. from aqueous solutions [21–23] and possess reasonably a good sorption capacity for these cations. Further, organo-modified sericite is exploited in the removal of phenol from aqueous solutions under the batch reactor operations [24]. The sericite is modified by poly (hydroxo aluminium) ions (Al) and followed by hexadecyltrimetrylammonium or alkyldimethylbenzylammonium ions to obtain the hybrid materials viz. Al-HDTMA-sericite (AH) and Al-AMBA-sericite (AA) [25]. These inorgano-organo-sericite samples are then employed in the removal of As(III) and As(V) from aqueous solutions under the batch and column reactor operations. The simulated batch reactor data indicated that As(V) is adsorbed specifically onto the solid surface whereas As(III) is sorbed mainly through electrostatic or even by the van der Waals attraction. Moreover, the results obtained under dynamic conditions show that the materials are reasonably useful in the speciation/attenuation of these two ions from water bodies. Similarly, the sericite is modified with the HDTMA or AMBA and further utilized in the remediation of arsenic contaminated wasters [26]. The encouraging results obtained previously prompted us further to employ the organo-sericite in the attenuation and speciation of arsenic. The present paper deals to obtain and assess the applicability of two different hybrid materials precursor to sericite i.e. tetramethylammonium-sericite (T) and dioctadecyldimethylammonium-sericite (D) in the remediation of arsenic contaminated waters under batch and column studies.

2. Materials and methods

2.1. Materials

Sericite is obtained from the Keuman deposit, Gagokmyun, Samcheok City, Kagwon province, Korea. It is crushed and sieved to obtain particle size 200–300 BSS (British Standard Sieve). The powder is washed with distilled water, dried and crushed in mortar for its further use. The CEC of sericite is obtained by the US-EPA method 9080 (http://www.epa.gov/osw/hazard/testmethods/sw846/pdfs/9080.pdf), which is found to be 37.22 meq/100 g of sericite. Sericite contained with various metal oxides primarily containing the silicon and aluminum oxides as reported elsewhere [23]. Tetramethylammonium chloride (TMA) and dioctadecyldimethylammonium bromide (DDDMA) are obtained respectively from Junsei Chemical Co. Ltd, Japan and Sigma Aldrich, USA. Sodium meta-arsenite and disodium hydrogen arsenate heptahydrate are obtained from Wako Pure Chemical Industries Ltd, Japan. The other chemicals are of AR grade. The deionized water is purified (18 MΩ-cm) using a Millipore water purification system (Milli-Q+).

The hybrid organo-sericite is obtained by incorporating the TMA/or DDDMA within the sericite network. Twenty grams of sericite powder is taken into 1.0 L of TMA or DDDMA solution containing the equivalent amount of 1.0 or 2.0 CEC of sericite; correspondingly named as T1 or D1 and T2 or D2 materials. The mixture is refluxed for 48 h at 60˚C under constant stirring. The slurries are filtered and washed with plenty of purified water. Soxhlet extraction is conducted to remove any excess of free surfactants. The sericite which is then loaded with organic surfactants i.e. T1, T2, D1 or D2 are dried at 90˚C and stored in the airtight polyethylene bottles for further experimentation.

2.2. Surface morphology of organo-modified-sericite materials

The surface morphology of sericite, T1 and D1 solids are obtained by the scanning electron microscope (SEM) images using a SEM (Model FE-SEM SU-70; Hitachi, Japan). X-ray diffraction (XRD) data is recorded using the XRD machine (PANalytical, Netherland; Model X'Pert PRO MPD). The Cu K_α radiation having wavelength 1.5418 Å is used for XRD. Fourier transform-infra red (FT-IR) data is obtained for these materials using a FT-IR machine (Bruker, Tensor 27, USA by KBR disk method).

2.3. Speciation studies of As(III) and As(V)

Speciation of arsenic(III) and arsenic(V) are conducted separately using the MINEQL+ (Version 4.5), a geochemical computer simulation program. The initial concentration of As(III) and As(V) is taken 2.0 mg/L at constant temperature 25˚C. The species distribution of As(III) and As(V) as a function of pH is obtained.

2.4. Batch reactor experiments

Stock solutions of As(III)/or As(V) 100 mg/L is prepared by dissolving an appropriate amount of respective arsenic salts in distilled water and the desired concentration is obtained by successive dilution of stock solution. 2.0 mg/L of As(III) /or As(V) solution (100 mL) is taken into polyethylene bottles and the pH is adjusted by a drop-wise addition of 0.1 mol/L HNO_3/or NaOH solutions. 0.2 g of solid i.e. organo-sericite is then added into these bottles. The bottles are kept in an automatic shaker (KUKJE, Shaking Incubator, Korea model 36-SIN-125) for 24 h at 25 ± 1˚C in order to achieve equilibrium between solid/solution interfaces. The samples are then taken out from shaker and filtered with 0.45 μm syringe filter and the pH is again checked and reported as final or equilibrium pH. The filtrates are subjected to its bulk sorptive concentration measurements using an AAS (Fast Sequential Atomic Absorption Spectrometer: Model AA240FS, Varian) as well to the TOC measurements using TOC analyzer (Shimadzu, Japan; Model: TOC-VCPH/CPN). The percent removal is calculated as stated elsewhere [23].

Sorptive concentration dependence data is collected taking arsenic concentrations from 1.0 to 20.0 mg/L at constant pH 4.5 and at constant temperature 25 ± 1˚C. A constant dose 0.2 g/L of solid is added into these solutions. The sorption process is carried out as described before. Further, the equilibrium concentration dependence sorption data are further employed in equilibrium modeling studies using the Freundlich and the Langmuir adsorption isotherms as discussed elsewhere [23,25].

The ionic strength dependence data is collected varying the background electrolyte concentrations of sorptive solutions from 0.0001 to 0.1 mol/L of $NaNO_3$. The sorptive pH (~4.5) and temperature (25 ± 1˚C) is kept constant throughout the experiments. Results are presented as percent removal as a function of background electrolyte concentrations.

2.5. Column reactor experiments

The column experiments are performed using a glass column (1 cm inner diameter) packed with 1.0 g of T1 or D1 (kept in the middle of the column); below and above to this, 2.0 g of virgin sand particles (14–16 BSS) are taken. It is then fully packed with glass beads. Sorptive solutions of As(III)/or As(V) 2.0 mg/L having a constant pH 4.5 is pumped upward from bottom of column using Acuflow Series II, High-Pressure liquid chromatographic pump, at a constant flow rate of 0.70 mL/min. Effluent samples are then collected using Spectra/Chrom CF-1 fraction collector. The liquid samples collected are filtered using a 0.45 μm syringe filter and the total bulk sorptive concentration is measured using an AAS. Further, the breakthrough data is utilized to optimize the removal capacity of these solids under the dynamic conditions using the Thomas Equation as described elsewhere [25,27,28].

3. Results and discussion

3.1. Characterization and surface morphology of organo-modified-sericite materials

SEM images are obtained for the solids sericite, T1 and D1 and shown in Fig. 1. Sericite sample possesses very compact and ordered layer structure which hardly has micro- or meso-pores on its surface. However, the organo-modified-sericite samples show heterogeneous and disordered surface structure having distinct visible pores on it. The layers are clearly propped-up in presence of organic cations. Moreover, at places, the organic molecules are aggregated onto the surface. It is assumed that the water molecules or even the potassium ions, which are present previously within the interspace of sericite, are replaced by the TMA or DDDMA organo cations. Hence, the surface of the sericite becomes more disordered. Similar results are obtained previously where sericite is pillared with aluminum and HDTMA or AMBA as to obtain the inorgano-organo-sericite [25].

The XRD data of these solids are recorded and presented graphically in Fig. 2. Characteristic peaks of sericite mineral is observed and marked in the XRD curve. The peaks are found at the 2θ values of 19.82, 20.83, 25.43, 26.62, 27.87, 36.00, 36.52, 42.41 and 50.12 assigned with the standards sericite mineral phase [27]. Samples T1 and Di showed almost an identical diffraction pattern with slight change in the d-spacings and intensities of peaks.

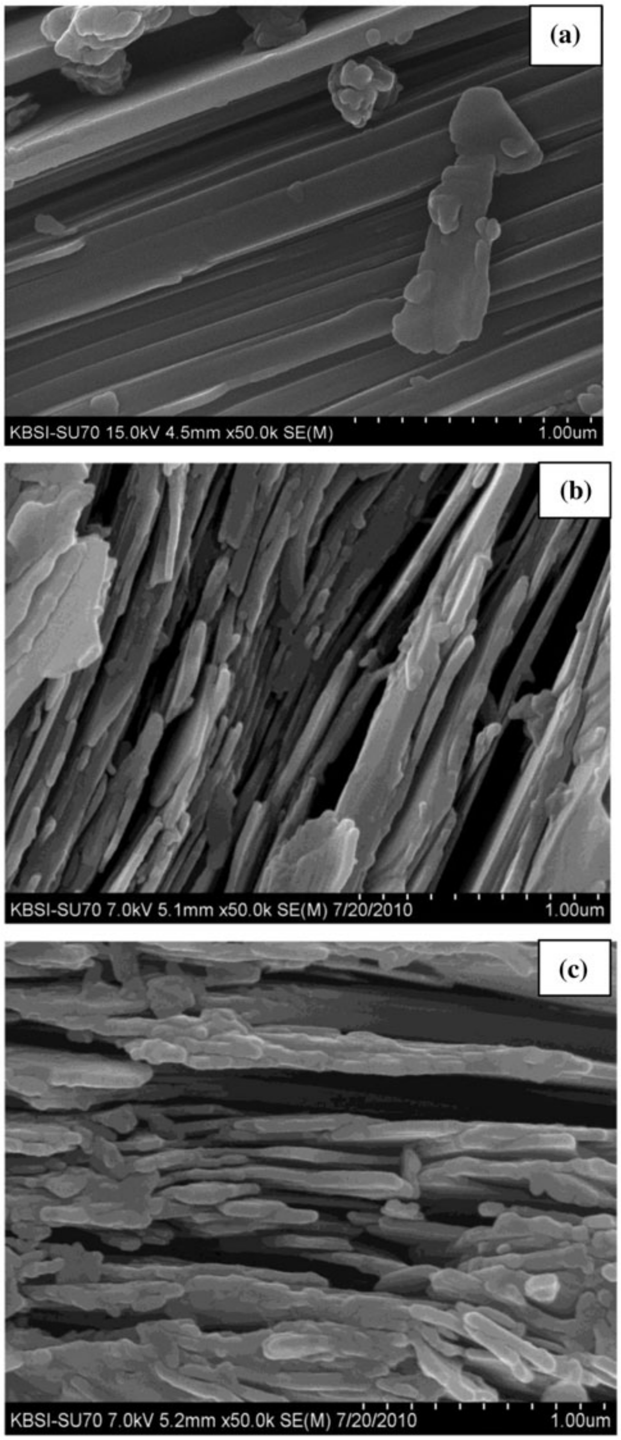

Fig. 1. SEM images of (a) Sericite, (b) T1 and (c) D1 solids.

Further, the FT-IR data is collected for the sericite and modified sericite samples i.e. T1 and D1. The FT-IR results are presented graphically in Fig. 3. Figure shows asymmetric and symmetric stretching vibrations of H-O-H are occurred around the wave number of 3,630 and 3,426 cm^{-1} (not much pronounced with sericite and D1). Similarly, H-O-H

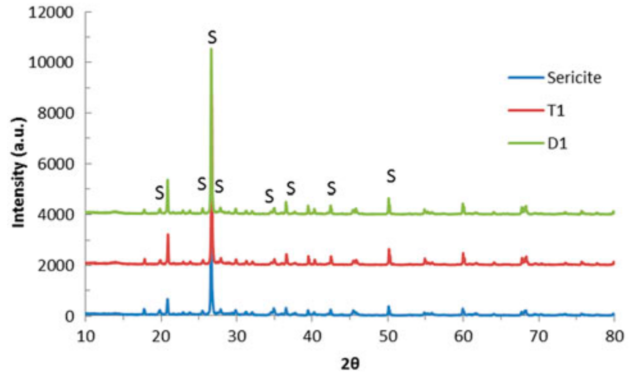

Fig. 2. XRD pattern of sericite, T1 and D1 solids.

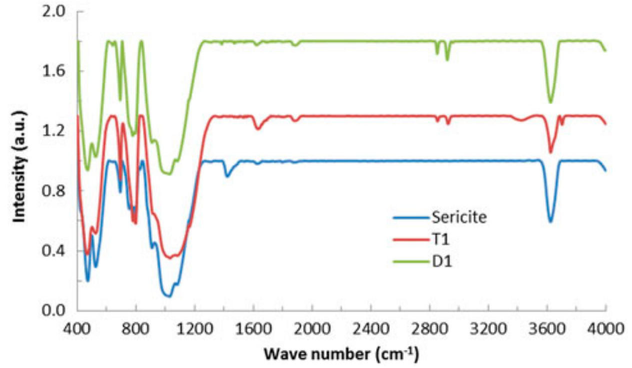

Fig. 3. FT-IR spectral data of sericite, T1 and D1 solids.

bending vibration is observed around the wavenumber of 1,625 cm^{-1} for these samples. This clearly indicates the presence of hydroxyl groups within the clay sheets and the water molecules present within the interlayer space of sericite [29–31]. A prominent IR peak centered around 1,030 cm^{-1} is an indicative of the Si–O stretching vibrations [32]. Moreover, couple of IR bands occurred around 690 and 790 cm^{-1} are assigned to the Si–O quartz vibrations [33]. Further, interesting to note that the modified samples T1 and D1 possessed prominent peaks centering around 2,930 cm^{-1} and 2,850 cm^{-1} are assigned as $-CH_2$ asymmetric stretching and $-CH_2$ symmetric vibrations, respectively [29]. This confirms the introduction of organo cations tetramethylammonium or dimethyldioctadecylammonium within the sericite network.

3.2. *Speciation study of As(III) and Arsenic(V)*

The speciation study of As(III) and As(V) is conducted at wide range of pH. Results are presented in Fig. 4(a) and (b), respectively for the As(III) and As (V). The Fig. 4(a) clearly demonstrates that uncharged H_3AsO_3 species is dominant below the pH 8 and above pH 8 the anionic species $H_2AsO_3^-$ is dominant. On the other hand, As(V) speciation data shows that at lower pH till pH 6.8, H_3AsO_4 and $H_2AsO_4^-$ species are dominated whereas above pH 7.0, $HAsO_4^{2-}$ anionic species are dominated (*cf* Fig. 4(b)).

3.3. *Batch reactor studies*

3.3.1. *pH dependence study*

Mechanism involved at solid/solution interfaces is, perhaps, better dealt with the pH dependence sorption studies. Therefore, the pH dependence sorption of As (III) or As(V) by these solids are obtained and presented graphically in Fig. 5(a) and (b) respectively for As(III) and As(V). In general, low to moderate pH values favor the percent uptake of As(III) or As(V) by these modified-sericite samples; whereas the high pH values greatly suppresses the uptake of these two sorbing species. On the other hand, very low percent uptake of As(III) and As(V) is obtained by the virgin sericite sample which is almost unaffected with the pH change. Quantitatively, increasing the pH from 2.0 to 10.0, the corresponding decrease in percent uptake of As(III) is found to be, respectively from 36.27 to 15.54% for T1; from 32.64 to 16.58% for T2; from 34.20 to 3.63% for D1 and from 18.13 to 1.04% for D2 samples. Similarly, the decrease in percent uptake of As (V) is recorded respectively from 56.44 to 23.11% for T1, from 39.11 to 20.89% for T2; 25.33 to 16.89% for D1. Unusually, very low percent uptake of As(V) by D2 sample is observed which is not affected significantly with pH. The values are found to be 24.89% and 26.22% at pH 1.94 and 9.34, respectively. It is clearly observed that increasing the dose of organic cations twice to CEC, i.e. the samples T2 and D2 show comparatively less percent removal of arsenic comparing to its corresponding samples of T1 and D1 having 1:1 CEC dose of organic cations. This is possibly due to the structural arrangements and number of monolayer formation of organic cations within the interspace of sericite having the basal spacing of *ca.* 8.0 Å. Possibly, the bilayer arrangement of organo cations within the interspace is not a suitable and stable arrangement and causing to decrease in As(III) or As (V) uptake. Earlier, however, it is reported that the HDTMA forms a stable bilayer within the interspace of zeolite when the surfactant addition is exceeded to the external CEC value [34,35]. Moreover, it is reported that the sorption of chromate on HDTMA-modified zeolite reached to its maximum value when modified to 200% to its external CEC [36]. However, the other studies, showed that 200% CEC loading of

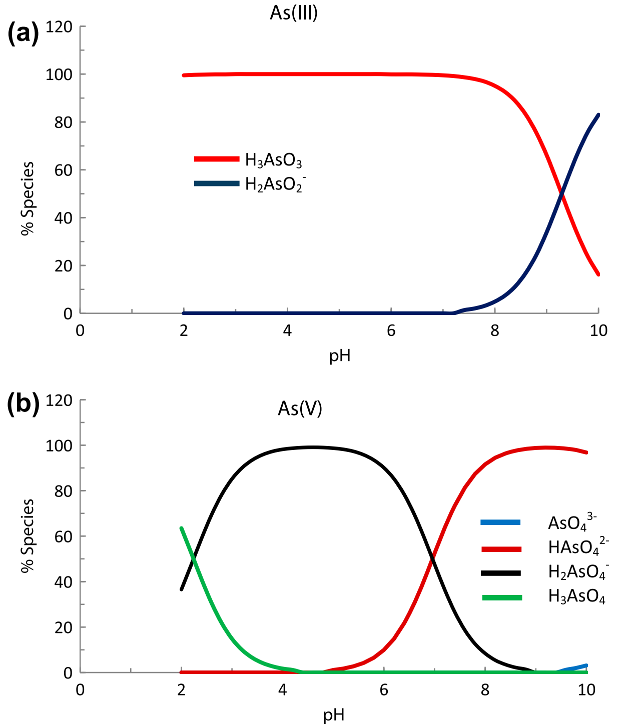

Fig. 4. Speciation of (a) As(III): 2 mg/L and (b) As(V): 2 mg/L as a function of pH.

some quaternary ammonium cations (QAC) onto montmorillonite is suppressed significantly the removal capacity of methylene blue and they inferred that QAC's already occupied the cation-exchange sites of the precursor clays, making it difficult for methylene blue to occupy place within the interspace [37].

Relatively high and almost constant percent uptake of As(III) is occurred within the pH region 2–6. The high uptake of As(III) is possibly due to dominating van der Waals attractive forces operative in between the arsenic and solid surface and this possibly enables an enhanced uptake of arsenic(III) in this pH region. However, the uptake of As(III) is decreased gradually increasing the pH beyond ~6. This is because of the fact that the acidic dissociation of H_3AsO_3 species takes place and gradually the anionic species $H_2AsO_3^-$ (negatively charged) increases in solution as the speciation results also indicated (vide Fig. 4(a)). This indicates that both solid and sorbate ions carrying net positive charge hence repulsive forces causing for an apparent decrease in sorption of As(III) at higher pH values. Moreover, at extreme high pH condition i.e. pH 10 there could be a competition between the OH^- ion and the anion of As(III) i.e. $H_2AsO_3^-$, towards solid surface, and the OH^- ions may significantly compete for solid surface [38]. Similarly, the uptake of H_3AsO_3 species by iron modified sand is reported to be adsorbed by the van der Waals attraction [39]. However, an electrostatic attraction is reported previously for the sorption of As(III) by hybrid materials, modified activated carbon or soil samples etc. [25,40–42].

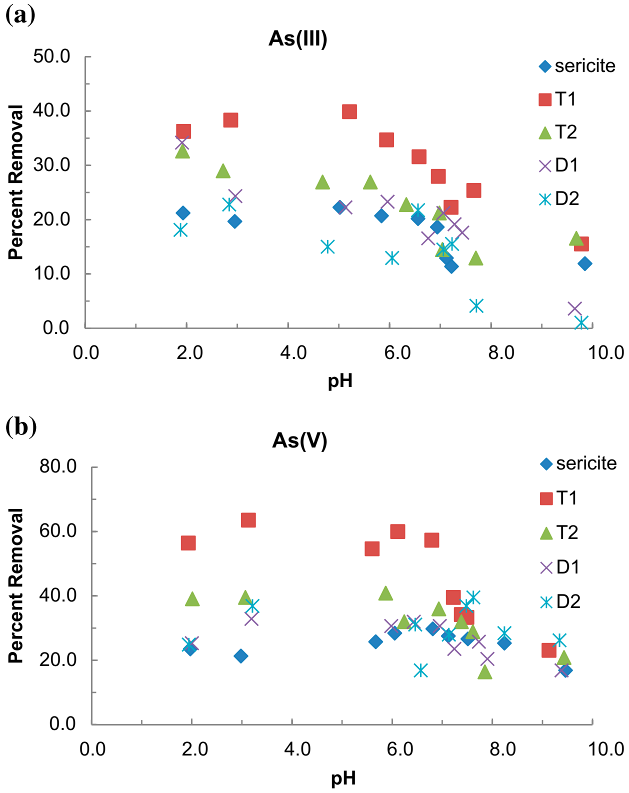

Fig. 5. Effect of pH in the removal of (a) As(III) and (b) As(V) using sericite and organo-modified sericite samples.

On the other hand, relatively high uptake of As(V) by T1 sample is almost unaffected up to the solution pH 6.7; beyond this it is greatly decreased. This could be explicable with the fact that at low pH values the surface carries net positive charge and mostly the As(V) present as anionic forms i.e. $H_2AsO_4^-$ or $HAsO_4^{2-}$ species (vide Fig. 4(b)), the electrostatic attraction favored the uptake of As(V) by these solids Eq. (1) [41].

$$\begin{aligned}&(\text{Sericite-T/or D})^+ + H_2AsO_4^- \\ &\quad \rightarrow (\text{Sericite-T/or D})^+ - H_2AsO_4^- \end{aligned} \tag{1}$$

This is the driving force caused to attract the arsenic species within the interspace of the sericite network. In fact, the sericite is muscovite type mineral, possessed a layered structure. It possesses three sheet layers having the T:O ratio of 2:1 (where T: tetrahedral $[SiO_4]^{4-}$ and O: octahedral $[AlO_3(OH)_3]^{6-}$) and the apices of these sheets are having the oxygen atom from which some are connected with protons (as –OH) and are perhaps taking part in surface complexation with the several heavy metal toxic ions including lead or copper [23]. However, it is assumed that the –OH group may be replaced with the arsenate and forming mono- or binuclear complexes with the Si or Al as demonstrated below Eq. (2) and (3):

$$> \mathrm{AlOH} + \mathrm{H_2AsO_4^-} \rightarrow\ > \mathrm{AlH_2AsO_4} + \mathrm{OH^-} \quad (2)$$

$$2(> \mathrm{AlOH}) + \mathrm{HAsO_4^-} \rightarrow\ > \mathrm{Al_2HAsO_4} + 2\mathrm{OH^-} \quad (3)$$

The specific sorption of As(V) by the modified sericite is again reaffirmed with the background electrolyte studies in later sections. Also the somewhat similar mechanism was suggested previously using the clay or aluminum hydroxide solids [43,44].

Further, increase in pH, there could possibly be a competition for the solid surface between the OH^- ions and the metal anions which seemingly restricts the uptake of As(V) by these solids [38].

3.3.2. Sorptive concentration dependence study

The sorptive concentration dependence data is collected for a wide range of initial arsenic concentration i.e. 1.0 to 20.0 mg/L. Results show that the organo-modified solids, at least T1 and D1, possess an enhanced amount of arsenic removal compared to the virgin sericite at all sorptive concentrations. Quantitatively, increasing the concentration from 1.0 to 20.0 mg/L of As(III), the corresponding decrease in percent removal is found to be, respectively from 30.21 to 1.68% for sericite; from 46.88 to 4.26% for T1; from 36.46 to 3.05% for T2; from 38.54 to 3.86% for D1 and from 33.33 to 2.39% for D2 samples. Similarly, the decrease in percent uptake of As(V) is found to be from 34.04 to 2.21% for sericite; from 47.87 to 7.39% for T1; from 42.55 to 5.70% for T2; from 43.62 to 6.31% for D1 and from 34.04 to 4.11% for D2 samples, respectively for an increase in sorptive concentration from 1.0 to 20.0 mg/L. This decrease in content of uptake is explained with the fact that at higher sorptive concentration of As(III)/or As(V); relatively lesser number of active sites are present whereas at lower concentrations less number of sorbing species are present for the same number of active sites available at the solid surface [45].

3.3.3. Equilibrium state modeling

The equilibrium state adsorption dependence data is further utilized to deduce various adsorption isotherm models viz. the Langmuir and the Freundlich models to its linear form. The equilibrium state concentration dependence data is fitted to these two models and hence, the Freundlich and Langmuir constants are estimated. These constants along with the R^2 values are returned in Table 1. The fitting data shows reasonably a good applicability of these two models is occurred for the systems studied. The difference in removal capacity estimated by these two models is attributing the different basic nature and assumptions of these two models. Further, organo-modified samples possess significantly higher adsorption capacity comparing to the virgin sericite; therefore shows its potential applicability in the remediation of waters contaminated with arsenic. Moreover, the sample T1 or D1 obtained by the 100% loading of surfactant to the sericite possess relatively higher adsorption capacity compared to its corresponding samples obtained by 200% loading of surfactant i.e. T2 or D2. These results again indicate the applicability of T1 and D1 samples with the stable monolayer structure of organo cation within the interlayer space of sericite. Among these two organo cations i.e. TMA and DDDMA; TMA-modified sericite shows relatively higher removal capacity than DDDMA-modified sericite at least towards the removal of As(III) or As(V) from aqueous solutions.

Further, the fractional values of Freundlich constant, i.e. $1/n$, obtained for these systems indicate a heterogeneous surface structure of solids with an exponential distribution of surface active sites [25]. Similarly, the Langmuir constant "*b*" reflected to the strength and affinity of these solids towards the adsorbing species [46].

3.3.4. Background electrolyte concentration study

The specific and non-specific adsorption of As(III) or As(V) onto the organo-modified-sericite, could be studied by carrying the ionic strength dependence study. It is reported previously that the specific adsorption is unaffected with the increase in ionic strength, whereas the non-specific adsorption is greatly influenced by the change of ionic strength because of the competitive adsorption with counter ions [47]. Hence keeping in view the study is conducted to observe the change in background electrolyte concentration i.e. $NaNO_3$ in the adsorption behavior of these solids in the removal of As(III)/or As(V)) at constant pH 4.5. The background concentration is increased from 0.0001 to 0.1 mol /L of $NaNO_3$ (1,000 times) and the corresponding percent removal of As(III)/or As(V) is obtained and

Table 1
Adsorption isotherm constants estimated for the sorption of As(III) and As(V) by sericite and organo-modified-sericite samples using linear adsorption equations

	Freundlich constants			Langmuir constants		
System	K_f (mg/g)	$1/n$	R^2	K_f (mg/g)	b	R^2
Sericite-As(III)	0.1942	0.314	0.829	0.4041	1.440	0.968
T1–As(III)	0.2986	0.454	0.959	1.0423	0.403	0.972
T2–As(III)	0.2162	0.488	0.972	0.8985	0.293	0.965
D1–As(III)	0.2342	0.513	0.937	0.9779	0.316	0.951
D2–As(III)	0.1891	0.467	0.887	0.6661	0.408	0.882
Sericite-As(V)	0.1941	0.579	0.969	1.1614	0.180	0.920
T1–As(V)	0.3381	0.577	0.988	1.9685	0.190	0.928
T2–As(V)	0.3006	0.519	0.978	1.3004	0.299	0.980
D1–As(V)	0.3006	0.536	0.966	1.3123	0.311	0.963
D2–As(V)	0.2377	0.477	0.767	0.6452	1.256	0.824

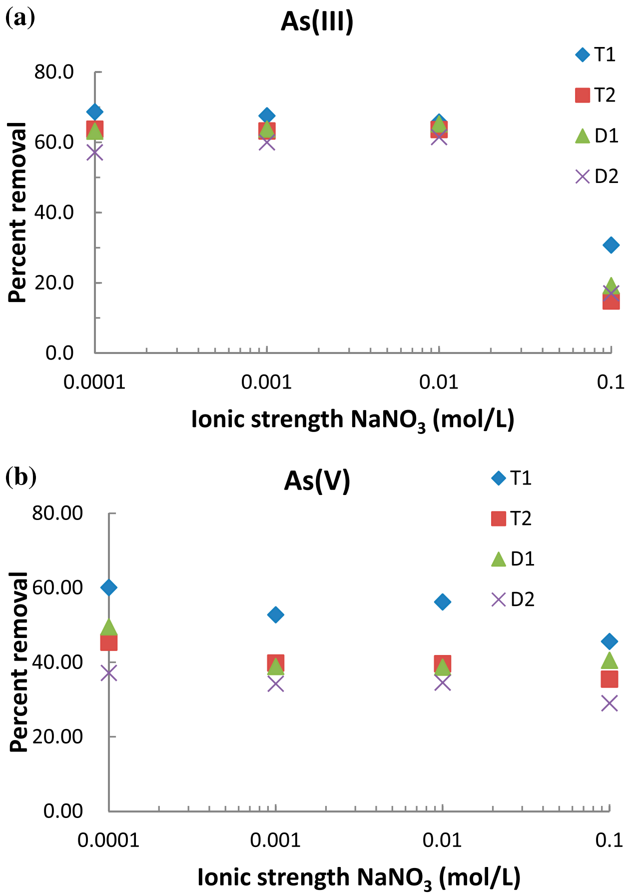

Fig. 6. Effect of ionic strength in the removal of (a) As(III) and (b) As(V) using organo-modified sericite.

represented graphically in Fig. 6(a) and (b) respectively for As(III) and As(V).

Quantitatively, increasing the background electrolyte concentration from 0.0001 to 0.1 mol/L NaNO$_3$ causes to decrease the As(III) uptake respectively from 68.68 to 30.77% for T1 i.e. 37.91% decrease; from 63.74 to 14.84% for T2 i.e. 49.9% decrease; 63.19 to 19.23% for D1 i.e. 43.96% decrease; and from 57.14 to 17.03% for D2 i.e. 40.11% decrease. Similarly, the uptake of As(V) is decreased from 60.09 to 45.62% for T1 i.e. 14.47% decrease; from 45.41 to 35.48% for T2 i.e. 10.03%; from 49.54 to 40.55% for D1 i.e. 8.99% decrease and from 37.16 to 29.03% for D2 i.e. 8.13% decrease. These results indicate that the 1,000 times increase of background electrolyte concentration causes significant decrease of As(III) by these solid materials. Therefore, it indicates that As(III) is adsorbed mostly with the weak attractive forces, perhaps van der Waals forces and forming an outer sphere complexes at the surface. On the other hand the uptake of As(V) is not significantly affected in presence of background electrolytes pointed it that As (V) is sorbed primarily by the strong chemical forces and forming an “inner sphere complexes” onto the solid surface of these modified sericite. As(III) sorption onto the zirconium(IV) oxide-ethanolamine is reported to be ion-exchange along with electrostatic attraction [48]. Vaisya and Gupta [39] also indicated that the major driving force in the sorption of As(III) onto the iron-modified sand was the van der Waals attraction.

3.4. Breakthrough curves for As(III) and As(V)

The applicability of the organo-sericite materials are further assessed in the removal of As(III) and As (V) under the dynamic conditions as performed with column experiments. The column data could be used for direct practical implication of these materials in the possible large scale or pilot scale treatment of water contaminated with arsenic. The column conditions are maintained as mentioned before and the results are presented graphically in Fig. 7(a) and (b), respectively for As(III) and As(V). It is interesting to note that the complete breakthrough is obtained for As(III) at the throughput volume of 1.22 L for T1 and 0.64 L for D1 solids. Similarly, it is obtained for the As (V) at 0.96 L for T1 and 0.29 L for D1. Relatively high value of throughput volume for these solids indicates its potential applicability in the remediation of water contaminated with arsenic. Further, the breakthrough data is utilized for the non-linear fitting to the Thomas equation [27] in order to optimize the two unknown parameters viz. q_0 and K_T known as loading capacity and Thomas rate constant. Reasonably a good fitting of breakthrough data is obtained for these systems as shown in Fig. 7(a) and (b). The Thomas constants are evaluated for these solids and are returned in Table 2. The high loading capacity is obtained for TMA modified sericite comparing to the DDDMA modified sericite at least for both the arsenic species i.e. As(III) and As(V). This clearly pointing its applicability in the treatment of arsenic contaminated waters. These results are in a line to the batch reactor data. Similar results are also reported previously using the biosorbents or manganese and iron coated sands, etc. [25,45,49,50].

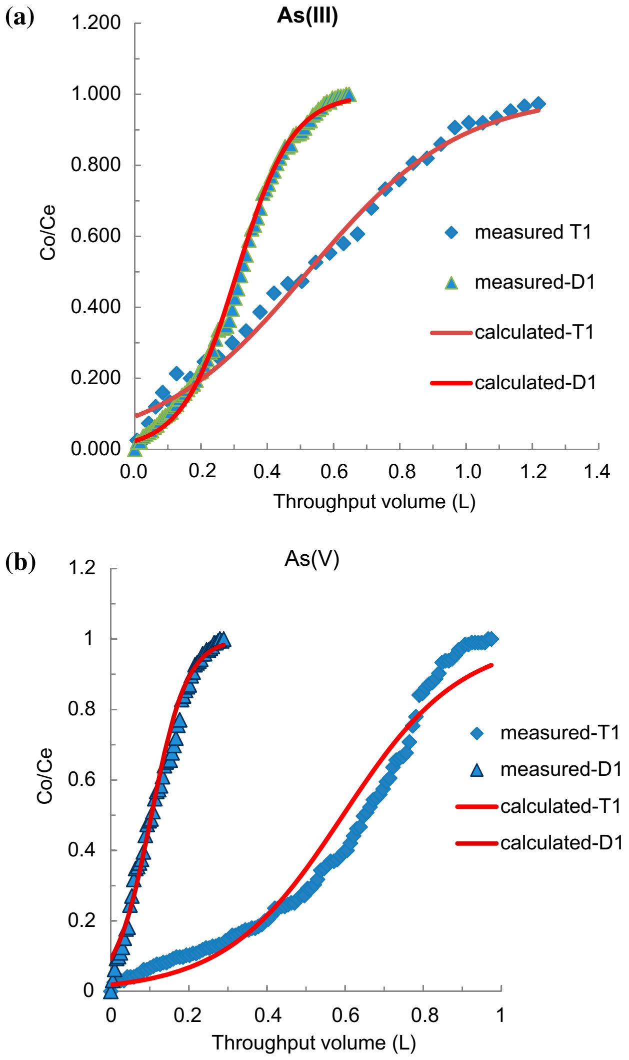

Fig. 7. Breakthrough curves for the removal of (a) As(III) and (b) As(V) by organo-modified-sericite fitted to the Thomas model.

Table 2
Thomas constants for the removal of As(III) and As(V) from aqueous solutions by organo-modified-sericite

Systems	q_0 (mg/g)	$K_T \times 10^{-3}$ (L/min/mg)
T1–As(III)	0.826	1.938
D1–(As(III)	0.589	4.427
T1–As(V)	1.160	2.388
D1–As(V)	0.199	7.998

4. Conclusions

Four different TMA/or DDDMA-modified sericite samples are obtained (viz. T1 and T2 or D1 and D2 obtained by 100 and 200% CEC loading of TMA/or DDDMA onto sericite). The surface morphology of these solids indicates that the presence of organo cations significantly disordered the compact and layered structure of sericite. The XRD data enables the presence of sericite minerals with these solids and IR data indicates the introduction of organic cations within the sericite framework. Further, the suitability and applicability of TMA and DDDMA modified sericite is assessed for the decontamination of arsenic contaminated waters. The studies are performed under batch and column reactor operations. Various parametric batch studies show that lower pH and high sorptive concentration favors greatly the uptake of As(III) and As(V) by these solids. The equilibrium state concentration dependence data is fitted well to the Freundlich and Langmuir adsorption isotherms. Moreover, the estimated capacity for these solids indicates that samples T1 and D1 possesses significantly higher sorption capacity than that of virgin sericite or samples T2 and D2. The 1,000 times increase in background electrolyte concentrations ($NaNO_3$) causes significant decrease in As(III) removal which indicates the arsenic(III) is predominantly sorbed by weak van der Waals attractive forces. However, As(V) sorption is insignificantly decreased by the similar increase in background electrolyte concentrations pointing that As(V) is sorbed with strong chemical forces and forming an inner sphere complexes at solid surface. Moreover, interesting to note that, no leaching of organic cations, i.e. TMA or DDDMA throughout the pH regions ~2–10, is occurred in the sorption of As(III) or As(V) by these organo-modified sericite sampels as obtained by bulk TOC data measurements. Further, the column reactor operations indicate very high value of breakthrough volume obtained for T1 and D1 solids. The breakthrough data is well fitted to the Thomas equation. Moreover, the T1 sample possesses significantly higher loading capacity than the sample D1.

Acknowledgements

This work is supported by the National Research Foundation of Korea (NRF) grant funded by the Korea government (MEST) (No. 2012R1A2A4A01001539). The work is also partly supported by the CSIR, New Delhi as in the form of sponsored research project to one of the author DT vide No. 01 (2567)/12/EMR-II.

References

[1] D. Mohan, C.U. Pittman Jr., Arsenic removal from water/wastewater using adsorbents—A critical review, J. Hazard. Mater. 142 (2007) 1–53.

[2] D.G. Kinniburgh, P.L. Smedley, Arsenic Contamination of Groundwater in Bangladesh, Vol. 2: Final Report, BGS Technical Report WC/00/19, British Geological Survey, Keyworth, 2001.

[3] S. Wang, X. Zhao, On the potential of biological treatment for arsenic contaminated soils and groundwater, J. Environ. Manage. 90 (2009) 2367–2376.

[4] S. Song, A. Lopez-Valdivieso, D.J. Hernandez-Campos, C. Peng, M.G. Monroy-Fernandez, I. Razo-Soto, Arsenic removal from high-arsenic water by enhanced coagulation with ferric ions and coarse calcite, Water Res. 40 (2006) 364–372.

[5] J.T. O'Connor, Arsenic in drinking water Part 2: Human exposure and health effects, Water Eng. Manage. 149 (2002) 35–37.

[6] E. Dopp, L.M. Hartmann, A.M. Florea, U. von Recklinghausen, R. Pieper, B. Shokouhi, A.W. Rettenmeier, A.V. Hirner, G. Obe, Uptake of inorganic and organic derivatives of arsenic associated with induced cytotoxic and genotoxic effects in Chinese hamster ovary (CHO) cells, Toxicol. Pharm. 201 (2004) 156–165.

[7] WHO, Guidelines for Drinking Water Quality, World Health Organization, Geneva, 1993.

[8] US EPA, Edition of Drinking Water Standards and Health Advisories, 2001. Available from: http://www.epa.gov/safewater/ars/arsenic.html.

[9] J. Su, H.G. Huang, X.Y. Jin, X.Q. Lu, Z.L. Chen, Synthesis, characterization and kinetic of a surfactant-modified bentonite used to remove As(III) and As(V) from aqueous solution, J. Hazard. Mater. 185 (2011) 63–70.

[10] S.M. Lee, D. Tiwari, Organo and inorgano-organo-modified clays in the remediation of aqueous solutions: An overview, Appl. Clay Sci. 59–60 (2012) 84–102.

[11] S.A. Boyd, S. Shaobai, J.F. Lee, M.M. Mortland, Pentachlorophenol sorption by organo-clays, Clays Clay Miner. 36 (1988) 125–130.

[12] W.F. Jaynes, S.A. Boyd, Clay mineral type and organic compound sorption by hexadecyltrimethylammonium-exchanged clays, Soil Sci. Soc. Am. J. 55 (1991) 43–48.

[13] G.M. Haggerty, R.S. Bowman, Sorption of chromate and other inorganic anions by organo-zeolite, Environ. Sci. Technol. 28 (1994) 452–458.

[14] Z. Li, Oxyanion sorption and surface anion exchange by surfactant-modified clay minerals, J. Environ. Qual. 28 (1999) 1457–1463.

[15] Z. Li, R.S. Bowman, Counterion effects on the sorption of cationic surfactant and chromate on natural clinoptilolite, Environ. Sci. Technol. 31 (1997) 2407–2412.

[16] J. Bors, A. Gorny, S. Dultz, Iodide, caesium and strontium adsorption by organophilic vermiculite, Clay Miner. 32 (1997) 21–28.

[17] Z. Li, R.S. Bowman, Retention of inorganic oxyanions by organo-kaolinite, Water Res. 35 (2001) 3771–3776.

[18] Z. Li, R. Beachner, Z. McManama, H. Hanlie, Sorption of arsenic by surfactant modified zeolite and kaolinite, Microporous Mesoporous Mater. 105 (2007) 291–297.

[19] S. Mandal, M.K. Sahu, R.K. Patel, Adsorption studies of arsenic(III) removal from water by zirconium polyacrylamide hybrid material (ZrPACM-43), Water Resour. Ind. 4 (2013) 51–67.

[20] B. Du, Q. Wei, J. Yang, L. Hu, L. Yan, W. Xu, Synthesis of amino functionalized magnetic graphenes composite material and its application to remove Cr(VI), Pb(II), Hg(II), Cd(II) and Ni(II) from contaminated water, J. Hazard. Mater. 278 (2014) 211–220.

[21] C. Jeon, T.N. Kwon, Adsorption characteristics of sericite for nickel ions from industrial waste water, J. Ind. Eng. Chem. 19 (2013) 68–72.

[22] J.O. Kim, S.M. Lee, C. Jeon, Adsorption characteristics of sericite for cesium ions from an aqueous solution, Chem. Eng. Res. Des. 92 (2014) 368–374.

[23] D. Tiwari, H.U. Kim, S.M. Lee, Removal behavior of sericite for Cu(II) and Pb(II) from aqueous solutions: Batch and column studies, Sep. Purif. Technol. 57 (2007) 11–16.

[24] D. Tiwari, W. Kim, M. Kim, S.K. Prasad, S.M. Lee, Organo-sericite in the remediation of phenol contaminated water, Desalin. Water Treat. Paper online (2014), doi: 10.1080/19443994.2013.846562.

[25] D. Tiwari, S.M. Lee, Novel hybrid materials in the remediation of ground waters contaminated with As (III) and As(V), Chem. Eng. J. 204–206 (2012) 23–31.

[26] S.M. Lee, D. Tiwari, Organo-modified sericite in the remediation of an aquatic environment contaminated with As(III) or As(V), Environ. Sci. Pollut. Res. 21 (2014) 407–418.

[27] H.C. Thomas, Heterogeneous ion exchange in a flowing system, J. Am. Chem. Soc. 66 (1944) 1664–1666.

[28] G. Yan, T. Viraraghavan, Heavy metal removal in a biosorption column by immobilized *M. rouxii* biomass, Bioresour. Technol. 78 (2011) 243–249.

[29] U.F. Alkaram, A.A. Mukhlis, A.H. Al-Dujaili, The removal of phenol from aqueous solutions by adsorption using surfactant-modified bentonite and kaolinite, J. Hazard. Mater. 169 (2009) 324–332.

[30] J.M. Trillo, M.D. Alba, A.A. Castro, A. Munoj, J. Poyato, M. Tobias, Local environment of lanthanum ions in montmorillonite upon heating, Clay Miner. 27 (1992) 423–434.

[31] S.E. Miller, G.R. Heath, R.D. Gonzalez, Effects of temperature on the sorption of lanthanides by montmorillonite, Clays Clay Miner. 30 (1982) 111–122.

[32] J. Madejová, P. Komadel, Baseline studies of the clay minerals society source clays: Infrared methods, Clays Clay Miner. 49 (2001) 410–432.

[33] B.J. Saikia, G. Parthasarthy, Fourier transform infrared spectroscopic characterization of kaolinite from Assam and Meghalaya, Northeastern India, J. Mod. Phys. 1 (1010) 206–210.

[34] S.M. Koh, J.B. Dixon, Preparation and application of organo-minerals as sorbents of phenol, benzene and toluene, Appl. Clay Sci. 18 (2001) 111–122.

[35] Z. LI, R.S. Bowman, Sorption of chromate and PCE by surfactant-modified clay minerals, Environ. Eng. Sci. 15 (1998) 237–245.

[36] Z. Li, I. Anghel, R.S. Bowman, Sorption of oxyanions by surfactant-modified zeolite, J. Dispersion Sci. Technol. 19 (1998) 843–857.

[37] R. Wibulswas, Batch and fixed bed sorption of methylene blue on precursor and QACs modified montmorillonite, Sep. Purif. Technol. 39 (2004) 3–12.

[38] Z. Li, T. Burt, R.S. Bowman, Sorption of ionizable organic solutes by surfactant-modified zeolite, Environ. Sci. Technol. 34 (2000) 3756–3760.

[39] R.C. Vaishya, S.K. Gupta, Modelling arsenic(III) adsorption from water by sulfate-modified iron oxide-coated sand (SMIOCS), J. Chem. Technol. Biotechnol. 78 (2003) 73–80.

[40] Y. Arai, E.J. Elzinga, D.L. Sparks, X-ray absorption spectroscopic investigation of arsenite and arsenate adsorption at the aluminum oxide–water interface, J. Colloid interface Sci. 235 (2001) 80–88.

[41] Lalhmunsiama, D. Tiwari, S.M. Lee, Activated carbon and manganese coated activated carbon precursor to dead biomass in the remediation of arsenic contaminated water, Environ. Eng. Res. 17(S1) (2012) 41–48.

[42] R. Xu, Y. Wang, D. Tiwari, H. Wang, Effect of ionic strength on adsorption of As(III) and As(V) on variable charge soils, J. Environ. Sci. 21 (2009) 927–932.

[43] B.A. Manning, S. Goldberg, Adsorption and stability of arsenic(III) at the clay mineral water interface, Environ. Sci. Technol. 31 (1997) 2005–2011.

[44] D. Haraguchi, C. Tokoro, Y. Oda, S. Owada, Sorption mechanism of arsenate in aqueous solution during coprecipitation with aluminum hydroxide, J. Chem. Eng. Jpn. 46 (2013) 173–180.

[45] S.M. Lee, C. Laldawngliana, D. Tiwari, Iron oxide nano-particles-immobilized-sand material in the treatment of Cu(II), Cd(II) and Pb(II) contaminated waste waters, Chem. Eng. J. 195–196 (2012) 103–111.

[46] V.K. Gupta, V.K. Saini, N. Jain, Adsorption of As(III) from aqueous solutions by iron oxide-coated sand, J. Colloid Interface Sci. 288 (2005) 55–60.

[47] K.F. Hayes, C. Papelis, J.O. Leckie, Modeling ionic strength effects on anion adsorption at hydrous oxide/solution interfaces, J. Colloid Interface Sci. 125 (1988) 717–726.

[48] S. Mandal, T. Padhi, R.K. Patel, Studies on the removal of arsenic (III) from water by a novel hybrid material, J. Hazard. Mater. 192 (2011) 899–908.

[49] A. Singh, D. Kumar, J.P. Gaur, Continuous metal removal from solution and industrial effluents using *Spirogyra* biomass-packed column reactor, Water Res. 46 (2012) 779–788.

[50] D. Tiwari, C. Laldanwngliana, C.H. Choi, S.M. Lee, Manganese-modified natural sand in the remediation of aquatic environment contaminated with heavy metal toxic ions, Chem. Eng. J. 171 (2011) 958–966.

ELSEVIER

Chemical Engineering Journal

An International Journal of Research and Development

The *Chemical Engineering Journal* focuses upon three aspects of **chemical engineering**: chemical reaction engineering, environmental chemical engineering, and materials synthesis and processing.

View full aims and scope

This journal supports the following content innovations

AudioSlides, **Interactive MATLAB Figure Viewer**, **Nomenclature Viewer**

Journal Metrics

Source Normalized Impact per Paper (SNIP): **1.905**

SCImago Journal Rank (SJR): **1.585**

Impact Factor: **4.321**

5-Year Impact Factor: **4.621**

Imprint: **ELSEVIER**

ISSN: **1385-8947**

Chemical Engineering Journal 263 (2015) 364–373

Contents lists available at ScienceDirect

Chemical Engineering Journal

journal homepage: www.elsevier.com/locate/cej

Efficient use of hybrid materials in the remediation of aquatic environment contaminated with micro-pollutant diclofenac sodium

Thanhmingliana, Diwakar Tiwari *

Department of Chemistry, School of Physical Sciences, Mizoram University, Aizawl 796004, India

HIGHLIGHTS

- Hybrid materials are obtained using bentonite and locally available clay.
- Materials are characterised by the FT-IR, XRD and SEM analysis.
- Materials are employed in efficient and effective attenuation of diclofenac from aqueous solutions.

ARTICLE INFO

Article history:
Received 29 August 2014
Received in revised form 27 October 2014
Accepted 29 October 2014
Available online 6 November 2014

Keywords:
Microporous
Diclofenac
Micro-pollutant
Hybrid materials
Partitioning

GRAPHICAL ABSTRACT

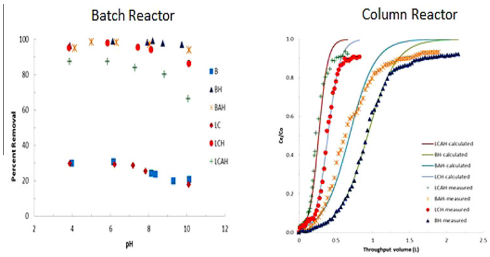

B: Bentonite; BH: HDTMA-B; BAH: HDTMA-Al-B; LC: Local Clay; LCH: HDTMA-LC; and LCAH: HDTMA-Al-LC

ABSTRACT

The aim of this study is to synthesise indigenously the hybrid materials and their efficient use to treat the wastewater contaminated with one of important micro-pollutant diclofenac. The hybrid materials are obtained modifying the commercial bentonite (B) and locally collected clay (LC) with the hexadecyltrimethylammonium bromide (HDTMA) as to obtain the organo-modified clay samples (BH and LCH). Moreover, the B and LC clay samples are pillared with aluminium and modified with the HDTMA as to obtain inorgano–organo-modified clay hybrid materials (*viz.*, BAH and LCAH solids). The hybrid materials are characterised by the XRD (X-ray diffraction) and FT-IR (Fourier Transform Infra-Red) analytical methods and the surface morphology is obtained by the FE-SEM (Field Emission Scanning Electron Microscope) images of these solids. pH_{PZC} (Point of Zero Charge) of these solids is obtained by acid base titrations. Further, these materials are assessed in the efficient and effective treatment of aquatic environment contaminated with diclofenac sodium under the batch and fixed-bed column reactor operations. Batch data is obtained for various physico-chemical parametric studies *viz.*, the effect of solution pH (3.8–10.0), sorptive concentrations (1.0–20.0 mg/L), and background electrolyte concentrations (0.0001–0.1 mol/L NaCl). The kinetics of the uptake of diclofenac by these solids is conducted using the pseudo-first, pseudo-second and fractal-like-pseudo-second order non-linear rate equations. The rate constants along with the removal capacity are, therefore, estimated. Further, the fixed-bed column reactor operations are performed to obtain the loading capacity of column for diclofenac under the dynamic conditions.

1. Introduction

Clay and minerals are fine particles of hydrous aluminosilicates. Crystal structure of clay and minerals possess layered sheets which are firmly and structurally arranged. Each layer is having two, three or four sheets. The sheets are having tetrahedral (T) $[SiO_4]^{4-}$ or octahedral (O) $[AlO_3(OH)_3]^{6-}$ units. The interiors of these sheets are composed with smaller cations and their apices are occupied by oxygen from which some are bonded with protons (as –OH). This basic structural element is arranged to form a hexagonal network with each sheet [1,2]. Bentonite is natural clay,

---

* Corresponding author. Tel.: +91 389 2301806; fax: +91 389 2330834.
E-mail address: diw_tiwari@yahoo.com (D. Tiwari).

http://dx.doi.org/10.1016/j.cej.2014.10.102
1385-8947/

mostly containing the smectite and kaolinite group of clays. The group of smectite is fairly an expanding three-sheet phyllosilicates, where the T:O ratio is 2:1 and the charge of the three-sheet layer (unit cell) is 0.5–1.2 e/uc (negative charge). This charge arises from the isomorphous substitution of Al^{3+} for Si^{4+} in the tetrahedral sheet for Mg^{2+} and Al^{3+} in the octahedral sheet. This possesses no hydroxyl functionality within the interlayer space. Whereas the kaolinite and serpentine group is a typical two-sheet phyllosilicates, where the T:O ratio is 1:1 and the charge of the two-sheet layer (unit cell) is 0 e/uc. Since bentonite contain dominantly the smectite mineral having permanent negative charge which is naturally compensated with the exchangeable cations (i.e., Na^{+}, K^{+}, Mg^{2+}, Ca^{2+}). These exchangeable cations are located within the interlayer space of bentonite sheets [3]. Therefore, bentonite possesses fairly a high cation exchange capacity (CEC), which termed it a good water replaced swelling type mineral. Moreover, because of high specific surface area enables this mineral to show high adsorption/absorption capacity towards several ionic or polar compounds.

Although clay and minerals are natural porous materials and used widely in decontamination of inorganic pollutants from wastewaters [4,5] however; show insignificant applicability in the treatment of several organic pollutants having non- or low-polarity [6]. Moreover, most of the clay materials show less settling capacity hence, limiting its wider practical implication in waste water treatment operations. However, since the clay materials are having exchangeable cations, hence this could be exchanged with the organo cations. Therefore, the modified materials possess an enhanced organophilicity and this, perhaps, be effective in attenuation of several organic pollutants from aqueous solutions. Similarly, the hybrid materials obtained by inorgano–organo-clay shows enhance applicability in waste water treatment since this could not only be effective in the removal of inorganic pollutants but also show fair affinity towards the organic impurities as well. Furthermore, these hybrid materials show achievable settling capacity makes easy for solid/aqueous separation. In a line, silylated pillared bentonite (SPILC) is obtained as inorgano–organo-composite [7]. These materials possess two different sorption sites enabling to remove both organic and inorganic pollutants from aqueous solutions simultaneously. Aluminium pillared sericite is modified with HDTMA and AMBA (alkyldimethylbenzylammonium chloride) surfactants and utilised in the removal of As(III) and As(V) from aqueous solutions even in presence of phenol [6]. Sericite, Na–montmorillonite and zeolite are modified with dimethyltetradecylbenzylammonium chloride, hyamine 1622® and trimethylbenzylammonium chloride organic cations. Further, these organo-modified materials are employed in the attenuation of several non-ionic organic contaminants (NOC) *viz*., benzene, phenol and toluene from aqueous solutions [8]. Previously, sericite was modified with HDTMA and AMBA, which is then employed in the removal of phenol from aqueous solutions [9]. Montmorillonite is pillared with aluminium and modified with the hexadecyl pyridine. The solid is found to be effective and efficient in the removal of phenol from aqueous solutions [10].

The presence of micro-pollutants (in particular, the pharmaceuticals and personal care products) in aquatic environment is received a serious environmental concern during recent past; since several micro-pollutants are persistent at low level, low biodegradability and the toxicity possessed by them. Therefore, these contaminants are known as emerging water pollutants. It is reported that the level of these contaminants increased significantly in the wastewater treatment plant (WWTPs) effluents, surface water, sewage water, ground water or even in the drinking water supply [11–14]. Further, the presence of such residual micro-pollutants in water bodies are found problematic in aquatic ecosystem (e.g., feminisation of fish) and potential concern towards human health (e.g., increasing antibiotic resistance) [15–17]. In addition to the pharmaceutical industries, the human urine and faeces is reported to be additional but significant sources which, elevating the level of pharmaceutical load in the municipal/sewage wastewaters since *Ca* 70% of consumed pharmaceuticals are excreted in human urine as active ingredients and metabolites [17–19]. Diclofenac (2-[-2′,6′-(dichlorophenyl)amino]phenyl acetic acid) is used mostly as its sodium salt. This is a non-steroidal anti-inflammatory drug (NSAID) and prescribed for the treatment of inflammatory and painful diseases of rheumatic, nonrheumatic and antiarthritic origin. It is also recommended to reduce menstrual pain, dysmenorrhea etc. [20,21]. Continued intake of diclofenac, even at low levels, by human shows several adverse biochemical effects e.g., cytotoxicity to liver, kidney and gill cells as well the renal lesions [22–26]. It may also influence the biochemical functions of fish and lead to tissue damage [27]. Further, it is pointed that due to the low solubility, high log K_{ow} value, low dipole moments and negative charges of diclofenac causes easy escape of this chemical from the nano-filtration unit [28]. The unit operations associated with ozonation [29], adsorption on activated carbon [30] and membrane filtration as nano-filtration and reverse osmosis [31,32] are the possible ways that could be employed for the removal of several pharmaceuticals (>99%) [33].

Previously, several materials including activated carbons [33] or advanced materials (Fe^0 based trimetallics (Pd, Cu and Ni)) [34], anion exchange polymer [19] is demonstrated in the possible attenuation of diclofenac from aqueous wastes. The granular activated carbon in the fixed bed column is found to be effective in the removal of diclofenac from aqueous solution as studied under column reactor operations [35]. The hybrid material precursor to carbon nanotubes and alumina is to be found effective materials in the removal of diclofenac from aqueous solutions [36]. In a line, hexagonal mesoporous silicate (HMS) and amine and mercapto-functionalised HMS derivatives are employed in the sorptive removal of diclofenac. Further, the mechanistic aspects are discussed using several physico-chemical parametric studies [37]. The Isabel grape (*Vitis labrusca* × *Vitis vinifera*) bagasse is employed in the diclofenac removal from aqueous solutions under the batch reactor operations [38]. Therefore, the present investigation aims to exploit the natural bentonite or locally available clay as to obtain the novel hybrid materials using the HDTMA or aluminium pillared HDTMA modified clay. The modified materials possess hydrophobic core, perhaps, provide an efficient partitioning of organic contaminants from aqueous solutions even at low level. The batch reactor operations are conducted at wide range of physico-chemical parametric studies; provides a plausible mechanism involved at solid/solution interfaces along with the fixed-bed column reactor operations performed to optimise the loading capacity of contaminants under the dynamic conditions.

2. Materials and methods

2.1. Materials

Bentonite clay was obtained from commercial supplier. It was mined at Bhuj, Gujarat, India. The bentonite was not separated anymore and used after simple washing with distilled water and dried at 90 °C in a drying oven. However, the local clay was collected from the field of Mizoram. Since this was having several impurities hence, was thoroughly separated using the standard ISRIC (International Soil Reference and Information Centre) method as detailed elsewhere (http://www.isric.org/isric/webdocs/docs/ISRIC_TechPap09_2002.pdf). The bentonite and local clay samples are crushed in mortar and sieved to obtain 100 BSS (British Standard Sieve) mesh size particles (0.150 mm). The bentonite and local clay powder is then subjected for its cation exchange capacity (CEC) determination using the standard US EPA (United States Environmental Protection Agency) method 9080 (http://www.epa.gov/osw/hazard/testmethods/sw846/pdfs/9080.pdf). The CEC of bentonite and local clay is found to be 69.35 and 46.38 meq/100 g of clay, respectively. Hexadecyltrimethylammonium bromide (HDTMA) and diclofenac sodium is procured from Sigma–Aldrich, USA. Aluminium(III) chloride is obtained from the Merck India. Sodium chloride, Extrapure is obtained from the HIMEDIA, India. The other chemicals are used of Analytical or equivalent grades. The deionised water is further purified (18 MΩ-cm) using a Millipore water purification system (Milli-Q+).

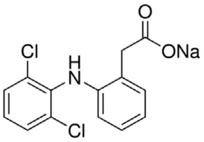

Structure of diclofenac sodium

2.2. Methodology

2.2.1. Preparation of HDTMA-modified clay

Bentonite and local clay is organically modified by the hexadecyltrimethylammonium bromide. The wet cation exchange process is followed as: 20 g of each clay powder is taken separately into 1 L of HDTMA solution containing 1.0 CEC of clay. The slurry is refluxed for 48 h at 60 °C under constant stirring. This is then filtered and the clay solid is washed with purified water. Excess or free surfactant is removed by the Soxhlet extraction. The organo-modified bentonite/or local clay is then dried at 90 °C in a drying oven. The solids are stored in the airtight polyethylene bottles. The HDTMA-modified bentonite/or local clay is then labelled as BH and LCH samples, respectively.

2.2.2. Preparation of inorgano–organo-modified clay

The bentonite/or local clay is pillared with aluminium and then modified with organo cation HDTMA as to obtain the HDTMA-Al-bentonite (BAH) or HDTMA-Al-local clay (LCAH) hybrid materials. A simple wet method is adopted as described elsewhere [6]. In brief, aluminium solution is prepared by mixing 100 mL of 0.4 mol/L NaOH and 100 mL of 0.2 mol/L aluminium chloride solutions under vigorous and constant stirring. The solution mixture is kept 7 days for ageing at room temperature. Further, in this aluminium solution a known amount of HDTMA (equivalent to 1:1 CEC of clay) is mixed under stirred conditions. Bentonite/or LC clay powders (4 g each) is taken in a round bottom flask and 300 mL water is then added. To this solution mixture, HDTMA mixed aluminium solution is introduced and stirred for *Ca* 5 h at room temperature. The slurry is then kept at room temperature for another 2 days. The modified bentonite/or local clay is separated carefully and the solid is washed with plenty of distilled water as to obtain the solid materials free from the halides. These solids are then dried at 60 °C in a drying oven and grounded gently in mortar. The powders (BAH and LCAH) are kept in the airtight polyethylene bottles for further investigations.

2.2.3. Characterisation and surface morphology of hybrid materials

The metal oxides present with the bentonite and local clay samples are obtained with the XRF analytical method using an X-ray Fluorescence Spectrometer (Model: ZSX 100e, Rigaku, Japan). Surface morphology of the hybrid materials along with the virgin clay is obtained taking the FE-SEM (Field Emission Scanning Electron Microscope) images using a Field Emission Scanning Electron Microscope (Model S-4700, Hitachi, Japan). X-ray diffraction (XRD) data is recorded using an X-ray diffraction machine (PANalytical, Netherland; Model X'Pert PRO MPD). The Cu K_α radiations having wavelength 1.5418 Å is used for X-ray diffraction analysis. FT-IR (Fourier Transform-Infra Red) data is obtained for these materials using a FT-IR machine (Bruker, Tensor 27, USA by KBR disk method).

2.2.4. pH_{PZC} measurements

The pH_{PZC} (Point of Zero Charge) of bentonite, local clay, BH, LCH, BAH and LCAH is obtained by the known method as described previously [6].

2.2.5. Batch reactor experiments

A stock solution of diclofenac sodium 50.0 mg/L is prepared; dissolving an appropriate amount of diclofenac sodium into purified water. The solubility is greatly enhanced with the sonication of solution mixture for 5 min. Further, the required diclofenac concentration is obtained by successive dilution of stock solutions. 10.0 mg/L of diclofenac solution (50 mL) is taken in the polyethylene bottles and the pH is adjusted using concentrated HCl/NaOH solutions. 0.1 g of solid sample is introduced with these solutions. The bottles are kept in an automatic incubator shaker (Incubator Shaker, TM Weiber, ACMAS Technologies Pvt. Ltd., India) for 24 h at 25 ± 1 °C. The prolonged period i.e., 24 h may enable to achieve an apparent equilibrium between the solid/solution interfaces. These bottles are then taken out from the shaker and filtered with 0.45 μm syringe filter and the pH is again checked and reported as equilibrium pH. The filtrates are then subjected to its bulk diclofenac concentration using UV–Visible spectrophotometer (Model: UV1, Thermo Electron Corporation, USA). The absorbance is recorded at 276 nm. The calibration curve is obtained using previously prepared standard diclofenac solutions having the concentrations of 1.0, 5.0, 10.0, 20.0 and 25.0 mg/L.

The diclofenac concentration dependence study is performed varying the diclofenac concentration from 1.0 to 20.0 mg/L at constant pH∼7.0 and at constant temperature 25 ± 1 °C. The adsorption process is conducted similar as detailed previously. Results are presented as percent removal of diclofenac as a function of initial diclofenac concentration (mg/L).

Time dependence sorption of diclofenac by these materials is obtained at different time intervals. The initial diclofenac concentration 10.0 mg/L with solid dose 2.0 g/L is taken as constant and the sorption experiments are conducted at constant pH ∼7.0 and temperature 25 ± 1 °C. Results are then reported as percent removal of diclofenac as a function of time (min).

Effect of background electrolyte concentration dependence sorption is studied varying the background electrolyte concentration from 0.0001 to 0.1 mol/L NaCl of diclofenac solution (10.0 mg/L). The solution pH (∼7.0) and temperature (25 ± 1 °C) is kept constant throughout the experiments. Results are presented as percent diclofenac removed as a function of background electrolyte concentrations.

2.2.6. Fixed-bed column experiments

The fixed-bed column experiments are conducted using a glass column (1 cm inner diameter) packed with 0.5 g of modified clay solid (kept middle in the column). Below and above to this solid, *Ca* 2.0 g of virgin sand particles are placed (14–16 BSS) and rest of the column is packed with glass beads. Diclofenac solution *Ca* 10.0 mg/L pH ∼7.0 is pumped upward from the bottom of column using peristaltic pump (KrosFlo Research I Peristaltic Pump, Spectrum Laboratories Inc., California, USA), at a constant flow rate of 1.0 mL/min. Effluent solution is collected using a fraction collector (Spectra/Chrom CF-2 Fraction Collector, Spectrum Laboratories Inc., California, USA). The collected effluents are then filtered using

0.45 μm syringe filter and the total bulk diclofenac concentration is measured using UV–Vis spectrophotometer.

The breakthrough data obtained by the fixed-bed column experiments is further utilised to optimise the loading capacity of diclofenac by the hybrid materials under the dynamic conditions employing the known Thomas Eq. (1) [39]:

$$\frac{C_e}{C_0} = \frac{1}{1 + e^{(K_T(q_0 m - C_0 V))/Q}} \tag{1}$$

where C_e and C_0 are the concentrations of effluent and influent solutions of diclofenac (mg/L), respectively; K_T refer to the Thomas rate constant (L/min/mg); q_0 is the maximum amount of diclofenac loaded (mg/g) under the specified column conditions; 'm' is the mass of hybrid materials taken in column (g); V is the throughput volume (L); and Q is flow rate of pumped diclofenac solution (L/min). The column data is fitted to a non-linear Thomas equation using the least square fitting method to estimate two unknown variables i.e., K_T and q_0.

3. Results and discussion

3.1. Characterisation of materials

The bentonite and local clay samples were subjected for the elemental composition using the XRF analytical method. The elemental data is then optimised to its oxide values. The results are then returned in Table 1. It is evident from the table that both the clay samples possessed mainly the silicon, aluminium and iron oxides. Also a significant amount of Na, Mg and K is present. This is, possibly, the exchangeable cations present within the interspace of clay. Moreover, both the clay samples possess almost an identical metal oxide composition.

The FT-IR data is collected for the bentonite and local clay based samples and presented in Fig. 1(a) and (b), respectively. It is found that characteristic and prominent IR stretching bands are occurred around the wave numbers 3625 and 3430 cm^{-1} are assigned as asymmetric and symmetric stretching vibrations of H–O–H. Similarly, H–O–H bending vibration is observed around the wavenumber of 1630 cm^{-1} for these samples. This clearly indicates the presence of hydroxyl groups within the clay sheets and the water molecule present within the interlayer space of bentonite [40–42]. A prominent IR peak centred around 1030 cm^{-1} is an indicative of the Si–O stretching vibrations [43]. Similarly, couple of IR bands centred around 690 and 790 cm^{-1} are assigned to the Si–O quartz vibrations [44]. The presence of Fe–O is ascertained with a prominent peak around the 540 cm^{-1} for all these solids. Further, interesting to note that the modified samples BH, BAH, LCH or LCAH, having with varied intensities, possessed prominent peaks centring around 2930 and 2850 cm^{-1} are to be considered as –CH$_2$ asymmetric stretching and –CH$_2$ symmetric vibrations, respectively [40]. This confirms the introduction of HDTMA within the clay network for all these modified solids.

Table 1
Various metal oxides present in bentonite and local clay samples estimated by the XRF analysis.

Components	Mass percentage	
	Bentonite	Local clay
Na_2O	2.11	2.17
MgO	2.77	2.72
Al_2O_3	21.87	21.89
SiO_2	54.51	54.57
P_2O_5	0.13	0.13
K_2O	1.39	1.38
CaO	0.98	0.95
TiO_2	2.51	2.47
Cr_2O_3	0.04	0.04
MnO	0.17	0.19
Fe_2O_3	12.46	12.45

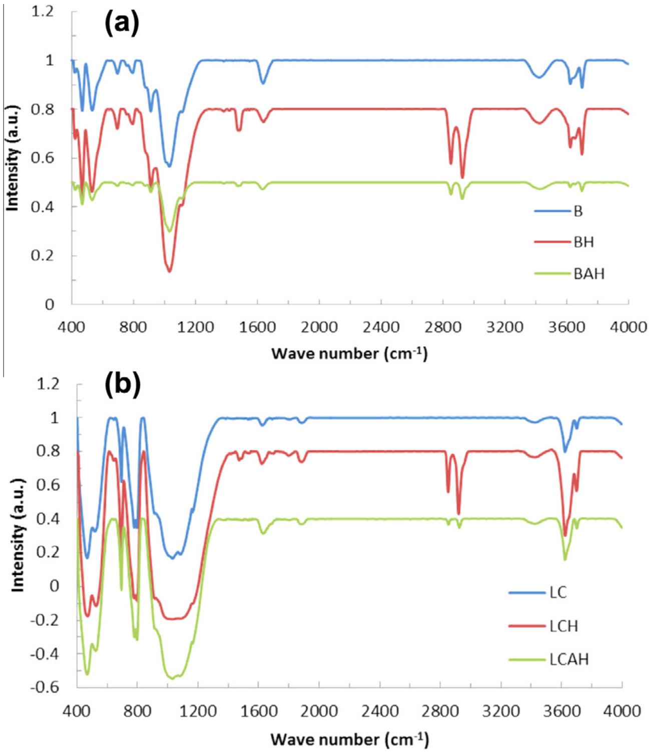

Fig. 1. FT-IR spectra of (a) bentonite and modified bentonite; and (b) local clay and modified local clay samples.

Further, the X-ray diffraction analysis is conducted for these solids i.e., B, BH, BAH, LC, LCH or LCAH. The results are presented graphically in Fig. 2(a) and (b), respectively for the bentonite and local clay based solids. Sharp diffraction peaks observed for these solids with a definite d-spacing makes possible to assign the peaks of different mineral phases of clay materials. XRD data of bentonite and local clay is matched with the standard ICDD (International Centre for Diffraction Data) reference pattern. It is noted that both the clay samples contained with the quartz, smectite, illite and kaolinite minerals with varied percent composition as characteristic peaks are assigned in the XRD diffraction pattern. Further, quantitatively, it is evaluated that bentonite is having the quartz, smectite, kaolinite and illite, respectively 43.71%, 23.17%, 1.73% and 31.39%. Similarly, the local clay is contained with the 79.35%, 6.20%, 0.45% and 14.01%, respectively the quartz, smectite, kaolinite and illite. Further, the other visible diffraction peaks are, perhaps, due to the presence of some impurity. The XRD pattern of modified clay samples is almost identical to its virgin clay having with slight change in d-values and intensities of peaks.

The surface morphology of these solids is obtained taking the FE-SEM images. The images are returned in Fig. 3(a–f), respectively for the solids B, BH, BAH, LC, LCH and LCAH. The images clearly show that the B and LC solids show relatively compact and ordered surface structure. Moreover, the surface of these solids is devoid of meso- or macro-pores. On the other hand, however, the organo-modified bentonite/or LC (i.e., BH or LCH) solids show more heterogeneous and disordered surface structures. It is assumed that the water molecules or the exchangeable cations present within the interspace of clay is exchanged with the HDTMA and firmly occupied within the interspace of bentonite or local clay. Also the surface structure seems more porous in nature. Further, the BAH and LCAH solids show the similar disordered structure but distinct and

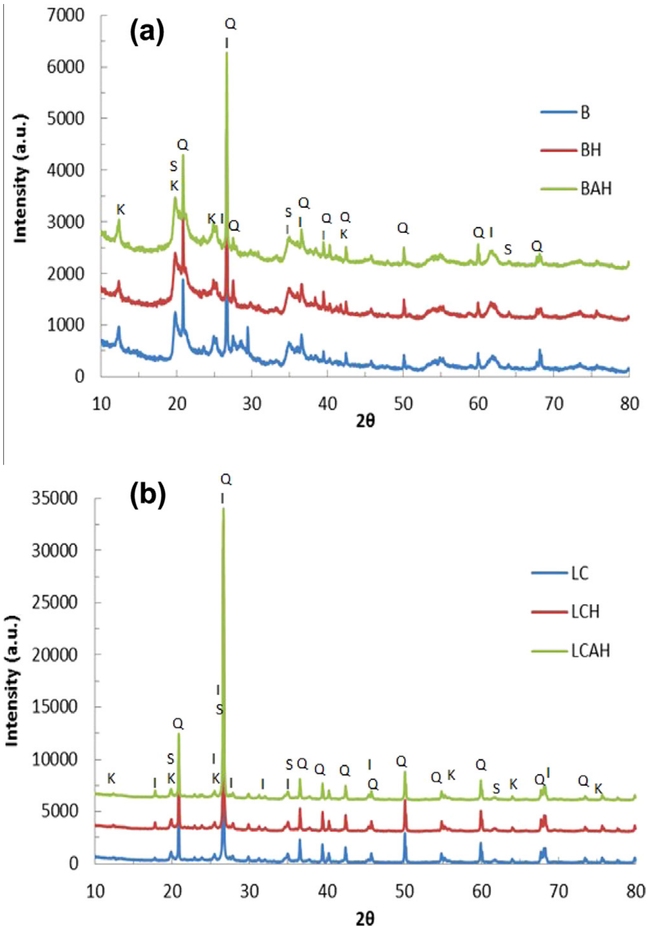

Fig. 2. X-ray diffraction pattern of (a) bentonite and modified bentonite; and (b) virgin local clay and modified local clay samples. [S: Smectite; K: Kaolinite; Q: Quartz; I: Illite.]

evenly distributed fine particles are observed onto the surface, perhaps aluminium is aggregated/immobilised as aluminium oxide onto the solid surface. It may also likely to pillar the clay sheet structure once entered within the interspace.

3.2. Batch reactor operations

3.2.1. Effect of pH

The pH dependence sorption of diclofenac sodium by these solids is carried out and results are presented graphically in Fig. 4. The pH_{PZC} value of these solids is found to be 10.0, 8.2, 6.1, 5.8, 5.1 and 5.1 for the samples B, BH, BAH, LC, LCH, LCAH, respectively. It is assumed that the solid carries net positive charge below this pH and beyond this pH the surface carries a net negative charge with the hydrolytic dissociation of surface functional groups (*cf* Eq. (2)).

$$\equiv SOH_2^+ \leftrightarrow \underset{pH_{PZC}}{\equiv} SOH^0 \leftrightarrow \equiv SO^- \qquad (2)$$

Moreover, on the other hand the diclofenac is having low dipole moment and acid dissociation constant value (pK_a) is 4.21 [45]. This implies that diclofenac carries negative charge beyond pH 4.2. The sorption of diclofenac sodium by these hybrid materials shows that a very high percent uptake (*Ca* 100%) of diclofenac is obtained for all these solids, which is almost independent of change in solution pH at least up to the pH 9.5 (*cf* Fig. 4). The uptake is therefore independent to the charge carried by the solid or solute species. Therefore, the possible mechanism of diclofenac sodium uptake by these modified solids is primarily demonstrated with the fact that the introduction of organic cation (HDTMA) with the clay network caused to enhance the organophilic behaviour of the surface having a strong hydrophobic core. The alkylammonium molecule preferentially resides at the layer surface, leaving the organic tail radiating away from the surface and providing a strong hydrophobic core [46,47]. This enables diclofenac to partition at the introduced hydrophobic core [48]. It was previously mentioned that sufficient loading of surfactant forms a bilayer and this results in a reversal of the charge on the external surface of clay. This provides the hydrophobic end of organic cation where neutral or slightly polar organic compounds can partition [2,48]. On the other hand, the Al pillared HDTMA modified local clay show slightly less uptake of diclofenac possibly due to the insufficient loading of the HDTMA cation which reduced the hydrophobic core within the clay network. Further, beyond pH 9.5 a slight decrease in the uptake of diclofenac is registered by these hybrid materials indicates that due to strong repulsive force seemingly restricts the partitioning of diclofenac within the modified clay samples [49]. Similar results are found for the uptake of BPA by ordered mesoporous carbon [50] or multi-walled carbon nanotubes [51]. Earlier, it was reported that the uptake of diclofenac by the hybrid solids novel granular carbon nanotubes (CNTs)/alumina (Al_2O_3) was greatly hindered at higher pH conditions whereas the uptake of carbamazepine was almost unaffected. The significant decrease in uptake of diclofenac was demonstrated due to the fact that (1) Electrostatic repulsion occurred between the diclofenac and CNTs (2) the size exclusion effect, which was found important in the sorption of monoaromatic and pharmaceutical compounds on CNTs, activated carbons and ordered micro-porous carbons [52,53], therefore, the larger molecular size of diclofenac and steric hindrance would limit its diffusion into inner adsorptive sites in the sorption process [36].

Further, it is noted that the virgin bentonite and local clay show very insignificant uptake of diclofenac (*Ca* 30% at pH 3.8). The uptake is further decreased slightly with increasing the solution pH and reaches about 17% at pH 10.1. These results therefore enable that the unmodified clay materials possess very low uptake capacity of diclofenac from aqueous solutions. However, the hybrid materials provide a strong hydrophobic core for effective partitioning of diclofenac and hence a high attenuation of diclofenac is achieved by the modified solids.

3.2.2. Effect of diclofenac concentration

The concentration dependence removal of diclofenac is studied for a wide range of initial diclofenac concentrations i.e., from 1.0 to 20.0 mg/L at constant pH 7.0. Results are presented graphically in Fig. 5. Figure reveals that increasing the concentration of diclofenac from 1.0 to 20.0 mg/L, a very high percent uptake of diclofenac, could not affect the percent removal of diclofenac from aqueous solution. These results again pointed a strong affinity of hybrid materials (BH, BAH and LCH) towards the attenuation of diclofenac. However, a slight less removal of diclofenac is observed (i.e., around 80%) using the LCAH solid. This is due to the less loading of HDTMA with the clay solid. The results are in consistent with the pH dependence study.

3.2.3. Time dependence removal

Further, the time dependence removal of diclofenac is studied and the amount of diclofenac removed as a function of time is presented graphically in Fig. 6. It is evident from the figure that the materials BH and BAH are extremely efficient particularly in the removal of diclofenac from aqueous solutions since within 2–3 min of contact almost an apparent equilibrium is achieved. This again reaffirms the affinity of these solids towards the diclofenac. However, the uptake of diclofenac onto the LCH and LCAH solids show comparatively slow uptake process and an apparent solid solution equilibrium is achieved within *Ca* 15 min of contact.

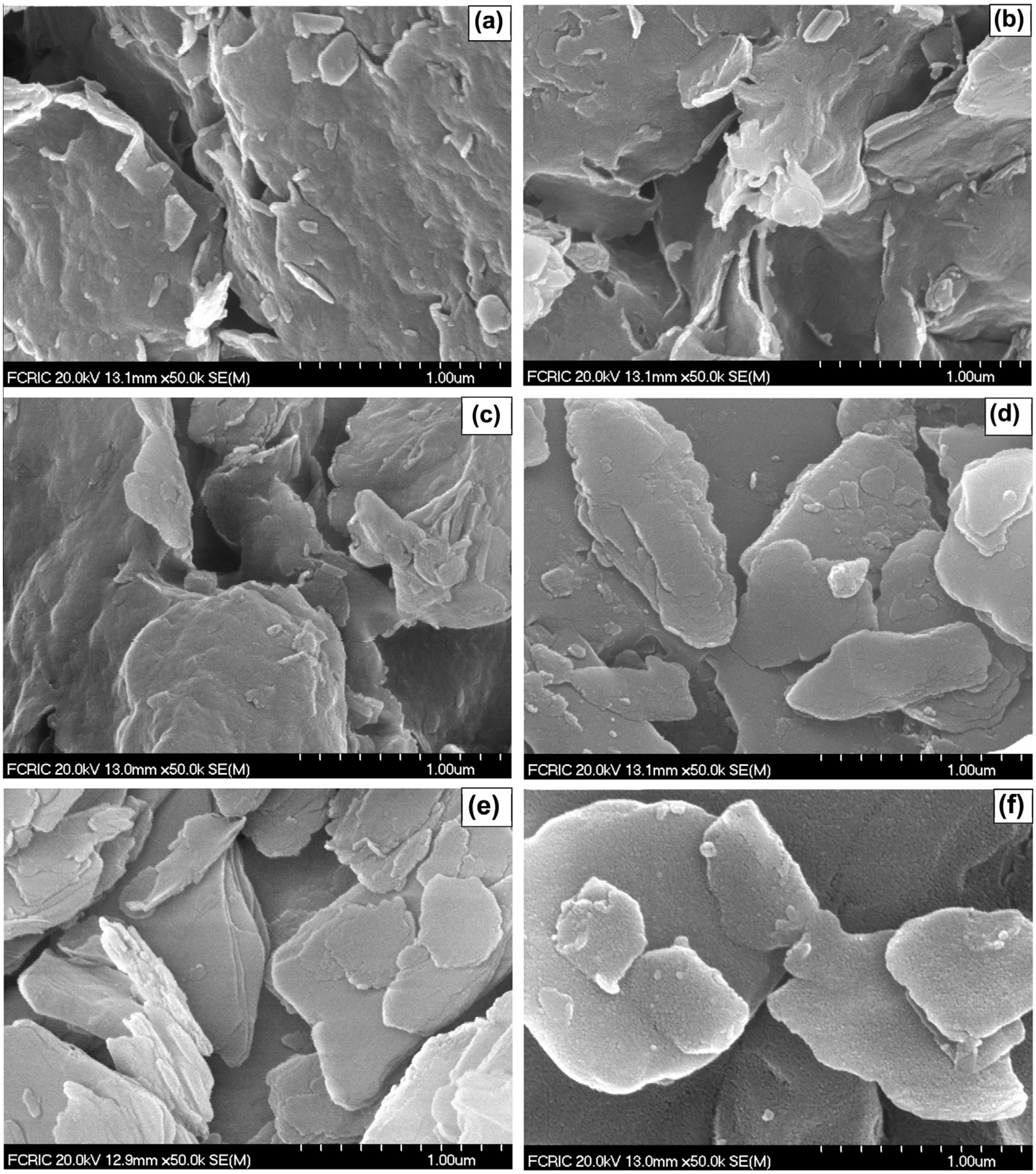

Fig. 3. SEM images of (a) virgin bentonite; (b) BH; (c) BAH; (d) LC; (e) LCH; and (f) LCAH solids.

The kinetic data is further utilised in the kinetic modelling to estimate the rate constants along with the removal capacity of these solids. Since the uptake of diclofenac by the BH and BAH is extremely fast hence, restricting to perform the kinetic modelling studies. However, the uptake process of diclofenac by the LCH and LCAH is relatively slow hence, this is utilised for the modelling studies. The three different kinetic models *viz.*, pseudo-first order (PFO) [54], pseudo-second order (PSO) [55] and fractal-like pseudo-second order (FL-PSO) [56] kinetic models to its non-linear forms (Eqs. (3–5)) are utilised:

$$q_t = q_e(1 - \exp(-k_1 t)) \quad (3)$$

$$q_t = \frac{k_2 q_e^2 t}{1 + k_2 q_e t} \quad (4)$$

$$q_t = \frac{k q_e^2 t^{\alpha}}{1 + k q_e t^{\alpha}} \quad (5)$$

where q_t and q_e are the amount of diclofenac removed at time 't' and removal capacity at equilibrium, respectively. k_1 and k_2 are the pseudo-first and pseudo-second order rate constants, respectively. Similarly, the constants k and α are referred to the rate constant and fractal constant, respectively. The pseudo-first-order kinetic model which is theoretically derived by the Lagergren could show the properties of the Langmuir rate at initial times of adsorption or close to equilibrium [54,57]. Similarly, the theoretical studies, conducted previously, indicates that the rate coefficient of pseudo-second-order model i.e., k_2 is virtually a complex function of the initial concentration of the sorbing species [54]. However, the FL-PSO model approach is basically implies to the fact that there are different paths of adsorption that take place in adsorption and the adsorption rate coefficient is a function of time [58]. A non-linear least square fitting is conducted for the estimation of unknown parameters. The estimated values of the unknown parameters along with the least square sum are tabulated in Table 2. Results are best

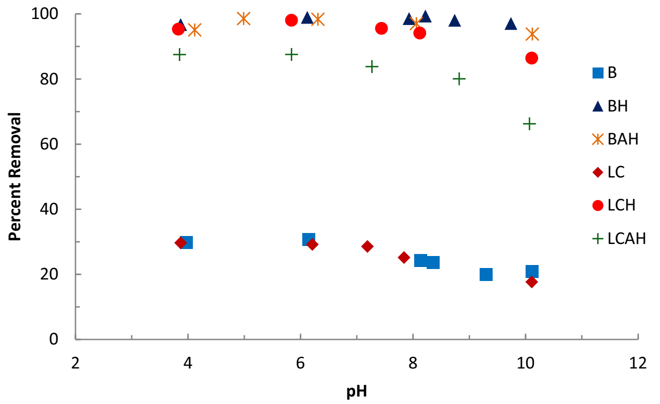

Fig. 4. pH dependence removal of diclofenac using modified and unmodified samples of bentonite and local clay.

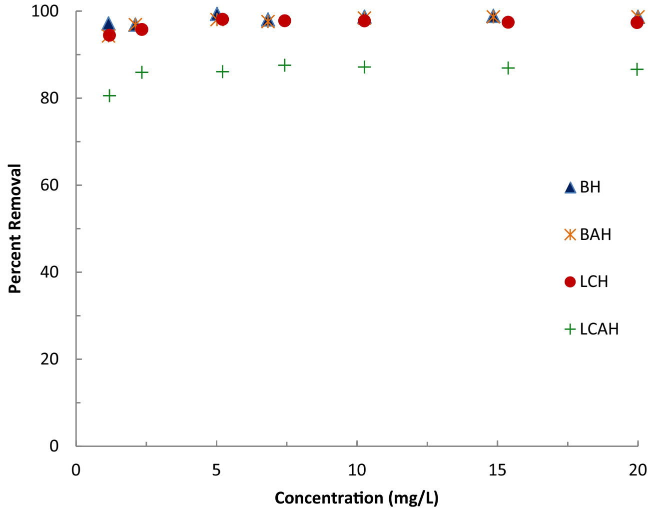

Fig. 5. Removal of diclofenac from aqueous solutions using various hybrid materials as a function of initial diclofenac concentration.

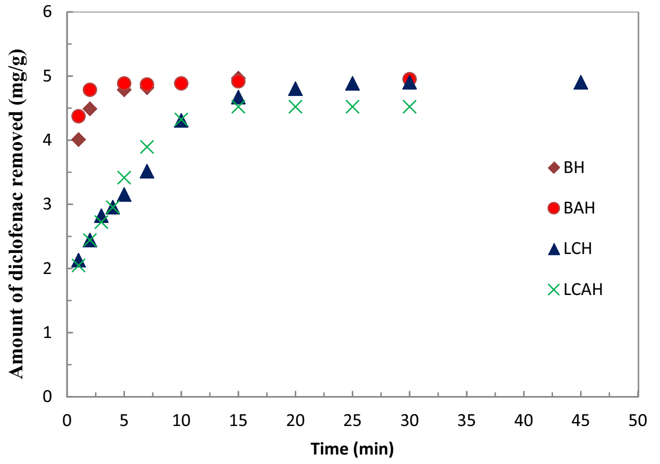

Fig. 6. Extent of diclofenac removal by the hybrid materials as a function of time.

fitted to the PSO and FL-PSO models comparing to the PFO model. The results again show that comparing to the LCAH the LCH possess higher removal capacity at least for the diclofenac removal. Moreover, the applicability of the PSO model indicates that the sorbate species are bound onto the surface of solids by strong forces. Earlier, it was mentioned that the adsorption of divalent metal cations onto the *sphagnum* moss peat followed the second-order rate laws. Hence, it is concluded that metal cations are bound with strong chemical forces as occurred between the valency forces sharing or the exchange of electrons between the peat and divalent metal ions forming covalent bonds [59,60]. Similarly, the diclofenac sorption onto the Isabel grape bagasse follows the pseudo-second order rate law. This concludes that the rate-controlling step depends on the physico-chemical interactions between the sorbing species and the solid adsorbent surface functional groups [38].

3.2.4. Effect of background electrolyte concentration

Effect of background electrolytes in the sorptive removal of diclofenac by these hybrid materials could enable to explain the mechanism involved at solid/solution interfaces [61]. The specific sorption is usually not much influenced with the change in background electrolyte concentrations; whereas the non-specific sorption is greatly influenced with the change in back ground electrolyte concentrations. Therefore, the sorption of diclofenac by BH, BAH, LCH and LCAH is assessed varying the background electrolyte concentrations from 0.0001 to 0.1 mol/L NaCl at an initial diclofenac concentration 10.0 mg/L and at constant pH 7.0. The percent removal of diclofenac is obtained as a function of background electrolyte concentrations. Results show that increasing the background electrolyte concentrations even up to 1000 times could not affect the percent uptake of diclofenac by these solids employed. Therefore, this infers the strong affinity of these solids towards the diclofenac. Also this implies that the partitioned diclofenac is bound with relatively stronger forces which retain firmly the diclofenac molecule onto or within the interspace of hybrid materials. The other report shows that the diclofenac removal by A520E resin (AER) is not affected significantly by the presence of phosphate or citrate which shows that an unfavourable electrostatic interaction occurs between the phosphate/or citrate and AER [19]. Previously, it was reported that the As(V) is adsorbed specifically onto γ-Al$_2$O$_3$ within the pH region 3.0–9.2; whereas As(III) is not adsorbed specifically within the pH region 4.5–9.0 [62,63].

3.3. Fixed-bed column reactor operations

Fixed-bed column reactor operations are performed to assess the removal/loading capacity of the hybrid materials BH, BAH, LCH and LCAH for diclofenac under the dynamic conditions. The fixed bed column experiments are conducted having the column conditions as stated previously. The breakthrough curves are presented graphically in Fig. 7. The figure reveals that relatively high breakthrough volume is obtained for diclofenac by these solids. A complete breakthrough volume is achieved at the throughput volume of 1.56, 1.32, 0.62 and 0.51 L, respectively for the BH, BAH, LCH and LCAH solids. Relatively high breakthrough volume is obtained for diclofenac loading, indicates strong affinity of these solids towards the diclofenac under the fixed-bed column conditions [64,65].

Further, the non-linear least square fitting is performed using the breakthrough column data employing the Thomas equation (Eq. (1)). The fitting is conducted to simulate two unknown parameters i.e., Thomas constants K_T and q_0 (*Cf* Fig. 7). The values of Thomas constants along with the least square sum are estimated and returned in Table 3. The data indicates that a high loading capacity is achieved for diclofenac by these solids under the dynamic conditions. Relatively, BH shows higher removal capacity comparing to the BAH solid. Similarly, LCH solid possesses relatively higher removal capacity for diclofenac than LCAH solid. This infers that Al pillared samples possess relatively less loading of HDTMA which

Table 2
Kinetic parameters estimated using various kinetic models for the removal of diclofenac by LCH and LCAH solids.

Systems	PFO model			PSO model			FL-PSO model			
	q_e	k_1	s^2	q_e	k_2	s^2	q_e	k	α	s^2
LCH-diclofenac	4.49	0.32	1.58	5.18	0.08	0.79	17.79	0.01	0.37	0.18
LCAH-diclofenac	4.39	0.35	0.86	5.04	0.09	0.41	6.64	0.06	0.61	0.23

s^2: Least square sum.

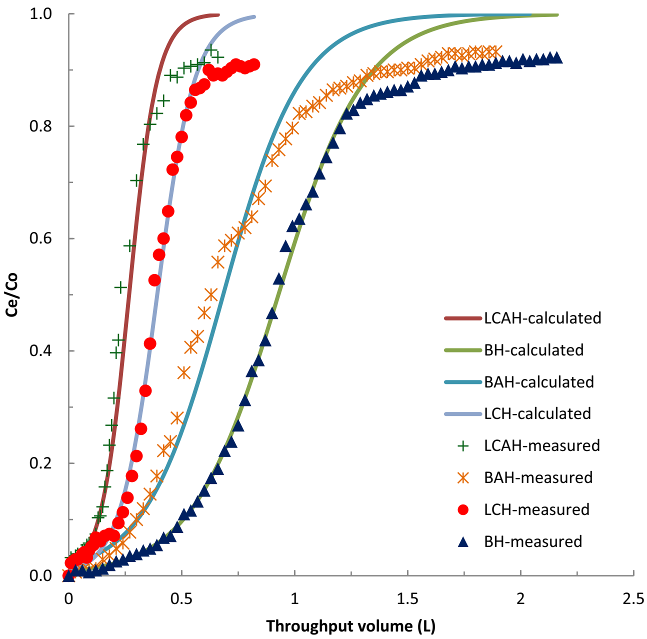

Fig. 7. Breakthrough curves obtained for the removal of diclofenac by hybrid materials.

causes in decrease of diclofenac partitioning. Overall the removal capacity follows the trend: BH, BAH, LCH and LCAH. It is further noted that the removal capacity of LCH or LCAH for diclofenac is found relatively higher by the fixed-bed column experiments comparing to the batch reactor operations as estimated by the PSO simulation method (vide Table 2). This is possibly due to the fact that a fixed-bed process is having an additional advantage of continuous contact of sorbing species with solid surface which may result in better exhaustion capacity than batch reactor operation [66]. Although, LCH sample possesses relatively less loading capacity for diclofenac but could be, an useful natural material, exploited in the removal/speciation of diclofenac from aqueous solutions. Therefore, this local clay, perhaps, an alternative material to be employed in the remediation of aquatic environment contaminated with diclofenac micro-pollutant. These results are similar to the findings of batch reactor experiments. Also results are in a line to other reports in which the Thomas equation is utilised to demonstrate the loading capacity of different sorbents [67,68].

Table 3
Thomas constants estimated in the removal of diclofenac by hybrid materials.

Materials	Thomas constants		Least square sum (s^2)
	q_0 (mg/g)	K_T (L/min/mg)	
BH	18.99	5.09×10^{-4}	3.2
BAH	13.99	5.65×10^{-4}	5.60
LCH	7.99	1.19×10^{-3}	0.99
LCAH	5.49	1.57×10^{-3}	3.50

4. Conclusion

The hybrid materials precursor to the natural bentonite and local clay is synthesised and characterised. The IR data shows that the organic molecule (HDTMA) is well introduced within the clay network. The XRD analysis enabled the presence of quartz, smectite, kaolinite and illite (having varied percentage) with these two clay samples i.e., bentonite and local clay. SEM images of these solids show disordered structure of HDTMA modified clay materials whereas Al pillared solids shows that fine particles of aluminium oxides are aggregated onto the clay surface. Further, the materials are utilised in the batch and column reactor operations in the remediation of diclofenac from aqueous solutions. The batch data implies that a very high uptake of diclofenac by these hybrid materials are almost unaffected with the increase in sorptive pH (pH 3.8–10.1), concentration (1.0–20.0 mg/L) and the background electrolyte concentration (0.0001–0.1 mol/L NaCl). Moreover, the uptake of diclofenac by these solids is extremely efficient as within 2 min of contact an apparent equilibrium is achieved by the BH and BAH solids whereas within 10–15 min of contact time the saturation is obtained by the LCH and LCAH solids. The fixed-bed column results show that relatively high breakthrough volume is obtained for attenuation of diclofenac using the hybrid materials. Further, the breakthrough data is fitted well to the Thomas equation therefore the loading capacity of diclofenac is estimated to be 18.99, 13.99, 7.99 and 5.49 mg/g for the solids BH, BAH, LCH and LCAH, respectively. The materials are found to be useful in the effective and efficient removal of diclofenac from aqueous solutions. Hence, these materials could have wider application in an efficient molecular sieving purpose for the decontamination of diclofenac from aqueous wastes.

Acknowledgements

One of authors DT wishes to acknowledge the CSIR, New Delhi for the financial support as in the form of Research Project (vide No.: 01 (2567)/12/EMR-II). The authors acknowledges Dr. G.V. Narasimha Rao, Head, Materials Characterization & Testing Group (MCTG), International Advanced Research Center for Powder Metallurgy & New Materials (ARCI), Department of Science & Technology (DST), Government of India, Balapur P.O., Hyderabad 500005, India for conducting the XRD analysis.

References

[1] J. Konta, Clay and man: clay raw materials in the service of man, Appl. Clay Sci. 10 (1995) 275–335.
[2] S.M. Lee, D. Tiwari, Organo and inorgano-organo-modified clays in the remediation of aqueous solutions: an overview, Appl. Clay Sci. 59–60 (2012) 84–102.
[3] F. Bergaya, G. Lagaly, General introduction: clays, clay minerals, and clay science, in: F. Bergaya, G. Theng, G. Lagaly (Eds.), Developments in Clay Science, Handbook of Clay Science, vol. 1, Elsevier, New York, 2006, pp. 1–18.
[4] Z.R. Liu, S.Q. Zhou, Adsorption of copper and nickel on Na–bentonite, Process Saf. Environ. Prot. 88 (2010) 62–66.
[5] C.M. Futalan, C.C. Kan, M.L. Dalida, K.J. Hsien, C. Pascua, M.W. Wan, Comparative and competitive sorption of copper, lead, and nickel using chitosan immobilized on bentonite, Carbohydr. Polym. 83 (2011) 528–536.

[6] D. Tiwari, S.M. Lee, Novel hybrid materials in the remediation of ground waters contaminated with As(III) and As(V), Chem. Eng. J. 204–206 (2012) 23–31.

[7] L. Zhu, S. Tian, J. Zhu, Y. Shi, Silylated pillared clay (SPILC): a novel bentonite-based inorgano–organo composite sorbent synthesized by integration of pillaring and silylation, J. Colloid Interface Sci. 315 (2007) 191–199.

[8] S.M. Koh, J.B. Dixon, Preparation and application of organo-minerals as sorbents of phenol, benzene and toluene, Appl. Clay Sci. 18 (2001) 111–122.

[9] D. Tiwari, W. Kim, M. Kim, S.K. Prasad, S.M. Lee, Organo-modified sericite in the remediation of phenol-contaminated waters, Desalin. Water Treat. Paper Online (2014), http://dx.doi.org/10.1080/19443994.2013.846562.

[10] P.X. Wu, Z.W. Liao, H.F. Zhang, J.G. Guo, Adsorption of phenol on inorganic-organic pillared montmorillonite in polluted water, Environ. Int. 26 (2001) 401–407.

[11] C.M. Dai, S.U. Geissen, Y.L. Zhang, Y.J. Zhang, X.F. Zhou, Selective removal of diclofenac from contaminated water using molecularly imprinted polymer microspheres, Environ. Pollut. 159 (2011) 1660–1666.

[12] T. Heberer, Occurrence, fate, and removal of pharmaceutical residues in the aquatic environment: a review of recent research data, Toxicol. Lett. 131 (2002) 5–17.

[13] S. Mompelat, B. LeBot, O. Thomas, Occurrence and fate of pharmaceutical products and by-products, from resource to drinking water, Environ. Int. 35 (2009) 803–814.

[14] X.F. Zhou, C.M. Dai, Y.L. Zhang, R. Surampalli, T. Zhang, A preliminary study on the occurrence and behavior of carbamazepine (CBZ) in aquatic environment of Yangtze River Delta, China, Environ. Monit. Assess. 173 (2010) 45–53.

[15] T.A. Ternes, A. Joss, Human Pharmaceuticals, Hormones and Fragrances. The Challenge of Micropollutants in Urban Water Management, IWA publishing, London, New York, 2006.

[16] J. Lienert, K. Gudel, B.I. Escher, Screening method for ecotoxicological hazard assessment of 42 pharmaceuticals considering human metabolism and excretory routes, Environ. Sci. Technol. 41 (2007) 4471–4478.

[17] J. Lienert, T. Buerki, B.I. Escher, Reducing micropollutants with source control: substance flow analysis of 212 pharmaceuticals in faeces and urine, Water Sci. Technol. 56 (2007) 87–96.

[18] A. Joss, E. Keller, A. Alder, A. Gobel, C. McArdell, T. Ternes, H. Siegrist, Removal of pharmaceuticals and fragrances in biological wastewater treatment, Water Res. 39 (2005) 3139–3152.

[19] K.A. Landry, T.H. Boyer, Diclofenac removal in urine using strong-base anion exchange polymer resins, Water Res. 47 (2013) 6432–6444.

[20] D. Vogna, R. Marotta, A. Napolitano, R. Andreozzi, M. d'Ischia, Advanced oxidation of the pharmaceutical drug diclofenac with UV/H_2O_2 and ozone, Water Res. 38 (2004) 414–422.

[21] Y. Zhang, S.U. Geissen, C. Gal, Carbamazepine and diclofenac: removal in wastewater treatment plants and occurrence in water bodies, Chemosphere 73 (2008) 1151–1161.

[22] R. Bort, X. Ponsoda, R. Jover, M.J. Gomez-Lechon, R.J.V. Castell, Diclofenac toxicity to hepatocytes: a role for drug metabolism in cell toxicity, J. Pharmacol. Exp. Ther. 288 (1998) 65–72.

[23] T. Haap, R. Triebskorn, H.R. Köhler, Acute effects of diclofenac and DMSO to Daphnia magna: immobilisation and hsp70-induction, Chemosphere 73 (2008) 353–359.

[24] C. Martínez, L.M. Canle, M.I. Fernández, J.A. Santaballa, J. Faria, Aqueous degradation of diclofenac by heterogeneous photocatalysis using nanostructured materials, Appl. Catal. B 107 (2011) 110–118.

[25] J.L.G. Oaks, M. Virani, M.Z. Watson, R.T. Meteyer, C.U. Rideout, B.A. Shivaprasad, H.L. Ahmed, S. Chaudhry, M.J.I. Arshad, M. Mahmood, S. Ali, A.A.A. Khan, Diclofenac residues as the cause of vulture population decline in Pakistan, Nature 427 (2004) 630–633.

[26] N. Zhang, G. Liu, H. Liu, Y. Wang, Z. He, G. Wang, Diclofenac photodegradation under simulated sunlight: effect of different forms of nitrogen and kinetics, J. Hazard. Mater. 192 (2011) 411–418.

[27] A.C. Mehinto, E.M. Hill, C.R. Tyler, Uptake and biological effects of environmentally relevant concentrations of the nonsteroidal anti-inflammatory pharmaceutical diclofenac in rainbow trout (*Oncorhynchus mykiss*), Environ. Sci. Technol. 44 (2010) 2176–2182.

[28] I. Vergili, Application of nanofiltration for the removal of carbamazepine, diclofenac and ibuprofen from drinking water sources, J. Environ. Manage. 127 (2013) 177–187.

[29] K. Ikehata, N.J. Naghashkar, M.G. El-Din, Degradation of aqueous pharmaceuticals by ozonation and advanced oxidation processes: a review, Ozone-Sci. Eng. 28 (2006) 353–414.

[30] S.D. Kim, J. Cho, I.S. Kim, B.J. Vanderford, S.A. Snyder, Occurrence and removal of pharmaceuticals and endocrine disruptors in South Korean surface, drinking and waste waters, Water Res. 41 (2007) 1013–1021.

[31] J. Radjenovic, M. Petrovic, F. Ventura, D. Barcelo, Rejection of pharmaceuticals in nanofiltration and reverse osmosis membrane drinking water treatment, Water Res. 42 (2008) 3601–3619.

[32] M.R. Boleda, M.T. Galceran, F. Ventura, Behavior of pharmaceuticals and drugs of abuse in a drinking water treatment plant (DWTP) using combined conventional and ultrafiltration and reverse osmosis (UF/RO) treatments, Environ. Pollut. 159 (2011) 1584–1591.

[33] E.S. Rigobello, A.D. DiBernardo, E.M.L.V. DiBernardo, Removal of diclofenac by conventional drinking water treatment processes and granular activated carbon filtration, Chemosphere 92 (2013) 184–191.

[34] A. Ghauch, H.A. Assi, H. Baydoun, A.M. Tuqan, A. Bejjani, Fe^0-based trimetallic systems for the removal of aqueous diclofenac: mechanism and kinetics, Chem. Eng. J. 172 (2011) 1033–1044.

[35] J.L. Sotelo, A. Rodríguez, S. Álvarez, J. García, Removal of caffeine and diclofenac on activated carbon in fixed bed column, Chem. Eng. Res. Design 90 (2012) 967–974.

[36] H. Wei, S. Deng, Q. Huang, Y. Nie, B. Wang, J. Huang, G. Yu, Regenerable granular carbon nanotubes/alumina hybrid adsorbents for diclofenac sodium and carbamazepine removal from aqueous solution, Water Res. 47 (2013) 4139–4147.

[37] N. Suriyanon, P. Punyapalakul, C. Ngamcharussrivichai, Mechanistic study of diclofenac and carbamazepine adsorption on functionalized silica-based porous materials, Chem. Eng. J. 214 (2013) 208–218.

[38] M. Antunes, V.I. Esteves, R. Guégan, J.S. Crespo, A.N. Fernandes, M.M. Giovanela, Removal of diclofenac sodium from aqueous solution by Isabel grape bagasse, Chem. Eng. J. 192 (2012) 114–121.

[39] H.C. Thomas, Heterogeneous ion exchange in a flowing system, J. Am. Chem. Soc. 66 (1944) 1664–1666.

[40] U.F. Alkaram, A.A. Mukhlis, A.H. Al-Dujaili, The removal of phenol from aqueous solutions by adsorption using surfactant-modified bentonite and kaolinite, J. Hazard. Mater. 169 (2009) 324–332.

[41] J.M. Trillo, M.D. Alba, A.A. Castro, A. Munoj, J. Poyato, M. Tobias, Local environment of lanthanum ions in montmorillonite upon heating, Clay Miner. 27 (1992) 423–434.

[42] S.E. Miller, G.R. Heath, R.D. Gonzalez, Effects of temperature on the sorption of lanthanides by montmorillonite, Clays Clay Miner. 30 (1982) 111–122.

[43] J. Madejova, P. Komadel, Baseline studies of the clay minerals society source clays: infrared methods, Clays Clay Miner. 49 (2001) 410–432.

[44] B.J. Saikia, G. Parthasarthy, Fourier transform infrared spectroscopic characterization of kaolinite from Assam and Meghalaya, Northeastern India, J. Mod. Phys. 1 (2010) 206–210.

[45] M. Meloun, S. Bordovska, L. Galla, The thermodynamic dissociation constants of four non-steroidal anti-inflammatory drugs by the least-squares nonlinear regression of multiwavelength spectrophotometric pH-titration data, J. Pharm. Biomed. Anal. 45 (2007) 552–564.

[46] M. Alexandre, P. Dubois, Polymer-layered silicate nano-composites: preparation, properties and uses of a new class of materials, Mater. Sci. Eng. Res. 28 (2000) 1–63.

[47] M. Zanetti, S. Lomakin, G. Camino, Polymer layered silicate nano-composites, Macromol. Mater. Eng. 279 (2000) 1–9.

[48] Z. Li, R.S. Bowman, Counter ion effects on the sorption of cationic surfactant and chromate on natura clinoptilonite, Environ. Sci. Technol. 31 (1997) 2407–2412.

[49] Thanhmingliana, S.M. Lee, D. Tiwari, Use of hybrid materials in the decontamination of bisphenol A from aqueous solutions, RSC Adv. 4 (2014) 43921–43930.

[50] Q. Sui, J. Huang, Y. Liu, X. Chang, G. Ji, S. Deng, T. Xie, G. Yu, Rapid removal of bisphenol A on highly ordered mesoporous carbon, J. Environ. Sci. 23 (2011) 177–182.

[51] L. Zhang, F. Pan, X. Liu, L. Yang, X. Jiang, J. Yang, W. Shi, Multi-walled carbon nanotubes as sorbent for recovery of endocrine disrupting compound – bisphenol F from wastewater, Chem. Eng. J. 218 (2013) 238–246.

[52] L.L. Ji, F.L. Liu, Z.Y. Xu, S.R. Zheng, D.Q. Zhu, Zeolite templated microporous carbon as a superior adsorbent for removal of monoaromatic compounds from aqueous solution, Environ. Sci. Technol. 43 (20) (2009) 7870–7876.

[53] L.L. Ji, F.L. Liu, Z.Y. Xu, S.R. Zheng, D.Q. Zhu, Adsorption of pharmaceutical antibiotics on template-synthesized ordered micro- and mesoporous carbons, Environ. Sci. Technol. 44 (2010) 3116–3122.

[54] S. Azizian, Kinetic models of sorption: a theoretical analysis, J. Colloid Interface Sci. 276 (2004) 47–52.

[55] Y.S. Ho, G. Mckay, A comparison of chemisorption kinetic models applied to pollutant removal on various sorbents, Process Safety Environ. Protect. 76 (1998) 332–340.

[56] M. Haerifar, S. Azizian, An exponential kinetic model for adsorption at solid/solution interface, Chem. Eng. J. 215–216 (2013) 65–71.

[57] Y. Liu, L. Shen, Kinetics to first- and second-order rate equations for adsorption, Langmuir 24 (2008) 11625–11630.

[58] M. Haerifar, S. Azizian, Fractal-like adsorption kinetics at the solid/solution interface, J. Phys. Chem. C 116 (2012) 13111–13119.

[59] Y.S. Ho, Review of second-order model for adsorption systems, J. Hazard. Mater. B136 (2006) 681–689.

[60] Y.S. Ho, G. Mckay, The kinetics of sorption of divalent metal ions onto *sphagnum* moss peat, Water Res. 34 (2000) 735–742.

[61] K.F. Hayes, C. Papelis, J.O. Leckie, Modeling ionic strength effects on anion adsorption at hydrous oxide/solution interfaces, J. Colloid Interface Sci. 125 (1988) 717–726.

[62] Y. Arai, E.J. Elzinga, D.L. Sparks, X-ray adsorption spectroscopic investigation of arsenite and arsenate adsorption at the aluminum oxide–water interface, J. Colloid Interface Sci. 235 (2001) 80–88.

[63] Z. Li, T. Burt, R.S. Bowman, Sorption of ionizable organic solutes by surfactant-modified zeolite, Environ. Sci. Technol. 34 (2000) 3756–3760.

[64] J.T. Matheickal, Q. Yu, Biosorption of lead(II) and copper(II) from aqueous solutions by pre-treated biomass of Australian marine algae, Bioresour. Technol. 69 (1999) 223–229.

[65] M.A. Stylianou, M.P. Hadjiconstantinou, V.J. Inglezakis, K.G. Moustakas, M.D. Loizidou, Use of natural clinoptilolite for the removal of lead, copper and zinc in fixed bed column, J. Hazard. Mater. 143 (2007) 575–581.

[66] A. Adak, M. Bandyopadhyay, A. Pal, Fixed bed column study for the removal of crystal violet (C.I. Basic Violet 3) dye from aquatic environment by surfactant-modified alumina, Dyes Pigm. 69 (2006) 245–251.

[67] D. Tiwari, S.M. Lee, Biomass derived materials in the remediation of heavy-metal contaminated water: removal of Cd(II) and Cu(II) from aqueous solutions, Water Environ. Res. 83 (2011) 874–881.

[68] S.M. Lee, D. Tiwari, K.M. Choi, J.K. Yang, Y.Y. Chang, H.D. Lee, Removal of Mn(II) from aqueous solutions using manganese-coated sand samples, J. Chem. Eng. Data 54 (2009) 1823–1828.

ELSEVIER

Chemical Engineering Journal

An International Journal of Research and Development

The *Chemical Engineering Journal* focuses upon three aspects of **chemical engineering**: chemical reaction engineering, environmental chemical engineering, and materials synthesis and processing.

View full aims and scope

This journal supports the following content innovations

AudioSlides, **Interactive MATLAB Figure Viewer**, **Nomenclature Viewer**

Journal Metrics

Source Normalized Impact per Paper (SNIP): **1.905**

SCImago Journal Rank (SJR): **1.585**

Impact Factor: **4.321**

5-Year Impact Factor: **4.621**

Imprint: **ELSEVIER**

ISSN: **1385-8947**

Chemical Engineering Journal 270 (2015) 496–507

Contents lists available at ScienceDirect

Chemical Engineering Journal

journal homepage: www.elsevier.com/locate/cej

Porous hybrid materials in the remediation of water contaminated with As(III) and As(V)

Seung Mok Lee [a], Lalhmunsiama [a], Thanhmingliana [b], Diwakar Tiwari [b],*

[a] Department of Health and Environment, Catholic Kwandong University, 522 Naegok-dong, Gangneung, Gangwon-do 210-701, Republic of Korea
[b] Department of Chemistry, School of Physical Sciences, Mizoram University, Aizawl 796004, India

HIGHLIGHTS

- Bentonite and locally collected clay employed to obtain the porous hybrid materials.
- The materials are characterized.
- The mechanism is proposed in efficient and effective attenuation of As(III) and As(V).
- The selectivity of materials obtained for arsenic.

GRAPHICAL ABSTRACT

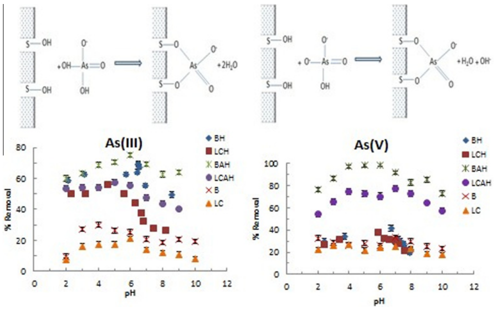

ARTICLE INFO

Article history:
Received 8 December 2014
Received in revised form 12 February 2015
Accepted 13 February 2015
Available online 21 February 2015

Keywords:
Porous hybrid materials
Arsenic
Phenol
Clay
Attenuation

ABSTRACT

The aim of this study is to synthesize novel hybrid porous materials using locally available clay and commercial bentonite and to assess their suitability in the attenuation of arsenic from ground water. Therefore, the clay samples are modified with hexadecylammonium bromide (HDTMA) or pillared with aluminium and then modified with HDTMA. The hybrid materials are characterized by the FT-IR, XRD and SEM analytical methods. Moreover, the BET (Brunauer–Emmett–Teller) specific surface area along with the pore diameter was obtained for these solids. Hybrid materials are then assessed in an effective and efficient remediation of aquatic environment contaminated with arsenic. Various physico-chemical parametric studies enable to deduce plausible mechanism involved at solid/solution interface. The sorptive pH (pH 2.0–10.0), concentrations (1.0–20.0 mg/L) and background electrolyte concentrations (0.001–0.1 mg L^{-1} $NaNO_3$) dependence sorption of As(III) and As(V) is studied by these solids. The sorption of As(III) or As(V) by these hybrid materials are further illustrated with the FT-IR analysis conducted for the arsenic loaded solids. Further, the simultaneous removal of phenol and arsenic is assessed and results show that the hybrid materials are useful in simultaneous remediation of water contaminated with phenol and, at least, As(V). The removal of arsenic is assessed separately in presence of several cations (Cd(II), Cu(II) and Mn(II)) and anions (glycine, iminodiacetic acid, ethylene diamine tetra acetic acid disodium salt, oxalic acid, phosphate and sulfate).

1. Introduction

Clay and minerals are useful natural porous materials widely employed in the treatment of wastewater contaminated with several heavy metals toxic ions [1,2]. However, the pristine clay materials are found less effective, in particular, in the remediation of several micro-pollutants of organic origin or oxyanions *viz.*, arsenic, chromium etc. [3–5]. Moreover, because of its low settling capacity, the clay materials found difficult to recover from the treated solutions [6]. Therefore, to enhance the applicability of natural clay materials, a strategic surface modification of clay minerals

---

* Corresponding author. Tel.: +91 389 2301806; fax: +91 389 2330834.
E-mail address: diw_tiwari@yahoo.com (D. Tiwari).

http://dx.doi.org/10.1016/j.cej.2015.02.053

attracted greater attention in the recent past. The modified clay materials find many applications not only in environmental engineering [3,7,8] but also in material sciences [9,10]. The modification of clay is basically of two types i.e., either by physical or by chemical. The exchange of exchangeable cations with surfactant molecule is a physical modification whereas silylation or pillaring with inorganic cations or polymer composites are the chemical modifications [1].

Bentonite is natural clay containing mainly the smectite and kaolinite mineral phases. Smectite is fairly an expanding three-sheet phyllosilicate, where the T:O (tetrahedral (T) $[SiO_4]^{4-}$ or octahedral (O) $[AlO_3(OH)_3]^{6-}$) ratio is 2:l and the charge of the three-sheet layer (unit cell) is 0.5–1.2 e uc^{-1} (negative charge). This charge arises from the isomorphous substitution of Al^{3+} and Si^{4+} in the tetrahedral sheet and Mg^{2+} for Al^{3+} in the octahedral sheet. This group possesses no hydroxyl functionality within the interlayer [3,11]. On the other hand, kaolinite and serpentine group is having two-sheet phyllosilicates, where T:O ratio is 1:1 and the charge of the two-sheet layer (unit cell) is 0 e uc^{-1}. Since bentonite contains dominantly the smectite mineral having permanent negative charge which is usually compensated by the exchangeable cations (i.e., Na^+, K^+, Mg^{2+}, Ca^{2+}, etc.). These cations are present within the interlayer space [11,12]. Therefore, bentonite clay shows fairly a high cation exchange capacity (CEC) and found good water replaced swelling type mineral [13]. The high specific surface area enables it for a useful material for adsorption/absorption of several ionic or polar compounds.

Arsenic is ubiquitous in natural environment. It is widely distributed in air, soil and water [14,15]. It is reported that the ground water, at several places of Bangladesh, India, USA, China, Mexico, Taiwan, is greatly contaminated with arsenic [16]. A rough approximation envisages that more than 100 million people are badly affected with arsenic poisoning around the globe [17–19]. Moreover, according to the International Agency for Research on Cancer (IARC), inorganic arsenic compounds are classified as Group 1 carcinogen (carcinogenic to humans) [20,21]. A long term exposure of arsenic causes lung, liver, kidney, bladder and skin cancer. Also it causes pigmentation change, skin thickening (hyperkeratosis), neurological disorders, muscular weakness, loss of appetite, nausea, etc. [16,22]. This compels regulatory bodies *viz*., WHO (World Health Organization) and US EPA (United States Environmental Protection Agency) to reduce the arsenic permissible level from 50 $\mu g\ L^{-1}$ to 10 $\mu g\ L^{-1}$ in the drinking water.

Several materials are used previously in the remediation of arsenic contaminated waters. The activated alumina is functionalized with the mercaptopropyl-silica (i.e., 3-mercaptopropyl triethoxysilane). The modified hybrid material, having mesoporosity, shows an enhanced uptake of As(III) as studied under the batch and fixed-bed column studies. It is proposed that the arsenic(III) is forming a strong covalent bond with the sulfhydryl site of hybrid solid [23]. Hybrid porous inorganic/organic polymer-type materials are synthesized by encapsulating the hydrated iron oxide with the polymer anion resin (styrene–divinylbenzene copolymer). The hybrid material is characterized and employed in the removal of arsenic from aqueous solutions under the fixed-bed column studies [24,25]. A sol–gel preparation route is adopted to obtain novel hybrid zirconium polyacrylamide (ZrPACM-43) material. The material is further utilized in the removal of As(III) under the batch reactor studies. The sorption data is collected for various physico-chemical parametric studies as to deduce the mechanism of sorption [26]. In addition, variety of hybrid materials, nano-structured hybrid materials are shown prominence in the removal of heavy metals or even several organic contaminants from aqueous solutions [27–30]. In a line, the porous organo-modified hybrid clay materials show applicability in the decontamination of several inorganic oxyanions [31–33]. It is reported that the incorporation of cationic surfactants within the clay interspace enhances the anions sorption capacity especially when the surfactant loading exceeds to the CEC (cation exchange capacity) of clay [3,34]. Li and Bowman [33] proposed following uptake mechanism for several anions (nitrate, arsenate and chromate) sorption onto the HDTMA modified kaolinite clay:

$$x(\mathrm{HDTMA-Clay-Br})+\mathrm{AO}_y=(\mathrm{HDTMA-Clay})_x-\mathrm{AO}_y+\mathrm{xBr}^- \qquad (1)$$

where '*A*' referred either N, Cr or As. Similarly, novel aluminium pillared HDTMA-modified-sericite is found to be useful in the removal of As(III) and As(V) from aqueous solutions. It is reported that the arsenate(V) is sorbed specifically onto the solid surface [22]. Surfactant modified-bentonites are prepared by varied dose of cationic surfactants, and are employed in the removal of As(V) and As(III) from aqueous solutions [35]. The results show that the adsorption capacities of bentonite modified with octadecyl benzyl dimethyl ammonium is significantly higher than the un-modified bentonite. The adsorption kinetics is fitted well to the pseudo-second-order rate model.

Therefore, keeping in view the wide applicability of porous clay materials, the present communication aims to obtain the novel hybrid materials using the natural bentonite and locally available clay. These hybrid materials are then assessed for the removal behavior of As(III) and As(V) from aqueous solutions in a wide range of physico-chemical parametric studies as to deduce mechanism involved at solid/solution interface. Further, the study aims to assess the selectivity and suitability of materials in the remediation of arsenic contaminated water in presence of several cations and anions.

2. Materials and methods

2.1. Materials

Bentonite is procured from commercial supplier and it was mined from Bhuj, Gujarat, India. The sample was washed with distilled water and dried in a drying oven at 90 °C. The local clay was collected from the field of Mizoram, India. Since this was having several impurities hence, was thoroughly separated using the standard ISRIC (International Soil Reference and Information Centre) method as described elsewhere (http://www.isric.org/isric/webdocs/docs/ISRIC_TechPap09_2002.pdf). These clay samples i.e., bentonite and local clay are crushed in mortar and sieved to obtain 100 BSS (British Standard Sieve) mesh particle size (0.150 mm). The cation exchange capacity (CEC) of these two samples (bentonite and local clay) is determined using the standard US EPA method 9080 (http://www.epa.gov/osw/hazard/ testmethods/sw846/pdfs/9080.pdf). The CEC of bentonite and local clay was found to be 69.35 and 46.38 meq/100 g of clay, respectively. Hexadecyltrimethyl ammonium bromide (HDTMA) and iminodiacetic acid was procured from Sigma–Aldrich, USA. Aluminium(III) chloride was obtained from the Merck India. Sodium chloride, Extrapure, obtained from the HiMedia, India. Manganese chloride, copper(II) sulfate, glycine, sodium phosphate, ethylenediaminetetraacetic acid (EDTA), nitric acid, sodium hydroxide were obtained from the Duksan Pure Chemicals Co., Ltd., Korea. Cadmium(II) sulfate was procured from Kanto Chemical Co., Inc., Japan and oxalic acid was obtained from Shinyo Pure Chemical Co., Ltd., Japan. Sodium metaarsenite and disodium hydrogen arsenate heptahydrate was obtained from Wako Pure Chemical Industries Ltd., Japan. The other chemicals were used of Analytical or equivalent grade. The deionized water was further purified (18 MΩ cm) using a Millipore water purification system (Milli-Q+).

2.2. Methodology

2.2.1. Preparation of organo-modified and inorgano-organo-modified clay

Bentonite and local clay was modified with hexadecyltrimethylammonium bromide employing simple cation exchange process. The detailed synthetic process is described elsewhere [36]. The HDTMA-modified bentonite/or local clay is named as BH and LCH samples, respectively. Similarly, Bentonite/or local clay was pillared with aluminium and modified with organic cations HDTMA i.e., the HDTMA-Al-bentonite (BAH) or HDTMA-Al-local clay (LCAH) materials. A simple wet synthesis was adopted as described elsewhere [22,36].

2.2.2. Characterization and surface morphology of hybrid materials

FT-IR (Fourier transform-infra red) data was obtained for these materials using the FT-IR machine (Bruker, Tensor 27, USA by KBR disk method). Similarly, the X-ray diffraction (XRD) data was recorded by the X-ray diffraction machine (PANalytical, Netherland; Model X'Pert PRO MPD). The Cu K_α radiation having wavelength 1.5418 Å is used for X-ray diffraction. Moreover, the surface morphology of these hybrid materials along with the neat clay was obtained taking the SEM (scanning electron microscope) images of these solids employing a field emission scanning electron microscope (Model S-4700, Hitachi, Japan). Similarly, the specific surface area, pore volume and pore size of these solids is obtained using the BET Analyzer Macsorb HM machine (Model-1201) Japan.

2.2.3. pH_{PZC} measurements

The pH_{PZC} (point of zero charge) of bentonite, local clay, BH, LCH, BAH and LCAH was obtained by the known method as described previously [22].

2.2.4. Batch reactor experiments

Stock solutions of arsenic(III) and arsenic(V) 100 mg L^{-1} was prepared taking appropriate amount of arsenic salt into purified water. Further, the required arsenic concentration was obtained by successive dilution of stock solutions. 10.0 mg L^{-1} of As(III)/or As(V) solution (50 mL) is taken into several polyethylene bottles and the pH of these solutions was adjusted using concentrated HNO_3/NaOH solutions. 0.1 g of solid sample was introduced in these solutions and bottles were capped tightly. These bottles were then kept in an automatic incubator shaker (KUKJE, Shaking Incubator, Korea model 36-SIN-125) for *Ca* 24 h at 25 ± 1 °C. A prolonged period i.e., 24 h of agitation could enable to achieve an apparent equilibrium between solid/solution interfaces. These bottles were then taken out from the shaker and filtered with 0.45 μm syringe filter and the pH was again checked and reported as equilibrium pH. The filtrates were subjected to measure the bulk arsenic concentration using atomic absorption spectrometer (Fast Sequential Atomic Absorption Spectrometer (FS-AAS): Model AA240FS, Varian, Australia). Additionally, in order to deduce the binding of As(III) or As(V) onto these hybrid materials, the solids (2.0 g/L) were equilibrated with the sorptive solutions (10.0 mg L^{-1}) at pH 4.5 and temperature 25 ± 1 °C for 24 h. It was filtered with syringe filter and the solids were washed with purified water for *Ca* 5 times and dried in a drying oven at 50 °C overnight. The dried solids were then subjected for the FT-IR analysis and data was produced along with the bare hybrid materials.

The sorptive concentration dependence study was performed varying the arsenic concentrations from ~2.0 to 18.0 mg L^{-1} and ~2.0 to 15.0 mg L^{-1} for As(V) and As(III), respectively at a constant pH ~4.5 and temperature 25 ± 1 °C. The sorption process was followed similar as detailed previously. Results were presented as percent of arsenic removed as a function of initial arsenic concentrations (mg L^{-1}).

Time dependence uptake of arsenic by these hybrid materials was obtained utilizing the sorption results obtained at different time intervals. The initial As(III)/or As(V) concentration 10.0 mg L^{-1} with a solid dose 2.0 g L^{-1} was kept constant. Moreover, the sorption experiments were conducted at constant pH ~4.5 and at 25 ± 1 °C. Results were then presented as percent removal of arsenic as a function of time (min).

Effect of background electrolyte concentration dependence sorption was collected varying the background electrolyte concentrations from 0.001 to 0.1 mol L^{-1} $NaNO_3$ of As(III)/or As(V) solution (10.0 mg L^{-1}). The solution pH (~4.5) and temperature (25 ± 1 °C) was kept constant throughout the experiments. Results were presented as percent arsenic removed as a function of background electrolyte concentrations.

The presence of phenol in the removal of arsenic was obtained varying the phenol concentration from *Ca* 2.0 to 15.0 mg L^{-1} keeping a constant arsenic (As(III) and As(V)) concentration 10.0 mg L^{-1} with a solid dose 2 g L^{-1}. The solution pH 4.5 and temperature 25 ± 1 °C was kept constant. The results were presented in two different ways i.e., the percent removal of arsenic as a function of initial phenol concentration as well the extent of phenol removed as a function of initial phenol concentration.

Further, the presence of co-cations (Cd(II), Cu(II) and Mn(II)) and co-anions (glycine, iminodiacetic acid, ethylenediaminetetra acetic acid, oxalic acid, sulfate and phosphate) in the removal of arsenic (both As(III)/or As(V)) by these hybrid materials was studied keeping a constant co-ion concentration 50.0 mg L^{-1} and arsenic concentration 10.0 mg L^{-1} with a constant solid dose 2.0 g L^{-1}. The sorption experiments were performed at constant temperature 25 ± 1 °C and pH 4.5. Results were presented as percent removal of arsenic in presence of various co-ions.

2.2.5. Statistical analysis

The data presented in tables and figures are mean values ± S.E. from the five replicates of observations. Where error bars are not visible, errors were smaller than or equal to the symbols. Modeling of non-linear sorption kinetic data was conducted using the Excel add-ins solver with user-defined functions to minimize the residuals between model-calculated and measured values.

3. Results and discussion

3.1. Characterization of materials

The FT-IR spectra of bentonite and local clay based samples were obtained and results presented elsewhere [36]. The results clearly show that the modified clay samples i.e., BH, BAH, LCH or LCAH possess with prominent IR peaks centring around 2930 cm^{-1} and 2850 cm^{-1}, which are assigned as $—CH_2$ asymmetric stretching and $—CH_2$ symmetric stretching vibrations, respectively [37]. This, therefore, concludes that the HDTMA is firmly occupied the place within the interspace of clay samples.

Further, the materials are subjected for its X-ray diffraction analysis and results show that the sharp diffraction peaks are observed for these solids i.e., modified and pristine clay samples with a definite d-spacing which enabled to assign the peaks of different mineral phases of clay materials [36]. The results of XRD data obtained for bentonite and local clay was matched with the standard ICDD (International Centre for Diffraction Data) reference pattern and it was noted that both the clay samples contained with the quartz, smectite, illite and kaolinite minerals with varied percent compositions as characteristic peaks were assigned in the spectra. Further, it was evaluated that bentonite contained with quartz, smectite, kaolinite and illite, respectively 43.71%, 23.17%, 1.73% and 31.39% whereas; the local clay was having the 79.35%, 6.20%, 0.45% and 14.01%, respectively, the quartz, smectite, kaolinite and illite.

The surface morphology of these solids is obtained taking the FE-SEM images of these solids and presented elsewhere [36]. The images show that the B and LC solids possess relatively compact and ordered surface structure, lacking with meso- or macro-pores on its surface. On the other hand, however, the organo-modified bentonite/or LC (BH or LCH) solids show more heterogeneous and disordered surface structure. It was concluded that the water molecules or the exchangeable cations present within the interspace of clay were exchanged with the HDTMA and the HDTMA molecules firmly occupied the space within the interspace of bentonite or LC. Moreover, the BAH and LCAH solids show similar disordered surface structure contained with newly borne fine particles of aluminium oxide.

The BET specific surface area, pore volume and pore sizes of these solids i.e., bentonite, local clay, BH, BAH, LCH and LCAH were obtained using the nitrogen adsorption and desorption. The results are presented in Table 1. It is evident from Table 1 that very high value of the BET specific surface area was obtained for the pristine bentonite having low pore volume and pore size. The high specific surface area is due to the presence of higher percentage of the smectite, kaolinite and illite content comparing to silica content. However, the HDTMA- or Al-HDTMA-modified bentonite materials showed a significant decrease of the specific surface area and increase in pore size (diameter) and pore volume of the materials. This is due to the fact that the HDTMA or aluminium occupied the interspace caused for decrease in specific surface area whereas the propping up of the interlayer caused to enhance in pore size and pore volume of the solids. The similar results were reported previously in the HDTMA modified montmorillonite using a regulated loading of HDTMA [38]. On the other hand the pristine local clay showed very low specific surface area i.e., 2.94 m^2/g. This is due to the compact surface structure of LC possessed dominantly the silica. Moreover, due to the silica content the solid showed relatively higher pore size and pore volume values. However, the presence of HDTMA or Al-HDTMA caused for relative increase in specific surface area as well decrease in pore diameter of the solid. It was reported previously that the specific surface area of bare sand was increased with the immobilized manganese oxide sand solid [39].

3.2. Batch reactor studies

3.2.1. pH variation study

Table 1
BET specific pore size, volume BET surface area values of the clay and hybrid clay materials.

Materials	Pore size (nm)	Specific pore volume (cm^3/g)	BET specific surface area (cm^2/g)
Bentonite	4.98	0.010	80.86
BH	36.60	0.050	4.68
BAH	27.45	0.075	9.55
Local clay	30.67	0.025	2.94
LCH	13.12	0.045	11.87
LCAH	8.04	0.010	4.55

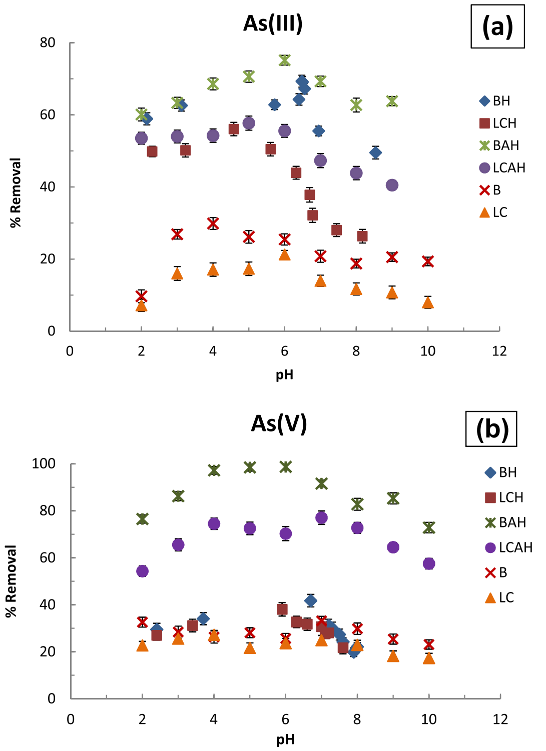

Fig. 1. pH dependence removal of (a) As(III) and (b) As(V) by the virgin clay and modified clay samples.

The uptake of As(III) and As(V) is obtained as a function of solution pH (pH 2.0–10.0). The results are presented graphically in Fig. 1(a) and (b) respectively for As(III) and As(V). In general, relatively a higher uptake of As(III) or As(V) is occurred at moderate pH values i.e., pH 4–7. However, relatively, a lower uptake of arsenic is occurred at extremely low and high pH values i.e., pH *Ca* 2.0 and 10.0. In order to demonstrate the mechanism involved at solid/solution interface, it is important to discuss the speciation of As(III) and As(V) in aqueous solution as well the pH_{PZC} of these solids employed. The point of zero charge of these solids are obtained by the acid and base titrations which is found to be 10.0, 8.2, 6.1, 5.8, 5.1 and 5.1 for the samples B, BH, BAH, LC, LCH, LCAH, respectively. The materials are positively charged below this pH and carry a net negative charge above to this pH. A simple acidic dissociation of surface functional groups could be deduced with the Eq. (2):

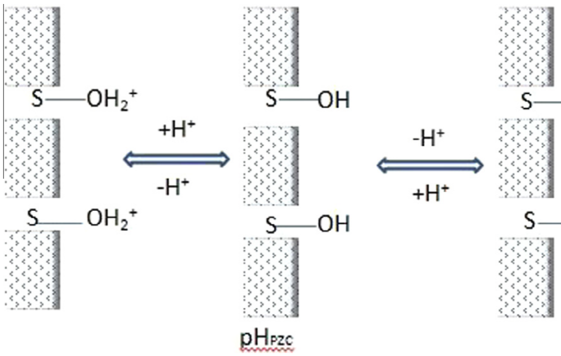

(2)

where 'S' represents the surface having the aluminium or silicon sites. The point of zero charge of the local clay samples show somewhat lower pH_{PZC} values whereas the bentonite and modified bentonite possess slightly higher pH_{PZC} values. The aluminium pillared samples i.e., BAH possess much lower pH_{PZC} i.e., 6.1 comparing to its corresponding pristine bentonite pH_{PZC} 10.0. This is because of the sufficient loading of aluminium along with the HDTMA.

The speciation of As(III) and As(V) is carried out previously which demonstrated that up until pH 8.0 the dominant species of As(III) is neutral H_3AsO_3 and beyond this pH the negatively charged species $H_2AsO_3^-$ is gradually dominating in aqueous solutions [40]. Relatively low uptake of arsenic(III) that occur at lower pH values i.e., pH ~2.0 is due to the fact that at this pH there is a strong competition between the H^+ ions and even the neutral arsenic species toward the surface and this hinders the attraction of arsenic species toward the solid surface [41]. However, with the increase in pH, the surface becomes uncharged or the charge density decreases which makes possible for the vander Waals attractive forces to dominate which results in an enhanced uptake of As(III) by these solids i.e., BH, BAH, LCH and LCAH. It seems that the aluminium pillaring could not affect significantly the uptake of As(III) since almost similar percent removal is obtained for the solids BH and BAH or LCH and LCAH. Similar mechanism was proposed for the uptake of arsenic(III) by the titanium oxide nanoparticles [42]. The vander Waals attractive sorption was reported previously for As(III) by the iron modified sand samples [43]. However, the other report shows that thiol-functionalized silica coated activated alumina sorbs As(III) by strong chemical bonds with the sulfhydryl group [23]. Further, at extreme high pH values (pH ~10.0), since the surface and arsenic species both possess negative charges hence, a strong repulsive forces causes for significant decrease in percent uptake of As(III) by these solids.

The FT-IR results obtained with the As(III) loaded BH and BAH or LCH and LCAH solids are presented graphically (Supplementary S1(a) and S1(b)) along with the unloaded As(III) hybrid materials. It is to be noticed that the $—CH_2$ asymmetric and $—CH_2$ symmetric stretching vibrations as occurred at the wave numbers 2930 cm^{-1} and 2850 cm^{-1} with the BH, BAH, LCH and LCAH are either diminished completely or the intensity is decreased significantly in presence of As(III). This indicates that the As(III) species are attracted by the organic core of the introduced HDTMA molecule with a feeble vander Waals attractive forces. Further, the vibrations around the wavenumbers 1114 and 1030 cm^{-1} which are assigned to the Si–O stretching vibrations [44] are almost unaffected in presence of As(III). Also the quartz Si–O vibrations centred around 695 and 795 cm^{-1} are unaffected in presence of As(III) [45]. A peak at 910 cm^{-1} which is due to the Al-OH hydroxyl bending [44] is unaffected in presence of As(III). These results clearly demonstrate that the arsenic(III) is not bound with the available functional groups of hybrid materials. This supports the assumption that As(III) was sorbed onto the solid surface with weak vander Waals forces. Additionally, the bands between the 467 and 533 cm^{-1} are due to the OSiO bending vibrations [22].

On the other hand, As(V) speciation shows that the oxyanionic species $H_2AsO_4^-$ is dominant within the pH region 3.5–5.5. Further, at higher pH region i.e., 6.0–10.0, the species $HAsO_4^{2-}$ is dominating in aqueous solutions. Moreover, below pH 3.5 the un-dissociated species H_3AsO_4 dominates in solution [40]. These species are important in deducing the mechanism involved at solid and surface interface. Fig. 1(b) clearly shows that an increase in pH from 2.0 to 4.0, there is an apparent increase in percent uptake of arsenic(V) by BAH and LCAH solids which further attains almost a constant percent uptake at around pH ~7.0 and beyond pH 7.0 there is a significant decrease in percent uptake of As(V). Since the acidic dissociation of H_3AsO_4 taking place at low pH and slowly the anionic species $H_2AsO_4^-$ increases in solutions also the surface carries positive charges which gradually facilitates in sorption of As(V). The driving force is perhaps the electrostatic attraction followed by the strong chemical bond formation. But within the pH region *Ca* 4.5–6.2, the uptake of As(V) attains to its maximum value. This is due to strong electrostatic attraction and, possibly, followed by a strong 'inner sphere complexation' at the surface. The inner sphere complexation is suggested based on the other study as well i.e., background electrolyte studies. The possible mechanism of As(V) sorption at the solid surface is suggested as given below (Eq. (3)):

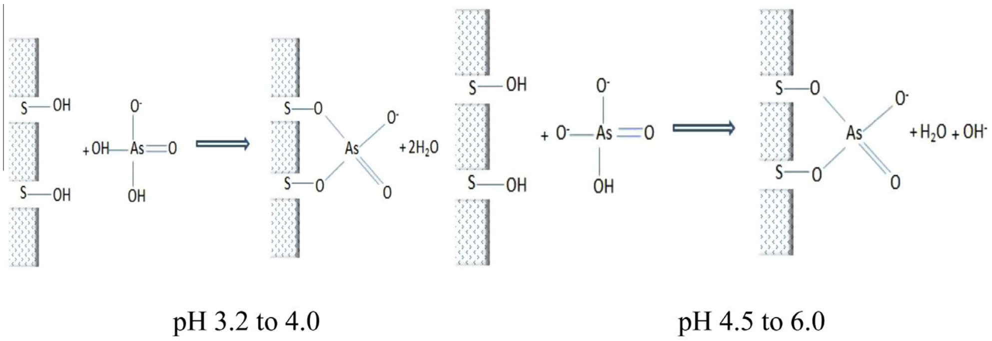

(3)

The strong inner sphere complexation was suggested for As(V) at pH 5.0 using the hybrid inorgano-organo polymeric materials [25]. It was suggested that at pH 5.0 the positively charged adsorption sites i.e., $FeOH_2^+$ attracting the oxyanions of arsenic $H_2AsO_4^-$ by the Coulombic interactions followed by the oxyanion could form inner sphere complexes with the surface active sites. The poly(vinylidene fluoride) PVDF-zirconia blend flat sheet membrane also showed a high uptake of arsenic(V) at pH *Ca* 5.0 and was suggested for the inner sphere complexation between the arsenic oxyanions and surface functional groups [46]. A constant and high percent uptake within the pH region 4–10 is suggested a strong chemisorptive uptake of arsenic(V) by the aluminium-loaded Shirasu-zeolite [47].

Further increase in pH i.e., above pH 7.0 there is a strong decrease in percent uptake of As(V). This is due to strong electrostatic repulsions operating between the negatively charged surface and the oxyanions of arsenic(V). This greatly hinders the sorption to proceed.

On the other hand, the HDTMA modified samples i.e., BH and LCH shows insignificant increase in percent removal of As(V) comparing to the pristine clay bentonite and local clay solids. It is to be assumed that a feeble electrostatic attraction restricts these oxyanions to enter within the interspace and, hence, to form therein a strong chemical bond with the residual active sites available by the aluminol or silanol groups of clay sheets. The positive end of the HDTMA molecule may take part in the electrostatic attraction of As(V) from aqueous solution, provided the organo-cation is loaded in excess of CEC value [3]. The similar electrostatic attraction was suggested previously for the sorption of several anions by the HDTMA modified kaolinite [33]. Moreover, it was referred previously that the incorporation of cationic surfactants within the clay interspace enhances the anions sorption capacity especially when the surfactant loading exceeds to the CEC (cation exchange capacity) of clay [3,34]. Since, the loading of the HDTMA is regulated to 1:1 CEC hence, the surface lacks with excess charge density. Therefore, it restricts the significant enhanced uptake of As(V) by the solids BH and LCH. The nature of binding could reaffirm with the background electrolyte studies as conducted in later sections.

Fig. 1(b) also demonstrates that the aluminium pillared clay samples possess significantly higher removal capacity for As(V) comparing to the HDTMA modified samples of clay. This clearly indicates that the loaded aluminium takes part predominantly in the sorption of As(V) species than the HDTMA. Therefore, the pillaring of the aluminium could be a synergistic effect as it could provide a mechanical strength of the material with enhanced settling capacity along with the enhanced removal capacity for arsenic.

Further, the qualitative studies in the sorption of the As(V) with the hybrid materials BH, BAH, LCH and LCAH are conducted taking the FT-IR spectra of bare hybrid materials and As(V) loaded hybrid materials. Results are presented graphically in figure (Supplementary 2(a) and 2(b)). Similar to the As(III) studies the characteristics IR bands for $-CH_2$ asymmetric and $-CH_2$ symmetric stretching vibrations are observed at the wave numbers 2930 cm^{-1} and 2850 cm^{-1} with the BH, BAH, LCH and LCAH are greatly suppressed or completely diminished in presence of As(V) (except As(V) loaded BAH solid). This suggests that the As(V) species are possibly attracted by the organic core of the introduced HDTMA molecule with a feeble vander Waals attractive forces or even by the electrostatic forces. Similarly, the vibration bands around the wavenumbers 1114 and 1030 cm^{-1} are assigned to the Si–O stretching vibrations [44] and the quartz Si–O vibrations centred around 695 and 795 cm^{-1} [45]. The absorption band at 910 cm^{-1} is due to the Al–OH hydroxyl bending vibrations [44]. This is noted that all these bands, for the As(V) loaded BAH and LCAH solids, showed a significant increase in the intensity which clearly marked that the As(V) is sorbed onto these solids with a strong chemical bonds [48]. Additionally, the bands between the 467 and 533 cm^{-1} which are attributed with the OSiO bending vibrations [22] are also possessed with increased intensity at least for the BAH and LCAH solids. Therefore, an increased uptake of the As(V) by the BAH and LCAH solids is due to the strong chemical bonds that occurred between the active silanol or aluminol groups present with the hybrid materials.

The bare clay samples, on the other hand, i.e., bentonite and local clay possess extremely low sorption capacity both for the As(III) and As(V) species. This enables that the modified clay materials, in particular the aluminium pillared, are having good applicability in the remediation of ground water contaminated with arsenic. Overall, the materials BAH and LCAH possess significantly higher removal capacity for the As(V) comparing to the As(III) which is in a line to other report where zero valent iron is sorbing significantly higher As(V) than As(III) [49].

3.2.2. Effect of arsenic concentration

The concentration dependence removal of arsenic(III) and arsenic(V) is studied for a wide range of initial arsenic concentrations i.e., from ~2.0 mg L^{-1} to 15.0 mg L^{-1} for As(III) and from ~2.0 mg L^{-1} to 18.0 mg L^{-1} for As(V) at a constant pH 4.5. Results are presented graphically in Fig. 2(a) and (b), respectively for arsenic(III) and arsenic(V). Figures reveal that increasing the concentration of arsenic, apparently causes to decrease in percent uptake of arsenic from aqueous solution. Quantitatively, increasing the arsenic(III) concentration from 2.46 to 15.60 the corresponding decrease in percent As(III) removal is from 77.64% to 32.18% (for BH solid); from 56.50% to 20.83% (for LCH solid); from 70.73% to 28.21% (for BAH solid); and from 52.44% to 22.82% (for LCAH solid), respectively. Similarly, increasing the As(V) concentration from *Ca* 2.0 to 18.0 mg L^{-1} the corresponding decrease in percent removal of As(V) is from 100.00% to 82.26% (for BAH); from 100.00% to 45.55% (for LCAH); 97.81% to 35.88% (for BH); and 74.86% to 17.35% (for LCH) solids, respectively. The high percent removal of arsenic by these hybrid materials at varied initial concentrations of the arsenic indicates the affinity of these solids toward the arsenic species in aqueous solutions.

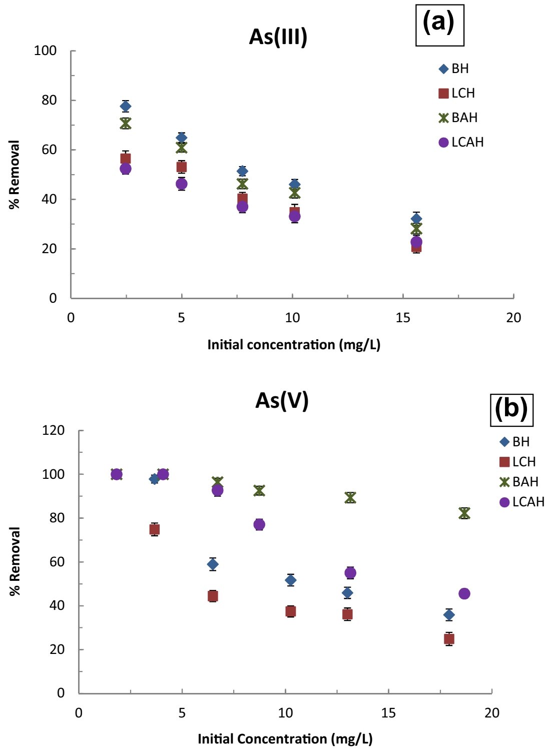

Fig. 2. Removal of (a) As(III); and (b) As(V) by the hybrid materials as a function of sorptive concentration.

3.2.3. Adsorption isotherm modeling

The equilibrium state adsorption data is further utilized to the modeling studies using standard Freundlich and Langmuir adsorption isotherm models. The linearized form of Freundlich and Langmuir Eqs. (4) and (5), respectively are utilized in the modeling studies [50,51].

$$\log a_e = \frac{1}{n}\log C_e + \log Kf \tag{4}$$

$$\frac{C_e}{q} = \frac{1}{q_0 b} + \frac{C_e}{q_0} \tag{5}$$

where a_e or q (mg g^{-1}) denotes the amount of arsenic sorbed at equilibrium by the solid, and C_e denotes bulk sorptive concentration (mg L^{-1}) at equilibrium. K_f and $1/n$ denote the Freundlich constants referring to the adsorption capacity and adsorption intensity or surface heterogeneity, respectively. The Langmuir constants i.e., q_0 denotes the Langmuir monolayer adsorption capacity, i.e., the amount of solute required to occupy all the available active sites in unit mass of solid sample (mg g^{-1}) and '*b*' represents the Langmuir constant (L g^{-1}).

The modeling studies indicate that Freundlich adsorption isotherm is not fitted well with the equilibrium state data since the

Table 2
Langmuir constants estimated for the sorption of As(III) and As(V) by hybrid materials.

Hybrid materials	As(III)			As(V)		
	Langmuir monolayer capacity (q_0 ± S.E.) (mg/g)	b ± S.E. (L/g)	R^2	Langmuir monolayer capacity (q_0 ± S.E.) (mg/g)	b ± S.E. (L/g)	R^2
BH	2.792 ± 0.045	0.816 ± 0.005	0.982	3.449 ± 0.039	0.896 ± 0.008	0.989
LCH	1.824 ± 0.027	0.971 ± 0.004	0.998	2.287 ± 0.056	1.074 ± 0.006	0.986
BAH	2.247 ± 0.051	0.787 ± 0.008	0.996	8.937 ± 0.120	1.634 ± 0.008	0.974
LCAH	2.184 ± 0.035	0.399 ± 0.007	0.995	4.255 ± 0.042	2.495 ± 0.003	0.992

R^2 values obtained are very low. However, the data is fitted well to the Langmuir adsorption model. Therefore, the Langmuir constants are evaluated and returned in Table 2. The results indicate that the Langmuir monolayer capacity for As(V) by the BAH and LCAH solids is extremely high comparing to the corresponding BH and LCH solids. However, the hybrid materials i.e., BH, LCH, BAH and LCAH possess almost a similar sorption capacity for As(III). These results are in a line to our previous observation on the pH dependence studies. Further, the Langmuir constant '*b*' is obtained for these systems which reflects the strength and affinity of these solids toward the adsorbing species [50].

Further, the removal capacity of As(III) and As(V) by these hybrid materials i.e., BH, BAH, LCH and LCAH as estimated with the Langmuir adsorption isotherm modeling is compared with several other materials obtained from literature and returned in Table 3. It is evident from the table that the materials BAH and LCAH showed a promising removal capacity for the As(V). Similarly, appreciably a high removal capacity of As(III) was achieved using these hybrid materials.

3.2.4. Effect of background electrolyte concentration

The specific and non-specific sorption of As(III) or As(V) onto these hybrid materials is studied; obtaining the sorption data at varied background electrolyte concentrations. It is reported that the sorption through the outer-sphere complexation is sensitive with the variation of background electrolyte concentrations since: (i) the background electrolyte ions may compete with the non-specific sorbed ions toward the solid surface, and (ii) the activity of the adsorbing species is to be greatly influenced by the variation of the interfacial potential because of the change in ionic strength as the outer sphere complexes are located at the same plane in the generalized triple layer model with the adsorbed background electrolyte ions. On the other hand, the inner sphere complexes are not influenced with the change in background electrolyte concentration since the adsorbed ions are residing at the plane which is closer to surface where usually background electrolyte ions are not located [52]. Therefore, the study is extended to observe the change in background electrolyte concentration i.e., $NaNO_3$ for the sorption of As(III) and As(V) by these solids at constant pH 4.5. The background electrolyte concentration is increased from 0.001 to 0.1 mol L^{-1} of $NaNO_3$ (100 times) and the corresponding percent removal of As(III)/or As(V) is obtained. Results are represented graphically in Fig. 3(a) and (b), respectively for As(III) and As(V).

This is observed that increasing the background electrolyte concentration from 0.001 to 0.1 mol L^{-1} $NaNO_3$ the corresponding decrease in percent uptake of As(III) is from 60.46% to 27.30% (for BAH); from 55.36% to 25.13% (for LCAH); from 47.10% to 20.60% (for BH); and from 45.50% to 14.20% (for LCH), respectively (*cf* Fig. 3(a)). This is evident that the increase in background electrolyte concentration has caused a significant decrease in the percent uptake of As(III) by these solids. This infers that the sorption of the As(III) by these solids is primarily with weak vander Waals forces and, possibly, forming an 'outer sphere complexes' onto the solid surface. These are in accordance with the mechanism pro-

Table 3
Langmuir monolayer sorption capacity of various materials for As(III) and As(V).

Adsorbents	Sorption capacity (mg/g)		Reference
	As(III)	As(V)	
Sericite	0.1616	0.4643	[22]
Al-HDTMA-sericite	0.4095	0.534	[22]
Al-AMBA-sericite	0.2720	0.4844	[22]
Activated alumina	8.45	–	[23]
Thiol functionalized activated alumina	8.41	–	[23]
Zirconium polyacrylamide	41.48	–	[26]
Surfactant modified bentonite	0.82	1.48	[35]
Rice hulls activated carbon	1.28	1.37	[46]
Areca nut activated carbon	0.87	1.39	[46]
Mn-oxide modified Rice hulls activated carbon	1.52	1.55	[46]
Mn-oxide modified areca nut activated carbon	1.24	1.50	[46]
Zero-valent iron-activated carbon	18.19	12.02	[52]
BH	2.792	3.449	Present study
LCH	1.824	2.287	Present study
BAH	2.247	8.937	Present study
LCAH	2.184	4.255	Present study

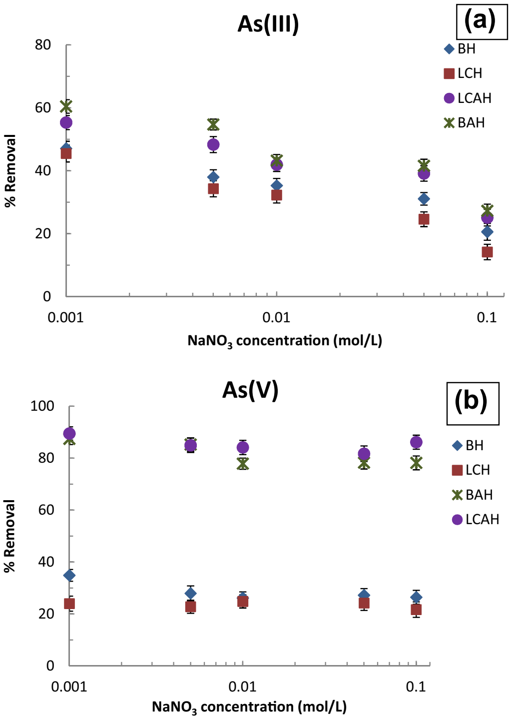

Fig. 3. Removal of (a) As(III); and (b) As(V) as a function of background electrolyte concentrations.

posed with the pH dependence studies or the FT-IR data obtained with the As(III) loaded solids. Previously, it was demonstrated that the sorption of As(III) or even As(V) by the iron hydroxides is somewhat suppressed in presence of coexisting solutes studied for ground waters of Bangladesh [53]. Similarly, the organo-modified sericite samples show similar outer sphere complexation for the As(III) [54].

Further, the increase in background electrolyte concentrations from 0.001 mol L^{-1} to 0.1 mol L^{-1} $NaNO_3$ causes to decrease the As(V) sorption from the 87.50% to 78.20% (for BAH); from 89.51% to 86.18% (for LCAH); from 34.88% to 21.69% (for BH); and from 24.00% to 21.69% (for LCH) solids, respectively (*cf* Fig. 3(b)). These results clearly show that the presence of background electrolytes even at 0.1 mol/L of $NaNO_3$ could not affect significantly the sorption of As(V) by these solids. Therefore, the sorption of As(V) is predominantly of chemisorptive type and As(V) is forming a strong chemical bond at the surface active sites and residing at the inner sphere plane. The results are in a line to the FT-IR studies conducted for the As(V) loaded solids. Similar results are reported previously for the organo-inorgano-modified sericite [22]. However, the removal of As(V) by the titanium dioxide showed a mixed removal mechanism i.e., inner and outer-sphere complexation [55].

3.2.5. Effect of time

The time dependence sorption of As(III) and As(V) by these hybrid materials is conducted and results are presented graphically in Fig. 4(a) and (b), respectively for As(III) and As(V). It is evident from the figures that a sharp initial uptake of arsenic is occurred onto the surface of solids which slowed down with the lapse of time and is reached to an apparent saturation value within *Ca* 180 min of contact. It is noted that within initial 60 min of contact most of the arsenic species are aggregated onto the solid surface. This indicates that the sorption of arsenic is relatively fast and efficient onto these solids. Comparing to these two oxyanions, the uptake of As(III) is relatively faster than As(V).

Further, the time dependence data is utilized to conduct the kinetic modeling and for this three different kinetic models *viz.*, pseudo-first order (PFO), pseudo-second order (PSO) and fractal-like pseudo-second order (FL-PSO) to its non-linear forms (Eqs. 6–8) are utilized [56–58]:

$$q_t = q_e(1 - \exp(-k_1 t)) \tag{6}$$

$$q_t = \frac{k_2 q_e^2 t}{1 + k_2 q_e t} \tag{7}$$

$$q_t = \frac{k q_e^2 t^\alpha}{1 + k q_e t^\alpha} \tag{8}$$

where q_t and q_e are the amount of arsenic removed at time '*t*' and removal capacity at equilibrium, respectively. k_1 and k_2 are the pseudo-first and pseudo-second order rate constants, respectively. Similarly, the constants k and α are referred to the rate constant and fractal constant, respectively. A non-linear least square fitting is conducted for the estimation of unknown parameters. The estimated values of the unknown parameters along with the least square sum are tabulated in Table 4. Table 4 reveals that the kinetic simulation data is best fitted to the PSO and FL-PSO models comparing to the PFO model since reasonably low least square sum is obtained for these two models. The results again show that BH or LCH materials possess relatively higher removal capacity for As(III) whereas BAH and LCAH hybrid materials show significantly high removal capacity for As(V) comparing to the BH and LCH materials. Moreover, fair applicability of the PSO model points that the arsenic species are bound onto the surface of these material by strong forces. Earlier, it was mentioned that the adsorption of divalent metal cations onto the *sphagnum moss* peat followed the second-order rate laws. Therefore, it was concluded that metal cations were bound with strong chemical forces that occurred between the peat surface active groups and divalent metal ions forming covalent bonds with valence forces sharing or the exchange of electrons [59,60].

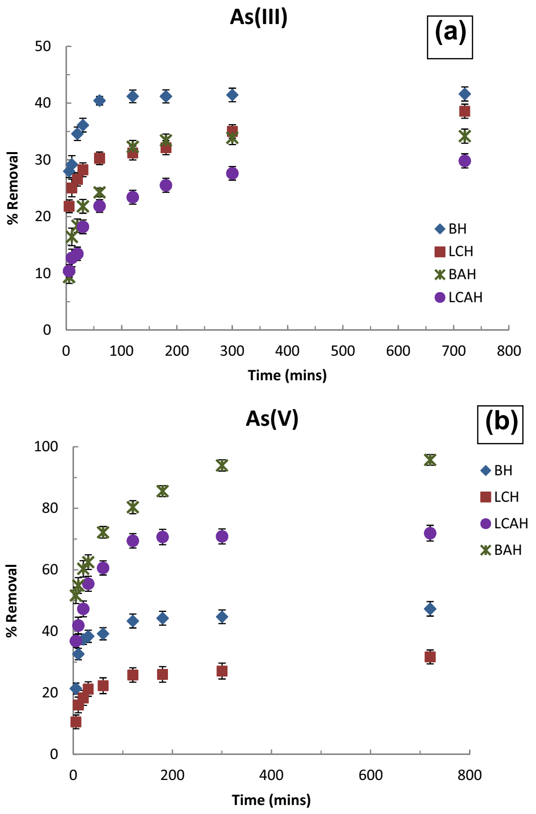

Fig. 4. Time dependence sorption of (a) As(III); and (b) As(V) by hybrid materials.

3.2.6. Effect of phenol

The hybrid materials BH, LCH, BAH and LCAH are utilized to assess the As(III) and As(V) removal at varied concentrations of phenol i.e., from *Ca* 2.0 to 15.0 mg L^{-1} keeping the arsenic concentration 10.0 mg L^{-1} and pH 4.5 as constant. Results are presented as the percent removal of arsenic as a function of phenol concentration and also the amount of phenol removed as a function of phenol concentration. It is to be noted that the percent removal of As(III) is significantly decreased with the increase in phenol concentration (vide Fig. 5(a)) whereas the similar increase in phenol concentration significantly increases the amount of phenol removal (vide Fig. 5(b)). The results clearly demonstrate that there is a competition between the phenol and As(III) toward the available active sites and the phenol is preferentially sorbed onto the solid surface. The increased extent of phenol removal is due to the preferential partitioning of phenol that took place at the hydrophobic core of HDTMA molecule and this suppresses the sorption of weakly bound arsenic(III). It was previously reported that the alkylammonium molecule preferentially resides at the surface layer of clay, leaving the organic tail radiating away from the surface and provides a strong hydrophobic core [61,62]. This possibly caused for increased phenol to partition at the hydrophobic core introduced [63].

On the other hand, interesting to note that the increase in phenol concentration from *Ca* 2.0 to 15.0 mg L^{-1} is not affected, sig-

Table 4
The kinetic data obtained for the sorption of As(III) and As(V) by the hybrid materials.

Systems	PFO model			PSO model			FL-PSO model			
	q_e ± S.E.	k_1 ± S.E.	s^2	q_e ± S.E.	k_2 ± S.E.	s^2	q_e ± S.E.	k ± S.E.	α ± S.E.	s^2
BH-As(III)	2.241 ± 0.025	0.209 ± 0.006	0.194	2.427 ± 0.036	0.137 ± 0.004	0.059	3.159 ± 0.045	0.172 ± 0.008	0.396 ± 0.002	0.019
LCH-As(III)	1.712 ± 0.035	0.251 ± 0.004	0.055	1.831 ± 0.025	0.237 ± 0.002	0.011	2.079 ± 0.038	0.356 ± 0.001	0.503 ± 0.004	0.002
BAH-As(III)	1.488 ± 0.032	0.063 ± 0.003	0.137	1.740 ± 0.018	0.043 ± 0.002	0.063	3.587 ± 0.032	0.0254 ± 0.006	0.471 ± 0.003	0.032
LCAH-As(III)	1.419 ± 0.012	0.047 ± 0.002	0.214	1.542 ± 0.016	0.043 ± 0.003	0.089	1.973 ± 0.012	0.081 ± 0.003	0.522 ± 0.002	0.021
BH-As(V)	2.339 ± 0.045	0.131 ± 0.002	0.177	2.483 ± 0.035	0.081 ± 0.003	0.061	2.499 ± 0.035	0.089 ± 0.005	0.947 ± 0.005	0.060
LCH-As(V)	1.437 ± 0.015	0.075 ± 0.003	0.189	1.552 ± 0.026	0.068 ± 0.004	0.069	1.880 ± 0.026	0.122 ± 0.002	0.528 ± 0.004	0.028
BAH-As(V)	4.284 ± 0.028	0.117 ± 0.007	3.21	4.618 ± 0.069	0.035 ± 0.008	1.413	8.973 ± 0.12	0.030 ± 0.008	0.247 ± 0.008	0.137
LCAH-As(V)	3.526 ± 0.042	0.093 ± 0.008	1.059	3.750 ± 0.068	0.039 ± 0.006	0.302	4.162 ± 0.065	0.072 ± 0.007	0.599 ± 0.007	0.102

S^2: the least square sum.

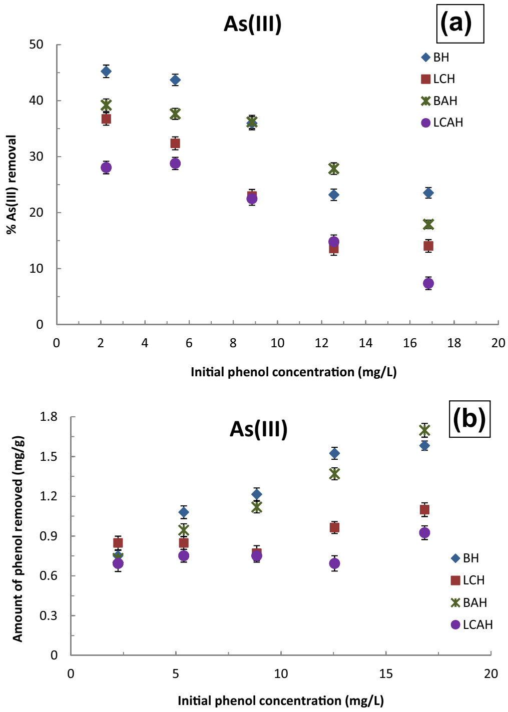

Fig. 5. (a) Removal of As(III) as a function of phenol concentration. (b) Removal of phenol as a function of phenol concentration.

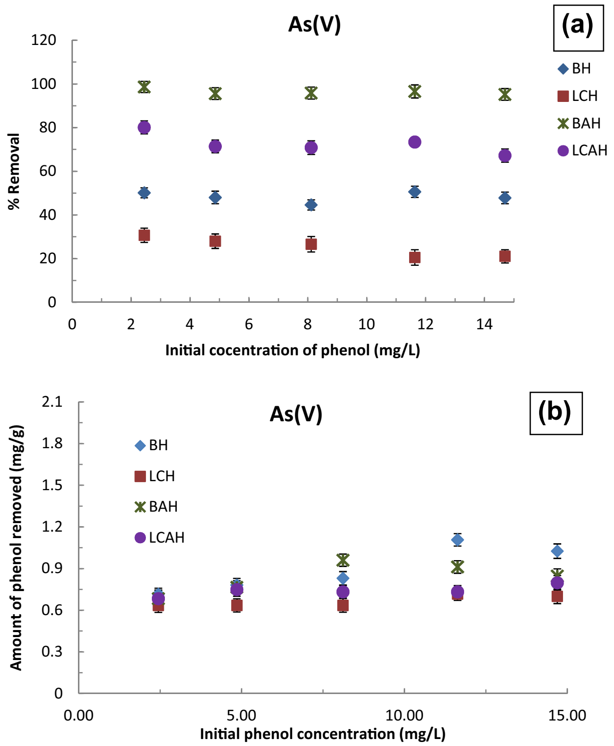

Fig. 6. (a) Removal of As(V) as a function of phenol concentration. (b) Removal of phenol as a function of phenol concentration.

nificantly, the uptake of As(V) (vide Fig. 6(a)). However, the amount of phenol removal is slightly increased (vide Fig. 6(b)). These results fully differ from the results obtained for the As(III) removal in presence of phenol concentrations. However, the results favor the assumption that the binding sites are different for these two different types of sorbing species. As proposed, the As(V) is specifically bound with the aluminol or silanol group and forming strong chemical bonds. However, the introduced HDTMA molecule is providing a strong hydrophobic core which enables to partition the phenol by the vander Waals forces. Therefore, there is no apparent change in the percent uptake of As(V) even at an increased phenol concentration from *Ca* 2 to 15 mg L^{-1}. However, the uptake of the phenol is increased slightly with the increase in phenol concentration. Earlier it was reported that the inorgano-organo-clay i.e., bentonite modified with Fe-polycations and cetyltrimethylammonium bromide materials showed fairly good applicability in the simultaneous removal of phosphate and phenanthrene from aqueous solutions. They further pointed that the hybrid material were possessed two different active sites capable to sequester different types of pollutants i.e., organic and inorganic pollutants from the aqueous solutions simultaneously [64]. Similarly, the aluminium pillared and HDTMA modified sericite showed similar results and found suitable for the simultaneous removal of phenol and arsenic from aqueous solutions [22].

3.2.7. Effect of co-ions

Further, the sorption of As(III) and As(V) is conducted in presence of several cations and anions separately keeping the arsenic concentration 10.0 mg L^{-1} and pH 4.5 as constant. The co-ion concentration is taken as 50.0 mg L^{-1}. The cations chosen are Cd(II), Cu(II) and Mn(II) whereas the anions taken are glycine, iminodiacetic acid, sulfate, oxalate, phosphate and ethylenediaminetetraacetic acid. The results are presented graphically in Figs. 7 and 8, respectively for the As(III) and As(V).

Fig. 7(a) shows that the presence of these cations, in general, causes a decrease in percent removal of As(III). However, the sorption of As(III) by the solids BAH and LCAH is not affected significantly in presence of Cd(II).

The presence of anions, at least for BH and LCH solids, is caused significant decrease in percent removal of As(III) (*cf* Fig. 7(b)). However, the BAH and LCAH solids possess almost identical percent removal of As(III) as compared to the blank sorption data.

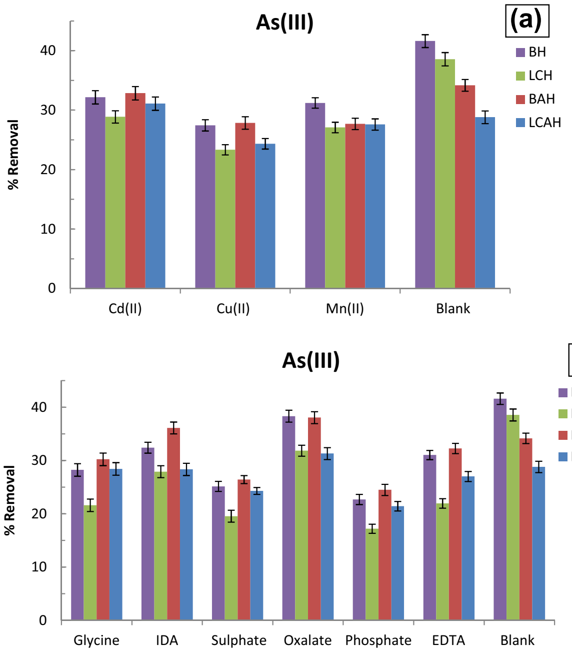

Fig. 7. Removal of As(III) in presence of (a) cations; and (b) anions.

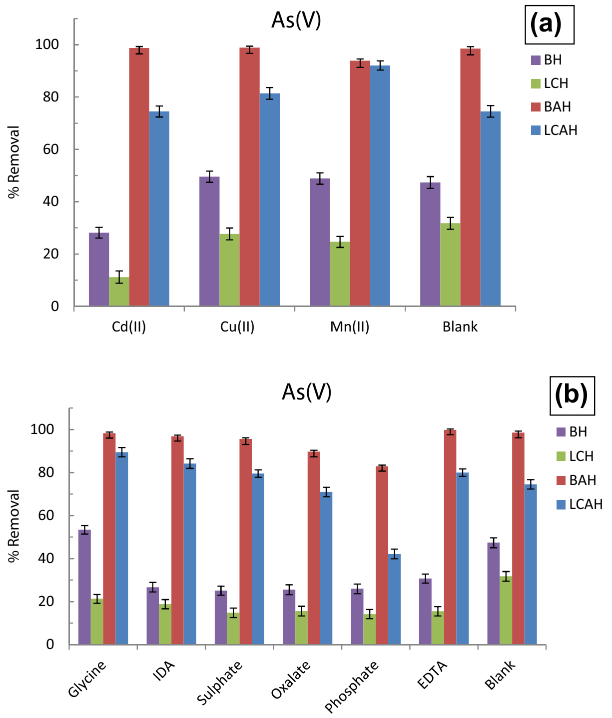

Fig. 8. Removal of As(V) in presence of (a) cations; and (b) anions.

Therefore, the solids BAH and LCAH are selective sorbing materials for the removal of As(III) even in presence of several anions. Earlier, it was reported that the presence of several anions viz., NO_3^-, Cl^-, SO_4^{2-}, HCO_3^- and CO_3^{2-} show a marked decrease in As(III) sorption by the hybrid materials zirconium (IV) oxide-ethanolamine (ZrO-EA). Moreover, the presence of CO_3^{2-} and HCO_3^- show practically no removal of arsenic (III) [65].

Unlike As(III), the uptake of As(V) is almost unaffected in presence of Cd(II), Cu(II) or Mn(II) for the solids BAH and LCAH (*cf* Fig. 8(a)). Moreover, for the solids BH and LCH the presence of Cu(II) and Mn(II) is not affected to a significant extent whereas the presence of Cd(II) is, definitely, caused to decrease the uptake of As(V) by the solids BH and LCH. Previously, it was reported that the presence of Ca^{2+} or Mg^{2+} enhances the arsenate sorption whereas Fe^{2+} decreases significantly the removal of arsenate by the iron based sorbing materials [66].

Similarly, the presence of glycine, IDA, oxalate and EDTA could not affect the uptake of As(V) by the solids BAH and LCAH (*cf* Fig. 8(b)). However, the presence of phosphate, to some extent, decreases the uptake of As(V) by these solids. The BH and LCH solids, in general, show that the presence of these anions could affect the removal of As(V) from aqueous solutions. These results again show the greater applicability of the aluminium pillared HDTMA modified clay samples in the effective and selective removal of arsenic from ground water samples. Previously, it was reported that the presence of phosphate significantly suppresses the arsenic removal by the ferrous based red mud sludge, however, carbonate shows no effect in arsenic removal [67]. Further, it was suggested that since phosphorous and arsenic elements are lying in the same group, and arsenate and phosphate are having similar molecular structures which causes for competitive sorption onto the surface active sites. The other report indicates that the anions viz., arsenate, phosphate, or even silicate readily forming inner-sphere complexes with the surfaces of iron oxides (or nano zero valent iron supported on activated carbon) and a competitive sorption occurs for the binding sites hence decreases the sorption of arsenic. Whereas the sulfate ions is sorbed both specifically and non-specifically and the bonding strength with iron (hydr)oxide is much weaker than that of arsenate hence, affecting insignificantly the uptake of arsenic [66,68]. Similarly, the presence of co-ions viz., chloride, nitrate, sulfate, chromate, and acetate was not interfered the sorption of As(V), whereas the phosphate greatly influenced the sorption by the aluminium-loaded Shirasu-zeolite [47].

4. Conclusions

Hybrid porous materials are obtained modifying the bentonite (B) and local clay (LC) using the HDTMA (BH or LCH) or aluminium pillared HDTMA (BAH or LCAH). The solids are characterized by the IR and XRD analytical methods. IR data shows that the HDTMA is inoculated within the clay structure. XRD data shows the characteristics diffraction peaks of quartz, smectite, illite and kaolinite phases are visible with these two clay samples i.e., bentonite and local clay. The SEM images reveal that the modified solids are porous and surface is heterogeneous in nature. The BAH and LCAH solids possess with additional fine particles of aluminium oxide onto the clay surface. The BET data showed that an appreciable porosity was obtained with the hybrid materials. Further, these solids are employed for the removal of As(III) and As(V) from aqueous solutions under various physico-chemical parametric studies. Both As(III) and As(V) shows relatively higher percent sorption at pH around 4–7. The BAH and LCAH solids possess much increased percent removal of As(V) comparing to the BH or LCH solids, whereas BH, LCH, BAH and LCAH possess almost identical removal percent for As(III). The modified solids show relatively increased percent removal both for As(III) and As(V) comparing to the pristine clay. The increase in concentration favors the removal of As(III) and As(V) by these solids. The increase in background electrolyte concentrations from 0.001 to 0.1 $\mathrm{mol\,L^{-1}}$ $NaNO_3$ causes insignificant effect in percent removal of As(V) by the hybrid materials whereas the As(III) is decreased significantly. This indicates that the As(V) is forming an inner sphere complexation onto the surfaces whereas As(III) is sorbed with weak vander Waals forces and forming outer sphere complexes at the solid surface. These results are further illustrated with the FT-IR results obtained for the arsenic loaded hybrid materials. Similarly, the increase in phenol concentration causes a significant decrease of As(III) removal but at the same time the phenol removal is increased significantly. On the other hand, As(V) removal is unaffected with the increase in phenol concentration whereas the phenol removal is also increased slightly. The uptake of As(III) and As(V) by these hybrid materials is rapid and follows the pseudo-second-order and fractal like pseudo-second-order rate kinetics. The presence of several cations (Cd(II), Cu(II) and Mn(II)) and anions (glycine, IDA, sulfate, oxalate, phosphate and EDTA) are examined. The BAH and LCAH is, overall, highly selective at least for As(V). The hybrid porous materials are found to be useful alternative materials in the effective and selective remediation of arsenic contaminated ground waters.

Acknowledgements

One of authors DT wishes to acknowledge the CSIR, New Delhi for the financial support as in the form of Research Project (vide No.: 01 (2567)/12/EMR-II). The work is also partly supported by the Korea Ministry of Environment as a “Converging technology project” (Proposal No. 2013001450001). The authors acknowledge Dr. G.V. Narasimha Rao, Head, Materials Characterization & Testing Group (MCTG), International Advanced Research Center for Powder Metallurgy & New Materials (ARCI), Department of Science & Technology (DST), Government of India, Balapur P.O., Hyderabad 500005, India for conducting the XRD analysis.

Appendix A. Supplementary data

Supplementary data associated with this article can be found, in the online version, at http://dx.doi.org/10.1016/j.cej.2015.02.053.

References

[1] D. Tiwari, H.U. Kim, S.M. Lee, Removal behavior of sericite for Cu(II) and Pb(II) from aqueous solutions: batch and column studies, Sep. Purif. Technol. 57 (2007) 11–16.

[2] J. Ikhsan, B.B. Johnson, J.D. Wells, A comparative study of the adsorption of transition metals on kaolinite, J. Colloid Interface Sci. 217 (1999) 403–410.

[3] S.M. Lee, D. Tiwari, Organo and inorgano-organo-modified clays in the remediation of aqueous solutions: an overview, Appl. Clay Sci. 59–60 (2012) 84–102.

[4] J.Q. Jiang, C. Cooper, S. Ouki, Comparison of modified montmorillonite adsorbents. Part I. Preparation, characterization and phenol adsorption, Chemosphere 47 (2002) 711–716.

[5] J. Smith, S. Bartlett-Hunt, S. Burns, Sorption and permeability of gasoline hydrocarbons in organo bentonites porous media, J. Hazard. Mater. B96 (2003) 91–97.

[6] H. He, Q. Tao, J. Zhu, P. Yuan, W. Shen, S. Yang, Silylation of clay mineral surfaces, Appl. Clay Sci. 71 (2013) 15–20.

[7] D.L. Guerra, S.P. Oliveira, R.A.S. Silva, E.M. Silva, A.C. Batista, Dielectric properties of organo functionalized kaolinite clay and application in adsorption mercury cation, Ceram. Int. 38 (2012) 1687–1696.

[8] H.P. He, Q. Zhou, W.N. Martens, T.J. Kloprogge, P. Yuan, X.F. Yunfei, J.X. Zhui, R.L. Frost, Microstructure of HDTMA$^+$-modified montmorillonite and its influence on sorption characteristics, Clays Clay Miner. 54 (2006) 691–698.

[9] K.A. Carrado, Synthetic organo- and polymer-clays: preparation, characterization and materials applications, Appl. Clay Sci. 17 (2000) 1–23.

[10] S.S. Ray, M. Okamoto, Polymer/layered silicate nanocomposites: a review from preparation to processing, Prog. Polym. Sci. 28 (2003) 1539–1641.

[11] J. Konta, Clay and man: clay raw materials in the service of man, Appl. Clay Sci. 10 (1995) 275–335.

[12] F. Bergaya, G. Lagaly, General introduction: clays, clay minerals, and clay science, in: F. Bergaya, G. Theng, G. Lagaly (Eds.), Developments in Clay Science; Handbook of Clay Science, Elsevier, New York, 1 (2006), 1–18.

[13] G.A. Ikhtiyarova, A.S. Ozcan, O. Gok, A. Ozcan, Characterization of natural- and organo-bentonite by XRD, SEM, FT-IR and thermal analysis techniques and its adsorption behaviour in aqueous solutions, Clay Miner. 47 (2012) 31–44.

[14] T. Yang, M.L. Chen, L.H. Liu, J.H. Wang, P.K. Dasgupta, Iron(III) modification of *Bacillus subtilis* membranes provides record sorption capacity for arsenic and endows unusual selectivity for As(V), Environ. Sci. Technol. 46 (2012) 2251–2256.

[15] M. Chen, Y. Lin, C. Gu, J. Wang, Arsenic sorption and speciation with branch-polyethyleneimine modified carbon nanotubes with detection by atomic fluorescence spectrometry, Talanta 104 (2013) 53–57.

[16] D. Mohan, C.U. Pittman Jr., Arsenic removal from water/wastewater using adsorbents – a critical review, J. Hazard. Mater. 142 (2007) 1–53.

[17] L. Cornejo, H. Lienqueo, M. Arenas, J. Acarapi, D. Contreras, J. Ya'nez, H.D. Mansillac, In field arsenic removal from natural water by zero-valent iron assisted by solar radiation, Environ. Pollut. 156 (2008) 827–831.

[18] M. Lin, C. Liao, Assessing the risks on human health associated with inorganic arsenic intake from groundwater-cultured milkfish in south western Taiwan, Food Chem. Toxicol. 46 (2008) 701–709.

[19] K. Tyrovola, E. Peroulaki, N. Nikolaidis, Modeling of arsenic immobilization by zero valent iron, Eur. J. Soil Biol. 43 (2007) 356–367.

[20] International Agency for Research on Cancer (IARC), Monographs on the Evaluation of Carcinogenic Risks to Humans, Supplement 7 (1987).

[21] R. Domínguez-González, L. GonzálezVarela, P. Bermejo-Barrera, Functionalized gold nanoparticles for the detection of arsenic in water, Talanta 118 (2014) 262–269.

[22] D. Tiwari, S.M. Lee, Novel hybrid materials in the remediation of ground waters contaminated with As(III) and As(V), Chem. Eng. J. 204–206 (2012) 23–31.

[23] J. Hao, M.J. Han, C. Wang, X. Meng, Enhanced removal of arsenite from water by a mesoporous hybrid material-thiol-functionalized silica coated activated alumina, Microporous Mesoporous Mater. 124 (2009) 1–7.

[24] C.M. Iesan, C. Capat, F. Ruta, I. Udrea, Characterization of hybrid inorganic/organic polymer-type materials used for arsenic removal from drinking water, React. Funct. Polym. 68 (2008) 1578–1586.

[25] C.M. Iesana, C. Capat, F. Ruta, I. Udrea, Evaluation of a novel hybrid inorganic/organic polymer type material in the Arsenic removal process from drinking water, Water Res. 42 (2008) 4327–4333.

[26] S. Mandal, M.K. Sahu, R.K. Patel, Adsorption studies of arsenic(III) removal from water by zirconium polyacrylamide hybrid material (ZrPACM-43), Water Resour. Industry 4 (2013) 51–67.

[27] K. Xia, R.Z. Ferguson, M. Losier, N. Tchoukanova, R. Brüning, Y. Djaoued, Synthesis of hybrid silica materials with tunable pore structures and morphology and their application for heavy metal removal from drinking water, J. Hazard. Mater. 183 (2010) 554–564.

[28] E. Petala, K. Dimos, A. Douvalis, T. Bakas, J. Tucek, R. Zboril, M.A. Karakassides, Nanoscale zero-valent iron supported on mesoporous silica: characterization and reactivity for Cr(VI) removal from aqueous solution, J. Hazard. Mater. 261 (2013) 295–306.

[29] I. Sheet, A. Kabbani, H. Holail, Removal of heavy metals using nanostructured graphite oxide, silica nanoparticles and silica/graphite oxide composite, Energy Proc. 50 (2014) 130–138.

[30] B. Bhattarai, M. Muruganandham, R.P.S. Suri, Development of high efficiency silica coated β-cyclodextrin polymeric adsorbent for the removal of emerging contaminants of concern from water, J. Hazard. Mater. 273 (2014) 146–154.

[31] S. Kaufhold, M. Pohlmann-Lortz, R. Dohrmann, R. Nueesch, About the possible upgrade of bentonite with respect to iodide retention capacity, Appl. Clay Sci. 35 (2007) 39–46.

[32] B.S. Krishna, D.S.R. Murthy, B.S.J. Prakash, Surfactant-modified clay as adsorbent for chromate, Appl. Clay Sci. 20 (2001) 65–71.

[33] Z. Li, R.S. Bowman, Retention of inorganic oxyanions by organo-kaolinite, Water Res. 35 (2001) 3771–3776.

[34] H. He, Y. Ma, J. Zhu, P. Yuan, Y. Qing, Organo clays prepared from montmorillonites with different cation exchange capacity and surfactant configuration, Appl. Clay Sci. 48 (2010) 67–72.

[35] J. Su, H.G. Huang, X.Y. Jin, X.Q. Lu, Z.L. Chen, Synthesis, characterization and kinetic of a surfactant-modified bentonite used to remove As(III) and As(V) from aqueous solution, J. Hazard. Mater. 185 (2011) 63–70.

[36] Thanhmingliana, D. Tiwari, Efficient use of hybrid materials in the remediation of aquatic environment contaminated with micro-pollutant diclofenac, Chem. Eng. J. 263 (2015) 364–373.

[37] U.F. Alkaram, A.A. Mukhlis, A.H. Al-Dujaili, The removal of phenol from aqueous solutions by adsorption using surfactant-modified bentonite and kaolinite, J. Hazard. Mater. 169 (2009) 324–332.

[38] L.-C. Juang, C.-C. Wang, C.-K. Lee, T.-C. Hsu, Dyes adsorption onto organoclay and MCM-41J, Environ. Eng. Manage. 17 (2007) 29–38.

[39] S.-M. Lee, W.-G. Kim, C. Laldawngliana, D. Tiwari, Removal behavior of surface modified sand for Cd(II) and Cr(VI) from aqueous solutions, J. Chem. Eng. Data 55 (2010) 3089–3094.

[40] Lalhmunsiama, D. Tiwari, S.M. Lee, Activated carbon and manganese coated activated carbon precursor to dead biomass in the remediation of arsenic contaminated water, Environ. Eng. Res. 17 (2012) S41–S48.

[41] D. Tiwari, C. Laldawngliana, S.M. Lee, Immobilized small sized manganese dioxide sand in the remediation of arsenic contaminated water, Environ. Eng. Res. 19 (2014) 107–113.

[42] D. Nabi, I. Aslam, I.A. Qazi, Evaluation of the adsorption potential of titanium dioxide nanoparticles for arsenic removal, J. Environ. Sci. 21 (2009) 402–408.

[43] R.C. Vaishya, S.K. Gupta, Modelling arsenic(III) adsorption from water by sulfate modified iron-oxide coated sand (SMIOCS), Sep. Sci. Technol. 39 (2004) 645–666.

[44] J. Madejova, P. Komadel, Baseline studies of the clay minerals society source clays: infrared methods, Clays Clay Miner. 49 (2001) 410–432.

[45] N. Jović-Jovičić, A. Milutinović-Nikolić, P. Banković, B. Dojčinović, B. Nedić, I. Gržetić, D. Jovanović, Synthesis, characterization and adsorptive properties of organobentonites, Acta Phys. Pol. A 117 (5) (2010) 849–854.

[46] Y.M. Zheng, S.-W. Zou, K.G.N. Nanayakkara, T. Matsuura, J.P. Chen, Adsorptive removal of arsenic from aqueous solution by a PVDF/zirconia blend flat sheet membrane, J. Membr. Sci. 374 (2011) 1–11.

[47] Y. Xu, T. Nakajima, A. Ohki, Adsorption and removal of arsenic(V) from drinking water by aluminum-loaded zeolite Shirasu, J. Hazard. Mater. B92 (2002) 275–287.

[48] V.M. Boddu, K. Abburi, J.L. Talbott, E.D. Smith, R. Haasch, Removal of arsenic(III) and arsenic(V) from aqueous medium using chitosan-coated biosorbent, Water Res. 42 (2008) 633–642.

[49] K. Tyrovola, N.P. Nikolaidis, N. Veranis, N. Kallithrakas-Kontos, P.E. Koulouridakis, Arsenic removal from geothermal waters with zero-valent iron-effect of temperature, phosphate and nitrate, Water Res. 40 (2006) 2375–2386.

[50] V.K. Gupta, V.K. Saini, N. Jain, Adsorption of As(III) from aqueous solutions by iron oxide-coated sand, J. Colloid Interface Sci. 288 (2005) 55–60.

[51] H. Zhu, Y. Jia, X. Wu, H. Wang, Removal of arsenic from water by supported nano zero-valent iron on activated carbon, J. Hazard. Mater. 172 (2009) 1591–1596.

[52] K.F. Hayes, C. Papelis, J.O. Leckie, Modeling ionic strength effects on anion adsorption at hydrous oxide/solution interfaces, J. Colloid Interface Sci. 125 (1988) 717–726.

[53] X. Meng, G.P. Korfiatis, S. Bang, K.W. Bang, Combined effects of anions on arsenic removal by iron hydroxides, Toxicol. Lett. 133 (1) (2002) 103–111.

[54] S.M. Lee, D. Tiwari, Organo-modified sericite in the remediation of an aquatic environment contaminated with As(III) or As(V), Environ. Sci. Pollut. Res. 21 (2014) 407–418.

[55] G.J. Liu, X.R. Zhang, L. McWilliams, J.W. Talley, C.R. Neal, Influence of ionic strength, electrolyte type, and NOM on As(V) adsorption onto TiO_2, J. Environ. Sci. Health A 43 (2008) 430–436.

[56] S. Azizian, Kinetic models of sorption: a theoretical analysis, J. Colloid Interface Sci. 276 (2004) 47–52.

[57] Y.S. Ho, G. McKay, A comparison of chemisorption kinetic models applied to pollutant removal on various sorbents, Process Saf. Environ. Protect. 76 (1998) 332–340.

[58] M. Haerifar, S. Azizian, Fractal-like adsorption kinetics at the solid/solution interface, Process Saf. Environ. Protect. 76 (1998) 332–340.

[59] Y.S. Ho, Review of second-order model for adsorption systems, J. Hazard. Mater. B 136 (2006) 681–689.

[60] Y.S. Ho, G. McKay, The kinetics of sorption of divalent metal ions onto sphagnum moss peat, Water Res. 34 (2000) 735–742.

[61] M. Alexandre, P. Dubois, Polymer-layered silicate nano-composites: preparation, properties and uses of a new class of materials, Mater. Sci. Eng. Res. 28 (2000) 1–63.

[62] M. Zanetti, S. Lomakin, G. Camino, Polymer layered silicate nano-composites, Macromol. Mater. Eng. 279 (2000) 1–9.

[63] Z. Li, R.S. Bowman, Counter ion effects on the sorption of cationic surfactant and chromate on natural clinoptilolite, Environ. Sci. Technol. 31 (1997) 2407–2412.

[64] J. Ma, L. Zhu, Simultaneous sorption of phosphate and phenanthrene to inorgano-organo-bentonite from water, J. Hazard. Mater. B136 (2006) 982–988.

[65] S. Mandal, T. Padhi, R.K. Patel, Studies on the removal of arsenic(III) from water by a novel hybrid material, J. Hazard. Mater. 192 (2011) 899–908.

[66] H. Zhu, Y. Jia, X. Wua, H. Wang, Removal of arsenic from water by supported nano zero-valent iron on activated carbon, J. Hazard. Mater. 172 (2009) 1591–1596.

[67] Y. Li, J. Wang, Z. Luan, Z. Liang, Arsenic removal from aqueous solution using ferrous based red mud sludge, J. Hazard. Mater. 177 (2010) 131–137.

[68] Y. Jia, G.P. Demopoulos, Adsorption of arsenate onto ferrihydrite from aqueous solution: influence of media (sulfate vs. nitrate), added gypsum, and pH alteration, Environ. Sci. Technol. 39 (2005) 9523–9527.

Publishing
Journals, books and databases

ROYAL SOCIETY OF CHEMISTRY

RSC Advances

2015, 5, Issue 58, Page 46834 to 46842

An international journal to further the chemical sciences

Impact Factor 3.840 Indexed in Web of Science

ISSN (Online): 2046-2069

About the journal

RSC Advances is an international, peer-reviewed journal covering all of the chemical sciences, including multidisciplinary and emerging areas. The criteria for publication are that the work must be high quality, well conducted and add to the development of the field. Articles submitted to the journal are evaluated by international referees for the overall quality and accuracy of the science presented.

RSC Advances publishes communications, papers and reviews. For more details on the scope of the journal read about our advanced topic modelling technology which assigns articles into 12 main topics and over 100 further sub-categories.

Subject categories

Advanced topic modelling technology with 12 main topics and over 100 sub-categories.

Editor

RSC Advances is supported by international Editorial and Advisory Boards, led by **Professor Mike Ward** (University of Sheffield, UK), which input into the development and strategy of the journal.

Contact the Journal

RSC Advances
Royal Society of Chemistry, Thomas Graham House, Science Park, Milton Road, Cambridge CB4 0W
Tel: +44 (0) 1223 420066
Fax: +44 (0) 1223 420247
Email: RSC Advances

RSC Advances

PAPER

Cite this: *RSC Adv.*, 2015, **5**, 46834

Efficient attenuation of 17α-ethynylestradiol (EE2) and tetracycline using novel hybrid materials: batch and column reactor studies

Thanhmingliana,[a] Seung Mok Lee,[b] Diwakar Tiwari*[a] and Shailesh K. Prasad[c]

Received 29th December 2014
Accepted 11th May 2015

DOI: 10.1039/c4ra17197g

www.rsc.org/advances

Hybrid materials were obtained by modifying natural bentonite (B) or locally collected clay (LC) using hexadecyltrimethylammonium bromide (HDTMA) to obtain bentonite-HDTMA (BH) and local clay-HDTMA (LCH), or by simultaneous pillaring with aluminum and modification with HDTMA to obtain BAH and LCAH. The hybrid materials were used for the efficient attenuation of micro-pollutants, 17α-ethynylestradiol (EE2) and tetracycline (TC), in aqueous solutions under batch and fixed-bed column reactor experiments. Batch data indicated that the uptake of EE2 and TC by the hybrid materials was slightly affected at low and high pH within the pH range of 4.0–10.0. The uptake was not affected by varying the initial sorptive concentration (1.0–10.0 mg L^{-1} for EE2 and 1.0–20.0 mg L^{-1} for TC) and the background electrolyte (NaCl) concentrations (0.0001–0.1 mol L^{-1}). Moreover, the attenuation of EE2 and TC by these hybrid materials was fairly efficient. Within a contact time of 60 min for EE2 and 240 min for TC, an apparent equilibrium between the clay and solution was achieved. Kinetic modeling showed that the data were fitted well to the pseudo-second order (PSO) and fractal-like-pseudo-second order (FL-PSO) kinetic models compared with the pseudo-first order (PFO) model because a low value of the least square sum was obtained for these two models. The fixed-bed column results showed that a high breakthrough volume was obtained for attenuation of EE2 and TC using the hybrid materials. Furthermore, the breakthrough data were fitted well to the Thomas equation; therefore, a very high loading capacity was estimated for EE2 and TC for the hybrid materials. These hybrid materials are useful materials in the remediation of aquatic environments contaminated with these two micro-pollutants.

1. Introduction

Clay minerals are composed of fine particles of hydrous aluminosilicates, and develop plasticity when mixed with water. A common characteristic of clay minerals is their layer structure, although they have diverse chemical, mineralogical, and physical characteristics. Clays possess a permanent net negative charge because of isomorphous substitution, which is responsible for the presence of exchangeable cations in the interspace region.[1–3] Therefore, the electrical charge possessed by clay minerals and their microscale porosity makes them suitable as natural sorbing materials for several pollutants in the treatment of contaminated water. Although clay minerals are used widely to decontaminate inorganic pollutants from wastewater, pristine clay minerals possesses low sorption capacity for several hydrophobic and low- or nonpolar organic pollutants owing to the hydrophilic nature of these materials.[4] Moreover, most clays show low settling capacity, limiting their wider practical application in wastewater treatment.[5] The exchange of clay cations with organic cations produces useful hybrid materials for the attenuation of several non-polar organic contaminants (NOC) from aqueous solutions.[6–10] Likewise, hybrid materials obtained by pillaring with poly(hydroxo-metal) cations and simultaneous intercalation of suitable organic cations are particularly suitable for wastewater treatment, because these materials show good affinity for organic impurities, and possess satisfactory settling capacity, allowing easy separation of solid and aqueous components.[3]

The presence of organic micro-pollutants, particularly pharmaceuticals and personal care products (PPCPs) in the aquatic environment is a serious environmental concern because several micro-pollutants are persistent, non-biodegradable and toxic even at low levels. The widespread distribution of PPCPs has been demonstrated by a number of monitoring studies and measurable concentrations of many PPCPs have been found in wastewater, surface water, sediments, groundwater, and even in drinking water.[11–13] PPCPs enter the terrestrial environment through direct runoff and

---

[a] *Department of Chemistry, School of Physical Sciences, Mizoram University, Aizawl-796004, India, +91-389-2330834. E-mail: diw_tiwari@yahoo.com; Tel: +91-389-2301806*

[b] *Department of Health and Environment, Catholic Kwandong University, 522 Naegok-dong, Gangneung, Gangwon-do 210-701, Korea*

[c] *Department of Chemistry, National Institute of Technology, Jamshedpur-831014, India*

excretion as unmetabolized drugs or active metabolites and degradation products.[14] Around 70% of pharmaceuticals consumed are excreted in urine as active ingredients or metabolites.[15–17] The normal sewage treatment system cannot eliminate antibiotics completely, which results in the presence of residual antibiotics in effluent.[18]

17α-ethynylestradiol (EE2) is a synthetic estrogen. It is a derivative of the natural hormone, estradiol (E2). EE2 is used in almost all modern formulations of combined oral contraceptive pills and hormone replacement therapy for treating conditions such as osteoporosis, menstrual disorders, and prostate and breast cancer.[19–21] EE2 is one of the most potent estrogenic chemicals of the known endocrine disruptors.[22] Tetracycline (TC) is a broad-spectrum antibiotic drug commonly prescribed for the treatment of bacterial infections.[23] TC is widely used in aquaculture and the livestock industry[24,25] as a food additive and growth promoter.[26] The consumption of tetracycline for veterinary purposes is higher than for other classes of antibiotics.[27]

Sorptive removal of PPCPs using natural and synthetic materials is a possible method of decontaminating the aquatic environment contaminated with PPCPs. de Rudder *et al.*[28] removed 17α-ethynylestradiol (EE2) from water in three upstream bioreactors (UBRs), filled with sand, granulated activated carbon (GAC), or MnO_2 granules. The removal of EE2 in the sand, GAC and MnO_2 reactors were 17.3%, 99.8% and 81.7%, respectively. They reported that the removal in the GAC reactor was mainly due to adsorption, whereas the removal in the MnO_2 reactor was possibly through the catalytic properties of MnO_2. Han *et al.*[20] studied the adsorption of ethynylestradiol (EE2) from aqueous solutions using industrial-grade polyamide 612 (PA612) particles. They observed that the adsorption of EE2 on PA612 followed pseudo-second order kinetics and the strong binding affinity between EE2 and PA612 was due to hydrophobic partitioning of EE2 solutes and hydrogen bonding interactions on PA612 amide groups. Combined coagulation–adsorption treatment using single-walled carbon nanotubes (SWCNTs), multiwall carbon nanotubes (MWCNTs), and powdered activated carbon (PAC) was studied for the removal of EE2.[29] The removal percentages using the combined coagulation–adsorption method were similar to those achieved using only an adsorbent. Al-Khateeb *et al.*[30] reported that the adsorption of EE2 on MWCNTs was a pseudo-second-order kinetic process it was exothermic in nature. Adsorption of tetracycline from aqueous solution by graphene oxide (GO) was investigated by Gao *et al.*[31] They reported that tetracycline strongly adsorbed on the GO surface *via* a π–π interaction and cation-π bonding. Activated carbon with different chemical and textural properties, sludge-derived materials, and the removal by the combined use of microorganisms and activated carbon (bioadsorption) were assessed for the adsorption of three different tetracyclines (TCs) (tetracycline, oxytetracycline, and chlortetracycline).[32] Sludge-derived materials possessed significantly higher removal capacity than the commercial activated carbon sample. Li *et al.*[33] investigated the adsorption of tetracycline on kaolinite with pH-dependent surface charges in aqueous solution by batch tests supplemented by FTIR analyses. The adsorption of TC on kaolinite was mainly on the external surfaces *via* cation exchange. TC adsorption was more pH dependent and the sorption capacity was much lower compared with that on swelling clays.

The present study uses porous clay materials, commercial bentonite and locally collected clay (local clay), to obtain the novel hybrid materials, hexadecyltrimethylammonium bromide (HDTMA) or aluminum-pillared HDTMA-modified clay. Organic cations with long-chain alkyl groups (*e.g.*, HDTMA) impart hydrophobic properties to the mineral surface, and these hybrid materials provide a hydrophobic core and organophilic properties, which aids hydrophobic bonding with several organic pollutants.[34] We use the hybrid materials to attenuate the important micro-pollutants, EE2 and TC, in aqueous solutions. Batch reactor experiments are conducted for physico-chemical parametric studies, which provide a plausible mechanism for the interfaces. Similarly, fixed-bed column reactor experiments are conducted to optimize the loading capacity of contaminants under dynamic conditions.

2. Materials and methods

2.1. Materials

Bentonite was procured from a commercial supplier, and was mined in Bhuj, Gujarat, India. The bentonite clay was used after simple washing with distilled water and drying at 90 °C in an oven for 24 h. Local clay was collected in Phullen, Mizoram, India. Because the local clay contained numerous impurities it was carefully separated using the International Soil Reference and Information Centre (ISRIC) standard procedure, as described elsewhere.[35] The bentonite and local clay samples were crushed in a mortar and sieved to obtain 100 British Standard Sieve (BSS) mesh size particles (0.150 mm). The cation exchange capacity (CEC) of bentonite and local clay powder were then obtained by using standard United States Environmental Protection Agency (US EPA) method 9080.[36] The CEC of bentonite and local clay were 69.35 and 46.38 meq/100 g of clay, respectively. Hexadecyltrimethylammonium bromide (HDTMA), 17α-ethynylestradiol (EE2) and tetracycline hydrochloride were procured from Sigma-Aldrich, USA. Aluminum(III) chloride was obtained from Merck, India. Sodium chloride (Extrapure) was procured from HiMedia, India. The other chemicals used were of analytical or equivalent grade. The water was purified by using a Millipore water purification system (Milli-Q$^+$).

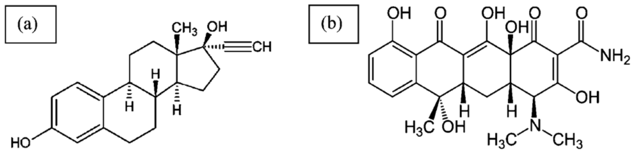

Structures of (a) EE2 and (b) tetracycline

2.2. Methodology

2.2.1. Preparation of organoclay and inorgano–organoclay.

Bentonite or local clay was organically modified by the standard wet cation exchange process. Hexadecyltrimethylammonium bromide (HDTMA) was loaded to saturate the clay CEC. HDTMA-modified bentonite and local clay were labeled as BH and LCH samples, respectively. The inorgano–organoclay was prepared by simultaneous pillaring with aluminum and modification with HDTMA to obtain HDTMA-Al-bentonite (BAH) or HDTMA-Al-local clay (LCAH) hybrid materials. A simple wet method was used as described elsewhere.[5,37]

2.2.2. Characterization and surface morphology of hybrid materials. The surface morphology of the hybrid materials and the virgin clay was determined from field emission scanning electron microscopy (FE-SEM; S-4700, Hitachi, Japan) images. X-ray diffraction (XRD) data was recorded by using an X-ray diffraction machine (X'Pert PRO MPD, PANalytical, Netherlands) with Cu-K$_\alpha$ radiation with a wavelength of 1.5418 Å. Fourier transform-infra red (FT-IR) spectroscopy was performed with an FT-IR spectrometer (Bruker, Tensor 27, USA, KBR disk method). The point of zero charge (pH$_{PZC}$) values of bentonite, local clay, BH, LCH, BAH and LCAH were determined by the pH drift method, as described previously.[38]

2.2.3. Batch reactor experiments. A stock solution (50 mg L^{-1}) of TC was prepared by dissolving an appropriate amount of TC in purified water. The required TC concentration was obtained by successive dilution of stock solution. A stock solution (10 mg L^{-1}) of EE2 was prepared by dissolving an appropriate amount of EE2 in purified water at elevated pH with dilute NaOH. The required EE2 concentration was obtained by successive dilution of stock solution and the pH was adjusted with HCl/NaOH. The pH dependence of sorption data was obtained as follows. A series of 5.0 mg L^{-1} EE2 or 10.0 mg L^{-1} TC solutions (50 mL) was placed in polyethylene bottles and the pH was adjusted by dropwise addition of conc. HCl/NaOH solutions. The clay (0.1 g) was added to these solutions. The bottles were kept in an automatic incubator shaker (Incubator Shaker, TM Weiber, ACMAS Technologies Pvt. Ltd., India) for 24 h at 25 ± 1 °C. The prolonged period of 24 h may allow an apparent equilibrium to be achieved between the clay and solution. The bottles were removed from the shaker and the mixture was filtered with a 0.45 μm syringe filter. The filtrate pH was reported as the equilibrium pH. Absorbance of the filtrates was measured with a UV-vis spectrophotometer (UV1, Thermo Electron Corporation, USA). The absorbance was recorded at 280 nm for EE2 and 360 nm for TC. The calibration curve was obtained by using standard EE2 and TC solutions with various concentrations. Results are presented as the percentage of EE2 and TC removed as a function of equilibrium pH. The spectrophotometric determination of EE2 and TC have been performed previously and are described elsewhere.[39,40] The blank EE2 (5.0 mg L^{-1}) or TC (10 mg L^{-1}) solutions at the appropriate pH were shaken without the hybrid materials in the polyethylene bottles for 24 h. The samples were filtered with a 0.45 μm syringe filter and their absorbance determined at wavelengths of 280 and 360 nm for EE2 and TC, respectively. No decrease in absorbance was observed, which indicated that negligible sorption to the polyethylene bottles occurred.

The concentration dependence study was performed by varying the EE2 concentration from 1.0 to 10.0 mg L^{-1} and the TC concentration from 1.0 to 20.0 mg L^{-1} at pH 7.0 and 25 ± 1 °C. The adsorption process detailed above was then followed. Results are presented as the percentage removal of EE2 or TC as a function of initial EE2 or TC concentration (mg L^{-1}). Time dependent sorption of EE2 and TC by the hybrid materials was obtained at different time intervals. The initial EE2 concentration of 5.0 mg L^{-1} and TC concentration of 10.0 mg L^{-1} for a clay sample of 2.0 g L^{-1} was taken as constant and the sorption experiments were conducted at pH 7.0 and 25 ± 1 °C. Results are reported as percentage removal of EE2 or TC as a function of time (min). The effect of background electrolyte concentration on sorption of EE2 or TC was studied varying the background electrolyte (NaCl) concentration from 0.0001 to 0.1 mol L^{-1} with EE2 and TC solution with initial concentrations 5.0 and 10.0 mg L^{-1}, respectively. The solution pH (7.0) and temperature (25 ± 1 °C) was kept constant throughout the experiments. Results are presented as percentage EE2 and TC removed as a function of background electrolyte concentration.

2.2.4. Fixed-bed column experiments. Fixed-bed column experiments were conducted with a glass column (1 cm inner diameter) packed with 0.25 g of hybrid materials in the middle of the column. Below and above the hybrid material, 1.0 g of virgin sand particles (14–16 BSS) was placed and the rest of the column was packed with glass beads. EE2 (5.0 mg L^{-1}) or TC (10.0 mg L^{-1}) solution at pH 7.0 was pumped upward from the bottom of the column with a peristaltic pump (KrosFlo Research I Peristaltic Pump, Spectrum Laboratories Inc., California, USA), at a constant flow rate of 1.0 mL min^{-1}. Effluent solution was collected by using a fraction collector (Spectra/Chrom CF-2 Fraction Collector, Spectrum Laboratories Inc., California, USA). The collected effluents were filtered with a 0.45 μm syringe filter and the filtrates were then subjected to UV-vis measurements.

Breakthrough data obtained from the fixed-bed column experiments were used to optimize the loading capacity of EE2 or TC on the hybrid material loaded column under dynamic conditions, using the Thomas equation,[41]

$$\frac{C_e}{C_0} = \frac{1}{1 + e^{(K_T(q_0 m - C_0 V))/Q}} \quad (1)$$

where C_e and C_0 are the concentrations (mg L^{-1}) of effluent and influent solutions of EE2 and TC, respectively; K_T is the Thomas rate constant (L min^{-1} mg^{-1}); q_0 is the maximum amount (mg g^{-1}) of EE2 or TC loaded under the column conditions; m is the mass (g) of hybrid materials in the column; V is the throughput volume (L); and Q is the flow rate (L min^{-1}) of EE2 or TC solution. The column data were fitted to a non-linear Thomas equation by using the least squares fitting method to estimate the two unknown parameters, K_T and q_0.

3. Results and discussion

3.1. Characterization of materials

FT-IR data indicated that the hybrid materials, BH, BAH, LCH or LCAH, possess prominent IR stretching bands at 2930 and 2850 cm^{-1} arising from –CH$_2$ asymmetric and symmetric stretching vibrations respectively. This confirmed the introduction of HDTMA in the clay network for all these hybrid materials.

Characteristic peaks in the X-ray diffraction analysis showed that both the clay samples contained quartz, smectite, illite and kaolinite in various proportions. The XRD patterns of the modified clay samples were almost identical to the virgin clay, with slight changes in *d*-values and peak intensities. The FE-SEM images clearly show that the organo-modified bentonite or LC (BH or LCH) had more heterogeneous and disordered surface structures. BAH and LCAH showed a similar disordered structure, although fine particles were observed on the surface that were possibly aggregated or immobilized as aluminum hydroxide or Al_2O_3. Detailed characterization of these hybrid materials has been described previously.[37,42]

3.2. Batch reactor experiments

3.2.1. Effect of pH. The pH dependent removal of EE2 (pH 4.01 to 10.14) and TC (pH 3.96 to 10.06) by the clays is presented in Fig. 1(a) and (b), respectively. The very high uptake of EE2 was not changed in the pH region of 4.0 to 8.0 by the clays. However, a further increase above pH 8.0 decreased the uptake of EE2. The uptake of EE2 by these clays may be increased by speciation of EE2 and the surface properties of the clays. EE2 has a pK_a of 10.4,[43] indicating that EE2 is a neutral molecule up pH 10.0 and carries a net negative charge above pH 10.4. However, the pH_{PZC} values of the clays were 10.0, 8.2, 6.1, 5.8, 5.1 and 5.1 for B, BH, BAH, LC, LCH and LCAH, respectively. This implies that except bentonite, the other clays possess a net negative charge around pH 7. Therefore, there is unlikely to be electrostatic attraction between the clay surface and EE2. Hence, the possible mechanism of EE2 uptake by these hybrid materials is demonstrated by the fact that the introduction of an organic cation (HDTMA) increases the hydrophobicity and organophilicity of the surface. This enables EE2 to partition at the HDTMA hydrophobic core.[44] However, Al-pillared HDTMA-modified local clay (LCAH) showed slightly less uptake of EE2, possibly because of the screening of HDTMA by small aluminum oxide/hydroxide particles on the clay surface. Furthermore, the removal of EE2 was decreased by increasing the solution pH to 10.0 because partial acidic dissociation of EE2 occurred at this pH. The dissociation caused electrostatic repulsion, reducing the partitioning of the EE2 in the hydrophobic core of the hybrid materials. Previously, hybrid materials obtained by modifying natural sericite with HDTMA and alkyldimethylbenzylammonium chloride were used in the remediation of wastewaters contaminated with BPA. The increase in pH from 2.0 to 10.0 did not significantly affect the percentage uptake of BPA by the hybrid materials. Furthermore, it was reported that organoclays containing longer chain surfactant molecules were less affected by the solution pH[45] and consistently possessed a high adsorption capacity for BPA even under alkaline conditions.[46] Virgin bentonite and local clay showed an insignificant uptake of EE2 (42% and 36% at pH 6.0 to 8.0 for B and LC respectively), which decreased further at low and high pH. The sorption of EE2 by all these hybrid materials showed a substantially higher percentage uptake (94%) compared with the unmodified clays. Interestingly, the high attenuation of EE2 was almost independent of the pH up to pH 8.5 (Fig. 1(a)).

TC has different functional groups with pK_{a1}, pK_{a2} and pK_{a3} values of 3.3, 7.7 and 9.7, respectively.[47] For the unmodified clays, B and LC, very high sorption of TC was achieved at lower pH values (pH 4), it decreased significantly between pH 4.0 and 6.0, remained nearly constant from pH 6.0–8.0, and then it decreased markedly at pH 10.0. These results agree well with other reports, in which TC adsorption was higher at low pH, and this was attributed to the cation exchange mechanism.[33,44] At pH values below 3.3, TC exists as a cation (TCH_3^+ or $TCH_3^{+\ 0\ 0}$), because of the protonation of the dimethyl-ammonium group. At pH 3.3–7.7, TC exists as a zwitterion (TCH_2^0 or $TCH_2^{0\ +\ -}$), because of the loss of a proton from the phenolic diketone moiety. At pHs greater than 7.7, TC exists as an anion (TCH^- or $TCH^{+\ -\ -}$), and at pH 9.7, it exists in di-anionic form (TC^{2-} or $TC^{0\ -\ -}$) through the loss of another proton from the tricarbonyl system and phenolic diketone moiety.[41] The higher removal at pH 6–8 for TC compared with EE2 for the unmodified clays indicates that the positive part of the TC zwitterions interacted with the clays. Because TCH_2^0 and TCH^- both contain a positively charged group in their structure, the molecules are probably arranged at the surface so that the positively charged group is close to the surface and the negatively charged group is furthest from the surface, which reveals that electrostatic attraction may play an important role in the sorption, not only of TCH_3^+, but also of TCH_2^0 and TCH^-.[48]

A slightly lower uptake of TC was observed for the hybrid material at pH 4.0. The uptake gradually increased at pH 6 (99.5%), and then remained nearly constant from pH 6.0 to 9.0. These results clearly indicate that hydrophobic interactions play a prominent role in TC sorption.[49] Above pH 9.0, a slight decrease in the removal of TC by the hybrid materials was observed, owing to the strong electrostatic repulsion. The slightly lower uptake of TC by LCAH may arise from the screening of HDTMA molecule by aluminum oxide/hydroxide particles on the clay surface, restricting the partitioning of TC in the hydrophobic core. Similar results were reported for the uptake of TC by $MnFe_2O_4$/activated carbon magnetic composite[50] and activated carbons.[32] Zhang *et al.*[51] observed similar behavior in the removal of TC by multi-walled carbon nanotubes (MWCNTs) and proposed that adsorption probably occurred *via* non-electrostatic π–π dispersion interactions between bulk π systems on the MWCNT surface and TC molecules containing benzene rings and double bonds, or *via* hydrophobic interactions between MWCNTs and TC.

3.2.2. Effect of EE2 or TC concentration. The effect of initial sorptive concentration can be used for estimating the sorption efficiency and capacity. The concentration dependence of removal was studied for initial EE2 concentrations from 1.0 to 10.0 mg L^{-1} and TC concentrations from 1.0 to 20.0 mg L^{-1} at pH 7.0. Results for EE2 and TC are presented in Fig. 2(a) and (b), respectively. Increasing the concentration of EE2 or TC did not affect the very high percentage uptake of EE2 and TC. These results also suggest the strong affinity of hybrid materials (BH, BAH and LCH) for EE2 and TC. At lower concentrations, the hybrid materials showed very high removal for TC, whereas the

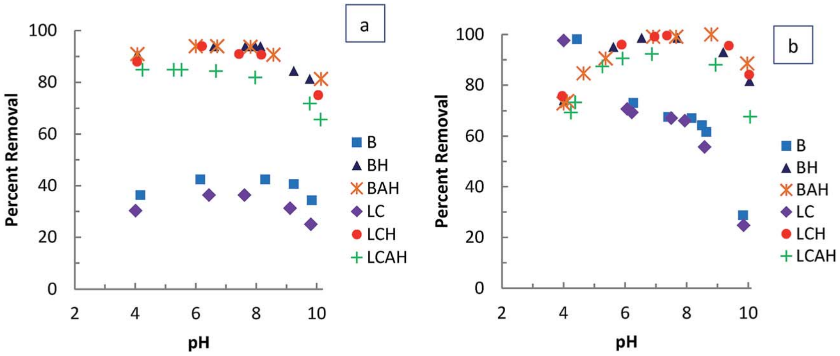

Fig. 1 pH dependence of sorption of (a) EE2 and (b) TC by B, BH, BAH, LC, LCH and LCAH.

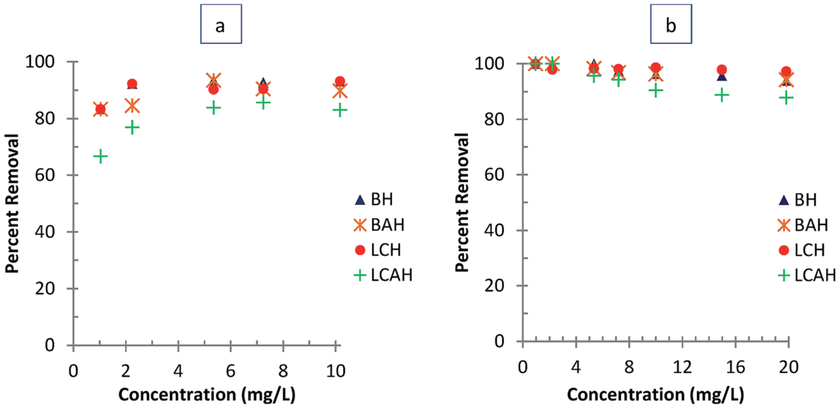

Fig. 2 Effect of concentration of (a) EE2 and (b) TC on the removal by BH, BAH, LCH and LCAH.

percent removal was slightly lower for EE2. A slightly lower removal of EE2 and TC was observed for LCAH. The results were consistent with the pH dependence study.

3.2.3. Effect of background electrolyte concentration. The effect of background electrolytes in the sorptive removal of EE2 and TC by the hybrid materials could help to explain the mechanism at solid/solution interfaces.[52,53] Specific sorption is not usually affected by the change in background electrolyte concentrations, whereas electrolyte concentration strongly affects non-specific sorption. Therefore, the sorption of EE2 or TC by BH, BAH, LCH and LCAH was assessed varying the background electrolyte concentrations from 0.0001 to 0.1 mol L^{-1} NaCl at an initial EE2 concentration of 5.0 mg L^{-1} and TC concentration of 10.0 mg L^{-1} at pH 7.0. The percent removal of EE2 and TC was obtained as a function of the background electrolyte (NaCl) concentrations. The results are presented in Fig. 3(a) and (b) for EE2 and TC, respectively. Increasing the background electrolyte concentrations even up to 1000 times did not significantly affect the percentage uptake of either EE2 or TC by the hybrid materials BH, BAH, LCH and LCAH. This indicated the strong affinity of the clays toward EE2 or TC. This implies that the partitioned EE2 or TC was bound strongly by van der Waals forces in the interspace of the hybrid materials. Previously, it was reported that increasing the NaCl concentration from 0 to 320 mM did not significantly change the adsorption of EE2 from landfill leachate on single-walled carbon nanotubes (SWCNTs).[54] Similarly, Zhang *et al.*[51] studied TC adsorption on multi-walled carbon nanotubes (MWCNT) at two ionic strengths (0.02 and 0.2 mol L^{-1} NaCl) and two initial TC concentrations (20.0 and 70.0 mg L^{-1}). In the pH range of 2.5 to 9, the ionic strength showed little effect on the sorption of TC on MWCNT.

3.2.4. Time dependence removal. The percent removal of EE2 or TC as a function of time was presented in Fig. 4(a) and (b). The materials are efficient in the removal of EE2 and TC from aqueous solutions because within the initial 10–15 min of contact time for EE2 and 60 min for TC, the uptake was very fast, and then it gradually increased until an apparent equilibrium was achieved within 60 min for EE2 and 240 min for TC. This also demonstrates the affinity of these clays for EE2 and TC. However, the uptake of EE2 and TC on LCAH was slower compared with the other hybrid materials.

The time dependence sorption data was then used to perform kinetic modelling. The three different kinetic models, pseudo-first order (PFO),[55] pseudo-second order (PSO)[56] and fractal-like pseudo-second order (FL-PSO)[57] models of its non-linear form (eqn (2)–(4)) were used.

$$q_t = q_e(1 - \exp(-k_1 t)) \quad (2)$$

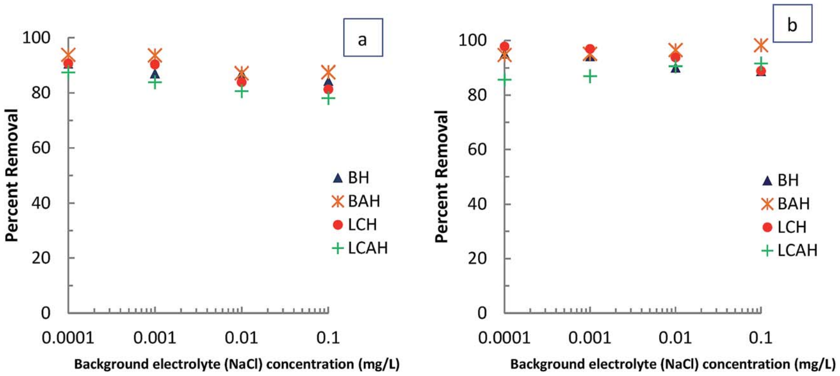

Fig. 3 Effect of background electrolyte (NaCl) concentration on the removal of (a) EE2 and (b) TC by BH, BAH, LCH and LCAH.

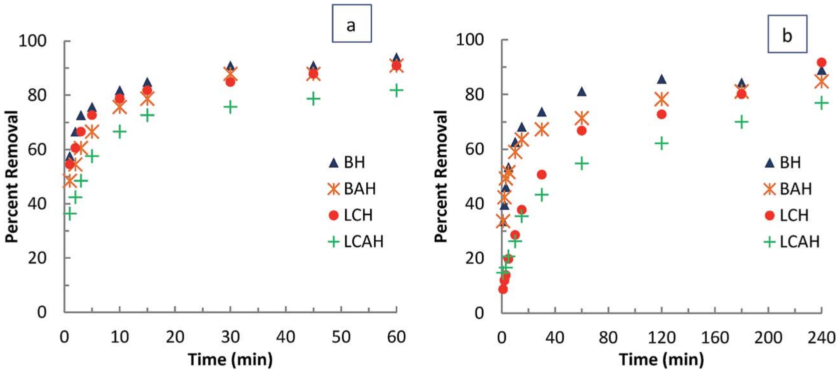

Fig. 4 Time dependence of the adsorption of (a) EE2 and (b) TC by BH, BAH, LCH and LCAH.

$$q_t = \frac{k_2 {q_e}^2 t}{1 + k_2 q_e t} \tag{3}$$

$$q_t = \frac{k {q_e}^2 t^\alpha}{1 + k q_e t^\alpha} \tag{4}$$

Here, q_t and q_e are the amount of EE2 or TC removed at time t and the removal capacity at equilibrium, respectively. k_1 and k_2 are the pseudo-first and pseudo-second order rate constants, respectively. k and α are the rate constant and fractal constant, respectively. A non-linear least squares fitting was performed and the unknown parameters were optimized. The estimated values of the unknown parameters along with the least square sum are shown in Table 1. The simulation data was best fitted by the PSO and FL-PSO kinetic models compared with the PFO model because a low value of the least square sum was obtained for these two models. These results showed that the removal capacity of these hybrid materials was higher for TC compared with EE2. Furthermore, the applicability of the PSO or FL-PSO models shows that the EE2 or TC species were bound to the surface of the hybrid materials with strong forces. Earlier reports indicated that the sorption of divalent metal cations on *Sphagnum* moss peat followed second-order rate laws. Therefore, metal cations were strongly bound by covalent bonds between the peat surface active groups and the divalent metal ions.[58,59] Similar results were obtained in the sorptive removal of bisphenol A by a hybrid material, made from a natural sericite precursor.[49]

3.3. Fixed-bed column reactor experiments

Fixed-bed column experiments were performed to assess the loading capacity of the hybrid materials BH, BAH, LCH and LCAH for EE2 and TC under dynamic conditions. The column experiments were carried out under various column conditions. The breakthrough curves are presented in Fig. 5(a) and (b) for EE2 and TC, respectively. A high breakthrough volume was obtained for EE2 and TC on these clays. A complete breakthrough volume was observed at throughput volumes of 7.68, 6.36, 6.24 and 5.041 L for EE2; and 1.33, 1.09, 1.06 and 0.94 L for TC; for BH, BAH, LCH and LCAH, respectively. The high breakthrough volume indicates the higher removal capacity of EE2 and TC by the modified clays under dynamic conditions. This further shows that the modified clays could be promising sorbing materials for the removal of EE2 and TC.

The non-linear least square fitting was conducted for the breakthrough column data employing the Thomas equation (eqn (1)). The fitting was performed to simulate the two unknown parameters, K_T and q_0. The values of the Thomas constants and the least square sum were estimated (Table 2).

Table 1 Kinetic parameters obtained for the sorption of EE2 and TC by hybrid materials by using various kinetic models[a]

	Kinetic models									
	PFO			PSO			FL-PSO			
Systems	q_e	k_1	s^2	q_e	k_2	s^2	q_e	k	α	s^2
BH-EE2	2.340	0.990	0.160	2.515	0.654	0.031	2.940	0.438	0.488	0.004
BAH-EE2	2.203	0.671	0.276	2.411	0.415	0.083	4.038	0.126	0.340	0.003
LCH-EE2	2.230	0.906	0.167	2.399	0.625	0.030	2.751	0.453	0.533	0.004
LCAH-EE2	2.002	0.463	0.164	2.221	0.292	0.045	2.673	0.217	0.611	0.013
BH-TC	3.868	0.289	1.699	4.127	0.100	0.481	4.691	0.108	0.571	0.035
BAH-TC	3.533	0.390	1.766	3.769	0.146	0.656	4.810	0.120	0.410	0.064
LCH-TC	3.940	0.039	0.882	4.506	0.010	0.350	5.534	0.013	0.712	0.143
LCAH-TC	3.296	0.046	1.192	3.700	0.016	0.608	7.395	0.011	0.457	0.088

[a] s^2: least square sum.

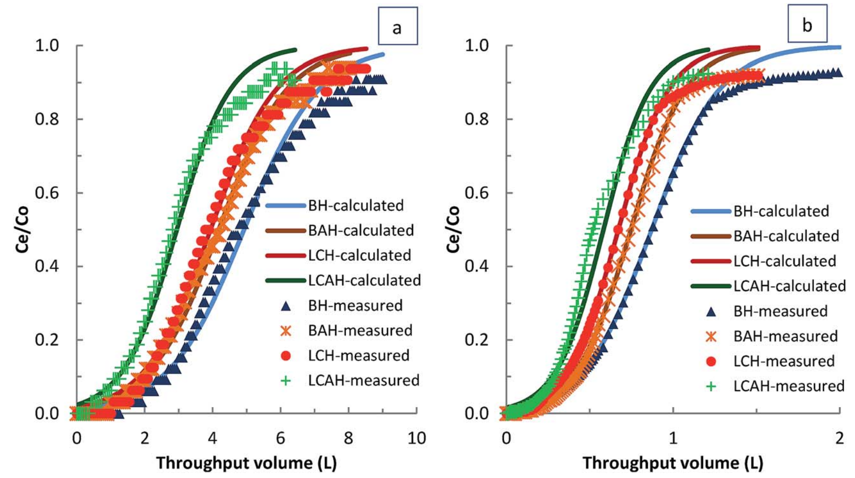

Fig. 5 Breakthrough curves for the removal of (a) EE2 and (b) TC by BH, BAH, LCH and LCAH.

A high loading capacity was achieved for EE2 and TC for these clays under dynamic conditions. BH showed a higher removal capacity for EE2 and TC compared with BAH. Similarly, LCH possessed a higher removal capacity than LCAH. The overall removal capacity was in the order BH > BAH ≈ LCH > LCAH. The removal capacity of BAH and LCH for EE2 and TC was comparable hence, the locally collected clay could be a useful natural material for the efficient, effective remediation of wastewater contaminated with the micro-pollutants EE2 and TC. Moreover, the removal capacity of BAH or LCAH for EE2 and TC was comparable with BH or LCH. Although a slight decrease was observed for BAH and LCAH, these materials showed a good settling capacity, and would be a superior alternative in solid/solution separation and wastewater treatment plants. These results were similar to the findings of the batch reactor experiments. The results were consistent

Table 2 Thomas constants and the least square sum for the removal of EE2 and TC by B, BH, BAH, LC, LCH and LCAH

	EE2			TC		
	Thomas constants			Thomas constants		
Materials	$K_T \times 10^{-4}$ (L min^{-1} mg^{-1})	q_0 (mg g^{-1})	Least square sum (s^2)	$K_T \times 10^{-4}$ (L min^{-1} mg^{-1})	q_0 (mg g^{-1})	Least square sum (s^2)
BH	1.59	111.979	10.0	4.89	34.976	12.0
BAH	1.70	97.987	11.0	6.09	29.963	12.0
LCH	1.88	86.965	11.0	6.59	26.956	12.0
LCAH	2.30	64.996	10.0	7.09	23.478	11.0

with previous reports in which the Thomas equation was used to demonstrate the loading capacity of different sorbing materials.[60,61]

4. Conclusion

Organo-modified clay and inorgano–organo-modified clays were synthesized from natural bentonite and local clay and characterized by IR and XRD. The IR data showed that HDTMA was introduced in the clay network. XRD analysis indicated the presence of quartz, smectite, kaolinite and illite in various proportions in bentonite and local clay. SEM images of the modified clays showed that the structures of HDTMA-modified clay materials were disordered, whereas Al-pillared clays contained fine particles of aluminum hydroxides or Al_2O_3 aggregated on the clay surface. The clays were used for the remediation of EE2 and TC contaminated waters in batch and column reactor experiments. The batch data implied that the uptake of EE2 and TC by the hybrid materials was slightly affected at low and high pH in the range 4.0–10.0. The uptake was not affected by varying the sorptive concentration (1.0 to 10.0 mg L^{-1} for EE2 and 1.0 to 20.0 mg L^{-1} for TC) and the background electrolyte concentration (0.0001 to 0.1 mol L^{-1} NaCl). Moreover, the attenuation of EE2 and TC by these hybrid materials was efficient; within 60 min of contact time for EE2 and 240 min for TC, an apparent equilibrium between clay and solution was achieved. The fixed-bed column results showed that a high breakthrough volume was obtained for attenuating EE2 and TC using the hybrid materials. Furthermore, the breakthrough data were fitted well to the Thomas equation; therefore, the loading capacity for EE2 was estimated to be 111.979, 97.987, 86.965 and 64.996 mg g^{-1} and that for TC was 34.976, 29.963, 26.956 and 23.478 mg g^{-1} for BH, BAH, LCH and LCAH, respectively. Hence, these hybrid materials are promising for the remediation of the aquatic environment contaminated with two important micro-pollutants, EE2 and TC.

Acknowledgements

DT wishes to acknowledge CSIR, New Delhi for the financial support through Research Project (no. 01 (2567)/12/EMR-II). The work is also partly supported by UGC (NERO) financial assistance (no. F.5-22/2013-14/(MRP/NERO)/261).

References

1 *Crystal structure of clay minerals and their X-ray identification*, ed. S. W. Bailey, G. W. Brindley and G. Brown, Mineralogical Society, London, 1980, pp. 1–113.
2 J. Konta, *Appl. Clay Sci.*, 1995, **10**, 275–335.
3 S. M. Lee and D. Tiwari, *Appl. Clay Sci.*, 2012, **59–60**, 84–102.
4 Y. Park, G. A. Ayoko and R. L. Frost, *J. Colloid Interface Sci.*, 2011, **354**, 292–305.
5 D. Tiwari and S. M. Lee, *Chem. Eng. J.*, 2012, **204–206**, 23–31.
6 Z. Li and R. S. Bowman, *Water Res.*, 2001, **35**, 3771–3776.
7 Z. Li, D. Alessi, P. Zhang and R. S. Bowman, *J. Environ. Eng.*, 2002, **128**, 583–587.
8 G. R. Alther, *Waste Manag.*, 2002, **22**, 507–513.
9 J. Q. Jiang, C. Cooper and S. Ouki, *Chemosphere*, 2002, **47**, 711–716.
10 J. Smith, S. Bartlett-Hunt and S. Burns, *J. Hazard. Mater.*, 2003, **96**, 91–97.
11 E. Benfenati, D. Barceló, I. Johnson, S. Galassi and K. Levsen, *Trends Anal. Chem.*, 2003, **22**, 757–765.
12 S. A. Snyder, P. Westerhoff, Y. Yoon and D. L. Sedlak, *Environ. Eng. Sci.*, 2003, **20**, 449–469.
13 M. Petrović, E. Eljarrat, M. J. L. de Alda and D. Barceló, *Anal. Bioanal. Chem.*, 2004, **378**, 549–562.
14 J. Niu, S. Ding, L. Zhang, J. Zhao and C. Feng, *Chemosphere*, 2013, **93**, 1–8.
15 J. Lienert, T. Buerki and B. I. Escher, *Water Sci. Technol.*, 2007, **56**, 87–96.
16 A. Joss, E. Keller, A. Alder, A. Gobel, C. McArdell, T. Ternes and H. Siegrist, *Water Res.*, 2005, **39**, 3139–3152.
17 K. A. Landry and T. H. Boyer, *Water Res.*, 2013, **47**, 6432–6444.
18 S. Larcher and V. Yargeau, *Environ. Pollut.*, 2013, **173**, 17–22.
19 Datapharm, EMC Medicine Guides (UK) – Ethinylestradiol, 2008, http://www.medicines.org.uk/guides/ethinylestradiol.
20 J. Han, W. Qiu, Z. Cao, J. Hu and W. Gao, *Water Res.*, 2013, **47**, 2273–2284.
21 A. Z. Aris, A. S. Shamsuddin and S. M. Praveena, *Environ. Int.*, 2014, **69**, 104–119.
22 USFDA, U.S. Food and Drug Administration (USFDA) and National Center for Toxicological Research (NCTR), Endocrine Disruptor Knowledge Base (EDKB), 2012, http://www.fda.gov/scienceresearch/bioinformaticstools/endocrinedisruptorknowledgebase/default.htm.
23 P. C. Heaton, S. R. Fenwick and D. E. Brewer, *J. Clin. Pharm. Ther.*, 2007, **32**, 483–487.
24 S. Yahiat, F. Fourcade, S. Brosillon and A. Amrane, *Int. Biodeterior. Biodegrad.*, 2011, **65**, 997–1003.
25 P. Gao, M. Munir and I. Xagoraraki, *Sci. Total Environ.*, 2012, **173**, 421–422.
26 W. Yang, Z. Tang, F. Zhou, W. Zhang and L. Song, *Environ. Toxicol. Pharmacol.*, 2013, **35**, 320–324.
27 H. Y. Kim, J. Jeon, J. Hollender, S. Yu and S. D. Kim, *J. Hazard. Mater.*, 2014, **279**, 428–435.
28 J. de Rudder, T. V. de Wiele, W. Dhooge, F. Comhaire and W. Verstraete, *Water Res.*, 2004, **38**, 184–192.
29 L. Joseph, L. K. Boateng, J. R. V. Flora, Y.-G. Park, A. Son, M. Badawy and Y. Yoon, *Sep. Purif. Technol.*, 2013, **107**, 37–47.
30 L. A. Al-Khateeb, A. Y. Obaid, N. A. Asiri and M. A. Salam, *J. Ind. Eng. Chem.*, 2014, **20**, 916–924.
31 Y. Gao, Y. Li, L. Zhang, H. Huang, J. Hu, S. M. Shah and X. Su, *J. Colloid Interface Sci.*, 2012, **368**, 540–546.
32 J. Rivera-Utrilla, C. V. Gómez-Pacheco, M. Sánchez-Polo, J. J. López-Peñalver and R. Ocampo-Pérez, *J. Environ. Manage.*, 2013, **131**, 16–24.
33 Z. Li, L. Schulz, C. Ackley and N. Fenske, *J. Colloid Interface Sci.*, 2010, **351**, 254–260.
34 S. A. Boyd, S. Shaobai, J.-F. Lee and M. M. Mortland, *Clays Clay Miner.*, 1988, **36**, 125–130.

35 ISRIC (International Soil Reference and Information Centre), *Procedures for soil analysis*, ed. L. P. van Reeuwijk, FAO, UN, Wageningen, The Netherlands, 6th edn, 2012, pp. 3.1–3.7, http://www.isric.org/isric/webdocs/docs/ISRIC_TechPap09_2002.pdf.

36 US EPA (United States Environment Protection Agency), *Method 9080, Cation-Exchange Capacity of Soils (Ammonium Acetate)*, 1986, pp. 1–9.

37 Thanhmingliana and D. Tiwari, *Chem. Eng. J.*, 2015, **263**, 364–373.

38 P. C. C. Faria, J. J. M. Órfão and M. F. R. Pereira, *Water Res.*, 2004, **38**, 2043–2052.

39 Y. Gao, Y. Li, L. Zhang, H. Huang, J. Hu, S. M. Shah and X. Su, *J. Colloid Interface Sci.*, 2012, **368**, 540–546.

40 M. Brigante and P. C. Schulz, *J. Hazard. Mater.*, 2011, **192**, 1597–1608.

41 H. C. Thomas, *J. Am. Chem. Soc.*, 1944, **66**, 1664–1666.

42 S. M. Lee, Lalhmunsiama, Thanhmingliana and D. Tiwari, *Chem. Eng. J.*, 2015, **270**, 496–507.

43 X. Yang, R. C. Flowers, H. S. Weinberg and P. C. Singer, *Water Res.*, 2011, **45**, 5218–5228.

44 Z. Li and R. S. Bowman, *Environ. Sci. Technol.*, 1997, **31**, 2407–2412.

45 Y. Park, G. A. Ayoko, R. Kurdi, E. Horváth, J. Kristóf and R. L. Frost, *J. Colloid Interface Sci.*, 2013, **406**, 196–208.

46 S. Zheng, Z. Sun, Y. Park, G. A. Ayoko and R. L. Frost, *Chem. Eng. J.*, 2013, **234**, 416–422.

47 P. Kulshrestha, R. F. Giese Jr and D. S. Aga, *Environ. Sci. Technol.*, 2004, **38**, 4097–4105.

48 M. E. Parolo, M. C. Savini, J. M. Vallés, M. T. Baschini and M. J. Avena, *Appl. Clay Sci.*, 2008, **40**, 179–186.

49 Thanhmingliana, S. M. Lee and D. Tiwari, *RSC Adv.*, 2014, **4**, 43921–43930.

50 L. Shao, Z. Ren, G. Zhang and L. Chen, *Mater. Chem. Phys.*, 2012, **135**, 16–24.

51 L. Zhang, X. Song, X. Liu, L. Yang, F. Pan and J. Lv, *Chem. Eng. J.*, 2011, **178**, 26–33.

52 K. F. Hayes, C. Papelis and J. O. Leckie, *J. Colloid Interface Sci.*, 1988, **125**, 717–726.

53 S. M. Lee, Lalhmunsiama and D. Tiwari, *Environ. Sci. Pollut. Res. Int.*, 2014, **21**, 3686–3696.

54 L. Joseph, Q. Zaib, I. A. Khan, N. D. Berge, Y.-G. Park, N. B. Saleh and Y. Yoon, *Water Res.*, 2011, **45**, 4056–4068.

55 T. Yang, M. L. Chen, L. H. Liu, J. H. Wang and P. K. Dasgupta, *Environ. Sci. Technol.*, 2012, **46**, 2251–2256.

56 Y. S. Ho and G. McKay, *Process Saf. Environ. Prot.*, 1998, **76**, 332–340.

57 M. Haerifar and S. Azizian, *Chem. Eng. J.*, 2013, **215–216**, 65–71.

58 Y. S. Ho, *J. Hazard. Mater.*, 2006, **136**, 681–689.

59 Y. S. Ho and G. McKay, *Water Res.*, 2000, **34**, 735–742.

60 D. Tiwari, C. Laldawngliana and S. M. Lee, *Environmental Engineering Research*, 2014, **19**, 107–113.

61 S. M. Lee, D. Tiwari, K. M. Choi, J. K. Yang, Y. Y. Chang and H. D. Lee, *J. Chem. Eng. Data*, 2009, **54**, 1823–1828.